VALORISATION OF STARCH PRODUCTION IN MICROALGAE BIOREFINERY

Imma Gifuni

Dottorato in Biotecnologie – XXX ciclo

Università degli Studi di Napoli Federico II

Dottorato in Biotecnologie – XXX ciclo

Università degli Studi di Napoli Federico II

VALORISATION OF STARCH PRODUCTION IN MICROALGAE BIOREFINERY

Imma Gifuni

Dottoranda: Imma Gifuni

Relatore: Prof. Antonio Marzocchella
Prof. Giuseppe Olivieri

Coordinatore: Prof. Giovanni Sannia

…to my family despite everything
…to my love for everything

Napoli, October 2017

TABLE OF CONTENTS

RIASSUNTO

I principali problemi ambientali della nostra epoca sono dovuti alla logica del "produrre-usare-gettare" che non presta attenzione alle limitate risorse ambientali e alla necessità di controllare la produzione dei rifiuti. Una soluzione innovativa, che tenga conto della domanda di beni di consumo e della salvaguardia dell'ambiente, è l'Economia Circolare. Essa propone l'utilizzo di materie prime rinnovabili per la produzione di beni che, dopo il loro utilizzo, costituiranno rifiuti riciclabili. Questo schema di economia circolare può essere implementato dalla produzione di materie prime tramite processi biologici che assimilano CO_2. In questo modo, la riduzione dell'effetto serra, causato dall'anidride carbonica, può essere associato alla produzione di beni e materie prime rinnovabili. Inoltre, per limitare la produzione di scarti, nuovi processi di *biorefinery* sono stati proposti. La bio-raffineria, analogamente alla raffineria petrolifera, è l'insieme strutturato di processi atti alla valorizzazione di tutte le componenti di interesse presenti nella materia di partenza, al fine di ridurre al minimo gli scarti generati dalla produzione e aumentare il profitto finale. La bio-raffineria può utilizzare diversi materiali di partenza tra cui scarti agricoli, forestali, biomasse acquatiche, residui industriali.

Nell'ambito delle biomasse acquatiche, le colture microalgali rivestono attualmente un ruolo di interesse per la loro variabilità, l'elevata efficienza fotosintetica e l'ampia gamma di prodotti di interesse industriale di cui sono costituite. Di questi prodotti fanno parte:

- ***pigmenti***, tra cui carotenoidi con attività antiossidante ampiamente richiesti da industrie farmaceutiche e cosmetiche, pigmenti utilizzati come coloranti naturali alimentari e non;
- ***proteine,*** ricche di amminoacidi essenziali e proprietà tecnico-funzionali che trovano applicazione come additivi alimentari o fonte primaria di proteine per uomo e animali;
- ***lipidi***, tra i quali acidi grassi polinsaturi (PUFA) di grande interesse per l'alimentazione umana e le proprietà terapeutiche, e gli acidi grassi saturi principalmente indirizzati alla produzione di biodiesel;
- ***carboidrati***, principalmente amido e glicogeno, attualmente proposti come fonte di zuccheri per la produzione di biogas tramite fermentazione microbica, interessanti applicazioni farmaceutiche derivano invece dai polisaccaridi solfati.

L'applicazione del concetto di bio-raffineria alla biomassa microalgale, consentirebbe di sfruttare contemporaneamente diverse delle componenti elencate, riducendo la produzione di scarti e aumentando il valore economico generato. Sebbene diversi schemi di bio-raffineria, applicati alla biomassa microalgale, sono stati proposti in questi anni (Zhu et al., 2015; Soh et al., 2014; Ansari et al., 2017), l'effettiva applicazione è ancora lontana. Alcune problematiche limitano lo sfruttamento della bio-raffineria delle microalghe e gli elevati costi di produzione confinano le applicazioni alle componenti ad elevato valore (antiossidanti, proteine, acidi grassi polinsaturi). La produzione di beni di largo consumo (e.g. biodiesel, bioplastiche) risulta tutt' oggi non vantaggioso dal punto di vista economico, senza possibilità di competizione con le materie fossili.

Le principali problematiche che limitano l'applicazione del concetto di bio-raffineria alla biomassa microalgale sono:

1. La selezione di ceppi robusti, che siano in grado di costituire la popolazione predominante, anche in condizioni non asettiche, e la selezione delle strategie di coltura adatte alla contemporanea produzione di differenti componenti.

Spesso le condizioni di coltura che favoriscono l'accumulo di un prodotto (es. lipidi, accumulati in carenza di azoto) riducono drasticamente la concentrazione delle altre componenti di interesse (es. contenuto di proteine diminuisce in carenza di azoto).

2. La valorizzazione di tutte le componenti della biomassa microalgale al fine di aumentare la convenienza economica dell'intero processo. A tal proposito, la frazione di carboidrati, contenuta nelle microalghe viene estremamente sottovalutata. Infatti, l'amido, che ne è il principale costituente nelle alghe verdi, potrebbe essere utilizzato direttamente nel settore industriale alimentare (come additivo o emulsionante), nel settore farmaceutico (come carrier per principi attivi) o per la produzione di biopastiche a base di amido. Il ricavo economico di tali applicazioni, supererebbe di gran lunga il guadagno derivante dall' attuale applicazione di produzione di biogas per via fermentativa.
3. L'intensificazione delle colture microalgali. Sebbene le alghe abbiano un'elevata efficienza fotosintetica, i sistemi di coltura più diffusi consentono di produrre colture estremamente diluite (0.8-2 g L^{-1}), le quali determinano un'eccessiva spesa nei processi di recupero.
4. Frazionamento e il recupero delle diverse componenti. Non sono state tuttora determinate delle strategie efficienti per il recupero e il frazionamento delle diverse componenti microalgali, che preservino l'integrità e le proprietà delle stesse. La maggioranza degli studi considera la massimizzazione del recupero del prodotto con più alto valore e, successivamente, propone la valorizzazione di ciò che resta nel residuo. Strategie innovative dovrebbero considerare la valorizzazione simultanea di più componenti, specialmente quelle indirizzate alla produzione di beni di largo consumo.

Scopo della tesi: Lo scopo della tesi è la valorizzazione della produzione di amido da microalghe nello schema della bio-raffineria e di proporre strategie innovative per l'intensificazione delle colture e il recupero di più componenti. I principali obiettivi di ricerca possono essere suddivisi in quattro gruppi: 1) Selezione di un ceppo microalgale robusto per la produzione di amido; 2) Caratterizzazione dell'amido da microalghe, per applicazioni industriali; 3) Progettazione un nuovo sistema di coltura intensivo; 4) Studio delle tecniche di *downstream* finalizzate al recupero di amido e proteine da microalghe.

Selezione di un ceppo microalgale robusto per la produzione di amido nello schema di bio-raffineria. Lo studio si è articolato in una prima fase di screening di ceppi microalgali per selezionare il ceppo con maggiore produttività di amido e capacità di produrre altre molecole di interesse. I ceppi investigati sono stati selezionati, sulla base di studi disponibili in letteratura, tra i più utilizzati per colture in larga scala. Essi sono stati: *Chlorella sorokiniana* e *Scenedesmus vacuolatus* (ceppi di acqua dolce), *Dunaliella tertiolecta* e *Tetraselmis chuii* (ceppi di acqua salata). Lo screening è stato effettuato in fotobioreattori a bolle inclinati. Il confronto ha portato alla selezione di *C. sorokiniana* come migliore ceppo per la produzione di amido e altre molecole. Successivamente, è stato valutato l'effetto della concentrazione di azoto e CO_2 sull'accumulo di amido e a produzione di biomassa di tale ceppo. Per intensità luminose di 300 µmol $m^{-2}s^{-1}$, le concentrazioni ottimali di azoto e CO_2 sono state riscontrate pari a 32 mg L^{-1} e 2% rispettivamente. Fornire elevate concentrazioni di azoto a parità di intensità luminosa non produce aumento nella crescita della biomassa e il contenuto di amido diminuisce. La CO_2, in concentrazioni uguali o superiori a 2%, è risultata non avere alcun effetto sull'accumulo di amido, ma concentrazioni di superiori al 5% determinano un drastico allontanamento del pH dal valore ottimale con

una conseguente diminuzione della crescita cellulare. Nelle condizioni ottimali di crescita individuate, una completa caratterizzazione biochimica della biomassa di *C. sorokiniana* è stata effettuata durante le varie fasi della crescita. Ciò ha consentito di valutare la dinamica di accumulo delle varie componenti microalgali e di stabilire la condizione ottimale che consentisse lo sfruttamento di più prodotti nell'ottica della bio-raffineria. A tal proposito, la fase di inizio di carenza di azoto è stata individuata come fase favorevole per il contemporaneo recupero di amido, proteine e lipidi (34, 37, 21 % del peso secco della biomassa, rispettivamente).

Caratterizzazione dell'amido delle microalghe per applicazioni industriali. L'obiettivo di questa sezione è stato la caratterizzazione fisico-chimica dei granuli di amido prodotti dal ceppo microlagale selezionato al punto 1. Limitate informazioni sono disponibili in letteratura sull'amido delle microalghe. Per validare la possibile applicazione di tale prodotto nell'ambito industriale, alcune proprietà devono essere studiate. Le principali caratteristiche che influenzano la processabilità dell'amido nell'ambito industriale sono: la forma dei granuli e la loro dimensione, il contenuto in amilosio e amilopectina, la cristallinità e le proprietà termiche. Quindi, un protocollo di estrazione e purificazione dell'amido è stato ottimizzato. Si è proceduto alla caratterizzazione dei granuli di amido prodotti da *C. sorokiniana* in collaborazione con il gruppo del Prof. Gerardino D'Errico del Dipartimento di Scienze Chimiche dell'Università "Federico II". I risultati relativi a peso molecolare, cristallinità, rapporto amilosio/amilopectina hanno evidenziato numerose analogie con l'amido prodotto dai cereali. La ridotta dimensione dei granuli d'amido delle microalghe (1-2 μm) ne suggerisce interessanti applicazioni. In particolare, ridotta dimensione e ampia superficie facilitano reazioni di funzionalizzazione e modifica chimica degli amidi, che risulta essere un settore in continua espansione. Ulteriori applicazioni sono state proposte come emulsificante alimentare e cosmetico, *carrier* di principi attivi per applicazioni farmaceutiche, produzione di film sottili per il packaging alimentare.

Progettazione di nuovi sistemi per colture microalgali intensive. L'aumento della concentrazione della biomassa e della produttività della biomassa stessa sono punti cruciali per l'ottimizzazione del processo produttivo. L'aumento della concentrazione della biomassa microalgale consente una significativa riduzione dei costi di *downstream*. La ridotta concentrazione ottenuta con gli attuali sistemi di coltura è principalmente dovuta a una scarsa penetrazione della luce nella coltura, pertanto la marggior parte del volume di coltura è scarsamente illuminata. Per superare tale limite è stato sviluppato un nuovo fotobioreattore caratterizzato da spessore estremamente ridotto (3 mm), definito *Ultra-flat panel PBR*. Le prestazioni del reattore sviluppato sono state determinate con riferimento al ceppo microalgale precedentemente selezionato: *C. sorokiniana*. L'effetto dell'intensità luminosa (fissata tra 50 e 1000 μmol m^{-2} s^{-1}), su crescita, fotosintesi e composizione biochimica, è stato valutato. La massima concentrazione di biomassa raggiunta è stata di 24 kg m^{-3} (rispetto a 2-5 kg m^{-3} dei tradizionali fotobioreatori) e una produttività di 0.34 kg m^{-3} h^{-1}. La massima velocità di crescita delle microalghe è stata di 0.1 h^{-1} ad irradianze di 1000 μmol m^{-2} s^{-1} e non è stata riscontrata inibizione dell'attività fotosintetica. L'analisi della composizione biochimica della biomassa alle diverse irradianze luminose dimostra che la disponibilità di luce influenza la concentrazione delle diverse biomolecole. In particolare, il contenuto di proteine aumenta dal 35 al 53% del peso secco all'aumentare dell'intensità luminosa. La concentrazione delle molecole di riserva (amido e lipidi), al contrario, diminuisce con l'aumento dell'intensità luminosa. Probabilmente, in condizioni in cui l'apporto fotonico non è limitante le microalghe investono più energia nella crescita e nella sintesi di proteine, anziché nell'accumulo

di riserve energetiche. Il massimo contenuto di amido è raggiunto a media irradianza luminosa (300 µmol m^{-2} s^{-1}), alla quale si stabilisce una sorta di bilancio tra crescita e accumulo di energia. Nonostante le migliorate prestazioni dell'*Ultra-flat panel PBR*, la concentrazione cellulare non supera i 24 kg m^{-3} sebbene l'irradianza sia stata aumentata significativamente nel corso della sperimentsaizone. Il modello del trasferimento della luce in colture microalgali, proposto da Pruvost e Cornet (2012), è stato quindi applicato ai dati sperimentali ottenuti al fine di individuare un eventuale limitazione che bloccasse la crescita. Nessuna limitazione da luce è stata riscontrata, pertanto ulteriori studi saranno necessari per individuare i fattori che limitano l'aumento della concentrazione microalgale oltre il limite rilevato (24 g L^{-1}).

Studio delle tecniche di downstream finalizzate al recupero di amido e altri componenti. L'attività è stata articolata in due lienee.

La prima linea è stata condotta in collaborazione con la Dr. Ganna Petruk studente dello stesso DdR attiva nel gruppo condotto dalla Prof.ssa R. Piccoli. Lo studio è stato finalizzato alla contemporanea valorizzazione di amido e antiossidanti prodotti dalla microalga *Chlorella sorokiniana*. L'estrazione con etanolo (*safe-solvent*) è stata ottimizzata con riferimento al recupero di amido e attivita antiossidante dell'estratto. I risultati hanno evidenziato un recupero di amido del 83% e una significativa attività antiossidante *in vitro* e *in vivo*.

La seconda linea è stata condotta presso Laboratoire de Génie des Procédés environnement agro-alimentaire (GEPEA) dell'Università di Nantes (FR) e ha riguardato tecniche di *downstream*. I processi di downstream investigati sono stati: i) distruzione cellulare accoppiata a centrifugazione blanda per il recupero di amido e proteine in due frazioni distinte (pellet e surnatante); ii) purificazione delle proteine recuperate nel surnatante per filtrazione su membrane. Gli studi sono stati effettuati utilizzando il ceppo microalgale dei punti precedenti: *C. sorokiniana*.

L'obiettivo della prima fase dell'attività presso GEPEA è stato l'ottimizzazione della distruzione meccanica delle cellule mediante *bead milling* al fine di recuperare l'amido nel pellet e le proteine nel surnatante dopo centrifugazione blanda. I parametri di centrifugazione sono stati fissati in modo da mantenere un basso consumo energetico associato a tale step e limitare la segregazione a particelle di diametro e densità dei granuli di amido (caratterizzati al punto 2). Dato che il processo di distruzione meccanica è influenzato da diversi parametri, un limitato numero di esperimenti è stato programmato ed effettuato, e lo *Stress model* (Kwade and Schwedes, 2007) è stato applicato ai dati sperimentali ottenuti. Lo Stress model è stato applicato con successo per descrivere la distruzione di microalghe tramite *bead milling* (Montalescot et al., 2015) e ha consentito di mettere in relazione i parametri di processo con la cinetica di distruzione cellulare e l'energia consumata. Il presente studio ha evidenziato una relazione tra l'estrazione dei prodotti intracellulari e le condizioni di esercizio del processo e l'energia consumata. Pertanto, selezionando opportunamente le condizioni di esercizio, la distruzione meccanica può portare all'estrazione selettiva di proteine invece che pigmenti. In particolare, è stato individuato un valore critico di energia somministrata per unità di massa di microalghe: 2.4 10^{+12} J kg^{-1}. Per trattamenti blandi (energia specifica somministrata inferiore al valore critico), la maggioranza dei detriti cellulari rimane nel surnatante con elevata resa in proteine (90% dell'iniziale contenuto della biomassa), 75% della clorofilla ritrovato nel surnatante e 75 % dell'amido recuperato nel pellet. Per trattamenti intensi (energia specifica somministrata superiore al valore critico), la maggioranza dei detriti cellulari è segregata nel pellet. Ciò determina un aumento del recupero dell'amido (85%) ma a purezza bassa. La resa del recupero di proteine nel surnatante diminuisce, lo stesso avviene per la clorofilla. In

corrispondenza del valore critico viene riscontrata la più alta resa e selettività per amido e proteine. Tali risultati, evidenziano la possibilità di prevedere la ripartizione dei prodotti intracellulari in pellet e surnatante, sulla base dell'energia investita nel processo di distruzione cellulare. Ciò costituisce un punto cruciale per la progettazione di un processo di downstream per il recupero di un prodotto di interesse e per applicazioni di bio-raffineria.

L'obiettivo della seconda fase dell'attività presso GEPEA ha riguardato la progettazione di un sistema di filtrazione articolato in tre step con lo scopo di purificare e concentrare le proteine recuperate nel surnatante della fase precedente. Le condizioni di esercizio selezionate per la distruzione cellulare sono state quelle corrispondenti alla condizione ottimale riscontrata al punto definito "critico". Il processo di filtrazione a più step è stato articolato come segue:

1. PREFILTRAZIONE, il surnatante è stato sottoposto a ultrafiltrazione con membrane di ceramica caratterizzate da cut-off di 0.22 μm. Tale step è finalizzato all'aliminazione di eventuali detriti cellulari presenti nella soluzione di partenza.
2. DIAFILTRAZIONE, in questa fase cinque dia-volumi di acqua distillata sono stati aggiunti al concentrato dello step precedente e un ulteriore filtrazione è stata effettuata sulla membrana 0.22 μm, al fine di recuperare eventuali proteine in esso bloccate.
3. CONCENTRAZIONE, il permeato raccolto nei primi due step è stato filtrato con una membrana ceramica di cut-off 3 kDa. Tale procedimento ha lo scopo di trattenere le proteine nel retentato e recuperarle in una soluzione concentrata.

Il procedimento di purificazione per filtrazione non ha portato i risultati auspicati. La resa totale del processo a tre step è risultata molto bassa: solo il 12% delle proteine iniziali è stato recuperato e, con una bassa purezza (18%). Il principale problema può essere identificato nell'utilizzo di un protocollo di conservazione della soluzione contenente le proteine siccome l'intero processo (harvesting della coltura, distruzione cellulare, prefiltrazione, diafiltrazione e concentrazione) ha la durata di più giorni. La conservazione può facilmente indurre alla denaturazione delle proteine. Probabilmente, lo step di diafiltrazione che utilizza acqua distillata diminuisce ulteriormente le prestazioni del processo causando aggregazione delle proteine presenti. Tale step potrebbe essere eliminato o sostituito con una diafiltrazione che faccia uso di buffer salini in sostituzione all' acqua distillata, per impedire l'aggregazione proteica. L'utilizzo della filtrazione con membrane nell'ambito della bio-raffineria microalgale, è ancora alle fasi iniziali, ma i bassi costi e la sostenibilità ad essa associati rappresentano un grande potenziale. Ulteriori studi saranno necessari per ottimizzare il processo e renderlo efficiente, inoltre grandi vantaggi nella progettazione dei processi di recupero, possono derivare da una completa caratterizzazione delle componenti cellulari liberate e dall'interazione tra esse.

SUMMARY

The present research project was aimed at the valorisation of microalgal starch production within a biorefinery approach. The activity was carried out at the Dipartimento di Ingegneria Chimica, dei Materiale e della Produzione Industriale and at the Dipartimento di Biologia of the Università degli Studi di Napoli 'Federico II'. Some tasks were carried out at the Laboratoire de Génie des Procédés environnement agro-alimentaire of the University of Nantes (France). The activity has been organized in four main paths:

T1) Selection of a robust microalgal strain for starch production.

This task was aimed to select a robust microalgal strain for industrial production of the biomass for biorefinery applications. The selection was based on the biomass and starch productivity. Two fresh water microalgae, *Chlorella sorokiniana* and *Scenedesmus vacuolatus*, and two seawater microalgae, *Dunaliella tertiolecta* and *Tetraselmis chuii* were investigated. *C. sorokiniana* was selected as the best starch producer. The effect of nitrogen and CO_2 concentration on the biomass and starch productivity was investigated. At light irradiance of 300 µmol $m^{-2}s^{-1}$, the optimal concentration of nitrogen and CO_2 were 32 mg L^{-1} and 2%, respevtively. A complete biochemical characterization of the microalgal biomass was carried out as a function of the growth time. The onset of nitrogen depletion was identified as the suitable condition for the simultaneous recovery of multiple products: starch, proteins, lipids (34, 37, 21 $\%_{DW}$, respectively).

T2) Characterization of the microalgal starch granules.

The goal of this task was to prove that the microalgal starch granules have interesting physic and chemical properties required for industrial applications. Limited information was available in literature about microalgal starch, then additional analysis were necessary to validate the potential applications of this starch type. *C. sorokiniana* starch extraction was optimized and a preliminary physic-chemical characterization was carried out. The results pointed out many similarities with cereals starch. However, the reduced size of the starch granules from microalgae addressed specific and high-value applications as emulsifier, molecules carrier, functionalization, bioplastics.

T3) Intensification of microalgal biomass production.

The increase in the microalgal biomass concentration and productivity are crucial issues for the process optimization. A new ultra-thin flat photobioreactor was designed and built. The performances were assessed for *C. sorokiniana*. The effect of the light intensity on the growth and the biochemical composition of *C. sorokiniana* was also investigated. Biomass concentration of 10 g L^{-1} was established in less than 100 hours at medium light irradiance of 300 µmol m^{-2} s^{-1}.

T4) Mild downstream processes for the recovery of starch and other components.

The goal was the exploitation of several microalgal components. The simultaneous recovery of starch and antioxidants was carried out in cooperation with Dr. Ganna Petruk, Biotechnology PhD student. The recovery of starch and proteins from microalgae was carried out at Laboratoire de Génie des Procédés environnement agro-alimentaire, Nantes University. The effect of bead milling cell disruption on products recovery was investigated. A model to describe the disruption process was successfully applied to the product recovery. Integration of microalagal mechanical disruption, centrifugation and membrane separation for the simultaneous recovery of starch and proteins from microalgal biomass was investigated.

1. INTRODUCTION

1.1 Circular bioeconomy and microalgal biorefinery

The environmental pollution is a growing concern for ecologist, worried about the stability of the ecosystems, and the World Health Organization worried for the toxicological risks for human health due to the pollution. The increase of the CO_2 emission, the associate increase of the greenhouse effect and climate change, the pollution and the reduction of fresh water source and the increase of waste production are the result of about two centuries of linear economy (Figure 1.1). Here, the logic of "make-use-dispose" used the environmental resources with no rationality and no plans for waste disposal or reuse.

The decrease of the natural resources and the increase of the environmental consciences have forced the industrial societies towards the concept of Circular Bioeconomy. The basic concept is that renewable materials must be used as feedstock for fuels and chemicals, all the by-products find feed or industrial applications and the wastes are completely degradable (Figure 1.1). This economy model promotes the sustainable development and it requires balanced and simultaneous consideration of the economic, environmental, technological and social aspects of an investigated economy sector as well as of the interaction among all these issues (FAO, 2002; Ghisellini et al., 2016). The Circular Bieconomy can find application only if it will be able to ensure the same supply rate of goods and services, no significant increase in the price of the final products, healthy and eco-friendly solutions. The investment for the application of the Circular Economy strategy are huge, but the Ellen Mac Arthur foundation estimated a final economic benefit of 1.8 trillion of euro in the 2030 and a reduction of the CO_2 emission of the 48% (www.ellenmacarthurfoundation.org).

Figure 1.1: Difference between linear economy and circular economy (www.ellenmacarthurfundation.org/education)

Mohan et al. (2016) highlight the possibility of implementing the Circular Bioeconomy based on the biological CO_2 capture for mitigating climate change and the simultaneous synthesization of feedstock for industries and value-added products. In this perspective, the biorefinery concept completely fulfil the objective. The concept of a biorefinery is analogous to a petroleum refinery (Figure 1.2). A petroleum refinery

exploite completely oil to produce fuels, oil-derived products from butane for cigarette lighters to asphalt, and a wide spectrum of petro-chemicals for the plastic industry. The same strategy is applied in the biorefinery for the exploitation of biomass: all the biomass components are used in different industrial field after separation and/or catalytic conversion. The residue streams of the processes are used, recycled, and valorised: no waste is produced (Moraes et al., 2014).

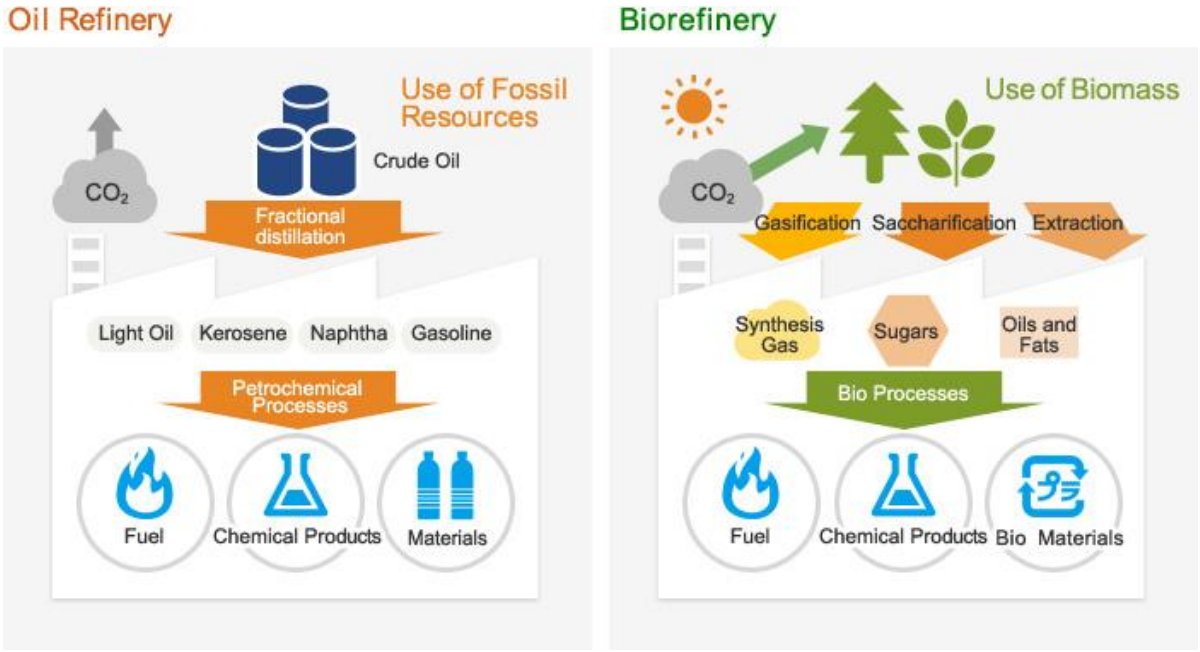

Figure 1.2: Similarities and differences between oil refinery and biorefinery (www.viaspace.com).

Biorefinery can use different raw materials such as biomass from forestry, agriculture, aquaculture, and residues from industry and households (Jong and Jungmeler, 2015). The different types of raw materials used defines different biorefineries: whole crop biorefineries, oleochemical biorefinery, lignocellulosic biorefinery, green and marine biorefineries. Marine biorefinery includes the use of photosynthetic microorganisms, such as microalgae and cyanobacteria. They have garnered enormous interest as tools to capture light energy and CO_2 to generate a variety of products, including fuels, chemicals, and materials (Rossi et al., 2015). In particular, the oxygenic photosynthesis realized by microalgae is more efficient than that of higher plant and the microalgae photosynthesis account for more than 70% of the total photosynthesis occurring on Earth (Masojídek and Torzillo, 2014). Moreover, the production of photosynthetic microorganisms does not compete with food/feed cultures for arable land because their cultivation may be carried out in area not favourable for crops culture.

1.2 Biorefinery products: valorisation of starch fraction

Nowadays, about 200,000 microalgal species are known, but less than 30 species are investigated for exploitation (Guiry, 2012). The metabolic diversity of algae and their ability to grow under different conditions of nutrition (autotrophic, heterotrophic, and mixotrophic) is the starting point for the synthesis of a huge number of products. It is expected that many functions and high-value products from algae are still unknown. Each of the metabolic processes for a single molecule production is governed by specific conditions and it can be influenced by altering the operating conditions. Moreover, some molecules production and their productivity are species

dependent. Single microalgal component may become feedstock for industrial productions and various applications have already been proposed. Some examples are:

- ***Pigments*** are widely used as natural colorants for food industry. Some of them- e.g. carotenoids - are strongly required in pharmaceutics and cosmetics for UV-protectors, anti-inflammatory and antioxidant properties (Ariede et al., 2017).
- ***Proteins*** from microalgae are widely recognised as vegetal souce of proteins for human nutrition and feed. Microalgae have traditionally been used as human food (Stengel and Walker, 2015). Today soluble proteins are proposed as food additive with high content of essential amino acids and functional properties as emulsifying activity (Schwenzfeier et al., 2011). Insoluble proteins fraction or damaged proteins resulting from the extraction of other microalgal components find application as animal feed, increasing the profit of the whole process.
- ***Lipids*** from algae are the object of many research studies and government investment for replacing traditional fossil fuel and producing biodiesel (Wijffels and Barbosa, 2010). Further interesting application of the microalglal lipid fraction are proposed: linoleic acid as substitute of rape seed, soy and sunflower fatty acids, PUFA (polyunsatured fatty acid) as food and drug additive with cardio vascular health benefit (Draaisma et al., 2013).
- ***Carbohydrates*** produced by microalgae are widely proposed as source of sugars for bacterial anaerobic digestion finalised to bioethanol and biohydrogen production (Fernandes et al., 2013; Zhu, 2015). Other applications regard the use of carbohydrates as food additive (carrageenan, alginate and agar) of chemical building block.

The cited industrial applications – and more others not cited – point out the microalgal potential to revolutionize many biotechnological processes by sequestering CO_2 and producing renewable feedstock for the industry. Nowadays, the energy costs of the microalgal biomass production (Tredici et al. 2010; Marzocchella et al. 2010) make the output confined to value-added products (sterols, PUFAs, phycobilins, chlorophyll, carotenoids) with applications as food additives, in cosmetics and health care. In this fields, many companies started to work and make profits (***Cyanotech***, ***Seambiotic***, ***Mera Pharma***, ***FujiChemical***, ***Algosource***), but the real change towards the sustainable development takes place when consumer goods are produced and commercialised. The biorefinery approach offers the solution for the realistic application of microalgal cultures in the circular bioeconomy. The current biorefinery strategies mainly valorise high value compounds, proteins for food (soluble proteins) and feed (unsoluble proteins). Lipids are still an interesting fraction for energetic applications (biodiesel). The remaining carbohydrates are suggested as feedstock for bioethanol or methane production because of the low cellulose content (Winck et al., 2013; Soh et al., 2014; Zhu and Hiltunen, 2016). The largest part of microalgal carbohydrates fraction is composed by starch. Starch polymer is widely used for food and non-food applications, which count more profit than bioethanol (0.75-3.7 vs. 0.21 €/kg). Moreover, common culture strategies used for the accumulation of lipids (such as nitrogen depletion) drastically reduce the protein content (Msanne et al., 2012) which is considered a valuable product for biorefinery. Chlorophyll content also decreases during the prolonged nitrogen depletion (Adesanya et al., 2014) and prolonged depletion reduce the high-value lipid content in favour of triacylglycerols (TAGs) (Guihé and Stengel, 2013). Then, for biorefinery application, a compromise need to be established for the exploitation of more number of components. A good compromise can be considered the early nitrogen depletion. In this phase,

carbohydrates (in particular starch) reach the maximum concentration, while proteins experience a reduction of 30-40% of the initial concentration with respect to 90% of reduction in the late nitrogen depletion (Breuer et al., 2012). Chlorophyll content follows the same story of carbohydrates (Shiratake et al., 2013). On the contrary, at the nitrogen depletion onset antioxidant pigments accumulation (carotenoids) take place (Mulders et al., 2014). The nitrogen depletion onset can be adopted for simultaneous production of proteins and starch. According to this scenario, chlorophyll and carotenoids could also be valorised.

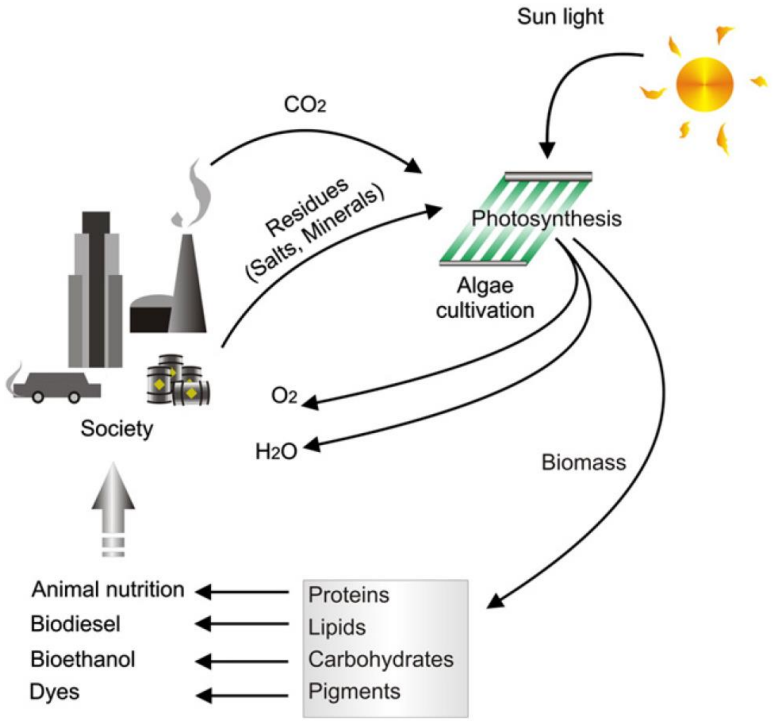

Figure 1.3: Current biorefinery scheme. Input and output streams of interest highlighted (Winck et al., 2013).

1.3 Starch applications and market

Starch is the principal storage polysaccharides produced by green plants. Starch consists of two D-glucose polymers: amylose and amylopectin. Amylose is a linear poli-structure with α-1,4-linked glucan. Amylopectin is a highly-branched molecule characterized byα-1,4-linked and α-1,6 branching links (Pérez and Bertoft, 2010). Short-branched amylopectin chains may form helical structures that may crystallize and cooperate to the formation of the granule structure (Figure 1.4). The granules also contain small amount of lipids and phosphate.

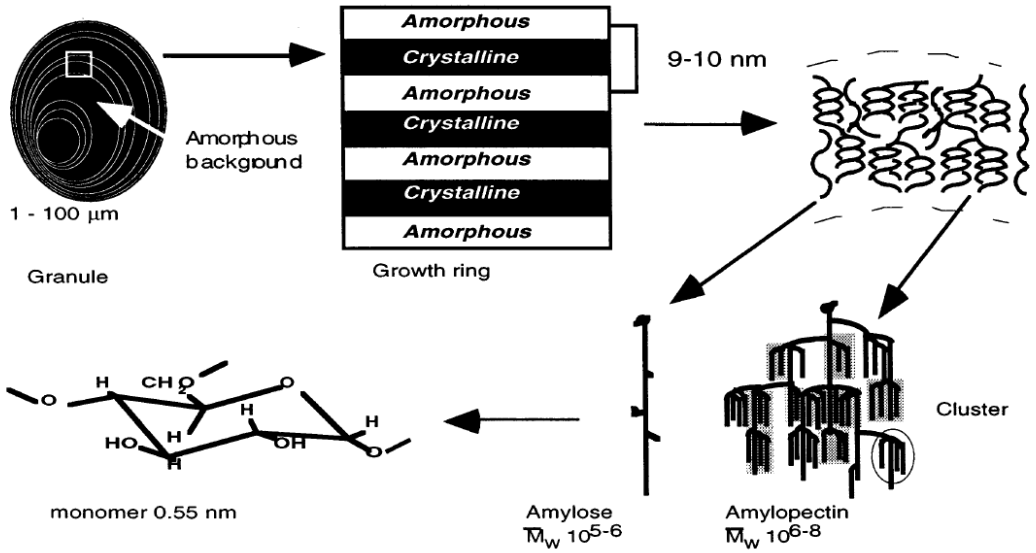

Figure 1.4: Schematic representation of the different structural level of the starch granule (Buleòn et al., 1998).

Starch find a wide spectrum of applications in food and non-food industries, apart from being a common constituent of human diet (35% of daily calories in UE and USA). The main applications are listed hereinafter and the market size of each application is showed in the Figure 1.5.

Food and beverages: starch and starch derivates (maltodextrine, glucose and cyclodextrine) are used for the formulation of sweet drinks, as flavor enhancer, and as inhibitor of sugar crystallization. It is added to frozen product to prevent dripping when defrosted, to absorb water, and to keep ingredients together. Its emulsifier properties lead its use as fat replacer in the formulation of low fat food. Native and modified starches are used also in the formulation of nutraceutical products as tablets, capsules, and baby powders (Crawshaw, 2004).

Feed: starch may be added in cattle and poultry feed. For esample, it is used as a tuning ingredient to adjust separately the energy and the protein content of the diet (Fuller, 2004).

Cosmetics and pharmaceutics: it is used as carrier and binders for fragrance and active compounds. It is an economic thickener and emulsifier for cream, lotion, make-up powder, wash products, and for capsule formulation.

Papermaking: starch aids the formation of better quality paper. It is used during the treatment of the cellulose and as wet-end additive for improving paper strength and increase fiber-to-fiber interaction.

Textiles and Laundry: starch provides maximum stiffer in the coating of fabrics for preserving them from the humidity (Schwartz et al., 2009).

Bio-plastics: film-forming properties of the starch allow its application in the production of biodegradable plastic films for food (*INSTANT PURE CATE*®), plastic bags (*MaterBi*®), and agricultural mulches.

Bio-ethanol: it can be an easy fermentable feedstock for bioethanol production (MojioviĆ et al., 2009).

Other non-food applications: starch is also known for its application in adhesive formulation and binder systems for building products (ceiling tiles, wallboard, paint and building adhesive).

The spectrum of starch non-food applications is increasing as a consequence of the expansion of green products, especially concerning biofuel and biomolecules. The global starch market is expected to increase 182 million metric tons by 2022, 14 million ton only for EU (Figure 1.5), driven by expanding use in food processing, papermaking, and pharmaceuticals. Nowadays, there is an increasing interest in chemically modified starch - to provide enhanced properties - (Filippov et al. 2015, Reddy et al. 2015) and its market size exceeded 8.9 million tons in the 2015. The key players in starch market are companies like *Tate & Lyle PLC*, *Cargill*, *Ingredion Incorporated*, *Roquette Fréres S.A.*, *BENED-Platinit GmbH*, *AGRANA Group*, *Grain Processing Corporation*.

The raw materials currently used as starch source are maize, waxy maize, potato, wheat, pea. However, the climate change and the environment parasitic contaminations strongly influence the price of the starch sources, the performances and the quality of the starch granules produced. Moreover, the increasing starch demand for non-food application open up to the competition with food crops.

Microalgae are considered novel high-efficient starch producers. Microalgal cultures do not compete with food culture for land and water and their starch granules diameter is around 1μm (Bránykiová et al., 2011). This microgranular starch is much appreciated in industrial applications because the high specific surface area gives more active site for crosslinking reaction finalized at starch modification, increases viscosity, surface adhesion, gelatinization temperature, and resistance to retrogradation. Thanks to these properties, microgranular starches are suitable for coatings, functionalization, as carrier for flavours and drugs and for bioplastic film formulation (Biliaderis et al. 1993). Other physic-chemical properties of the starch are critical for considering its industrial applications. The most important are: shape distributions, crystallinity, amylose/amylopectin ratio, thermochemical properties. For the real application of microalgal starch granules in the starch industry, a complete physic-chemical characterization is required. To our knowledge, limited informations are available in literature (Suzuki E. and Suzuki R., 2013) about physic-chemical characteristics of microalgal starch, so additional characterization is required to validate the potential applications of this starch type.

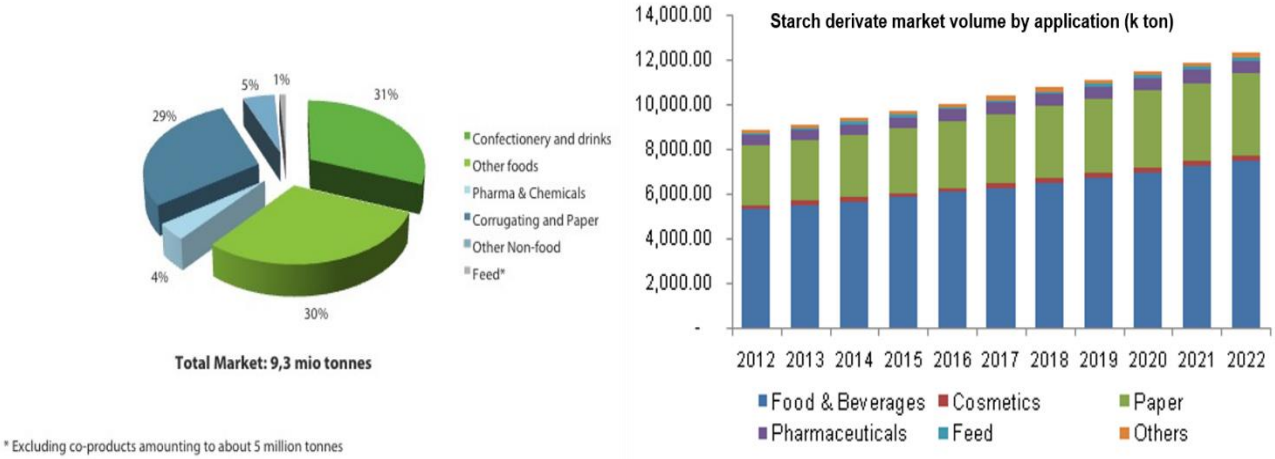

Figure 1.5: Main starch application and forecast of the increase of starch derivate market in EU up to 2022 (Global Industry Report, 2016).

1.4 Microalgae for protein supply

Proteins are significant constituent of plants and animals, and they are the only source of essential amino acids for humans and animals. The increase of world population implicates the necessity of a durable and sustainable source of proteins. The figure 1.6 shows the increase of the world demand of proteins from 1961 to 2010 and the projection for the next years forecast a demand of 300 million tonnes/year. The application of vegetal proteins in the food industry is currently limited because of the lower nutritional value with respect to the animal proteins, but the lower price and the higher availability are pointing the interests towards vegetal sources. Moreover, there is an increasing attention to the quality of the food and the general opinion is the limitation in the use of animal proteins for healthy and ideological reasons (Tilman and Clark, 2014). Innova Market Insights (www.newfoodmagazine.com/innova-market-insights) reported an increase of 24% in the use of plant proteins from 2013 to 2014. The current sources of vegetal proteins are maize, rice, wheat, potato and soy bean. Vegetal proteins are mainly used in feed, food and concentrates (food supplements) and they are hardly ever used for bio-based technical applications (adhesive, coating, surfactants, plastics). However, soil resources for plant growth are also limited and a huge interest is now pointed towards aquatic biomass such as duckweed, macroalgae and microalgae. In particular, microalgae are characterized by the higher proteins content: 30-60% of the dry weight with respect to 4-40% of macroagae and duckweed.

The high extraction costs and relative low protein content and quality still limit the use of the new vegetal sources of proteins. Threfore, the most sustainable proteins supply chains consider the valorisation of protein rich side stream such as: ethanol production, starch extraction, oil extraction. This biorefinery approach - the co-exploitation of different marketable products - offers the opportunity of a competitive business and a sustainable biomass use of microalgae in the circular bioeconomy. Similar approaches are already used for soy beans and wheat flour in order to obtain oil, sugars, and proteins from the first and starch and gluten form the second one (Bikker et al., 2016). Equivalent cascade extraction is proposed for new protein sources such as microalgae but the research is still exploring efficient and sustainable processes.

For food applications, the quality of proteins and their functional properties are the most important parameters to validate the applicability of a protein-containing source. The quality of the proteins is expressed as amino acidic profile, digestibility, availability and allergens content. The presence of essential amino acids and the good digestibility of microalgal proteins was already proved (Becker, 2007; Skrede et al., 2011; Tibbetts et al. 2017) and recent studies are now focused on functional properties required by food industries. The functional properties include the solubility, binding capacity, gel-forming ability, emulsifying and foaming activity.

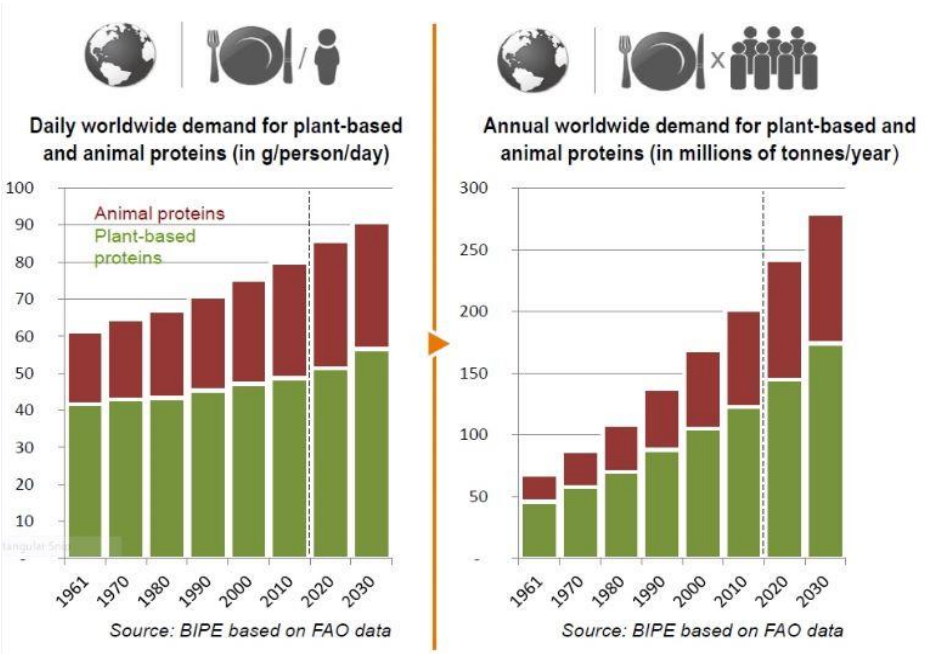

Figure 1.6: Increase of plant and animal based proteins demand (http://www.foodnavigator.com/Market-Trends/Changing-diets-Plant-protein-sustainability-crucial-for-food-security).

1.5 Current issues of microalgal biorefienery

The innovation related to the biorefinery approach to microalgal biomass and the aptitude of the microalgal components to become feedstock for many industrial fields, lead the penetration of microalgal production in the developing “green” market. Moreover, the maximum number of products output increases the profit from a single raw material (Chew et al., 2017). The possibility of exploitate multiple products from the biomass and microalgal biomass was first proposed in the 1993 by Wyman and Goodman. However, the environmental consciousness and the expected reduction of the raw material resources have induced the increase of the research effort in the microalgal refinery. At present, the microalgal biorefinery scheme still displays some critical points to be optimized. The main stages of microalgal biorefinery still present some bottleneck limiting their fulfilment: they are identified in upstream processes, culture systems and downstream processes. The bottleneck is highlighted in the *Cellana* biorefinery model, Figure 1.7.

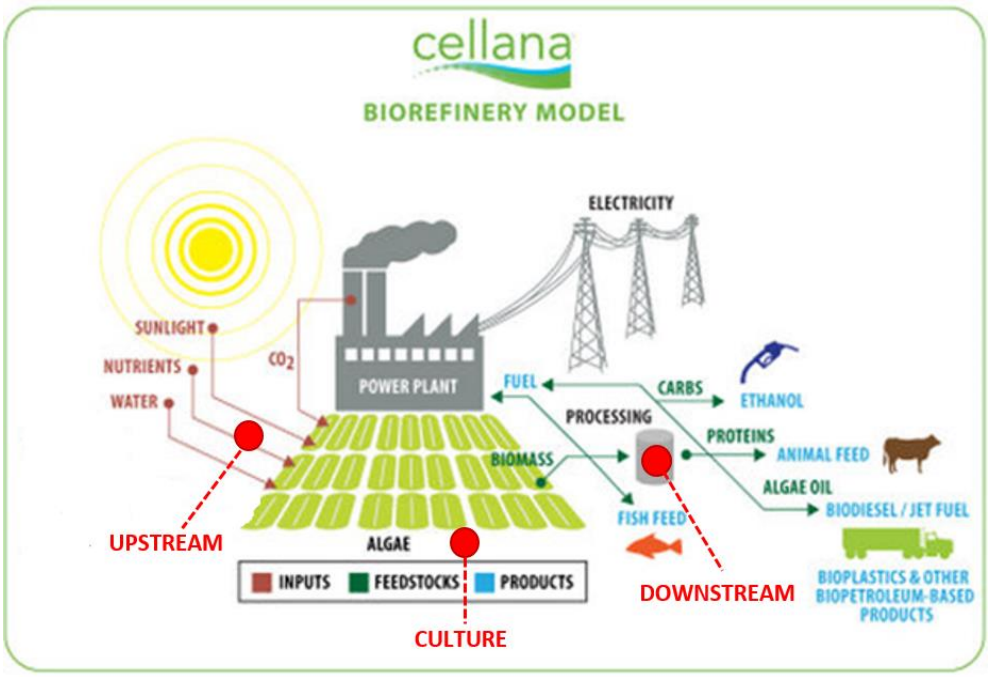

Figure 1.7: Bottleneck of the microalgal biorefinery are in upstream processes, culture system and downstream processes (modified scheme from *Cellana Inc.*).

Selection of a robust strain for industrial application

Upstream processes involve the selection of the microalgal strain, the supply of carbon dioxide (CO_2), and nutrient source such as nitrogen and phosphorus, and source of illumination (Vanthoor-Koopmans et al., 2013). The supply of CO_2 and illumination source are mainly determined by economic and logistic reasons. The main goal of the microalgal refinery is the production of biomass from sunlight energy and CO_2 from industrial exhausted gas stream. The concentration of the CO_2 in the exhausted gas stream generally does not match the optimal condition for microalgal biomass production and this value is often strain dependent (Rossi et al., 2015). Then the optimal CO_2 concentration should be set as a function of the selected strain and the dilution of the gas stream with air could be applied. The supply of nitrogen and phosphorus are depending on the selected strain and the main target products. Indeed, the single nutrient concentration affects the metabolic balances in favour of a molecule instead of another (Arora et al., 2015). The issue remains the selection of the strain for microalgal biorefinery.

The main quality required to a strain is the robustness. To limit the production costs, the microalgal growth should not be carried out in completely aseptic systems. Threfore, the selected microalgal strain should be able to grow in non-aseptic conditions and competitive operating conditions should be selected to overwhelm bacterial and parasitic contaminations.

The most cultured species were: *Chlorella*, *Scenedesmus*, *Nannochloropsis*, *Spirulina*, *Tetraselmis*, *Dunaliella*. Clearly, the selection of the strain is based on the ability to produce the main target molecule, although for biorefinery applications and large consuming products, a versatile strain able to produce different molecules is preferred.

Culture strategy and nutrient supply

Nutrient supply is the most used strategy for customizing the microalgal biochemical composition in favour of a target molecules accumulation. Nitrogen

depletion normally cause a reduction in the protein content of microalgae and an increase in carbohydrates and lipids content (Fernandes et al., 2013). In some species, N depletion is a trigger of lipid accumulation, in other species the starch is the mayor storage molecule during the depletion. Moreover, it has been reported that the prolonged N-depletion causes the conversion of carbon sources in lipids instead of starch (Msanne et al., 2012). The chlorophyll content also reduces by the N depletion. However, commercially interesting pigments (carotenoids, astaxantin, lutein) are accumulated in this phase too (Adesanya et al., 2014; Mulders et al., 2014). As regard high value lipids (e.g. polyunsatured fatty acids, PUFAs), they are generally accumulated in the onset of the nitrogen depletion, while the major lipids content became TAGs during the late depletion. The same effect is produced by the light intensity: high light intensity improves the cell growth and the protein synthesis, as well the concentration of antioxidant and secondary pigments, and it reduces the chlorophyll content (Ferreira and Sant'Anna, 2017).

The effect of the nutrient supply is specie-specific. Therefore, when the goal is the microalgae biorefinery, it is necessary to select a compromise for the accumulation of the higher number of exploitable products for a cost-effective process and the strategy have to be designed on the selected microalgal strain. As regard the production of large market products by robust microalgal strains, interesting solutions are offered by the co-exploitation of carbohydrates and proteins. Carbohydrates accumulation is enhanced in the early nitrogen depletion and, in this condition, protein content is still high.

Intensification of microalgal biomass production

The culture system used for the microalgal growth are generally classified in open systems (open ponds, thin layer cascade) and closed systems (photobioreactors, PBRs). Both systems count on a wide spectrum of technological solutions with benefit and limitations (Carvalho et al., 2011). The global microalgal productivity largely exceeds the crops cultures (40-80 ton/year). The photosynthetic efficiency reached in vertical photobioreactor was about 1.3 g $mol_{photons}^{-1}$ close to the theoretical maximum of 1.8 $mol_{photons}^{-1}$ (Barbosa and Wijiffles, 2013). The areal productivity remarkably depends on the photobioreactor design and operating conditions: results reported in the literature ranges between 10 and 33 g m^{-2} d^{-1} (Richmond, 2013). However, the investment costs due of the industrial plants and the relatively low biomass concentration achieved make the closed systems not competitive at the industrial scale. The current research efforts are directed to the intensification of the microalgal culture for obtaining high concentrated culture, which can reduce the harvesting costs. In this optic, the key parameter to optimize is the conversion of light energy into biomass. The limitation to the maximum exploitation of the light received by the photosynthetic system is due to the establishment of a dark zone along the optical path of the culture system as the microalgal concentration increases. In the dark zone, the light availability is reduced or absent due to the shadowing effect of the cells, then the photosynthesis and the biomass production are reduced in this zone (Cuaresma et al., 2009; Sforza et al., 2014). Janssen et al. (2016) calculated that, reducing the optical path to values equal or lower than 0.01 m it is possible to increase the photosynthetic efficiency of 5-8%. Then, the efforts of many research groups are directed to the development of reduced optical path culture systems for maximize the microalgal biomass concentration and productivity (Pruvost et al., 2017; Doucha et al., 2008; Qiang and Richmond, 1996).

Recovery and separation of different microalgal products

The downstream processes are all the unit processes that occur after the micrroalgal cultivation. They include the concentration of the microalgal culture (harvesting), the extraction (cells disruption and/or product release) and the purification (solvent based, supercritical CO_2, membrane filtration). The integration of microalgal harvesting, extraction methods, and separation techniques requires the integration of multiple steps (Lopes et al., 2014). The downstream processes should be directed toward the use of mild separation technologies to recovery the desired compounds without damaging other fractions (Vanthoor-Koopmans et al., 2013) because the industrial success of the microalgal products is stringly related to their functionality. Currently, the separation of the different fractions is considered the main bottleneck of the microalgal biorefinery (Chew et al., 2017) and the attention payed to this point is still insufficient. Just 72 articles on *Scopus* search could be found on the topic of multiple product separation in microalgal biorefinery. Moreover, the recovery studies are mainly focused on a single target product and propose potential solution to valorise the residual fraction. Pireto et al. (2017), Lupatini et al. (2016), Zhu and Hiltunen (2016) proposed the valorisation of the defatted biomass obtained after lipids extraction. Pireto et al. (2017) proposed the fermentation of the residual oil cake for microabial poly-hydroxybutyrate and the use of the digestate for heat and fertilizer generation. Lupatini et al. (2016) simulate the possibility to optimize ultrasonication in alkaline conditions of the defatted biomass to extract proteins and obtain carbohydrates in the residual fraction. Gilbert-lòpez et al. (2017) suggest a more complete cascade-recovery process. It consists in three extractions: supercritical CO_2 extraction for triglycerides recovery, gas expanded liquid extraction (supercritical CO_2 supplemented with ethanol) for the recovery of a fraction enriched in luteins and β-carotene, pressurized water extraction for the recovery of soluble proteins and sugars. In this case, the yield of proteins and sugars in the third extract was very low, most remained in the residue. Probably, it was due to the lipids and pigments extraction, which can denaturise the proteins. The denaturation causes aggregations and loss in the solubility. Indeed, Ansari at al. (2017) have analysed several scenarios of sequential product recovery and they have concluded that the sequence protein-lipid-carbohydrates allowed the optimum recovery of individual metabolites. In fact, if high value compounds (such as antioxidants and pigments) are not damaged by aqueous proteins extraction: the proteins can precede the high value compounds recovery. Moreover, the lipid extraction should consider non-invasive and sustainable techniques in order to recover the polysaccharides (starch) from the residue fraction. The subject of the sequential extraction of the different microalgal products is still in its infancy, and further studies are required to reach an optimized strategy. However, different strategies should be designed on the basis of the microalgal strain selected and its main product.

2. AIM OF THE THESIS

The present Ph.D project was aimed at the valorisation of microalgal starch production as parte of a biorefinery scheme. The main interest is to propose a new approach to implement the sustainable production of building blocks for materials and chemicals required by the modern industry. The proposed approach includes the exploitation of non-valorised microalgal component (such as starch), the intensification of the microalgal biomass production through the design of new performing photobioreactors and the application of mild and "green" downstream technologies for the recovery of the different microalgal products.

The multidisciplinary subject characterizing the proposed project required the collaboration of experts operating in different scientific fields. Indeed, the research activities were carried out at the Dipartimento di Ingegneria Chimica, dei Materiale e della Produzione Industriale, at the Dipartimento di Biologia, and at the Dipartimento di Scienze Chimiche of the Università degli Studi di Napoli 'Federico II'. Some activities were carried out at the Laboratoire de Génie des Procédés environnement agro-alimentaire of the University of Nantes (France).

The research activities are presented in four sections explained hereinafter and illustrated in the Figure 2.1.

The selection of a robust microalgal strain for starch production in the biorefinery scheme.

This task was aimed to select a robust microalgal strain for industrial production of the biomass for biorefinery application. The selection was based on the biomass and starch productivity. Two fresh water algae, *Chlorella sorokiniana* and *Scenedesmus vacuolatus*, and two seawater algae, *Dunaliella tertiolecta* and *Tetraselmis chuii*, were investigated. *C. sorokiniana* was selected as the most promising strain. The effect of nitrogen and CO_2 concentration on the biomass and starch productivity was investigated for the selected strain. A complete biochemical characterization of the microalgal biomass was also carried out during the different growth phases in order to quantify all the exploitable molecules produced by the selected strain and to asses its potential for biorefinery applications.

Physic-chemical characterization of the microalgal starch for industrial applications.

The goal of this task was to charactrerize the microalgal starch granules with respect to physic and chemical features required for industrial applications. The characterization was a preliminary study made in collaboration with a research group of the Dipartimento di Scienze Chimiche.

Intensification of the microalgal biomass production by photobioreactor design innovation.

The increase in the microalgal biomass production and productivity is nowadays one of the critical issue for the process optimization. A new designed ultra-thin flat photobioreactor was designed, built up and operated. Performances were assessed for cultures of the strain selected in the previous task. The effect of the light intensity on the growth and on the biochemical composition of the microalga *C. sorokiniana* was also investigated.

Study of mild and sustainable downstream processes for the recovery of starch and other bioproducts form microalgae.

The downstream processes continue to be the less explored field of the microalgal biorefinery. The activity carried out in the present PhD thesis is part of a program aiming at the complete exploitation of the different microalgal components. The

simultaneous recovery of starch and antioxidants was carried out in cooperation with Dott. Ganna Petruk, Biotechnology PhD student at the Università degli Studi di Napoli Federico II. The recovery of starch and proteins from microalgae was carried out at the Laboratoire de Génie des Procédés environnement agro-alimentaire, Nantes University. The latter regarded mechanic disruption of the microalgal cells and the influence of the disruption parameters on the product recovery. A consolidated model describing the disruption process was successfully applied to the product recovery. A preliminary study was carried out about the possibility of integrating mechanical disruption, centrifugation and membrane separation of the supernatant for the simultaneous recovery of starch and proteins from microalgal biomass.

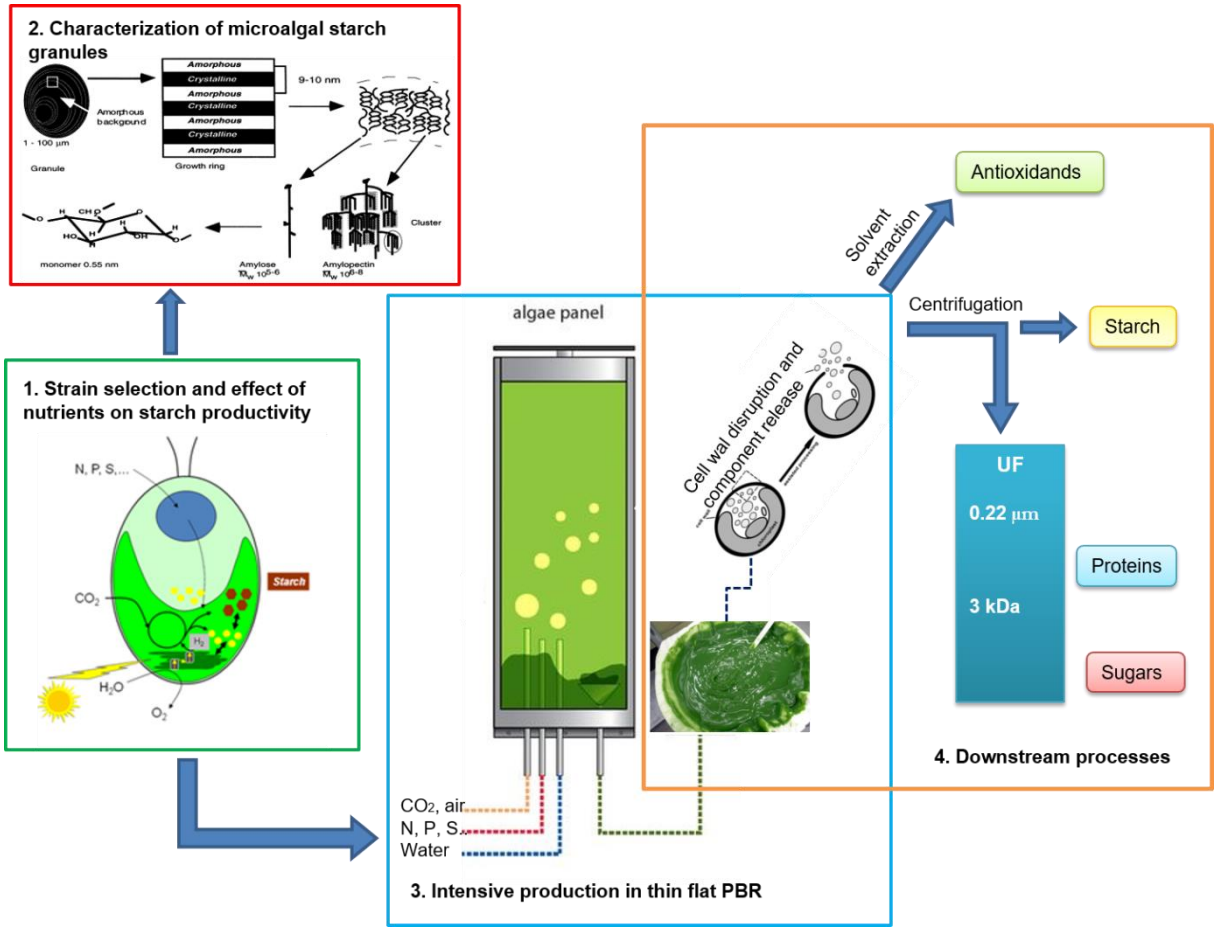

Figure 2.1: Schematic representation of the Ph.D aims.

3. SELECTION OF A ROBUST STRAIN FOR STARCH PRODUCTION

The selection of a robust microalgal strain able to accumulate starch and produce other molecules of interest was the first action of the PhD program. Two fresh water microalgae, *Chlorella sorokiniana* and *Scenedesmus vacuolatus*, and two seawater microalgae, *Dunaliella tertiolecta* and *Tetraselmis chuii* - used for industrial production - were investigated. The selection was based on the microalgal starch fraction and starch productivity. Indicators taken into account for the strain selection were: biomass nitrogen content during nitrogen depletion; yield of biomass with respect to the light provided; biomass productivity; starch fraction of the biomass. *C. sorokiniana* was selected as the most promising strain. The effect of the main nutrient concentration on the selected strain (*C. sorokiniana*) was investigated. In particular, several tests were carried out to assess the effect of nitrogen and CO_2 concentration on starch fraction and starch productivity of *C. sorokiniana*. The biochemical composition, in terms of proteins, starch, lipids and total sugars, was investigated at the different growth phases.

3.1 Identification of an industrial microalgal strain for starch production in biorefinery context: the effect of nitrogen and carbon concentration on starch accumulation.

I. Gifuni[1*], G. Olivieri[1], A. Pollio[2], A. Marzocchella[1]

[1]Dipartimento di Ingegneria Chimica, dei Materiali e della Produzione Industriale, Università degli Studi di Napoli Federico II, Piazzale Tecchio 80, 80125 Napoli, Italy
[2]Dipartimento di Biologia, Università degli Studi di Napoli Federico II, Via Cinthia, 80125 Napoli, Italy

Abstract

The recent trends in microalgal cultures are focused on the biorefinery of the biomass components. Some of them are not completely valorised, for example starch. Since there is a wide market for starch products in food and non-food industries, the exploitation of microalgal starch fractions could improve the economic sustainability of microalgae production. In this perspective, the optimization of nitrogen and carbon source uptake for starch accumulation is a critical point for reducing the nitrogen requirement footprint and to increase CO_2 capture. In this study, four robust microalgal strains, already known as starch-accumulating strain, were investigated: *Chlorella sorokiniana*, *Scenedesmus vacuolatus*, *Dunaliella tertiolecta*, and *Tetraselmis chuii. C. sorokiniana* was selected as the best starch producer in the biorefinery context, and the role nitrogen and CO_2 concentration had on the starch production was investigated. For light irradiance of 300 µmol $m^{-2}s^{-1}$ the optimal nitrogen concentration for growth and starch accumulation resulted 32 mg L^{-1}. The CO_2 concentration clearly does not influence the starch accumulation, but concentrations distant from 2% negatively influence microalgal growth, affecting the final starch productivity. The biomass composition during the batch growth of *C. sorokiniana* was also analysed in order to explicitly characterise the dynamic of starch accumulation during the different growth phases. Protein content decreased during N-depletion, carbohydrates were mainly produced during the early N-depletion, followed by the accumulation of lipids in the late depletion.

Highlights

- *C. sorokiniana* was selected as robust strain for starch production in biorefinery context.
- The effect of NO_3 and CO_2 concentration fed was investigated.
- The dynamic of biomolecules accumulation during the growth was analysed.
- An optimal harvesting time was proposed for starch recovery and biorefinery applications.

Keywords

microalgae; biorefinery; starch; nitrate demand; CO_2 supply

Introduction

The current increase in the demand for goods and awareness of environmental issues, calls for new and sustainable industrial production approaches. Microalgal cultures have been extensively investigated in recent years as a resource for the sustainable production of feed, food, and biofuels (Mata et al., 2014; Olivieri et al., 2013; Draaisma et al., 2013). However, the exploitation of a single microalgal component is not cost-effective. Indeed, the current trend is to exploit microalgae within the biorefinery concept, where all biomass components are valorised. Currently the biorefinery strategies mainly valorise proteins for food and feed; lipids for biodiesel, food or cosmetic additives; pigments as sources for natural dyes and antioxidants; the carbohydrates as feedstock for bioethanol productions (Soh et al., 2014; Zhu and Hiltunen, 2016). Improvements in microalgal exploitation are required in order to make the process competitive. This study proposes the valorisation of starch (carbohydrates part) directly as feedstock for food and non-food industries (Copeland et al., 2009; Pérez-Pacheco et al., 2014).

This purpose for the starch allows for a higher profit than that coming from the use of the entire carbohydrates fraction as feedstock for bioethanol production: 0.75-3.7 €/kg for food and non-food products vs. 0.21 €/kg for ethanol (Penloglou et al., 2016; Cheali et al., 2015). Furthermore, the use of starch for food and non-food applications typically only requires mechanical extraction without any fermentation step, as is required for the bioethanol production. In fact, the global starch market is projected to exceed 150 million metric tons by 2020 (Global Industry Analysts, Inc, 2014), especially due to the increase in demand for non-food production. Current starch production by microalgal cultures can provide a solution to prevent competition between food and non-food starch cultures: microalgae do not compete for arable lands and freshwater. Gifuni et al. (2017) have already reported on the starch production by non-conventional *Chlamydomonas* strains. However, strains characterised by a high starch accumulation and robustness are required to support large scale industrial production and biorefinery applications. In general, *Chlorophycae* species are already reported to be good starch accumulators (Mizuno et al., 2013; Ho et al., 2013; Wang et al., 2013; Kim et al., 2015; Li et al., 2015; Yao et al., 2013), but a real comparison among robust microalgal strains under the same culture conditions (PBR geometry, light and nutrient input) is missing in the literature.

Moreover, much research has reported that starch accumulation is enhanced during nitrogen depletion (Msanne et al., 2012; Wase et al., 2014; De Farias Silva et al., 2016; Arora et al., 2015). Since nitrogen is also an important nutrient required for food culture and is mainly produced by fossil fuels, nitrogen depletion is not only highly regarded for rich carbon product accumulation, but also for reducing the nutrient consumption (Chen et al., 2013). Nevertheless, a clear indication of the minimum nitrogen concentration required for growth and starch production, related to the specific strain and culture conditions, is not reported in the literature.

The increase of carbon source concentration is also reported to enhance carbohydrate accumulation (De Farias Silva et al., 2016), but the resulting effect on the pH of the media can generate stressful conditions responsible for the reduced carbohydrate content (De Farias Silva et al., 2017). The response to CO_2 concentration is always strain dependent, and a clear identification of the effect on starch accumulation is required for a large-scale application projecting to use exhaust gas from industrial plants (Rossi et al., 2015). The aim of this paper is to: 1) identify a robust microalgal strain for starch production in the biorefinery context; 2) the identification of the N and CO_2 concentration which provides the best performances in starch productivity and the lowest nutrient and energy consumption; and 3) the identification of the growth phase where the biomass composition is the most promising for biorefinery usage. For this purpose, two freshwater microalgae, *Chlorella sorokiniana* and *Scenedesmus vacuolatus*, and two seawater microalgae, *Dunaliella tertiolecta* and *Tetraselmis chuii*, extensively recognised as starch producers and which are all favourable for large scale usage, were compared for starch and biomass production. The effects on the concentration of key nutrients (nitrogen source, inorganic carbon source) on growth and starch accumulation were investigated. Attention was also given to characterise the dynamic of the biochemical composition of the selected strain for biorefinery applications.

Materials and methods

Strains and medium

Four strains were selected from the ACUF collection (www.acuf.net): *Chlorella sorokiniana* Shihiraet Krauss strain ACUF 318; *Dunaliella tertiolecta* Butcher strain ACUF 333; *Tetraselmis chuii* Butcher strain ACUF 593; *Scenedesmus vacuolatus* Shihiraet Krauss, strain ACUF 35. *C. sorokiniana* and *S. vacuolatus* are fresh-water microalgae. The inorganic medium for their growth was Bold Basal Medium (BBM) and this was sterilised by autoclave for 20 minutes. *D. tertiolecta* and *T. chuii* are seawater microalgae. The medium for their growth was the Enriched Sea Water Medium (Bold and Wynne, 1978). The natural seawater was provided by the Stazione Zoologica Anton Dohrn of Naples. The medium –natural seawater supplemented with nutrients - was sterilised by microfiltration (0.22 µm).

Both BBM and Enriched Sea Water medium contained $NaNO_3$ as nitrogen sources. The standard concentration of the nitrate was 0.25 g L^{-1}.

Apparatus

The growth was carried out in inclined square bubble column photobioreactors (height 0.27 m, length 0.11 m, thickness 0.08 m) characterised by 1.5 L working volume (Olivieri et al., 2013). The aeration/mixing of cultures was provided by feeding air supplemented with CO_2 at the bottom of the photobioreactors. The photobioreactors were housed in a climate chamber (*Heraeus Vötsch GmbH; type: HPS 500*) equipped with white fluorescent tubes (*M2M engineering*) located along the ceiling-chamber. A gas mixer (*Bronkhorst, model: El-flow Select Series)* provided the gas stream at the pre-set CO_2 concentration. A hydrophobic filter (0.2 µm) sterilised the gas flow stream fed to the photobioreactors.

Operating conditions

The temperature in the climate chamber was set at 25±1 °C. The irradiance was 300 µmol m^{-2} s^{-1} 24/24h. The irradiance value was chosen as it corresponded to the average yearly conditions, during outdoor production, in Europe (Pruvost et al., 2012). The volumetric gas flow rate was set at 0.2vvm.

The $NaNO_3$ concentration was set at ½, 1, 2 and 4-fold the standard concentration (0.25 g L^{-1}) to investigate the effect of the initial N-content on starch accumulation. At the selected $NaNO_3$ concentration, the N content of the mediums was 20, 30, 60 and 120 mgL^{-1}.

The CO_2 concentration in the gas stream fed to the photobioreactors depended on the tests' objective. The tests aimed at screening strains and at initial N-concentration effect, were carried out setting the CO_2 at 2% in the gas stream. The tests aimed at the investigation of the effect of the CO_2 concentration on starch accumulation were carried out setting the CO_2 at 0.04% (air), 0.5%, 5%, and 10%.

Analysis and assays

The microalgal concentration was measured as optical density (OD) by a spectrophotometer (*Specord 50 – Analytik Jena*) at 750 nm wavelength. The relationship between the optical density and the biomass dry weight was assessed for the different strains and the different growth phases (exponential, early N-depletion, late N-depletion phase).

Nitrogen concentration in the medium was measured as nitrate, by the spectrophotometric method reported by Collos et al. (1999). The sample of medium was diluted, 10 µL of HCl 0.1 M were added in order to eliminate carbonate interferences and the absorbance was measured at 220 nm. The absorbance of the sample was converted in NO3 concnetration by appropriate calibration curve with $NaNO_3$.

The concentration of the nitrogen released in the medium as proteins, N_P, was measured spectrophotometrically as absorbance at 280 nm. It should be noted that the N_P measured in all tests was lower than 1mg L^{-1}, therefore, the nitrogen related to the secreted proteins was considered negligible. It was believed that the consumed nitrogen was completely converted into biomass.

The pH of media was measured daily by pHmeter (*Mettler Toledo)*.

Microalgal biomass was characterised in terms of lipids, proteins and carbohydrates content.

Lipid concentration*.* Lipids were extracted according to the protocol proposed by Breuer et al. (2013). 20 mg of dried biomass were suspended in 1 mL of methanol and disrupted by means of bead beater (2500 rpm for 3 cycles of 4 min alternated with 1 min break in ice) equipped with 0.5 mm glass beads. The disruption was followed by methanol/chloroforform extraction (3:1). The chloroform extract was dried at 100°C for 1 hour and the lipid mass was measured gravimetrically.

Protein concentration*.* Proteins were assayed by means of the BCA Protein Assay Kit (*Thermo Scientifi*c). 10mg of biomass dried pellet were suspended in 1mL of lysis buffer (60mM Tris, 2% SDS) and mechanically disrupted by means of bead beater (2500 rpm for 3 cycles of 4 min alternated with 1 min break in ice) equipped with 0.5 mm glass beads. The samples were incubated at 100°C for 30 min to extract the membrane proteins, then they were centrifuged at 2000 rpm for 10 min. The supernatant was assayed by means of the BCA Kit.

Carbohydrate composition. Carbohydrates were characterised in terms of total sugars and starch content. *Total sugar* concentration was measured by means of a spectrophotometric method based on that proposed by Anthrone - described in Chen and Vaidyanathan (2013) – and modified in the present research. The cell disruption was carried out according to the procedure described for the protein assay. Then, the Anthrone method was used as colorimetric method for sugar concentration assessment. *Starch fraction*: the concentration of microalgal starch (ω_{Starch}, the starch weight fraction on the dry biomass) was assayed by using Total

Starch kit by Megazyme (*Wicklow, Ireland*). The manufacture's protocol for the starch assay was modified as follows: the amount of sample was set at 10 mg, the microalgal samples and the cell disruption was carried out according to the procedure described for the protein assay. Then, the free sugars and the pigments were removed by ethanol extraction at 80°C. After centrifugation the enzymatic digestion and the quantification of the starch recovered in the pellet, was carried out following the manufacture's protocol.

The composition assays were performed in triplicates.

Procedure and data processing

The light yield ($Y_{X/E}$, g $mol_{photons}^{-1}$) was defined as the ratio of the produced biomass and the light energy irradiated over the cultivation time. Thus:

$$Y_{X/E} = \frac{(X - X_0) \cdot V}{A \cdot I \cdot t} \qquad (3.1)$$

where the produced biomass is the product of the culture volume (V, L) and the biomass concentration produced ($X - X_0$, g L^{-1}) during the culture time (t, s). The irradiated energy is the product of the irradiated surface (A, m^{-2}), the irradiance (I, µmol m^{-2} s^{-1}) and of the culture time.

The biomass nitrogen yield ($Y_{X/N}$, g g^{-1}) was defined as the ratio between the maximum produced biomass (($X_{max} - X_0$) ·V, g) and the nitrogen consumed ($N_0 \cdot V$, g):

$$Y_{X/N} = \frac{X_{max} - X_0}{N_0} \cdot \left[\frac{V}{V}\right] \qquad (3.2)$$

where X_{max} is the maximum biomass concentration, and X_0 is the initial biomass concentration.

The biomass nitrogen concentration (φ_N) was defined (Eq. 3.3) as the ratio between the nitrogen fixed by the cells and the produced dry biomass. The nitrogen fixed by the cells was assessed as the product of V and the difference between the initial nitrogen concentration (N_0 , g L^{-1}) and concentration of nitrogen released in the medium as protein (N_P, g L^{-1}). The φ_N was:

$$\varphi_N = \frac{N_0 - N_p}{X - X_0} \cdot \left[\frac{V}{V}\right] \qquad (3.3)$$

The biomass productivity (P_X, kg m^{-3} day^{-1}) was assessed as the ratio between the biomass concentration at the instant t_{smax} at which ω_{Starch} is maximum (X_{tsmax}, g L^{-1}) and the culture time ($t_{smax} - t_0$, day):

$$P_x = \frac{X_{tsmax}}{t_{smax} - t_0} \qquad (3.4)$$

where t_0 is the beginning of the culture.

Starch productivity (P_{starch}, kg m^{-3} day^{-1}) was assessed as the ratio between the maximum starch concentration and the culture time at which the ω_{Starch} is maximum. Starch concentration was calculated as the product between biomass starch content ω_{Starch} and biomass concentration (X, g L^{-1}), calculated at the instant at which the starch content reached the maximum level (t_{smax}, day):

$$P_{starch} = \frac{\omega_{Starch}(t_{smax}) \cdot X(t_{smax})}{t_{smax}} \qquad (3.5)$$

The specific time of N depletion (t_N , day g^{-1}) was calculated as the ratio between the culture time required for the nitrogen starvation (t_d, day) and the initial amount of nitrogen present in the broth:

$$t_N = \frac{t_d}{N_0 \cdot V} \qquad (3.6)$$

Results

Batch tests were carried out in the inclined square bubble column photobioreactors at 25°C and irradiated 24/24 h at 300 µmol m^{-2} s^{-1} (yearly-averaged experimented irradiance in outdoor conditions). The cultures were sparged with CO_2-supplemented air stream at the flow rate of 0.2 vvm. The performances of two fresh water and two seawater strains were investigated in terms of growth, nitrogen uptake, light conversion into biomass and starch production. Figure 3.1 reports the time resolved data of biomass concentration (X), medium nitrogen concentration (N), and starch biomass fraction (ω_{Starch}) for the investigated strains. The biomass concentration increased continuously with time and approached a constant value: the biomass growth rate and the ultimate biomass concentration depended on the strain. *C. sorokiniana* and *S. vacuolatus* were characterised by a high biomass production (at culture time of 12 days), 2.8 and 2.2 g L^{-1}, respectively. *D. tertiolecta* and *T. chuii* were characterised by a low biomass production, 1.2 and 1.5 gL^{-1}, respectively. The starch fraction (ω_{Starch}) vs. time was characterised by a maximum during the second day of nitrogen depletion for *C. sorokiniana*, *T. chuii*, and *S. vacuolatus*, while it reached a maximum during the stationary phase for *D. tertiolecta* (Figure 3.1 b).

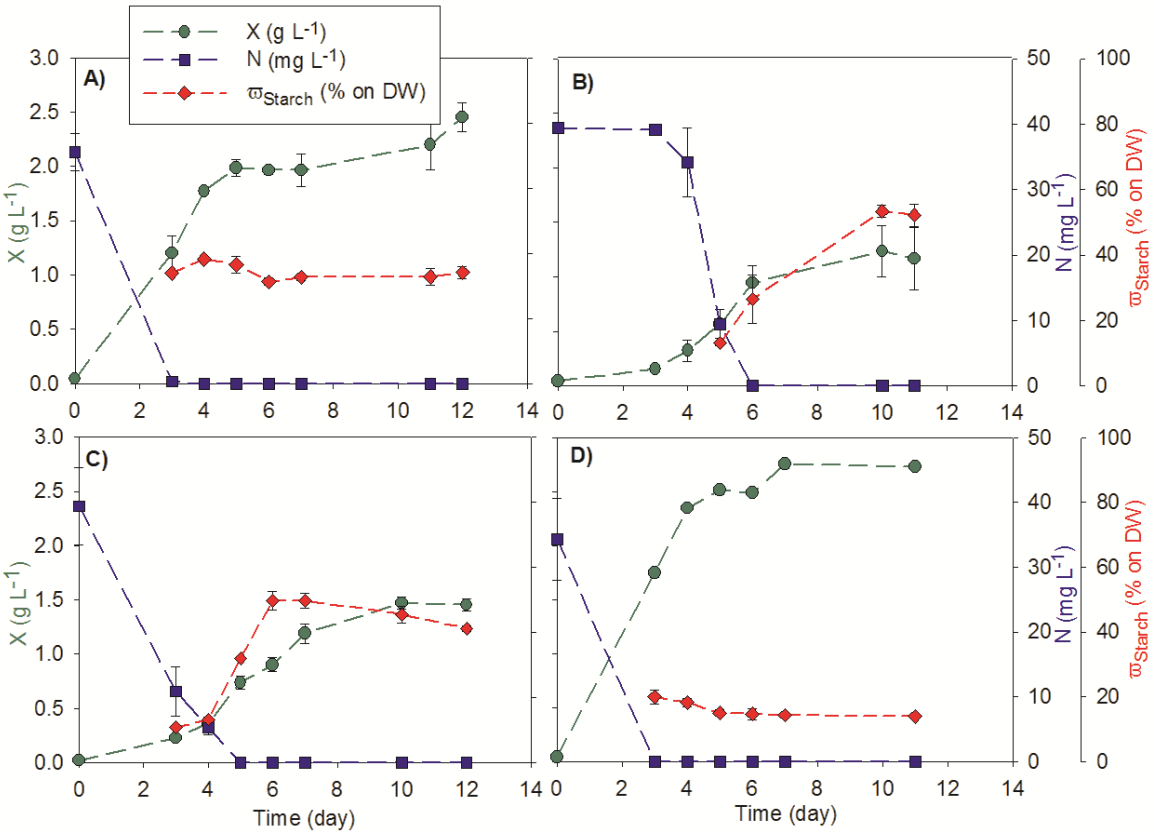

Figure 3.1: Time resolved data - concentration of biomass (X) and of nitrate (N), microalgal starch fraction (ω_{Starch}) - measured during the fermentation tests of: A) *C. sorokiniana*; B) *D. tertiolecta*; C) *T. chuii*; D) *S. vacuolatus*.

Figure 3.2 reports the light energy conversion into biomass ($Y_{X/E}$), the biomass nitrogen content under initial nitrogen starvation (φ_N), the starch productivity (P_{Starch}), and the biomass productivity (P_X). The highest measured light yield was 1.2

$g_X/mol_{photons}$ for *S. vacuolatus,* whereas for *C. sorokiniana it was* 0.9 g_X $mol_{photons}^{-1}$, while it drastically decreased for *D. tertiolecta* and *T. chuii* (0.3 g_X $mol_{photons}^{-1}$).

The starch accumulation was maximum (53% on microalgal dry weight) for *D. tertiolecta* and the starch productivity was maximum (0.17 kg $m^{-3}day^{-1}$) for *C. sorokiniana*. The higher productivity of *C. sorokiniana* with respect to *D. tertiolecta* was due to the higher biomass productivity measured for the former strain. The role of combined effects of starch content and biomass productivity is still more evident when data of *S. vacuolatus* is analysed: the highest biomass productivity (0.586 kg $m^{-3}day^{-1}$) did not entail a high starch productivity because the starch content was quite low (22% on DW).

C. sorokiniana was selected as the most promising starch producer in the biorefinery context as it demonstrated a high growth rate and starch productivity. Furthermore, the role of the initial nitrogen concentration on the biomass and starch production was investigated, and the minimum N concentration required for good productivity was identified. For this reason, a batch growth of *C. sorokiniana* was carried out in the inclined PBRs, irradiated at 300 µmol m^{-2} s^{-1}, and sparged with a gas stream composed of air supplemented with 2% of CO_2. The initial nitrogen concentration (nominal value) tested was: 20, 30, 60, and 120 mg L^{-1}.

Figure 3.3 shows the biomass concentration, the nitrogen concentration and the starch content of the cells during the cultures that were carried out in the PBRs at the four initial N-concentration investigations. It is worth noting that the X vs. t and the ω_{Starch} vs. t data are almost coupled at low initial N-concentration and un-coupled at high initial N-concentration.

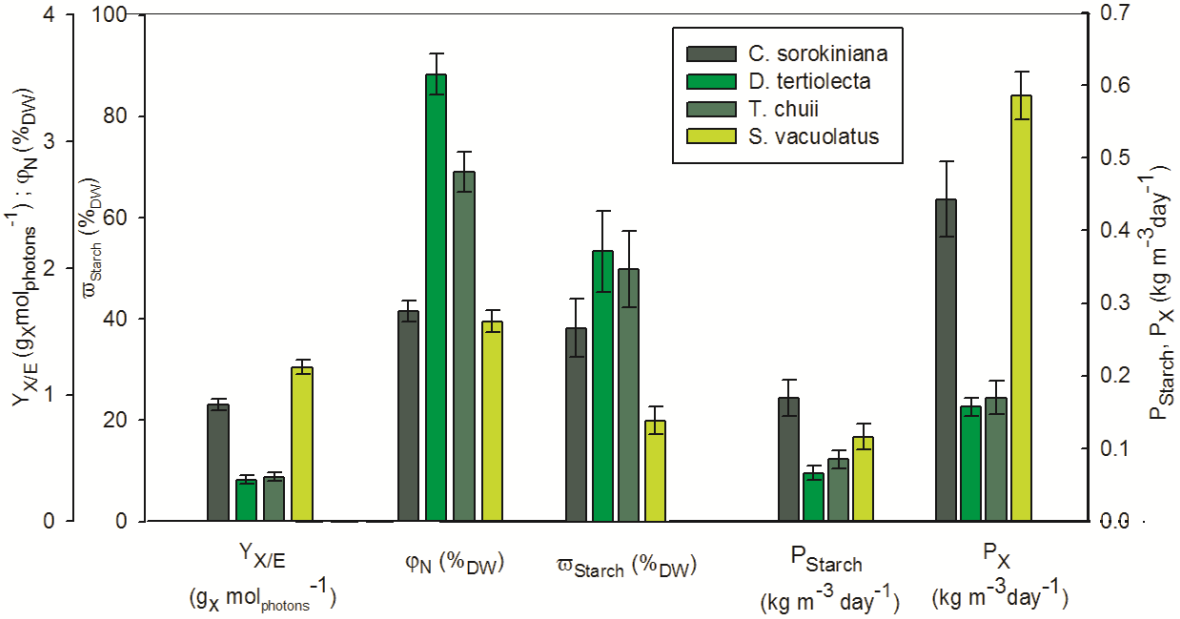

Figure 3.2: Light yield ($Y_{X/E}$), biomass nitrogen content (φ_N) under incipient N-stravation, starch fraction (ω_{Starch}), starch productivity (P_{starch}) and biomass productivity (P_x) assessed for the investigated strains.

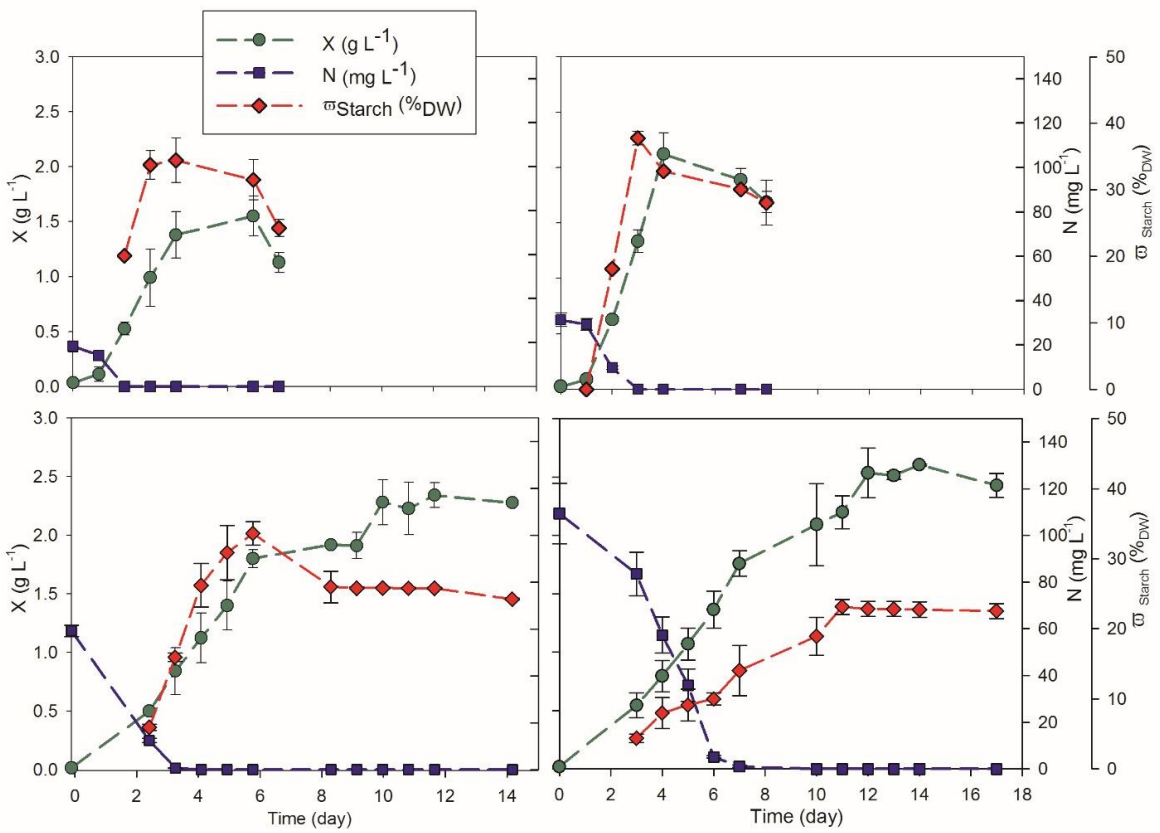

Figure 3.3: Time resolved data of growth (X), nitrogen uptake (N) and microalgal starch fraction (ω_{Starch}) of *C. sorokiniana* at different initial N concentration in the medium.

Figure 3.4 A reports the biomass concentration at the N-depletion onset ($X_{N=0}$) and the maximum biomass concentration (X_{max}) as a function of the initial nitrogen concentration. Results confirm that the biomass concentration still increased under nitrogen depletion. X_{max} and $X_{N=0}$ increased with the N-concentration, except for the point of $X_{N=0}$ at 61 mg L^{-1} of N.

The effect of the initial nitrogen concentration on the specific time for N uptake (t_N) and the biomass-nitrogen yield ($Y_{X/N}$) is reported in Figure 3.4 B. The t_N decreases with the N concentration: a behaviour that can be described by first order uptake kinetics.

Figure 3.4 C shows the maximum starch fraction, and the starch and biomass productivities assessed from the tests at different initial nitrogen concentrations. Reported data are characterised by a maximum at initial nitrogen concentration of 30 mg L^{-1}: starch content, starch productivity and biomass productivity were 38%, 0.17 and 0.45 kg $m^{-3}day^{-1}$, respectively.

The effect of the CO_2 concentration in the sparged gas stream was investigated. *C. sorokiniana* cultures were carried out in PBRs at 300 µmol m^{-2} s^{-1} and initial nitrate concentration of 30mgL^{-1} selected in the previous tests. The air stream was supplemented with CO_2 concentrations of: 0.04 (air without CO_2 integration), 0.5, 1, 2, 5, 10 %.

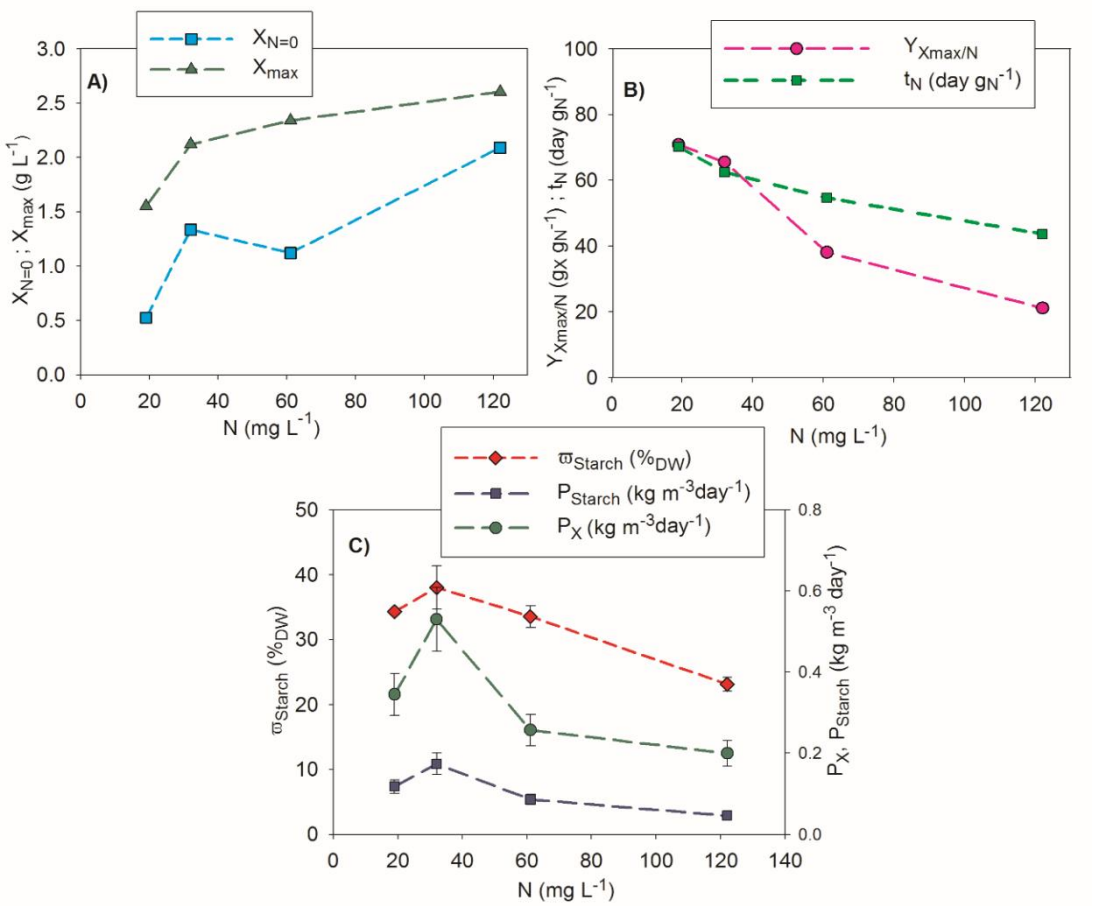

Figure 3.4: A) Biomass concentration at N=0 ($X_{N=0}$) and maximum biomass concentration (X_{max}); B) biomass nitrogen yield ($Y_{X/N}$) and specific time for nitrogen uptake (t_N); C) maximum starch fraction (ω_{Starch}), starch productivity (P_{starch}) and biomass productivity (P_x) as function of the initial N-concentration in the medium.

Biomass concentration was reported as a function of the time in Figure 3.5 A for the different CO_2 concentrations investigated. The pH measured during the cultures was reported in the legend for each CO_2 concentration in the gas stream. The tests carried out at 0.5, 2 and 5% of CO_2, have the same growth performances, regardless of the CO_2 concentration. The cultures carried out at 0.04 and 10% of CO_2 were characterised by lower growth performances with respect to the other tests. This behaviour was due to the CO_2 effect on the pH of the culture.

The biomass concentration at the onset of the N-depletion depends on the CO_2 concentration in the sparged gas stream, and the data are reported in Figure 3.5 B. The $X_{N=0}$ was characterised by a maximum at 2% CO_2. The X_{max} was also characterised by a maximum but less pronounced: X_{max} was approximately 2 g L^{-1} for CO_2 between 0.5 and 2% of CO_2.

The maximum ω_{Starch} was reached at the second day of nitrogen depletion for 0.04, 0.5 and 2% tests (data reported in figure 3.6). For the test at 5% of CO_2, microalgae took 6 days under N-depletion to reach the maximum starch content; whereas at 10% of CO_2, the maximum starch content was reached before the N-starvation.

Figure 3.5 C reports the effect of CO_2 concentration on starch fraction, starch and biomass productivity. The biomass and starch productivity were maximum at 2% CO_2, the starch fraction increased with the CO_2 and approached the maximum at 2% CO_2. The low productivities were measured for the test that was carried out with air and 10% CO_2.

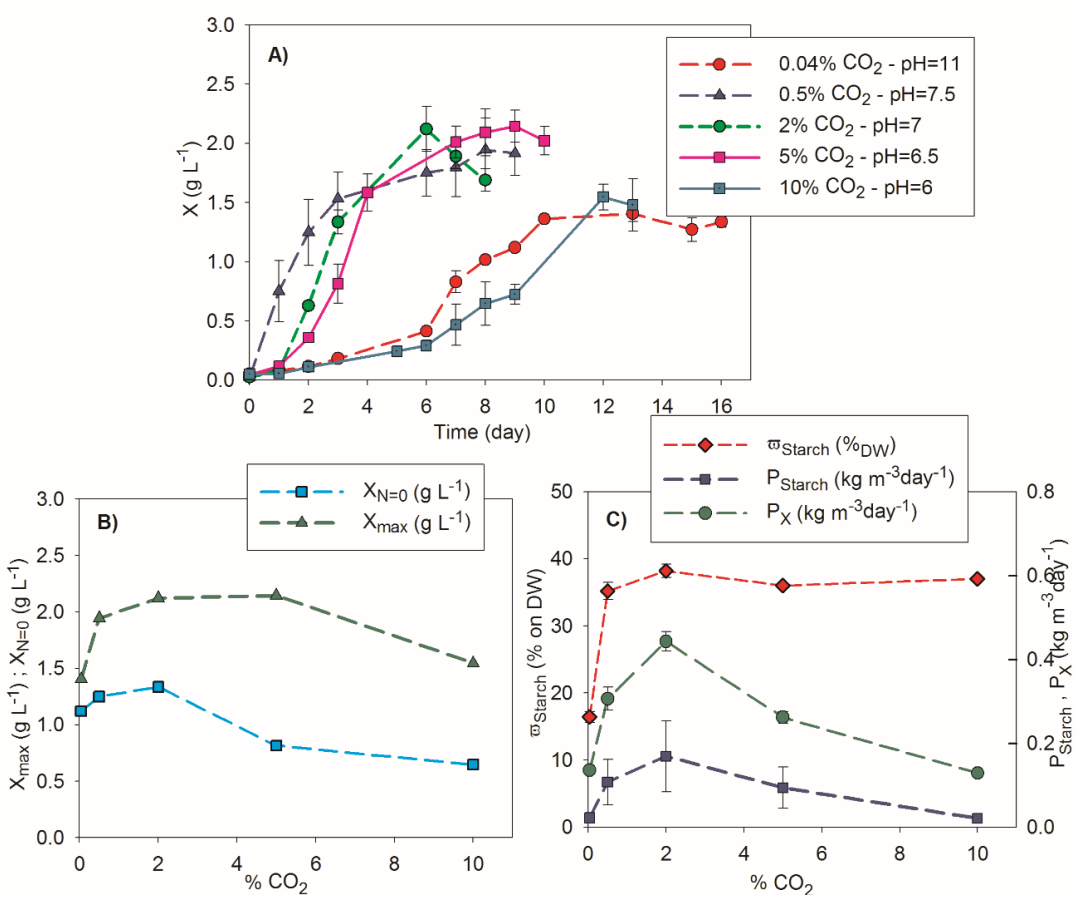

Figure 3.5: A) Growth curves of *C. sorokiniana* at different %CO_2 and pH. B) Biomass concentration when nitrogen in the medium comes out ($X_{N=0}$) and maximum biomass concentration (X_{max}); C) maximum starch fraction (ω_{Starch}), starch productivity (P_{starch}) and biomass productivity (P_x) as function of the CO_2 concentration in the feed.

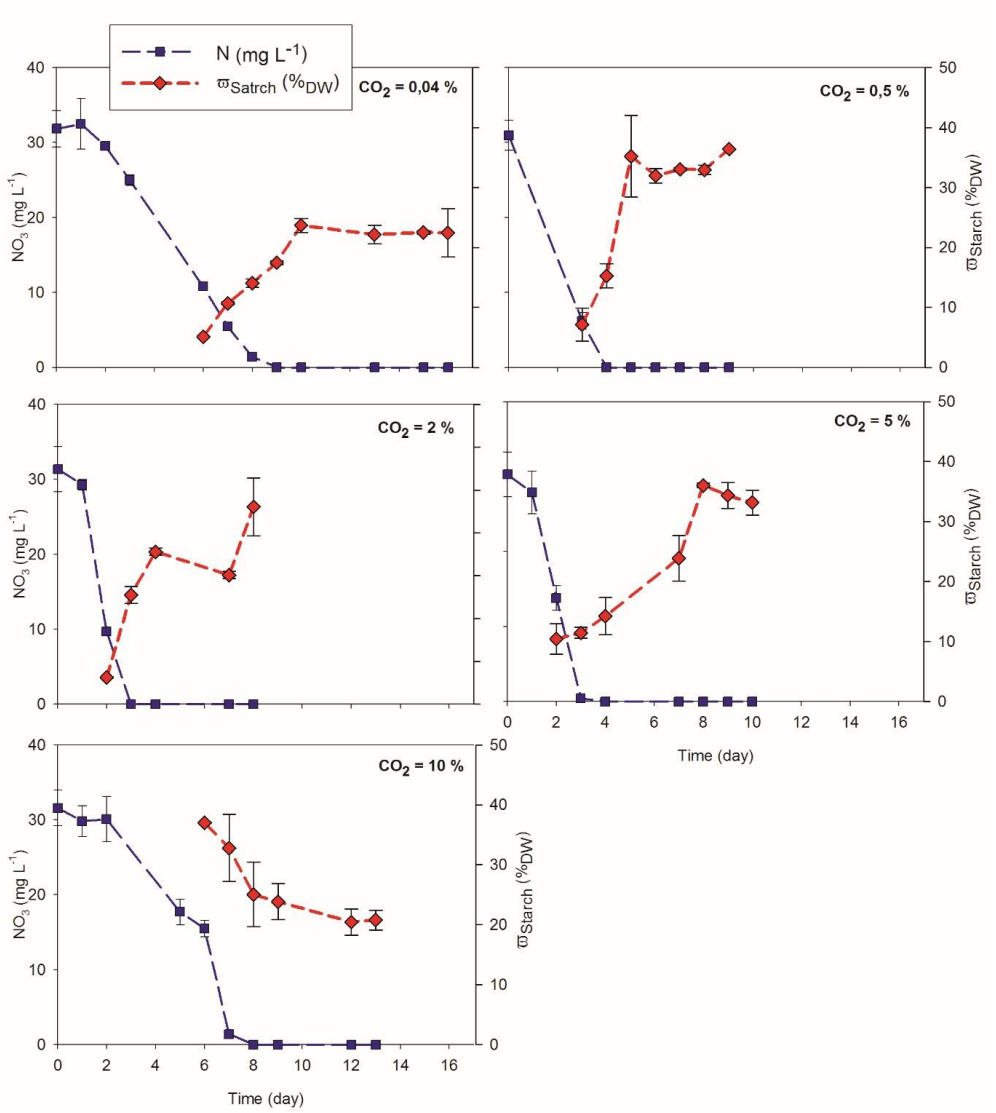

Figure 3.6: Dynamic of nitrogen uptake (N) and microalgal starch fraction (ω_{Starch}) of *C. sorokiniana, grown* at different CO_2 concentration in the gas stream.

The microalgal biochemical composition of *C. sorokiniana* was analysed during the batch culture at 2% of CO_2 and 30 mg L^{-1} of nitrogen in the medium (best conditions selected for strain, nitrogen and CO_2 in the feed).

Figure 3.7 illustrates the dynamic of protein, lipids, carbohydrates and starch fraction of the biomass throughout growth phase under nutrient replete conditions, at the onset of the N-depletion, and under x-day (with x=1, 3 and 6) in N-deplete conditions. Protein content of the biomass significantly decreased with nitrogen depletion. Protein concentration was relatively high (37%$_{DW}$) the first day of N-depletion, then its content decreased to 15% of DW in the late depletion. Carbohydrates, in particular starch, increased during the early N-depletion reaching a maximum of 47% and 38% of DW respectively, after the first day of depletion. Subsequently, they slightly decreased in favour of lipids accumulation. Lipid concentration increased slower than carbohydrates and reached a maximum of 41% of DW on the last day of depletion.

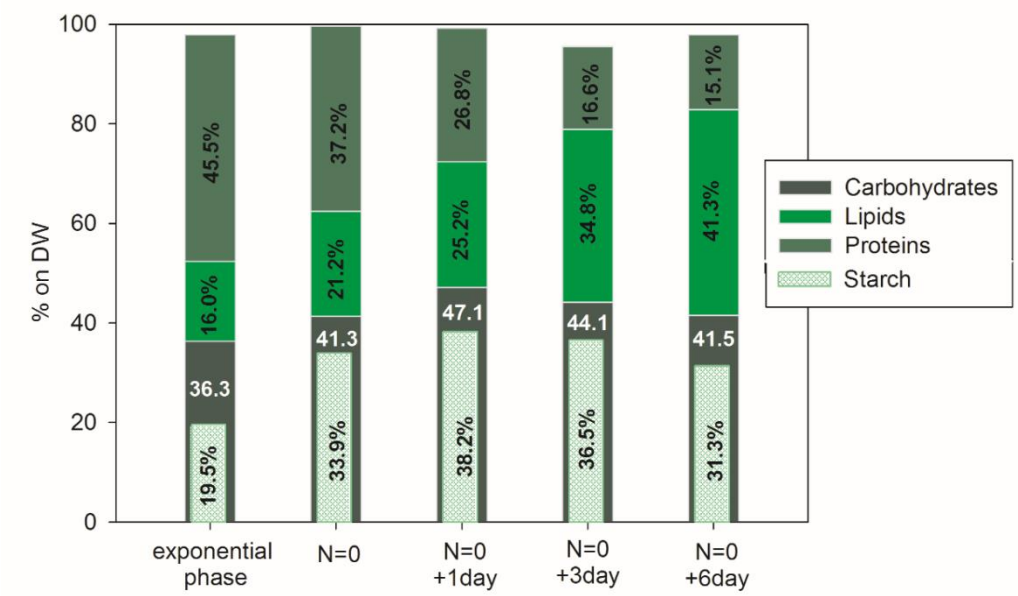

Figure 3.7: Biochemical composition of *C. sorokiniana* n (ash-free basis content) at different culture times. Batch test carried out at 300 µmol $m^{-2}s^{-1}$, air flow of 0.1vvm, 2% CO_2, 25°C.

Discussion

The aim of the tests was threefold: i) to select the most promising strain to produce starch in a biorefinery context; ii) to investigate the effect of nitrogen and CO_2 on growth and starch accumulation; iii) to assess the dynamic of the biochemical composition of the selected microalgal strain in order to identify the best conditions for a biorefinery application.

Strain selection for starch production

The objective function was starch productivity, but both the components contributing to P_{Starch} -starch fraction and the biomass concentration- were assessed as a function of the time for the four investigated strains: *C. sorokinina*, *D. tertiolecta*, *T. chuii*, *S. vaquolatus*. Even if all four strains are reported as good starch producers, these results compare the performances at the same culture conditions and nutrient-energy input. Moreover, the results indicate how the two fresh water strains resulted as higher biomass producers, while the seawater strains were the best starch accumulators, thus, the choice is ambiguous, and the compromise between both properties guides the selection.

It is worth noting that the biomass still increased even though the nitrogen source depleted. In particular, the biomass concentration of *C. sorokiniana*, *T. chuii* and *S. vacuolatus* increased by about 1 g (35 -50 % of the ultimate concentration) since the beginning of the nitrogen depletion. The increase of the biomass, under these conditions, is not due to cell growth/division because nitrogen sources for protein synthesis terminated. The increase of cell concentration was due to the cell accumulation of carbon rich molecules. This behaviour has already been reported in several papers (Packer et al., 2009; Breuer et al., 2012), but a comparative study on the difference among the species is now evident.

The observed starch accumulation during the early nitrogen depletion is in agreement with previous observations reported in literature for other microalgal species: *C. vulgaris* (Adesanya et al., 2014)*; S. obliquus* (Breuer et al., 2013); *C. reinhardtii* (Chen et al., 2013). The observed decrease in the starch content was clearly associated with the prolonged nitrogen starvation. Msanne et al. (2012) proposed that the reduction of starch content in *C. reinhardtii* during prolonged starvation is due to

the microalgae metabolism shift to triacylglycerols (TAGs) synthesis. With regard to the dynamic of the starch accumulation in *D. tertiolecta*, to the best of the authors' knowledge, no data are reported in literature. Indeed, it was the only strain accumulating starch during the stationary phase.

Data regarding light yield ($Y_{X/E}$), are in agreement with the growth data. They confirm that *C. sorokiniana* and *S. vacuolatus* are able to convert light energy in biomass better and faster than the other investigated strains. Relating light yield results with starch content aid to identify how light energy is addressed in the metabolism of the different strains. The energy is mainly used for biomass production in *S. vacuolatus*, while it is directed to starch accumulation in the marine species (*D. tertiolecta and T. chuii*). The compromise between starch accumulation and biomass growth is reached by *C. sorokiniana*.

Under initial N-depletion conditions, the φ_N was as low as 4% of DW in all strains, that is less than the N content of microalgal biomass generally measured - between 7 and 14% - under nutrient replete conditions (Tibbetts et al., 2017). The low value measured under N-depletion conditions indicated a good flexibility of the investigated microalgae to modify their biomass composition during nutrient depletion, and confirm that microalgae can change the chemical composition under a non-balanced medium – one of the N, P, S, sources being not sufficient - moving towards carbon rich molecules accumulation. It is known that, during the early N-depletion, the cells divert the accumulation of the surplus of energy from photosynthesis into glucose because the absence of nitrogen sources do not support protein synthesis and cell division. The produced glucose is then polymerised to starch by an endothermic reaction and the φ_N further decreases. According to this scenario, low φ_N should be associated to high ω_{Starch}. For the investigated strains, a more articulated scenario was found: *D. tertiolecta* and *T. chuii* were characterised by a high starch content (53% and 49% of DW, respectively); *C. sorokiniana* and *S. vacuolatus* strains were characterised by the lowest value of φ_N, but also low values of ω_{Starch} (38% and 22% respectively). The first pair of strains suggest the hypothesis that under N-depletion most of the energy is accumulated in the form of starch. On the other hand, the second pair of strains support the hypothesis that the energy from photosynthesis in some strains is not accumulated mainly as starch, but other energetic reserves can be accumulated such as TAG (e.g. *Scenedesmus* species accumulated TAGs as reported by Gardner et al. (2013).

The sea water strains resulted as better starch accumulators, while maintaining the nitrogen content over 3% of microalgal dry weight in the analysed conditions. However, the selection of the strains was essentially based on the starch productivity, therefor *C. sorokiniana* was selected as the most promising starch producer in a biorefinery context, as it showed a high growth rate and starch productivity. Moreover, the maximum starch content of 38% of DW during the early nitrogen depletion condition, suggests a good ability to accumulate other biomolecules in significant concentration.

The data regarding the starch productivity of *C. sorokiniana* were compared with those reported in other studies regarding the same strain. It should be noted that the comparison between the starch productivity reported in the literature and the present data is a not easy task, as cultures were carried out in different typologies of photobioreactors and under different irradiances and nutrients supply. Nevertheless, the starch productivity obtained in this study was higher than that reported by Tanadul et al. (2014) and Takeshita et al. (2014) using similar culture conditions.

Effect of initial nitrogen concentration on starch production

The effect of initial nitrogen concentration in the medium was analysed for *C. sorokiniana*. Indubitably, the phosphorus is also reported to influence the starch or lipid

accumulation and it is also required as a fertilizer in agriculture, but this work focused on the nitrogen since it is known that P-depletion causes a reduction in photosynthesis, thus, starch –which requires a photosynthesis derived precursor- cannot be synthetised (Belotti et al., 2013).

Interesting data were found regarding the growth performances and starch accumulation along the culture time. The results suggest that: the maximum biomass concentration and the time to reach the N-depletion increased with the initial N-concentration; furthermore, the instant at which the ω_{Starch} is maximum depends on the initial N-concentration; the delay between the nitrogen depletion and the instant at which the ω_{Starch} is maximum increased with the initial N-concentration. In particular, the larger availability of nitrogen seems to enhance growth, while simultaneously reducing the starch accumulation. The increase in biomass concentration is not significant, considering the reduction in biomass and starch productivity. Moreover, the biomass concentration at the N-depletion onset ($X_{N=0}$) could be a critical factor for the further increase of microalgal mass and starch accumulation. Indeed, at higher microalgal concentrations the light availability is reduced and so is the energy to fix carbon as organic molecules (starch).

The $Y_{X/N}$ decreased with the initial N-concentration: the nitrogen is not converted directly in biomass but it is stored in the cells and mobilised during nutrient shortage, as reported by Lavín and Laurenço (2005). Indeed, at a high initial nitrogen concentration, the biomass concentration increased for a long time even during N-depletion (Figure 3.3, N=120 mg/L), proving that cells were re-converting some stored nutrients. Jerez et al. (2016) also reports that low nitrogen concentration in the medium caused high starch fraction and productivity in microalgae, but low biomass concentration was obtained. Therefore, a compromise between biomass productivity and starch concentration has to be established. Our tests showed that, for the analysed conditions, the best results correspond to 32 mgL^{-1} of nitrogen in the medium. Different results are reported in other work on *Chlorella* species (De Farias Silva et al., 2016; Li et al., 2015) but, as previously mentioned, the comparison is not possible since the mediums used, the PBR design and the light irradiance are different. Moreover, the analysis of the reported results indicated that the cell concentration at the beginning of the N-depletion is a critical factor: low concentration means low productivity, but also high concentration means high light absorption that can affect photosynthesis, glucose and starch accumulation.

Effect of CO_2 concentration on starch production

The effect of the concentration of the inorganic carbon source (CO_2), was analysed for batch culture of *C. sorokiniana*. The pH of the culture, when only air was fed, increased to 11 due to the absence of the buffer effect of the dissolved CO_2. The pH during the cultures carried out sparging the 0.5, 2 and 5 % of CO_2, was controlled by the buffer effect of CO_2 and it ranged between 6.5 and 7.5, while for the cultures grown at 10 % of CO_2, the pH dropped to 5.5, too distant from the optimal condition. The decrease in X_{max} for air test can be due to insufficient carbon source. The decreasing trend of $X_{N=0}$ and X_{max} for 5 and 10% tests, can be due to stress conditions (pH ~ 6) that influence the growth both in N replete and deplete conditions. Moreover, a higher CO_2 concentration fed into the gas stream does not correspond to a higher biomass production. The effect of the pH was also analysed in other papers, such as De Farias Silva et al. (2017) but the behaviour reported was not the same as this study, most likely because of the different strain analysed.

For the test at 5% of CO_2, microalgae took 6 days under N-depletion to reach the maximum starch content, probably due to stress conditions; whereas at 10% of CO_2,

the maximum starch content was reached before the N-starvation. It is possible to explain these observations considering that the microalgae accumulated nutrients and stored molecules (e.g. starch) during the lag phase (day 0 to 6), then the accumulated starch was consumed under the growth phase (day 6).

The low productivities measured for the test carried out with air were mainly due to the low biomass produced, because of the reduced carbon source concentration. In the test at 5 and 10% CO_2, the reduced performances in terms of productivities, are essentially due to the low pH that causes stress conditions for *C. sorokiniana*.

Supplementing CO_2 (carbon source) to the air stream (mix of air and exhaust gas streams) until 2% proved to be an efficient strategy to improve biomass production, while no effect is noticed on starch accumulation, on the contrary of that reported by Chen et al. (2013). Carbon is essentially directed towards biomass production instead of carbon reserves accumulation (starch). Tanadul et al. (2014) also reported that 2% of CO_2 provided better conditions than air for biomass and starch production. The comparison of his results regarding *C. sorokiniana* (P_{starch} of 0.02 kg $m^{-3}day^{-1}$, at 120 µmol $m^{-2}s^{-1}$,2% CO_2 and N of 140 mgL^{-1}) with that of the present study (P_{starch} of 0.17 kg $m^{-3}day^{-1}$, at 300 µmol $m^{-2}s^{-1}$,2% CO_2 and N of 32 mgL^{-1}) suggests that the real limiting factor influencing the starch productivity is the light irradiance. Moreover, to the best of the authors' knowledge, this is the first time that the CO_2 concentration, provided to the culture, is directly correlated to the accumulation of sugars as starch reserves and no increase is found for CO_2 higher than 2% if the incident light irradiance is maintained constant.

Effect of growth phase on microalgal biochemical composition

The biochemical composition of *C. sorokinina* was monitored during the batch growth in order to identify the optimal balance of biomolecules for the exploitation in the biorefinery. As reported by Adesanya et al. (2014), the carbohydrates accumulation occurs when the photosynthetic system and chlorophyll are not already affected by depletion of their structural element (N), then lipids accumulation occurs. The overall behaviour of the microalgal composition is also reported in other works (Klok et al., 2014; Zhang et al., 2015), but the present results analyse the biochemical composition day by day during nitrogen depletion, providing more detailed data. This allows for a better understanding of the biochemical response to the nitrogen depletion in *C. sorokiniana,* and subsequently, to consider the optimal component balance for biorefinery applications. In particular, harvesting the biomass at N=0 + 1day, it is possible to have the highest starch content (and productivity) for its exploitation in industrial field, already proved by a physico-chemical characterisation of *C. sorokiniana* starch (Gifuni et al., 2017). Moreover, proteins and lipid fraction could also be recovered in large amounts for food or cosmetic applications (Schwenzfeier et al., 2012; Christaki et al., 2011).

Conclusions

C. sorokiniana was found to be the most promising candidate for starch production in the biorefinery context. Moreover, this study not only proves that N-depletion is a key issue for starch accumulation, but also that the light availability is essential. A concentration of CO_2 higher than 2% is proven to not have any effect on starch accumulation, if the light provided is 300 µmol m^{-2} s^{-1}. The biochemical composition of *C. sorokiniana*, during the early nitrogen depletion, suggests its exploitation for the biorefinery context. Indeed, at the same time it is possible to not only recover starch (38%$_{DW}$), but also proteins (27%$_{DW}$) and lipids (25%$_{DW}$) with many commercial applications. Further studies are required for the separation of the different

components of the microalgal biomass for its effective valorisation on an industrial scale.

Acknowledgements
The authors would like to thank the ACUF collection for providing the microalgal strains and the "Ministero dell'Istruzione, dell'Università e della Ricerca" for supporting this research activity.

4. PHYSIC-CHEMICAL CHARCTERIZATION OF MICROALGAL STARCH GRANULES

The physic-chemical characterization of the microalgal starch granules was one of the aim of the PhD research project. Although starch features are relevant to assess the effective application in the industrial fields, limited information regarding microalgal starch are available in the literature. Indeed, the physic and chemical properties of the starch affect the performances of material produced from starch. The main fetaures investigated were: molecular weight, shape, size distribution, amylose/amylopectine content, crystallinity, and thermal properties. Specific applications were proposed based on the experimental results.

4.1 Microalgae as New Sources of Starch: Isolation and Characterization of Microalgal Starch Granules

I. Gifuni[a], G. Olivieri*[a], I. Russo Krauss[b], G. D'Errico[b], A. Pollio[c], A. Marzocchella[a]

[a] Dipartimento di Ingegneria Chimica, dei Materiali e della Produzione Industriale, Università degli Studi di Napoli "Federico II", Piazzale Tecchio, 80, Naples, Italy.
[b] Dipartimento di Scienze Chimiche, Università degli studi di Napoli "Federico II", Complesso Universitario Monte Sant'Angelo, Via Cinthia, 47, Naples, Italy.
[c] Dipartimento di Biologia, Università degli studi di Napoli "Federico II", Complesso Universitario Monte Sant'Angelo, Via Cinthia, 47, Naples, Italy.

Abstract

Starch is a very important biopolymer used in the modern society. It is a basic element of our diet (35% of daily calories in UE and USA). Moreover, it is widely used in the non-food industries. Indeed, the market of the non-food applications is nowadays growing and it includes chemical additives, bulking agents, and bioplastics productions (e.g. Mater-Bi by Novamont). The key starch features for industrial applications are: size and shape distributions of starch granules, crystallinity, amylose-amylopectin ratio, thermal properties. These features are critical to address the starch processing in the industrial production. Nowadays the main sources of small starch granules that fulfil the industrial requirements are maize, wheat, rice, oats, and amaranth. However, the reduced availability of arable lands and the increase of food demand ask for alternative sources for starch, not in competition with food cultures. Microalgae are considered novel highly efficient starch producers. Their starch content can reach the 40%w. They do not require arable land and fresh water for their cultivation. Nevertheless, limited information is available in literature about physic-chemical characterization of microalgal starch. Therefore, additional analysis about molecular weight, crystallinity, and amylose fraction are required to validate the potential industrial applications of this starch type. The present contribution reports a study on starch granules present in the microalga *Chlorella sorokiniana*. The granules were isolated and a preliminary physic-chemical characterization was carried out. The microalgal starch was characterized by small granules of about 1µm with a narrow size distribution (key feature for some applications). The molecular weight of microalgal starch is comparable with that of plant- starch sources. The amylose content and crystallinity pattern were similar to cereal starch. Moreover, the high gelatinization temperature of 110 °C makes these granules suitable for system requiring high processing temperature such as for biodegradable materials.

Published in Chemical Engineering transactions, 2017, 57, 1423-1428

Introduction

Starch is the principal storage polysaccharides produced by green plants. Starch consists of two D-glucose polymers: amylose and amylopectin. Amylose has a linear structure with α-1,4-linked glycan, while amylopectin is a highly branched molecule characterized by α-1,4-linked and α-1,6 branching links (Pérez and Bertoft, 2010). Starch is a very important biopolymer with a wide use in human life. It is a basic element of our diet (35% of daily calories in UE and USA) and of the commercially produced starch (50 million ton/year) two third are used in food industries and a third in non-food industries (Morton Satin – FAO Report, 2007). In food industries, it performs various functions as thickener, binder, disrupting agent, stabilizer, texture modifier, gelling and bulking agent, useful in the preservation of canned and frozen foods, in the formulation of syrups, essences and beverages, in confectionery and bakery, snacks and marshmallows (Copeland et al., 2009). Starch use is extended also in non-food industries. It is used for adhesives and rubbers production (already by Romans and Egyptians), as a cement additive to reduce the stabilization time; in paper and textile industry as filling agent and to improve the ink adhesion; it is used also as a bulking agent, humectant and thickening agent in the formulation of cosmetic and pharmaceutical products. Not least is its use in the production of plastic products and for food packaging, food containers and cutlery and agriculture (Pérez-Pacheco et al., 2014). Non-food applications have increasing importance also for consumers that become more aware of “green” issues, moreover this kind of application requires specific properties as well as increasing production yield.

Plants starch properties and yield mostly depend on environmental conditions - hardly controllable- so many studies are aimed at chemical starch modification or functionalization (Filippov et al., 2015; Chauhan et al., 2015). The most interesting starch properties are: size and shape distributions, crystallinity, amylose/amylopectin ratio, which influence physico-chemical behaviour during product productions. In particular, there is a recent interest in small starch granules applications because of their high specific surface area. This property increases viscosity, gives more sites for crosslinking reaction finalized at starch modification, better surface adhesion, high gelatinization temperature and resistance. Recently, there is interest in small starch granules for peculiar applications: fat replacers in free-fat food formulation; carrier material in pharmaceutics and cosmetics and flavour essences; thick coatings for fabrics, paper, in high quality biodegradable film production (Lindeboom et al., 2014).

The current major sources of small starch granules are rice, oats, amaranth, which contain about 30% of small granules (0.5-3 μm) (Wilhelm et al., 1999), but expensive separation process limits their commercial applications. Moreover, the European reduction of agricultural land urges new and sustainable production that avoid the competition with food production.

Microalgae are considered a novel highly efficient starch producer (Brányiková et al., 2010) and they produce only small starch granules with a narrow size distribution range (0.5-2.1 μm) (Tanadul et al., 2014). The recovery of microalgal starch allows to have only enriched small size granules avoiding a wasteful granules separation. As higher plant, microalgae are able to accumulate sugars- synthesized during photosynthesis, as starch granules in the plastids (Ho et al., 2011). Starch concentration of microalgae, especially in *chlorophycae* strains, may be as large as 40% of the dry biomass when nitrogen depletion conditions establish (Gifuni et al., 2017). Moreover, microalgae as feedstock source are characterized by a wide spectrum of advantages compared to higher plants: i) high growth rate; ii) high photosynthetic efficiency and high level of CO_2 fixed per unit of biomass synthesized

(reduction of greenhouse effect); iii) they do not require arable land and fresh water; iii) their exploitation do not compete with food market. Microalgae cultures have been extensively studied in the last decades, particularly for biodiesel production (Perin et al., 2014; Sforza et al., 2014; Gargano et al., 2015). However, the analysis of the large-scale productions points out that the current technologies to produce liquid fuels are not self-sustainable from an economic point of view. Therefore, the biorefinery approaches to exploit as much as possible all the macrocomponents of the microalgae – lipids, carbohydrates and proteins – as well as the high-value products become the key issue for the industrial development of microalgal processes. Including starch production in this microalgal biorefinery approach also makes possible to develop an economical feasible process for the small high-quality starch granules recovery. Furthermore, to the author knowledge, limited informations are available in literature about physic-chemical characteristics of microalgal starch, so additional analysis about molecular weight, crystallinity and amylose content and thermoplastic properties are needed to validate the potential applications of this starch type.

The aim of the present paper is to report on the investigation regarding the mentioned physical and chemical properties of *Chlorella sorokinana* starch granules. The selected strain belongs to *chlorophyiceae* and it is already used for large-scale production. It is suitable for biorefinery application and it is known to accumulate large amount of starch during nitrogen depletion.

Materials and methods

Starch source

Microalgal strain *Chlorella sorokiniana* Shihiraet Krauss ACUF 318, was provided by ACUF collection (www.acuf.net). Photoautotrophic batch growth of this strain was carried out in inclined square bubble column photobioreactors in order to obtain the required amount of biomass for starch extraction. Further details can be found elsewhere (Gargano et al. 2015). The photobioreactors were housed in a climatic chamber at the temperature of 25°C, under continue illumination of 300 µE $m^{-2}s^{-1}$. The flow rate of the gas sparged at the bottom of the photobioreactors was set to 0.02 vvm. The gas was air additioned with 2% of CO_2. The inorganic medium used was Bold basal medium (BBM) described by Olivieri et al. (2013). The biomass was harvested when nitrogen source in the medium became depleted, to verify if this condition enhances starch accumulation in microalgae.

Purification of starch granules

Starch granules extraction, was carried out on fresh microalgal biomass according to the protocol by Derlue et al. (1992) with some modifications. Briefly, microalgal biomass was suspended in ethanol and mechanically disrupted by beat beating (equipped with glass beads of 0.5 mm). The entire lysate was recovered and heated at 75°C in order to complete cells disruption, fragmentation of the debris and pigments extraction, preserving starch granules structure. The resulting samples were centrifuged at 10,000 g for 20 min. The pellet, containing starch granules and cells fragments, were resuspended in cold distilled water and centrifuged twice through Percoll gradient at 10,000 g for 20 min in order to separate high density starch granules and low-density cell debris. The purified starch pellets were washed two times with distilled water and acetone. Then, 10 mg of the obtained starch was assayed by total starch kit (Megazyme - Ireland) to establish the purity of the sample. The purity was calculated as follows:

$$\%\text{Purity} = \frac{m_{\text{Starch measured}}}{m_{\text{Starch assayed}}} \cdot 100 \qquad (4.1)$$

Starch characterization

Purified starch granules were characterized in terms of granules morphology, average size and size distribution, amylose and amylopectine content, molecular weight, crystallinity and gelatinization temperature. *Granule morphology.* The shape of starch was examined by a scanning electron microscopy (SEM). Starch samples were mounted on a metallic slide and the examination was performed with a scanning electron microscopy.

Size distribution analysis. The measure of the average size of microalgal starch granules and size distribution in the sample, was performed using laser granulometer (Master-sizer 2000 Malvern Instruments) after the dispersion of the powders in water under mechanical agitation of the suspension and with the application of ultrasound.

Amylose amylopectine ratio. Amylose content of the *C. sorokiniana* starch was determined using enzymatic assay (Amylose/Amylopectin kit - Megazyme). The amylopectin content is assessed as difference at 100%.

Molecular weight. An estimation of the starch molecular weight was derived from the hydrodynamic volume of the particles, as determined by Dynamic Light Scattering (DLS), considering the volume completely filled by glucose monomer of known molecular weight. DLS measurements were performed with a home-made instrument composed of a Photocor compact goniometer, a SMD 6000 Laser Quantum 50 mW light source operating at 5325 Å, a photomultiplier (PMT-120-OP/B) and a correlator (Flex02-01D) from Correlator.com. The experiments were carried out at the constant temperature (25.0 ± 0.1) °C, by using a thermostatic bath, at the scattering angle θ of 90°. The scattered intensity correlation function was analysed using a regularization algorithm. The diffusion coefficient of each population of diffusing particles was calculated as the z-average of the diffusion coefficients of the corresponding distributions. Considering that the mixtures are dilute, the Stokes–Einstein equation was used to evaluate the hydrodynamic radius, R_H, of the starch particles, assumed to be spherical, from their translation diffusion coefficient, D.

Crystallinity. X-ray diffraction patterns were obtained with Ni filtered Cu Kα radiation. The powder profiles were obtained with an automatic Philips diffractometer. Starch was placed into the sample holder, and XRD patterns were recorded in reflection mode with 2θ ranging between 5 and 80° operating at 40 kV and 40 mA, at room temperature. The crystallinity was evaluated from the X-ray powder diffraction profiles by the ratio between the crystalline diffraction area and the total area of the diffraction profile.

Thermal properties. Starch gelatinization was measured using a differential scanning calorimeter (DSC 822 Mettler Toledo, Switzerland) with the method reported by Homer et al. (2014). 10 mg of starch was weighed in a small aluminum pan and 20 µL of distilled water were added. The sample was stabilized for 1 hour at room temperature before the measurement. The DSC was calibrated using an empty aluminum pan as a blank. The aluminum pan containing the starch and water was heated at a temperature ranging from 20 to 150 C with a heating rate at 10°C/min. The initial temperature (T_o), peak temperature (T_p), finishing temperature (T_c), enthalpy of gelatinization (ΔH_{gel}) and peak height index were calculated. The thermogravimetric analysis was also carried out using TGA 50 Shimadzu, Japan. 10 mg of starch were heated from room temperature to 400°C at a heating rate 10 C/min.

Results

C. sorokiniana was grown under autotrophic conditions at light irradiance of 300 µmol m^{-2} s^{-1}. The biomass was harvested after the first day of nitrogen depletion. This

condition was previously found to give the highest starch content and productivity. In particular, the starch fraction reached the 38% of the microalgal dry weight and the starch productivity resulted 0.17 kg m^{-3} day^{-1}. Starch fraction and biomass productivity of the plants commonly used for starch production are reported in table 4.1. The values assessed in the present study for *C. sorokinina* strain were also reported. *C. sorokiniana* is characterized by starch fraction lower than the other higher plants but its biomass productivity (as for microalgae in general) is significantly higher than plants species. Therefore, the starch productivity was higher than that of higher than plant species. Moreover, microalgae can be grown in closed photobioreactors where culture conditions can be controlled, so the amount of biomass and starch produced is not influenced by environmental and climatic conditions.

Species	Starch fraction (%on DW)	Biomass productivity (ton ha^{-1} y^{-1})	Starch productivity (ton ha^{-1} y^{-1})
Corn	78	8	6
Rice	80	10	8
Potato	85	17	15
Oat	61	6	4
Amaranth	69	8	6
C. sorokiniana	40	150	58

Table 4.1: Comparing starch fraction and productivity of the most used plant species (www.FAO.org) and microalga *C. sorokiniana* (this study).

The starch powder produced according to the optimized protocol for microalgal starch purification was characterized by 87% of purity. The produced starch granules were characterized from the morphological point of view by means of SEM. Pictures of *C. sorokiniana* starch granules are reported in the figure 4.1. Granules shape resulted ovals and spheres, similar to wheat and potato starch. Even if there are many aggregates, no composite granules are present.

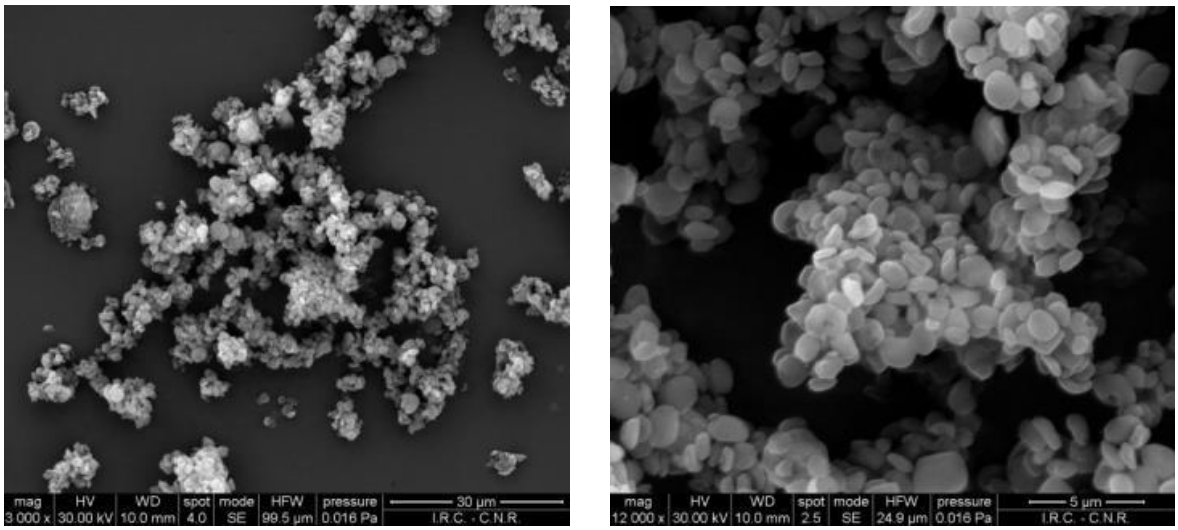

Figure 4.1: SEM micrograph of granular starch isolated from *C. sorokiniana*.

Figure 4.2 shows the results of granulometric analysis in terms of size distribution of the sample particles. The 80% of the analysed particles have a mean diameter of 1.5 µm, the size distribution range was 0.8-5.3 µm, the last 15% of particles exceeding 5.3 µm are probably associated to the impurities of the sample. These data are in agreement with that reported by Tanadul et al. (2014), moreover the microalgal starch is effectively enriched in small starch granules, more than 80%, with respect to the other plant sources for which small granules count the 30% of the total (Wilhelm et al., 1999). This feature is particularly advisable for applications as fat replacers in free-fat food formulation, as carrier material in pharmaceutics, as one-layer-thick honeycomb coatings in the cosmetic, paper, textile industries and for bioplastics film formulation for garbage bags and agricultural mulches (Lindeboom et al., 2004).

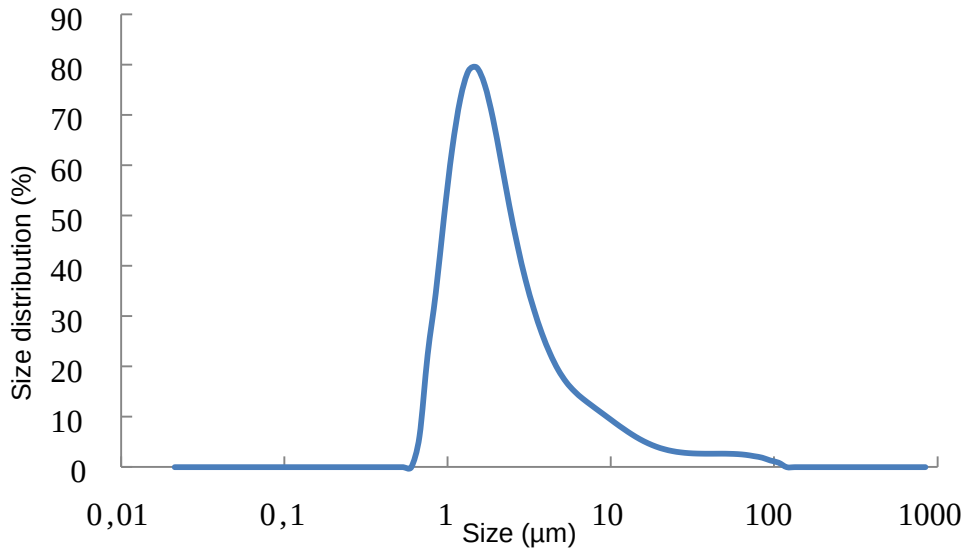

Figure 4.2: Size distribution of starch powder obtained from *C. sorokiniana*.

The molecular weight of microalgal starch resulted about $6.35 \cdot 10^8$ kDa, comparable with that plant sources (10^8-10^{12} kDa). Molecular weight strongly influences starch properties, high molecular weight is required for bioplastic production. It is connected

to the amylopectin content of starch, since the highly branched polymer has the highest molecular weight.

The amylose/amylopectin ratio was also measured. Amylose content of starch from *C. sorokiniana* is 17%, amylopectin content is 83%. The amylose fraction is nearby that of cereals starch (19-28%). The amylose/ amylopectin ratio is mainly influenced by biological origin and environmental factors then, probably amylase content could be increased changing microalgal culture conditions in order to obtain a good film forming starch. Indeed, high-amylose starch shown to form stronger and stiffer thermoplastic films, but amylopectin fraction contributes to increase swelling properties that lead to gel and film formation.

In the figure 4.3, XRD pattern of *C. sorokiniana* starch is reported. Peaks at 15° and 23°, and a double peak at 17 and 18° 2θ are clearly recognizable. This pattern indicates a crystalline structure classified as A-type, typical of cereal starches (Pérez and Bertoft, 2010). The crystallinity of the starch was about 30%, straightly linked to the amount of crystalline and amorphous structure (amylopectin fraction).

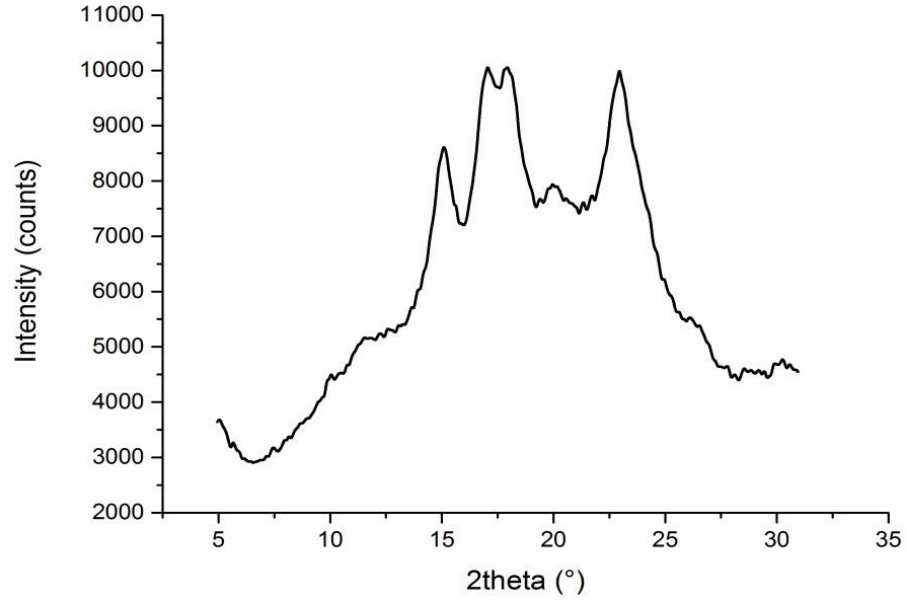

Figure 4.3: XRD diffractograms of *C. sorokiniana* starch.

The thermal properties of starch granules were also analyzed in order to assess the thermal processability of the starch in the industrial field (food and plastics industries). For microalgal starch, the gelatinization started at 24°C (T_o) and it was completed at 97°C (T_c), with a peak at 69°C (T_p). The gelatinization enthalpy was 5.49 Jg^{-1} (ΔH_{gel}) with a peak height index of 1.55°C. Gelatinization properties seemed similar to other starch sources, except for the onset temperature; probably the swelling of the starch started at lower temperature because of the higher specific surface (associated to small starch granules) which facilitate the water diffusion into starch granules and the crystallinity loss. The thermal degradation and stability assays were also carried out. The total weight loss, after the complete combustion, was 85.81%. The first step of the thermogravimetric analysis, showed a rapid dehydration of the sample below 100°C for approximately 10% of the weight. The second step, representing the degradation of amylose and the amylopectine breakage, occurred in the range 250-350°C. The third step, of the complete combustion took place at 349°C. The thermal decomposition temperature was 321°C, indicating a good thermal stability, since it does not decompose under 190°C (Elmi Sharlina et al., 2017).

Conclusions

Microalgae are a sustainable source of starch for industrial applications and they are characterized by far outweigh productivity than higher plants. *C. sorokiniana* starch granules purification was optimized and the physico-chemical characterization showed interesting features. Small granules with narrow distribution range find application as additives in cosmetics, pharmaceutics, food and plastics industries. Crystallinity, molecular weight and thermal properties are very close to starch from other sources, suggesting microalgal starch as valid alternative to plant starch in several fields.

5. INTENSIFICATION OF MICROALGAL BIOMASS PRODUCTION

The increase in the microalgal biomass concentration and productivity is a critical issue for the economic/energetic success of industrial processes. As regards the biomass concentration in the conventional culture system, a limiting factor is the exponential decrease of the light availability along the optical path of the culture. A potential solution to reduce the shaded culture volume is the use of thin photobioreactor. Many thin protobioreactors reported in the literature are characterized by a thickness (optical path) in the range of 1.5-0.7 cm. In this part of the thesis, the design of an ultra-thin flat photobioreactor, characterized by an optical path of 3 mm. The ultra-thin flat photobioreactor was built up and suvccessfully operated. The performance of the ultra-thin flat photobioreactor was charcaterized by the culture of the strain selected, *C. sorokiniana* (chapter 3). The effect of the light intensity on the growth, photosynthesis and biochemical composition of the microalga *C. sorokiniana* was also investigated for the proposed culture system.

5.1 New designed ultra-flat photobioreactor for intensive microalgal production: the effect of light irradiance.

I. Gifuni[a]*, A. Pollio[b], A. Marzocchella[a], G. Olivieri[a]

[a] Dipartimento di Ingegneria Chimica, dei Materiali e della Produzione Industriale, Università degli Studi di Napoli "Federico II", Piazzale Tecchio, 80, Naples, Italy.
[b] Dipartimento di Biologia, Università degli studi di Napoli "Federico II", Complesso Universitario Monte Sant'Angelo, Via Cinthia, 47, Naples, Italy.

Abstract

One of the main bottlenecks for the microalgal exploitation are the low biomass concentration and productivity that asks for high harvesting costs and large cultivation area. These bottlenecks may be due to the low light availability along the optical path of photobioreactors. An ultra-flat photobioreactor (UFP) characterized by 3 mm thickness was proposed to increase biomass concentration and productivity. The performance of the UFP was investigated. The effect of incident light intensity – ranged between 50 and 1000 μmol m^{-2} s^{-1} - on cell growth rate, photosynthesis, and biochemical composition of *Chlorella sorokiniana* was characterized. The maximum microalgal concentration and the maximum volumetric productivity were 24 kg m^{-3} and 0.34 kg m^{-3} h^{-1}, respectively. The cell growth rate was as large as 0.1 h^{-1} at 1000 μmol m^{-2} s^{-1} and no deleterious effect was observed on the photosynthetic activity at the highest light intensity investigated. The microalgal biochemical composition changed with the light irradiance. Protein content increased from the 35 to the 53% of DW with the light intensity. The concentration of storage compounds (starch and lipids) decreased from 30 to 20% and from 25 to 8%, respectively, with the light intensity. A light transfer model was applied to assess if maximum biomass concentration was due to the light availability: no light limitation was found.

Highlight

- A new design ultra-thin flat PBR was proposed.
- The biomass concentration reached 24 kg m^{-3} with a medium light input of 300 μmol $m^{-2}s^{-1}$.
- High light irradiances do not decrease the photosynthetic efficiency in the ultra-thin flat PBR.
- Biomass composition is influenced by the incident light irradiance, in favor of proteins production and not for carbon rich molecules accumulation.

Keywords

Ultra-thin flat PBR; *C. sorokiniana*; intensive culture; light irradiance; biochemical composition, biorefinery.

Introduction

The potential of microalgal cultures have led their applications in many industrial fields. Dozens of enterprises have been founded in the recent years with the aim to produce sustainable bioproducts: renewable oils for powerhouse and more sustainable fuels; ingredients for healthy foods; industrial products for personal care (Vigani et al., 2014). In particular, microalgae are a source of proteins characterized by high nutritional value and emulsifying properties (Schwenzfeier et al., 2014). The lipid fraction is currently used as source for omega-3, other polyunsatured fatty acids as food additives (Cuellar-Bermudez et al., 2015) and TAG (triglycerides) as feedstock for biodiesel production. Pigments, like chlorophylls, are used as food colorant (Gouveia et al., 2007). Moreover, more valuable pigments such as β-carotene, lutein, tocopherols and astaxanthin are also exploited in cosmetics and pharmaceutics fields (Monari et al., 2016). Carbohydrates fraction are proposed for fermentation and bio-ethanol production (Fernandes et al., 2013) or as bulk chemicals (Gifuni et al., 2017). Bioproduct production by microalgae is currently limited because of the low biomass concentration and productivity. Although microalgal productivity far exceed crops culture, the plant and the processing costs still negatively affect the economy of the process (Ruiz et al., 2016; Tredici et al., 2016) and confine the microalgal productions to high value compounds. The low biomass concentration is one of the key factors that increase the processing costs and it is mainly caused by the low light availability in the large-scale culture systems currently used. Indeed, as the biomass concentration in a photobioreactor (PBR) increases an extended inner dark zone establishes. The low light irradiance in this zone becomes even smaller than the energy required for the maintenance of the cells and the photosynthetic efficiency of the culture is low (Janssen, 2016). In order to avoid light limitation, flat-panel PBRs (Qiang and Richmond, 1996; Cuaresma et al., 2011; Sforza et al., 2014; Pruvost et al., 2017) and open thin-layer (Doucha and Lìvansky, 2008) pounds have been proposed by several research groups. These culture systems are characterized by a short optical path (≤1cm) that reduces the PBR volume for unit irradiated area and the mutual shadowing effect among microalgal cells. The concentration and productivity of microalgae measured for these culture systems are quite high. Moreover, the flat-panel PBRs are easy to scale up and some applications as building-integrated PBR have already been proposed (Pruvost et al., 2016).

The current configuration of flat PBR systems are characterized by thickness larger than 7 mm (Quiand and Richmond, 1996; Pruvost et al., 2017). In this study a new designed ultra-flat PBR has been developed. The innovation is in the extremely reduced optical path of 3 mm aimed to increase the microalgal concentration and productivity. The production of the proposed PBR has been characterized with reference to a robust microalgal strain previously selected: *Chlorella sorokiniana* (Gifuni et al., 201-). The effect of the light intensity on growth, photosynthesis, and biochemical composition of the strain in the proposed PBR has been investigated. The light transfer model proposed by Pruvost and Cornet (2012) was applied to assess light limitation in the PBR and potential effects of light intensity limitation on the maximum biomass concentration and productivity.

Materials and methods

Ultra-flat photobioreactor system

The experimental apparatus consisted of an ultra-flat photobioreactor (UFP), an irradiance system, a cooling system, and a gas feeding system. The sketch of the new designed ultra-flat photobioreactor is reported in the Figure 5.1. It consists of three

Plexiglass panels (86 × 18 cm) spaced out by two silicone sheets, characterized by a thickness of 3 mm, conveniently cut out to outline the reactor. The thickness of the panels was 0.5 mm for each and they globally absorbed 1% of the incident irradiance (measured by light sensor Li-cor). Two compartments were formed by the sandwich structure panel-sheet-panel-sheet-panel. A compartment was exposed to the light and housed the microalgal culture. The other compartment was the cooling jacket equipped with four ports (two at the top and two at the bottom of the panel) for the cooling stream circulation. The final volume of the culture was 0.3 L. Gas stream was sparged into the culture from the bottom of the photobioreactors through four 1 mm orifices. The head of the PBR was equipped with four ports for the sampling and the vent. The reactor was chemically sterilized by 2% *Steril-C* sterilizing solution.

The irradiance system was made of two indoor and outdoor LED floodlight lamps (Tech-mar, Prince 4) able to irradiate up to 3500 µmol m^{-2} s^{-1}. The lamps irradiated the front side of the PBR. The irradiation was continuous (24/24 h) and the average light irradiance was set at different values between 50 and 1000 µmol m^{-2} s^{-1}.

The temperature of the PBR was kept at 25 ± 2° C by using an external thermos-cryostat connected to the cooling jacket.

The gas feeding system consisted of: air and pure CO_2 pressurized vessels; a gas mixing device (gas flow mixer *Bronkho*rst, model: *El-flow Select Series*); a hydrophobic filter (0.2 µm) to sterilize the gas stream fed to the PBR. The gas flow rate was set at 4 vvm. The CO_2 concentration was set between 2 and 18 % to control the pH of the culture at 7.

Strain and nutrients

The microalgal strain was *Chlorella sorokiniana* Shihiraet Krauss strain ACUF 318, provided by ACUF collection (http://www.acuf.net). The used media was BBM (Bold's Basal Medium) at modified nutrient concentration. The medium composition was (in g L^{-1}): $NaNO_3$ 1; $CaCl_2 \cdot 2H_2O$ 0.038; $MgSO_4 \cdot 7H_2O$ 0.15; K_2HPO_4 0.35; KH_2PO_4 0.35; NaCl 0.05; EDTA 0.1; KOH 0.124; H_3BO_3 0.023; $FeSO_4 \cdot 7H_2O$ 0.01; H_2SO_4 (2µL); $ZnO_4 \cdot 7H_2O$ 0.018; $MnCl_2 \cdot 4H_2O$ 0.003; MnO_3 0.002; $CuSO_4 \cdot 5H_2O$ 0.003; $Co(NO_3)_2 \cdot 6H_2O$ 0.001.

5 mL of 50-fold concentrated modified BBM were added to the culture when the nitrogen concentration was less than 10% of the initial in order to prevent any nutrient limitation.

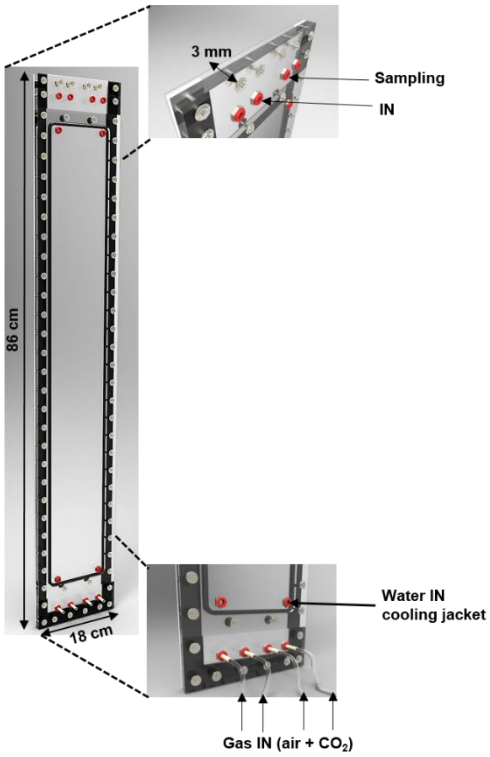

Figure 5.1: Sketch of the utra-thin flat photobioreactor

Measurements and assays

The microalgae concentration was measured by a spectrophotometer (*Specord 50 – Analytik Jena*) as optical density at 750 nm wavelength. The conversion factor between the optical density to the dry weight was assessed at different stage of the culture.

The nitrogen concentration in the medium was measured according to the spectrophotometric method reported by Collos et al. (1999).

The pH of the medium was measured by a pHmeter (*Mettler Toledo*).

The incident light irradiance on the PBR surface and the transmitted light irradiance at the back side of the PBR were constantly monitored by a light sensor (Li-cor quantum sensor LI-190).

The photochemical efficiency of the photosysthem II (f_V/f_M) was measured by fluorometer apparatus as described by Gargano et al. (2015). The microalgal sample concentration was set at 7 OD_{750nm}, the sample was dark adapted for 30 min, then it was exposed to actinic light at different intensity (0-1400 μmol m^{-2} s^{-1}).

Biochemical composition of microalgal biomass was carried out. Protein content, lipid content, total carbohydrates, and starch fraction were assayed according to the methodologies reported in Gifuni et al. (submitted) for microalgae harvested at different growth phase. It is worth to note that starch is the storage fraction of the total carbohydrates.

Chlorophyll a was measured by a fluorimeter (AquaFluorTM; Handheld Fluorometer/Turbidimeter; Turner Designs) was used to measure the content of chlorophyll a in vivo, in the untreated samples. The concentration of chlorophyll a was used to measure the amount of photsynthetic active pigments during thetests at the different light irradiances (Bilger et al., 1995).

Data analysis of the microalgal growth

The X_{max} was the maximum concentration reached in the PBR.

The specific growth rate (μ) of the strain was estimated under the exponential growth phase according to the relationship:

$$\mu = \frac{1}{t} \cdot \ln \frac{X_t}{X_0} \quad (5.1)$$

where X_t and X_0 are the biomass concentration at time t and at the beginning of the culture.

The biomass volumetric productivity (P_x, kg m^{-3} h^{-1}) was assessed as the ratio between the biomass concentration produced ($\Delta X = X_t - X_0$, kg m^{-3}) and the time t:

$$P_x = \frac{\Delta X}{t} \quad (5.2)$$

The biomass superficial productivity (A_x, g m^{-2} h^{-1}) was calculated as the product between the biomass volumetric productivity and the thickness of the reactor (δ, m).

$$A_x = \frac{\Delta X}{t} \cdot \delta \quad (5.3)$$

Data of productivity and biochemical composition were assessed at X_t about 10 kg m^{-3}. This value allowed considering all the tests during their exponential growth phase and at the same culture concentration. The tests carried out at irradiance set at 50 μmol m^{-2} s^{-1} make an exception for the biomass reference concentration (10 kg m^{-3}) because the culture did not reach the adopted concentration.

All culture tests were carried out in triplicates. The reported standard deviation referred to independent experimental replicates.

Light transfer model

The kinetic of cell growth in photosynthetic organisms is closely related to the rate of useful light energy absorption. The useful light energy for microalgae is a fraction of the total light spectra defined Photon Active Radiation (PAR) ranging between 400 and 700 nm (λ). Considering microalgae growth in a PBR, the absorbed useful energy is the ammount of photons absorbed per unit of time and unit of biomass weight (A; μmol g^{-1} s^{-1}). The available useful energy depends on the specific absorption cross-section of the microalgal species ($A_{abs,\lambda}$; m^2 kg^{-1}) and the radiation gradient along the optical path (z) of the PBR (G_z; μmol m^{-2} s^{-1}) as detailed in Pruvost and Cornet (2012). According to this approach, the mean available useful energy ($< A >$; μmol kg^{-1} s^{-1}) is the average value of A along the PBR thickness and can be expressed as:

$$< A >= \frac{1}{L} \int_{400}^{700} \int_0^L A_{abs,\lambda} \, G_z(z) \, dz d\lambda \quad (5.4)$$

L is the total thickness of the PBR (m), and z the depth coordinate of the PBR.

The minimum specific rate of photon absorption required for the cell maintenance is defined as $\mathcal{A}_C$, specific rate of photon absorption at the compensation point. Its value was equal to 1.5 μmol g^{-1} s^{-1} for *C. vulgaris* (Souliès et al., 2016).

This model proposed by Pruvost anfd Cornet (2012) was used to predict the maximum biomass productivity in a PBR. The same model was applied by Kandilian et al. (2014) to calculate the minimum $< A >$for maximizing the TAG production during nitrogen depletion. Souliès et al. (2016) adapted the model to *C. vulgaris* cultures to predict irradiative transfer, pigment adaptation, and biomass productivity as a function of specific irradiation conditions. In this study, experimental data were used for the calculation of $< A >$ at the end of the microalgal growth and to verify if it match the compensation point. Parameters related to spectral mass absorption and spectral mass scattering were set as reported by Souliés et al. (2016) for *C. vulgaris* under no nutrient limitation.

Results

Batch testes were carried out in the new designed ultra-flat PBR using the microalgal strain *C. sorokiniana*. The first batch test was carried out at medium incident light irradiance (300 µmol m^{-2} s^{-1}) already set in previous studies carried out with different typology of PBR (Gifuni et al., submitted; Pruvost et al., 2017). The campaign was addressed to assess the performances of the proposed UFP in terms of maximum biomass concentration, productivity and biochemical composition. A second campaign of tests was carried out to investigate the effect of the incident light irradiance on the biomass production, the biochemical and photochemical response of microalgae. The light transfer model was applied to investigate the potential presence of an upper limit in the increase of biomass concentration in this culture system depending on the light availability.

Batch growth in UFP

Preliminary tests were carried out with *C. sorokiniana* to select the optimal inoculum conditions (growth phase and initial concentration, X_0) to support the growth in the investigated UFP. The optimal initial conditions consist in: inoculum cultures under exponential growth phase and initial microalgal concentration of 0.3 kg m^{-3}. Under the selected conditions, the growth lag phase was almost absent.

The Figure 5.2 reports the growth curve of *C. sorokiniana* measured in the UFP operated at irradiance of 300 µmol m^{-2} s^{-1}. The lag phase was absent. The exponential growth phase extended over the first 40 h of culture until the biomass concentration was about 10 kg m^{-3}. Then the growth became linear until about 20 kg m^{-3} and approached a stationary phase. The average specific growth rate under exponential growth phase was about 0.05 h^{-1}. The maximum biomass concentration was 24 kg m^{-3}. The volumetric and superficial productivity were 465 g m^{-3} h^{-1} and 1.34 g m^{-2} h^{-1}, respectively. The biochemical composition of *C. sorokiniana* under exponential growth conditions was: 35%$_{DW}$ of proteins, 29%$_{DW}$ of starch, and 15 %$_{DW}$ of lipids.

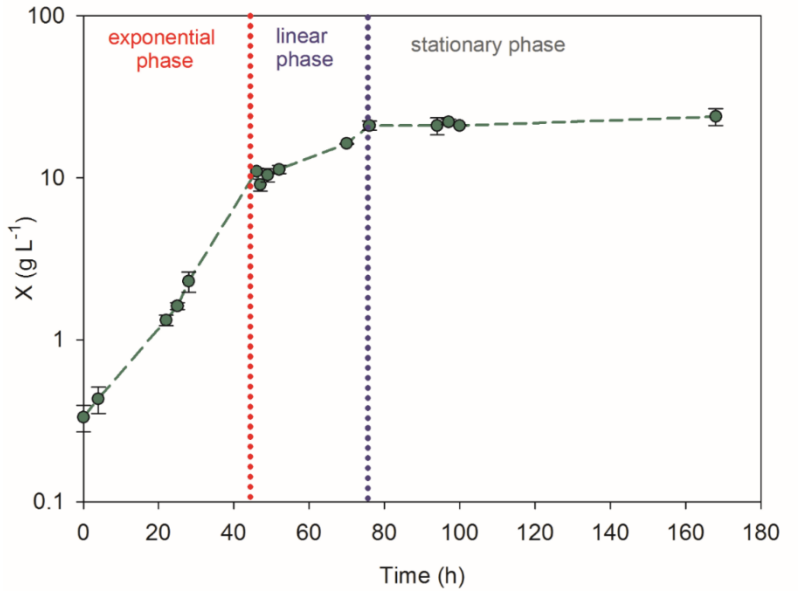

Figure 5.2: Growth curve of *C. sorokiniana* in the ultra-flat PBR. Light irradiance: 300 µmol $m^{-2}s^{-1}$.

Effect of incident light intensities

The extremely reduced optical path (0.003 m) of the UFP proposed in this work strongly increased the light availability throughout the optical path. Then, the critical point is the investigation of the effect of the different light irradiances on the microalgal photosynthesis, growth and biochemical composition, in the proposed UFP.

The Figure 5.3 reports the biomass superficial productivity, the cell growth rate and the maximum biomass concentration as a function of the light irradiance I_0. The superficial productivity was calculated at X_t=10 kg m^{-3} except for the tests carried out at 50 µmol m^{-2} s^{-1}. The specific growth rate and the superficial productivity show that the increase of light irradiance effectively causes an increase in the microalgal growth during exponential phase. It is possible to notice a significant improvement in growth rate and productivity between 50 and 150 µmol m^{-2} s^{-1}. Then, the curves slow down keeping almost constant values between 150 and 300 µmol m^{-2} s^{-1} and further increase for 750 and 1000 µmol m^{-2} s^{-1} reaching a maximum at 1000 µmol m^{-2} s^{-1}. The maximum growth rate was 0.1 h^{-1}, while the maximum superficial productivity reached was 3.45 g m^{-2} h^{-1}.

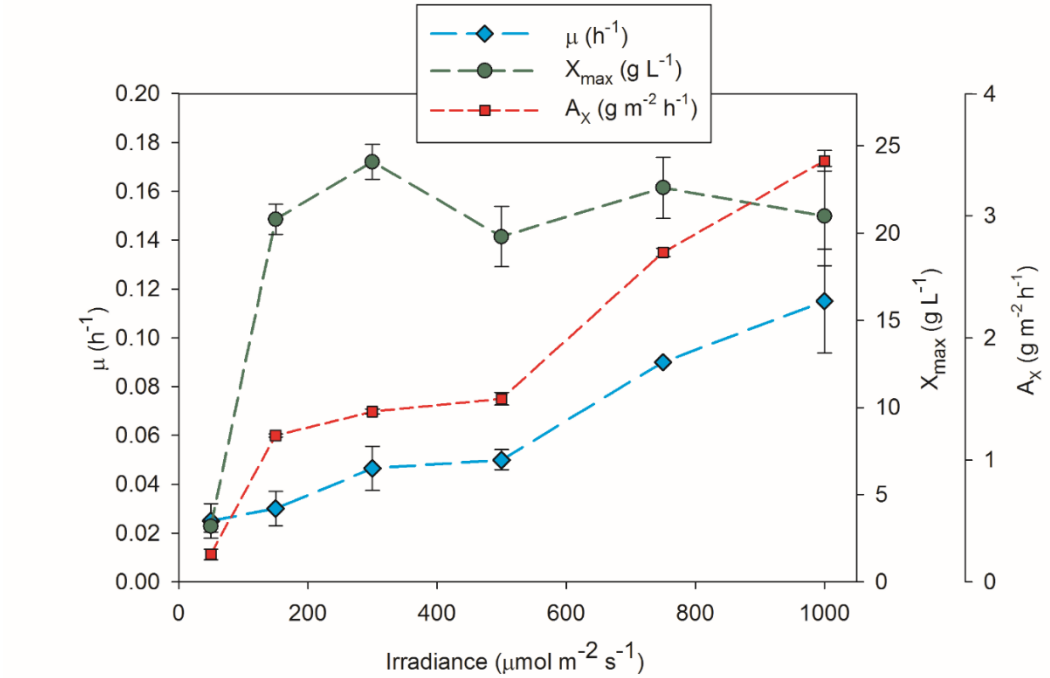

Figure 5.3: *C. sorokiniana* superficial productivity (A_X), cell growth rate (µ) and cell maximum concentration (X_{max}) vs. the incident light irradiance.

The maximum biomass concentration X_{max} increased with the irradiance and approached 2 kg m^{-3} at 300 µmol m^{-2} s^{-1}. X_{max} was almost constant at higher light irradiances: a biological/physical limit of the system appears to be reached.

Data about photochemical efficiency of the photosysthem II are reported in the Figure 5.4. The data are representative of cultures carried out at three light irradiances significantly different each other: low (50 µmol m^{-2} s^{-1}), medium (300 µmol m^{-2} s^{-1}), and high (1000 µmol m^{-2} s^{-1}). f_V/f_M ranged between 0.6 and 0.76, typical of healthy microalgae and efficient photosynthetic activity (Masojídek and Torzillo, 2014). The highest f_V/f_M value (0.76) was measured for samples grown at 50 µmol m^{-2} s^{-1}, a condition of low light intensity that stimulated an intensive use of the photosynthetic apparatus to support cell surviving. On the contrary, the high light intensity of1000 µmol m^{-2} s^{-1} did not stimulate the photosynthetic apparatus and f_V/f_M ranged between 0.6 and 0.65.

The biochemical composition of *C. sorokiniana* - expressed in terms of starch, total carbohydrates, proteins and lipids for the test at different light irradiance - is reported in the Figure 5.5. The biochemical composition of the biomass reflects how the energy of the received photons was used for biomolecules synthesis. The carbohydrate and starch content were characterized by a maximum at light irradiance 300 µmol m^{-2} s^{-1}:

40 and 30%$_{DM}$, respectively. At the highest light irradiance, their content reduced to 30 and 16% of DW, respectively. The opposite behavior can be observed for the protein content: it was constant (about 35%) up to light irradiances of 300 µmol m^{-2} s^{-1} and it increased up to 50% of the DW at the highest investigated irradiance. Lipid content decreased with the light irradiances: the maximum (50 µmol m^{-2} s^{-1}) was measured at 30%$_{DW}$ at 50 µmol m^{-2} s^{-1} and decreased at the 10%$_{DW}$ at 1000 µmol m^{-2} s^{-1}.

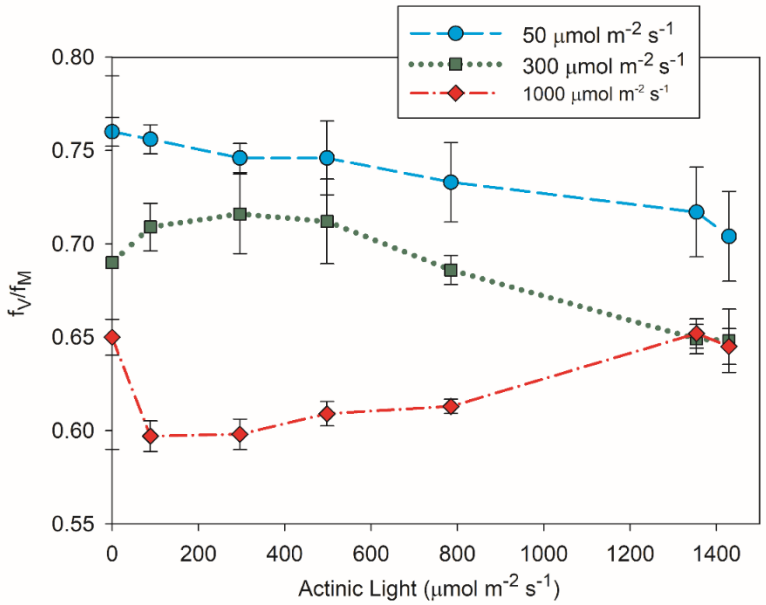

Figure 5.4: Photochemical efficiency of the photosysthem II (f_V/f_M) of *C. sorokininana* during exponential growth phase (10 kg m^{-3}) Data refer to tests carried out at low (50 µmol m^{-2}s^{-1}), medium (300 µmol m^{-2}s^{-1}), and high (1000 µmol m^{-2} s^{-1}) light irradiance.

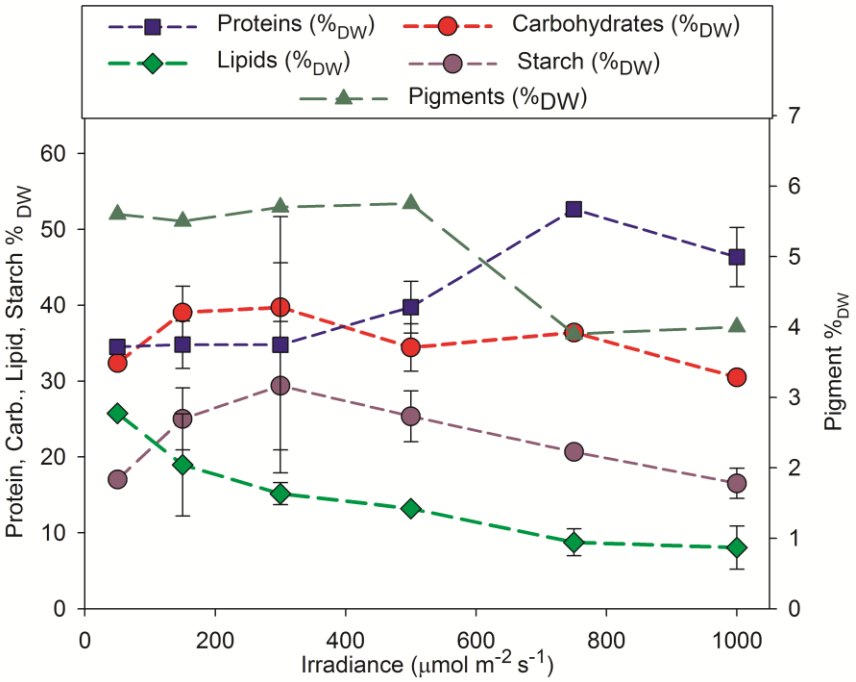

Figure 5.5: Starch, total carbohydrates, proteins, lipids and pigments content of *C. sorokiniana* growth in the ultra-flat PBR as a function of the light irradiances. Pigment standard deviation is negligible (≤5%).

Discussion

Improvement of the ultra-flat PBR

The biomass concentration of the cultures carried out in the new ultra-flat PBR was 10 times higher than that measured in cultures carried out in the conventional bubble column PBRs (Mizuno et al., 2013). The high biomass concentration reduces the energy and costs of the culture exploitation processes. Indeed, the centrifugation energy (cost) for microalgal harvesting is about 1/10 than that required to harvest microalgae from dilute cultures that it is about the 33% of the energy stored by the biomass (Ancièn et al., 2012).

Gifuni et al. (submitted) reported that the key limiting factor for microalgal growth and starch accumulation is the light availability when the culture concentration increases over 1 kg m^{-3}. The table 5.1 reports the biomass concentration, the volumetric and the superficial biomass productivity, and the biomass composition of *C. sorokiniana* measured in the cultures carried out in the bubble column PBR and in the UFP with the same strain and under the same operating conditions. The comparison of the data reported in the table 1 points out that the light exploitation in the UFP is higher than in the bubble column photobioreactor. Volumetric productivity increased of a factor of about 20 when the ultra-flat PBR is used. The superficial productivity is slightly reduced from 1.75 to 1.34 g m^{-2} h^{-1} when moving from bubble column PBR to ultra-flat PBR due to the high surface/volume ratio typical of thin PBR. Starch fraction was reduced in flat PBR (29% instead of 38% of bubble column PBR) while protein content increased (from 27% to 35%). The increase of the light availability for the UFP cultures enhanced the cell growth and the associated protein synthesis: more energy is spent for cells reproduction than for energy storage as starch and lipids.

	Thickness (m)	P_X ($gm^{-3}h^{-1}$)	A_X ($gm^{-2}h^{-1}$)	ωStarch ($\%_{DW}$)	ωProteins ($\%_{DW}$)	ωLipids ($\%_{DW}$)	Ref
Bubble column PBR	0.08	22 ±0.2	1.75 ±0.1	38.2 ±3.9	26.8 ±3.2	16.0 ±1.8	Gifuni et al., (submitted)
Ultra-flat PBR	0.003	465 ±0.7	1.34 ±0.02	29.4 ±8.5	34.8 ±6.9	15.2 ±1.5	This work

Table 5.1: *C. sorokinina* productivity and composition in two type of PBRs. Light irradiance: 300 μmol m^{-2} s^{-1}.

The table 5.2 reports biomass concentration and productivity reported in the literature for cultures carried out in flat PBRs. Reported data refer to cultures carried out under controlled conditions of temperature, pH, gas flow rate, and CO_2 concentration. Typically, the temperature was set between 20 and 35°C (depending on the used strain), the pH between 6-8, the air flow ranged between 0.2-6.2 vvm, the initial CO_2 percentage was between 2 and 5%. The light irradiance sources and intensity supplied in the different studies were also reported in the table 2. Cuaresma et al. (2011) investigated simulated outdoor conditions. Doucha et al. (2008) investigated outdoor cultures. The other investigations applied continuous irradiation at selected specific intensities. The spectrum of operating conditions, strains, and type of reactors make difficult a direct comparison of the data reported in the literature. The productivity measured in the present study is in agreement with that reported by Pruvost et al. (2017) for cultures carried out under comparable light irradiance. The

highest volumetric productivity of 0.57 kg m^{-3} h^{-1} reported by Prouvost et al. (2015) may be due to the reactor's thickness of 7 mm that allowed a faster cell growth and about 20 kg m^{-3} at irradiance of 430 µmol $m^{-2}s^{-1}$. The highest surface productivity reported by Cuaresma et al. (2009) (7 g m^{-2} h^{-1}) for cultures carried out in a 14 mm flat PBR may depend on the high light irradiance (2100 µmol m^{-2} s^{-1}) and the continuous mode applied. The biomass concentration achieved 6 kg m^{-3}. The biomass concentration achieved in the ultra-flat PBR is lower than Doucha et al. (2008) which reached 40-50 kg m^{-3} even though the productivity is about 1/3 of that measured in the present investigation. Probably the better productivity is due to different mixing system which is provided by the gravity (in the cascade layer) instead of the bubbling (thin-flat panel).

Altogether, the proposed ultra-flat PBR was characterized by high potential when compared with the PBRs reported in the literature and characterized by the same design. The proposed system effectively provides efficient use of the irradiated light.

PBR O.P. (mm)	Strain	P_X (kg $m^{-3}h^{-1}$)	A_X (g $m^{-2}h^{-1}$)	X_{max} (kg m^{-3})	Irradiance (µmol $m^{-2}s^{-1}$)	$Y_{X/E}$ (g mol^{-1})	Reference
14	*C. sorokiniana*	0.5*	7	6	2100	0.07	Cuaresma et al. 2009
7	*C. vulgaris*	0.57	4	20	430	0.37	Pruvost et al. 2015
6	*Chlorella sp.*	0.18	1.1	40-50	outdoor	0.17	Doutcha et al. 2008
3	*C. sorokiniana*	0.47	1.3	24	300	0.44	This study
1.3-2.2	*C. vulgaris*	0.08 0.29**	0.15 0.52	30 22	120 270	0.19 0.31	Pruvost et al. 2017

*continuous mode; **semi-continuous mode

Table 5.2: Comparison of performance measured for cultures carried out in flat PBRs.

Growth limitation and light availability

The plots of the biomass concentration, growth rate and productivities (Fig. 5.3) measured for cultures carried out in the UFP highlights the presence of a maximum for the biomass concentration: about 20 kg m^{-3}. Although the growth rate and the productivities increased with the light irradiance, the biomass concentration growth stopped at 20 kg m^{-3}. Several phenomena could be responsible of this maximum concentration and they are hereinafter discussed. The continuous gas supply and the vent of the PBR avoided the accumulation of oxygen and potential growth inhibition by gaseous species. The increase of the CO_2 concentration in the inlet gas stream up to 20% was proved to be tolerated for *Chlorella* species (Acién et al., 2012, Hussain et al., 2017). Moreover, if we consider a constant mass transfer coefficient for the CO_2 from gas to liquid (K_{La,CO_2}), the CO_2 concentration in the culture will increase with the its concentration in the gas stream. It means that the rate of CO_2 supply to the culture increases. Since the biomass production rate is also proportional to the CO_2 supply rate, the more we increase the CO_2 concentration the more should increase the biomass concentration. Doucha and Lìvansky (2006) supposed that the increase of the CO_2 supply rate caused a coalescence of the bubbles, which decrease the specific gas-liquid interface and then the CO_2 mass transfer to the culture. Anyway, further investigations are needed to prove this phenomenon. The observed limit of biomass concentration could depend on the saturation of photosynthetic system: it could not convert all the received light into chemical energy to be channeled into biomass production. However, the measurements of the f_V/f_M (Figure 5.5) point out that the maximum photosynthetic efficiency of dark-adapted cells (0 µmol m^{-2} s^{-1}) was the same found for the actinic irradiance corresponding to light intensity of the growth of each

sample. Therefore, it could be inferred that the cultures were well adapted and they were not stressed whatever the irradiances set for the tests. In addition, the increase/decrease of tested actinic light intensity caused a slightly reduction in f_V/f_M pointing out cell resistance to high light irradiances. Photosynthetic data proved that the investigated strain was characterized by high tolerance to the investigated light intensity. The photosynthetic apparatus of the strain can quickly adapt to the operating conditions. This feature is also supported by the constant content of the photosynthetic active pigments (Chl a) until the stationary phase established.

The light transfer model reported in method section points out that the absorbed light depends on the light received and on the ability of the cells to absorb the light. The absorption ability is a function of the pigment content, which it is affected by the light intensity. Indeed, Kandilian et al. (2014) proposed that the key factor affecting the cell growth rate is the absorbed light by the microalgal culture at high concentration and it is not the rate of the mixing in the PBR. The reported light transfer model proposed that the biomass concentration in cultures characterized by no limiting nutrient (light included) increases up to the $< A >$ matches the compensation point A_C of 1.5 µmol g^{-1} s^{-1} (Souliés et al., 2016). Figure 5.6 reports the measured X_{max} vs. the estimated $< A >$ as a function of the irradiance. Assuming the parameter proposed by Souliés et al. (2016), the scenario proposed by the model does not fit with the cell growth results. Indeed, the maximum biomass concentration in the ultra-flat PBR is not related to the $< A >$. The medium rate of energy absorption under stationary phase was higher than the compensation value except for the incident light irradiance of 1000 µmol m^{-2} s^{-1}. For incident light irradiance of 50 and 300 µmol m^{-2} s^{-1} the medium rate of energy absorption at the end of the growth was about 3 µmol kg^{-1} s^{-1} (twice the compensation value). For irradiance of 500 and 750 µmol m^{-2} s^{-1} the medium rate of energy absorption was about 7 µmol kg^{-1} s^{-1}. $< A >$ is 1.3 µmol kg^{-1} s^{-1} (about the A_C) at 1000 µmol m^{-2} s^{-1} but the measured maximum biomass concentration does not change with respect to that measured for the other tests (500-750 µmol m^{-2} s^{-1}).

The supply of CO_2 to the culture at high biomass concentration was provided by increasing the CO_2 concentration in the gas stream - at constant gas flow rate - and keeping the pH at 7-7.5. Under these conditions, it may be assumed that the CO_2 was not a limiting substrate. Therefore, CO_2 depletion can not be responsible of the maximum biomass concentration.

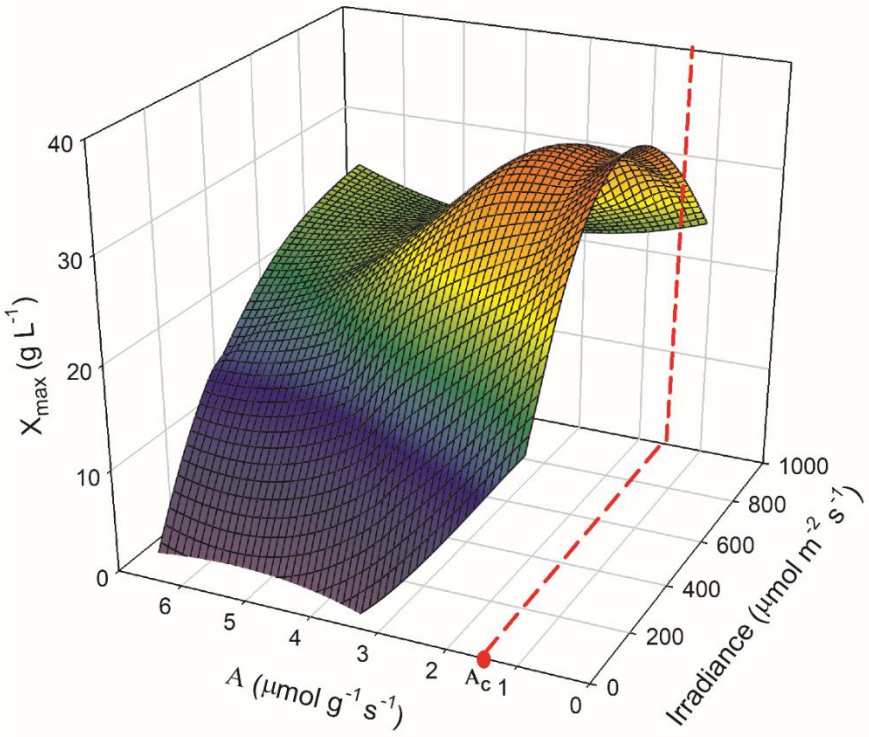

Figure 5.6: Maximum biomass concentration (X_{max}) vs. the incident irradiance and of the mean rate of photon absorption (A).

Biochemical composition and biorefinery applications

The biochemical composition of microalgae depends on the growth conditions and nutrient supply strategy. In the present study, the tests were carried out at different light irradiance and without limiting nutrients. The biochemical composition was characterized for microalgae sampled during the exponential growth phase (Figure 5.5). The fraction of protein and of the energy storage molecules depended on the irradiance. In particular, the biochemical composition can be related to the photon flux and the photon investment strategy of cells in the growth and energy storage pathways. According to the model proposed by Klok et al. (2013), the electrons produced by photosynthesis can have different allocations: functional biomass (mainly proteins), storage molecules (starch and lipids), maintenances and respiration. Moreover, Klok et al. (2013) concluded that high photon flux (> 300 µmol m^{-2} s^{-1}) stimulates functional biomass synthesis and cell growth: at high light irradiance, more energy is diverted in the growth to the detriment of starch and lipid accumulation. The model proposed by Klok et al. (2013) is in agreement with the results of the present results as regards the starch and total sugar productions. The productions were characterized by a maximum at irradiance of 300 µmol m^{-2} s^{-1}. At this irradiance, the photosynthetic rate is still higher than the growth rate and the produced energy is accumulated as starch. The presence of a theoretical maximum for the sugar production at irradiance of about 300 µmol m^{-2} s^{-1} was also pointed out by Janssen et al. (2016) that reported a model of specific sugar production. Janssen et al. (2016) demonstrate that the irradiance 300 µmol m^{-2} s^{-1} is effectively a turning point between the storage specie accumulation and the cell growth. For photon flux higher than 300 µmol m^{-2} s^{-1}, the energy is mainly diverted to protein synthesis to support the cell growth and the cellular division. Lipids accumulation is generally associated to stress conditions, such as nutrient depletion. The nutrient supply strategy adopted in the present investigation kept the nutrient

concentration always above the depletion level and just a small lipid accumulation was measured, especially at high irradiance.

The light decrease of pigment content - from 5.5 to 4 $\%_{DW}$ - with the irradiance was not associated to any decrease in the cell growth rate and in the synthesis of proteins and carbohydrates. The absence of any effect on growth and synthesis was expected because the measured pigment content is close to the non-stressed cultures (5%). The decrease of the pigment content from 5.5 to 4% was probably due to the high irradiance (750-1000 µmol m^{-2} s^{-1}). Under these conditions, the microalgae did not need high pigment concentration to capture the light because the light was already provided at large rate.

The possibility to address the biomass composition by tuning the irradiance or to forecast the biomass composition as a function of the sun light irradiance is a key issue to exploit microalgae according to the biorefinery concept. All the characterized biomolecules find a variety of applications and the increase of the biomass concentration and productivity effectively provide the opportunity to make the production process cost-effective reducing of harvesting and processing costs. The high growth rate under exponential phase cultures effectively increases the productivity of the single molecules even though their fractions of the microalgal dry weight (see starch and lipids) are smaller than those measured by adopting nutrient-depletion strategies. In particular, the strong increase of the protein production suggests promising applications for the productions of food additives (Wijffels et al., 2010).

The reported results also suggest the possibility of predicting the biomolecules production as a function of the light irradiance experimented by cultures in an outdoor large-scale flat-panel biorefinery system.

Conclusions

This study provided that the reduction of the optical path of PBR to 0.003 m enhance the biomass productivity. Microalgal concentration of 10 kg m^{-3} may be established in less than 100 h at medium light energy input of 300 µmol m^{-2} s^{-1}. Moreover, the increase of the light irradiance provided an increase in the growth rate and protein fraction of the biomass. Further investigation is required to increase the biomass concentration for the complete exploitation of the ultra-flat PBR potential. Indeed, the effective light absorption by cells does not match the compensation value.

6. DOWNSTREAM PROCESSES FOR THE RECOVERY OF STARCH AND OTHER BIOPRODUCT FROM MICROALGAE

This activity was focused on the downstream processes for the simultaneous recovery of starch and other bioproduct from microalgae. This activity is divided in three sections. The section 6.1 reports an extended abstract regarding the simultaneous recovery of starch and antioxidant molecules from *Chlorella sorokiniana* biomass, the full article is reported in the appendix (Petruk et al.-Appendix). It was the result of a fertile collaboration with Dr. Ganna Petruk, Biotechnology PhD student at the Università degli Studi di Napoli Federico II. Both PhD project shared the objective to recover natural and renewable products of commercial interest. The section 6.2 is focused on the bead millng cell disruption and the prediction product fractionation after a mild centrifugation. The section 6.3 is focused on the purification of the proteins, recovered in the supernatant of the previous task, using membrane filtration.

6.1 Simultaneous production of antioxidants and renewable molecules from microalga *Chlorella sorokiniana*.

G. Petruk[a], I. Gifuni[b], A. Illiano[a], M. Roxo[c], G. Pinto[a], A. Amoresano[a], A. Marzocchella[b], R. Piccolia[d], M. Wink[c], G. Olivieri[b]*, D.M. Monti[ad]*.

[a]Department of Chemical Sciences, University of Naples Federico II, Complesso Universitario Monte Sant'Angelo, via Cinthia 4, 80126, Naples, Italy
[b] Dipartimento di Ingegneria Chimica, dei Materiali e della Produzione Industriale, Università degli Studi di Napoli Federico II, Piazzale Tecchio, 80, Naples, Italy.
[c]Institute of Pharmacy and Molecular Biotechnology, University of Heidelberg, Heidelberg, Germany
[d] Istituto Nazionale di Biostrutture e Biosistemi (INBB), Rome, Ital

Keywords: antioxidants/ *Chlorella sorokiniana*/eukaryotic cells/ microalgae/*Caenorhabditis. elegans*

Abbreviations: **DCF**, 2',7'-dichlorofluorescein; **DTNB**, 5,5′-dithiobis-2-nitrobenzoic acid; **EDTA**, ethylene diamine tetra acetic acid; **EE**, ethanol extract; **H_2-DCFDA**, 2',7'-dichlorodihydrofluorescein diacetate; **P-p38**, phosphorylated p38 MAP kinase; **P-MAPKAPK-2**, phosphorylated MAP kinase-activated protein kinase; **ROS**, reactive oxygen species; **r.t.**, room temperature; **TFA**, trifluoroacetic acid; **TNB**, 5-thio-2-nitrobenzoic acid.

Extended Abstract

Microalgae are considered an interesting resource for circular bioeconomy. Microalgal biomass is renewable, besides for its production, the industrial byproduct CO_2 and the sun light energy are required. No competition exists with food culture for arable land. The recent studies are mainly focused on the exploitation of various microalgal component in order to obtain the maximum economic benefit, moreover the conversion of biomass into different product produce minimal waste to the environment, then it can be considered certainly sustainable (Chew wt al., 2017; Ruiz et al., 2016). It encourages the investigation of new biorefinery approaches towards a multicomponent cascade extraction process. Previous works investigated the opportunity of using starch carbohydrates fraction of microalgae for bioplastics and selected *Chlorella sorokiniana* as robust strain for large scale production (section 3.1). Moreover, the conditions selected for the starch accumulation (early nitrogen depletion) are also reported to increase the procustion of pigments with antioxidant activity (Goiris et al., 2015). The lab-scale optimized protocol for starch purification (Gifuni et al., 2017)

consider the removal of the pigments by ethanol extraction also considered a safe solvent (law 2009/32/CE). Then, the goal of the study was the application of ethanol extraction and the estimation of: i) the antioxidant activity of ethanol extract of the microalga *Chlorella sorokiniana* and ii) the starch recovery in the extracted pellet. The recovery of other molecules (such as lipids, proteins and simple sugars) in the extracted pellet was also measured. The materials and methods adopted are reported in the full-length article (Appendix). With the extraction protocol proposed, it was possible to recover 82.9% of the initial starch, with a significant amount of proteins (78.3%). Only 17.0% of the initial lipid content remained in the pellet after the extraction. Therefore, starch recovery was considered satisfying. Simple sugars seem to increase in the pellet with respect to the untreated biomass, probably because part of the initial starch is reduced in simple sugars during the treatment. The composition in proteins and lipids of extracted pellet suggests applications as feedstock for bioplastics or as feed or food complements without further treatments. Introducing further separation steps, all the components of the pellet could be separated and exploited as biochemicals in different industrial fields, with higher profit. For example, proteins could be used for animal feed (Gifuni et al., 2017), starch as bulk chemicals in food or pharmaceutical industries (Zhu, 2015) and lipids as food emulsifier or for biofuel production (Fernandes et al., 2013). The ethanol extract was characterized in terms of biochemical composition and it resulted that: most of the lipids were extracted (29.5 ± 3.6 mg); small amount of proteins and simple sugars were detected (12.5 ± 1.3 mg and 4.9 ± 0.8 mg, respectively); carotenoids, chlorophyll a and b content were 0.17 ± 0.23 mg, 0.79 ± 0.11 mg and 0.66 ± 0.09 mg, respectively. The in vitro activity on human cancer colon cells (LoVo), showed high biocompatibility and no oxidative stress induction by the microalgae extract. The in vivo activity was tested on Caenorhabditis elegans and the results confirmed that the microalgal extract effectively reduces the injury caused by oxidative stress by inhibiting ROS production and activating DAF-16/FOXO transcription factor pathway. We observed that a pool of molecules from three different classes (fatty acids, photosynthetic pigments and carotenoids) were synergistically responsible for this activity. This study does not identify which class of molecules the antioxidant activity is due, or if there is a synergistic effect among them. It has to be taken into account, that the novelty of the present work is in the proved feasibility of the cascade approach to isolate two different high value products, starch and antioxidants from renewable and sustainable feedstock.

6.2 Effect of bead milling parameters on the product recovery in microalgal biorefinery

I. Gifuni[a], T. R. Zinkone[b], J. Pruvost[b], L. Marchal[b*]

[a] Dipartimento di Ingegneria Chimica, dei Materiali e della Produzione Industriale, Università degli Studi di Napoli "Federico II", Piazzale Tecchio, 80, Naples, Italy.
[b] GEPEA, UMR CNRS 6144, University of Nantes, 37 bd de l'Université 44602 Saint Nazaire Cedex, France

Keywords
Bead mill, microalgae, biorefinery, stress model, specific energy.

Abstract
Microalgae biorefinery represents a sustainable solution for renewable feedstock supply. One of the key issues of the microalgal biorefinery is the cell disruption for intracellular product release. In this study, bead milling disruption is analyzed and the relation between disruption parameters and the effective recovery of the products in two different fractions, after mild centrifugation, was investigated. The stress model was applied and the optimal parameters range, to balance efficient disruption and efficient energy use, was identified. Then, the product fractionation yield and selectivity were correlated to the different energetic region identified by the stress model. A clear behaviour appeared. Before the critical energy, the highest proteins yield was obtained (80%), but high chlorophyll is also released in the supernatant. For specific energy higher than the critical values, it was measured higher starch yield (85%) in the pellet and lower selectivity for pigment in the supernatant (0.02).

Graphical abstract

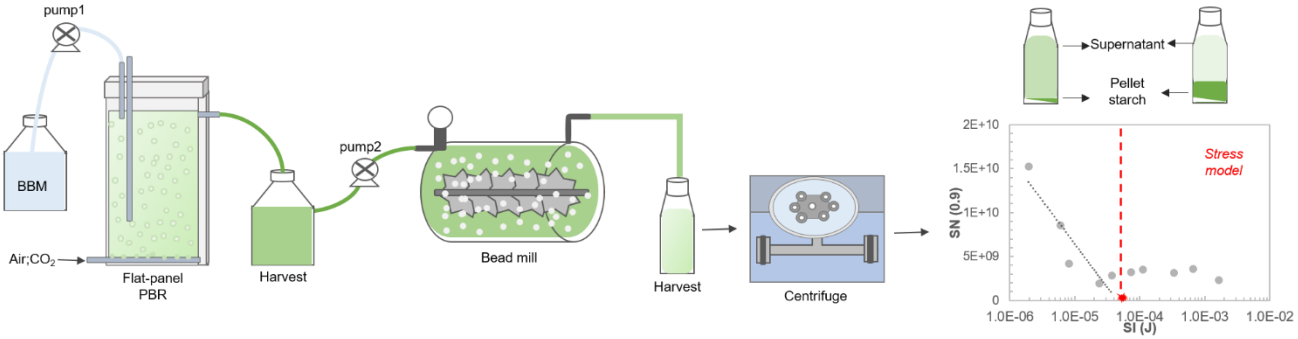

Introduction

Nowadays, microalgae are considered as sustainable source of feedstock for different industrial fields: food, fuels, pharmaceutics (Chisti et al., 2006; Wijffels and Barbosa 2010; Draaisma et al., 2013). The recent trends in microalgae production are focused on the biorefinery of the biomass for the simultaneous exploitation of different components for a more cost-effective process (Chew et al., 2017; Moreno-garcia et al., 2017). In this context, one of the bottlenecks of the microalgae production is the downstream. Downstream processes include harvesting, cell disruption, extraction, purification and characterization of the products and it counts more than 50% of the overall production costs (Davis et al., 2016). The recovery of the microalgae products is highly influenced by its release from the cells; in this sense, the cell disruption is a

crucial step. Mechanical cell disruption, in particular bead milling, is now considered the most suitable technique for industrial scale application because of the high efficiency and the commercially available equipment even at large scale (Günerken et al., 2015). Moreover, mild cell disruption conditions can be selected to preserve the integrity and the value of the product (Phong et al., 2017). The drawbacks are the high energy demand and heat production, the process is considered not selective for the product release and producing fine cell debris, difficult to process.

Regarding the bead milling cell disruption, several studies were addressed to the description of the process from the mathematical point of view in order to find the main parameters for the optimization. In particular, the cell disruption kinetic was successfully described with a first order kinetic by Balasundaram et al. (2012), Garrido et al. (1994), Montalescot et al. (2015). Kwade and Schwedes (2007) proposed the Stress model to describe the comminution of the cells as function of the process parameters and the calculation of the energy input as function of these parameters was also carried out. The stress model allows the identification of critical region corresponding to the optimal parameters to balance efficient disruption and efficient energy use. This model, initially used for yeast disruption was also applied to microalgae (Montalescot et al., 2015; Postma et al., 2017). Moreover, the increase of biomass concentration was reported to be a key issue for the reduction of bead milling energy consumption (Postma et al., 2017).

The effective target of the milling for microalgae biorefinery application is not only the cell disruption, but also the release of the intracellular metabolites. Cell disruption and product release were considered two different phenomena occurring in the mechanical disruption and the release of some molecules do not follow a linear model (Heim et al., 2007). Postma et al. (2015) suggested to apply a first order kinetic model for pigment and proteins release and the kinetic constant was related to the localization of the component in the cytoplasm or intracellular organelles.

A real breakthrough in the microalgae products exploitation will came from a thorough knowledge of the relation between bead mill disruption parameters and the effective recovery of the products. In the present study, the recovery of the products is analyzed as further step following cell disruption and product release. The recovery considers the effective collection of the desired molecules in a liquid of solid fraction after the centrifugation step. Three different products were analyzed: proteins, chlorophyll and starch. Proteins fulfil considerable importance in the food industry, but their combination with highly coloured pigment as chlorophyll are not appreciated. Starch is a storage polysaccharide with many industrial applications (Gifuni et al., 2017). The recovery of the starch structure as insoluble granules entails its location in the pellet after disruption and centrifugation. The centrifugation parameters were set in order to ensure low energy investment in the centrifugation step and compatibility with low-cost and large-scale equipments.

The aim of this study is to identify a relation between bead milling parameters, elaborated with the stress model, and the selectivity for specific cell metabolite recovery for a more aware process optimization and customization. To this end, the repartition of the proteins, pigment and starch between pellet and supernatant was analysed and related to the energetic input of the bead milling.

Materials and methods

Microalgal strain and culture

The microalgal strain used in this study was *Chlorella sorokiniana* Shihiraet Krauss strain (ACUF 318) provided by ACUF collection (http://www.acuf.net). The growth was performed in autotrophic conditions using modified BBM medium (Van Vooren et al., 2012). The culture of this strain was carried out in a flat panel photobioreactor (PBR) of 5 L characterized by a thickness of 3 cm and continuously illuminated on the front side by white light at 280 µmol m^{-2} s^{-1}. The PBR was operating in continuous mode with a dilution rate of 0.4 day^{-1} in order to have every day the minimum amount of culture for disruption experiments with constant and reproducible biomass conditions for each test. The microalgal culture, at steady state (concentration of 1 g L^{-1}) was directly processed by bead milling without previous concentration step.

Bead milling disruption

Disruption experiments were performed in Dyno-mill multi lab from Willy A Bachofen AG (4 kW, Muttenz, Switzerland). The bead milling was operated in pendulum mode as already described by Montalescot et al. (2015). The temperature was maintained at 20°C, the flow rate was set at 200 mL min^{-1} and the filling ratio of the grinding media at 80%. Beads density (glass, zirconia), beads diameters (0.2-1.3 mm) and the rotation speed (8-14 $m.s^{-1}$) were varied in order to test different stress intensities referred to the stress model. First order kinetic was applied to the cell disruption and product recovery, taking into account the non-ideal flow inside the chamber (Montalescot et al., 2015). Specific energy requirement for the 90% of cell disruption was calculated according to Montalescot et al. (2015) and Postma et al. (2017). The equations for the calculation of kinetic constant (k), stress intensity (SI), stress number for the 90% of cell disruption ($SN_{0.9}$) and specific energy requirement for the 90% of cell disruption (E_m) are reported hereinafter:

$$x = 1 - e^{-kt} \quad (6.2.1)$$

$$t_{0.9} = -\frac{\ln(1-0.9)}{k} \quad (6.2.2)$$

$$SI \propto d^3\, \rho\, v^2 \quad (6.2.3)$$

$$SN_{0.9} \propto \frac{\varphi\,(1-\varepsilon)}{\{1-\varphi(1-\varepsilon)\}\cdot C}\,\frac{n\cdot t_{0.9}}{d} \quad (6.2.4)$$

$$E_m \propto \frac{SN_{0.9}\cdot SI}{m} \quad (6.2.5)$$

Where, x is the fraction of disrupted cells (or recovered product); $t_{0.9}$ is the comminution time to reach the 90% of disruption (s); d is the beads diameter (m); ρ is the beads density (kg m^{-3}); v is the impeller tip speed (m s^{-1}); φ is the beads filling ratio; ε is the bulk porosity; C is the cells number (or cell concentration); n is the rotational speed (s^{-1}); and m is the total biomass treated.

Centrifugation

The microalgal lysate generated by bead milling was centrifuged before carrying out the analysis of the released products. Centrifugation parameters were selected in order to ensure the efficient settling of dense and insoluble particles (such as starch) and minimum energy consumption. Mild centrifugation at 2,500 g (24,525 $m.s^{-2}$) was selected as optimal speed for low cost large-scale applications and the time, necessary to settle starch granules (dense and insoluble), was calculated according to the known equation:

$$t = \frac{9H\eta_L}{2(\rho_P - \rho_L){r_P}^2 g} \quad (6.2.6)$$

Here, t is the time to achieve the starch settling (s); H is the radial movement covered by the particles (m); η_L is the lysate viscosity (Pa s); ρ_P and $\rho_L$are the density of the starch particles and of the lysate, respectively (kg m^{-3}); r_P the mean diameters of microalgal starch granules; g the angular velocity (m s^{-1}). The microalgal lysate was assumed to have physical properties close to those of the water because it is quite dilute (Souliès et al., 2013; Montalescot et al., 2015). The properties of the microalgal starch granules were reported in Gifuni et al. (2017). The calculated time was 3 minutes, for the precipitation of starch granules suspended in 3 mL of lysate.

Analysis of the released products

After disruption and centrifugation two fractions were obtained: pellet and supernatant. The released products investigated were starch, proteins and pigments. The dry weight of the total particles recovered in the two fractions was also analysed.
The dry weight of the total particles recovered in the pellet was measured by weighting the pellet after drying at 100°C for 24 hours. The dry weight of the total biomass was measured by filtering a known amount of culture by cellulose filter, then dried at 100°C for 24 hours and weighted.

The fraction of the dry weight released in the supernatant or recovered in the pellet was calculated as difference from the total dry weight of the biomass.
The starch concentration was assayed in the pellet by Total Starch Kit by Megazyme (Wicklow, Ireland). Proteins concentration was assayed in the supernatant by BCA Protein Assay Kit (Thermo Scientific). Pigments concentration was measured in the pellet by spectrophotometric quantification after methanol extraction.

The fraction of recovered product was defined as the ratio between the concentration of the released component in the pellet or supernatant after mild centrifugation and the concentration in the not disrupted biomass.
The amount of released product after bead milling disruption were compared with the initial concentration in the total biomass. The initial concentration in the biomass was assumed as the starch concentration in the pellet after two passes in high pressure disrupter (CellD, Constant System) at 270 MPa and centrifugation at 3,000g for 5 minutes; and the protein concentration in the total high-pressure lysate. The total pigment content was measured on the intact cells after centrifugation and methanol extraction.

The fraction of the dry weight in the pellet and supernatant (X) was calculated as follow:

$$X_f = \frac{m_f}{M_{tot}} \quad (6.2.7)$$

Here, X_f is the generic indication of the fraction of dry weight in the pellet (p) or in the supernatant (s). The symbol f will be conveniently replaced by p or s in the result section. m_f is the generic indication of the pellet or supernatant mass ($m_p; m_s$) divided for the total mass of the cells before the disruption (M_{tot}).

For the different products analysed, the yield and the selectivity of the recovery after bead milling disruption and centrifugation were calculated.
In particular, the yield (Y) was defined as the ratio between the mass of the product (m_α) in the recovered fraction (pellet for starch, supernatant for proteins and pigments) and the total mass of the product *α* in the initial biomass (M_α):

$$Y_\alpha = \frac{m_\alpha}{M_\alpha} \quad (6.2.8)$$

α, is the generic symbol adopted for product. It will be conveniently replaced by the name of the product in the results session.
The selectivity (S^α) was defined as the ratio between the mass of the product in the recovering fraction (m_f^α) and the total mass of the fraction (m_f).

$$S^\alpha = \frac{m_f^\alpha}{m_f} \quad (6.2.9)$$

α is the generic product and f indicate pellet or supernatant fraction, both of them will be replaced as previously described in the results section.

Results and discussion

Overall kinetic of disintegration and product recovery

The kinetic of cell disruption and product recovery was analyzed for the different bead milling parameters investigated. The protein and pigment recovery are referred to the supernatant fraction, while the starch recovery is referred to its concentration as free granules in the pellet (starch included in not disrupted cells, precipitating into the pellet, was not considered).

In the figure 6.2.1, the kinetics of the cell disruption, proteins, pigments release and starch recovery are reported for two distant bead milling conditions. The figure 1a and 1b differs for the use of 0.375 mm and 1.3 mm glass beads, the rotational speed was 10 m s^{-1}, filling ratio of 0.8 for both conditions. The fitting with the first order kinetic model is also reported. Beads diameter highly influences the disruption and recovery rate as already reported by Postma et al. (2017). For *C. sorokiniana* treated with 0.375 mm glass beads (figure 6.2.1 a), 4 minutes were required to reach the 90% of disruption, the recovery of the 90% of the initial proteins, 85% of the total chlorophyll in the supernatant and 70% of the starch in the pellet after centrifugation. When 1.3 mm glass beads were used (figure 1 b), the 90% of cell disruption was reached after 10 minutes. At the same time, 50% of the initial proteins were recovered in the supernatant with 30% of the total chlorophyll, 85% of the initial starch was recovered in the pellet. Highest efficiency for the proteins recovery was obtained by the use of little beads, but high pigments content polluted the protein extract. Lower proteins recovery associated to the use of big beads ensured higher purity and lower selectivity for the pigments. Starch was recovered in the pellet in lower amount for little beads instead of big beads. This could be caused by excessive disintegration causing harm to the starch granules structure, reducing their size or changing their conformation. The first hypothesis can be followed by a limited settling of the little starch granules by centrifugation, then lower recovery in the pellet. The second hypothesis can cause solubilisation of the disrupted starch granules. These results differ from Postma et al. (2017) because the selectivity of the process parameters for the carbohydrates fraction is analyzed in terms of polysaccharides (starch) recovered in the pellet after centrifugation, instead of fragmentation and solubilisation of all the carbohydrates fraction in the supernatant. Moreover, mild centrifugation parameters were chosen for the analysis of the product recovery.

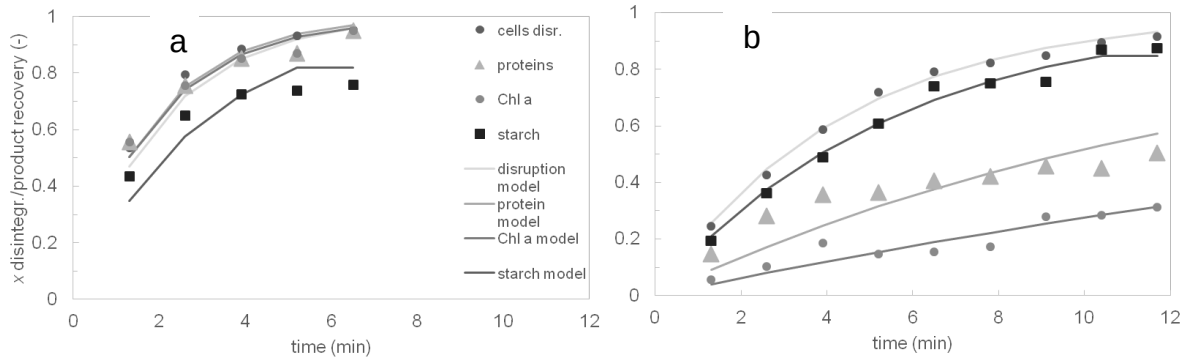

Figure 6.2.1: The fraction of disrupted cells, recovered proteins and pigments in the supernatant and starch recovery in the pellet are reported as function of the time for two bead milling conditions differing for beads diameters: a) 0.375 mm and b) 1.3 mm. The first order kinetic model is also reported for disruption, protein, chlorophyll and starch.

Application of stress model for C. sorokiniana

Kwade and Schwedes (2002) first proposed the stress model for yeast and bacteria then, it was successfully transposed to microalgae by Montalescot et al. (2015). The calculation of the specific energy consumption was also proposed and applied in the microalgal milling (Postma et al., 2017) in order to find the optimal condition for disruption, product release and energy saving. As indicated by Kwade et al. (2007), following SI and SN values are indicators proportional to the necessary intensity (J) or stress events for disruption but can differ from real value for several orders of magnitude. They are then convenient for process optimisation but not for energy consumption prediction.

In the figure 6.2.2 a, the SI/SN parameters are reported for the microalga *C. sorokiniana* in semi-log scale. The relation between the number of stress events necessary to reach the 90% of cell disruption ($SN_{0.9}$) and the stress intensity applied in the milling system (SI), shows a trend in agreement with that already reported for *N. oculata* and *P. cruentum* (Montalescot et al. 2015). After SI of 1 10^{-4} joules, even if the stress intensity increases, the stress number reaches a constant value. On the other hand, before SI of 1 10^{-5} joules the number of stress events increases with the reduction of the stress intensity. The transition between these two regimes is characterized by the critical stress intensity SI_C. SI_C was 4.5 10^{-5} joules a closed value to that found for *N. oculata* and *P. cruentum* (5.5 10^{-5} and 1 10^{-4} joules respectively).

In the figure 6.2.2 b, the relation between the specific energy required for the 90% of cell disruption and the stress intensity is presented in a semi-log scale to highlight the sudden increase of the energy consumption when the SIc is crossed. The energy consumption is almost constant for SI ≤ SIc, suggesting that all the bead milling conditions, characterized by these SI values, are almost equivalent for the energetic consumption. For SI higher than SIc, the energy consumption rapidly increases for small change in SI. For the analysed strain, the optimal condition (Si_c) was for 0.6 mm glass beads, with a filling ratio of 80% and a tip speed of 14 $m.s^{-1}$. The specific energy (E_m) required for the 90% of cell disruption in the critical zone was in the range 5 10^{+11} - $3 \cdot 10^{+12}$ joule kg^{-1}. This value is higher than that reported by Doucha and Lívanský (2008) and Postma et al. (2014), for *Chlorella* species, but the higher energy requirement is mainly due to the very low biomass concentration tested in this experiment in order to avoid overloading effects (1 g L^{-1} of this study with respect to 25-145 g L^{-1} of the other papers). Anyway, this study is not finalized to the optimization

of the energy consumption, but to the relation between the energy and the product recovery and selectivity.

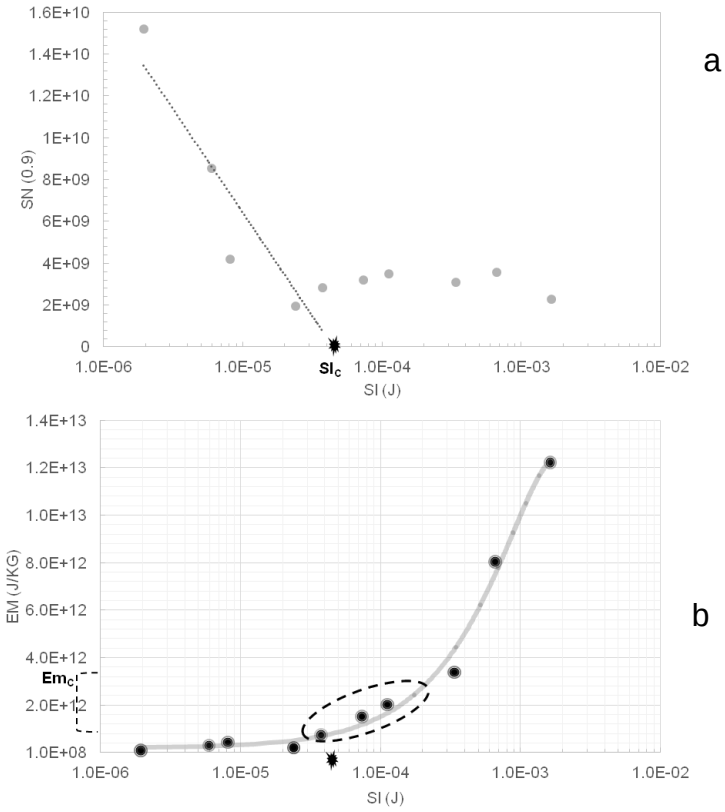

Figure 6.2.2. a)Number of stress event required to reach the 90% of cell disruption (SN - 0.9) is reported in function of the stress intensity applied in the milling (SI) of *C. sorokiniana.* (Semi-log scale). b)The specific energy required for the 90% (E_m) of cell disruption as function of the stress intensity (SI). (semi-log scale).

Prediction of metabolites recovery with optimal energy consumption

The amount of product recovered for different bead milling energy conditions was analysed in order to understand if there is a critical zone effect. The recovery was referred to the selected centrifuge parameters calculated in the section 3. The choice of mild centrifugation parameters lies in the perspective of reducing the energy consumption, without reintroducing the expensive centrifuge step we tried to overcame by intensive culture (see chapter 5).

In the figure 6.2.3, the repartition of the dry weight, starch, protein and chlorophyll between pellet and supernatant is shown for different specific energy requirements at the 90% of cell disruption (E_m). In the figure 6.2.3. a, the repartition of the dry weight in pellet and supernatant is shown; in the figure 6.2.3. b, c and d the yield and the selectivity of starch in the pellet, proteins and chlorophyll in the supernatant are reported. A clear transition appeared around the SIc. Below the critical E_m range (5 10^{+11} - $3 \cdot 10^{+12}$ joule kg^{-1}) most of the particles are still in the supernatant after mild centrifugation. It results in high protein recovery in the supernatant (up to 90% of the initial biomass content), but at the same time a high amount of chlorophyll (about 75% of the total chlorophyll content of the biomass). 75% of the total starch is recovered in the pellet in this zone. After the critical value, most of the initial mass (60%) is found in the pellet. It produces higher starch recovery than in the low energy region, to the detriment of the starch selectivity. The protein yield in the supernatant decreases to

the 50%, with a minor increase in the selectivity. The same trend is shown for the recovery and the selectivity of the chlorophyll in the supernatant. The critical energy range corresponds to the highest starch yield and selectivity, high proteins release and lower selectivity for pigments. E_m of 1.5 10^{+12} ensure the best compromise for starch yield and selectivity in the pellet (0.8 and 0.2 respectively), high protein yield in the supernatant (0.8) and lowest selectivity for chlorophyll in the supernatant (0.02). Clearly, the high proteins yield obtained is not due only to the high cell disruption efficiency, but also to the mild centrifugation applied. As a result, some unsoluble proteins can still be in the supernatant after centrifugation, then it should be moted that the proteins yield is not referred to soluble proteins yield, strictly.

These results could be correlated to the disruption kinetics, high rate of cell disruption corresponds to lower energy input in the bead milling (figure 6.2.1 a), but lower selectivity for the products recovery in pellet and supernatant after centrifugation. In fact, low SI and energy investment (before critical zone), correspond to the use of small beads and resulted in an excessive comminution of the cell fragments and most of them remain in the supernatant after the centrifugation step. Then, higher selectivity for the starch in the pellet is obtained, but lower selectivity for proteins with respect to pigments in the supernatant. The opposite trend is related to the high SI and E_m, the lower kinetics required, reduces the miniaturization of the bigger cells, resulting in large fragments that settle in the pellet during centrifugation. As a result, more starch is recovered in the pellet, but together with all the insoluble components of the microalgae. The protein content recovered in the supernatant for high E_m is then reduced (yield of 50 %). Safi et al. (2017) concluded that the maximum amount of protein released by bead milling is the 50% of the initial protein content of the biomass. The comparison of present results with the conclusion reported in Safi et al. (2017), suggests that only cytoplasmic, water-soluble proteins are released for high E_m value, even if the 90% of cell disruption was reached. While, low E_m correspond to higher comminution and the release of part of the non-soluble proteins.
As a conclusion, lower energetic investment in the bead milling does not correspond to mild disruption, while the mild disruption can be considered for E_m higher than the critical value.

In fact, for high E_m, the lowered disruption kinetics result in a slower but gentle disruption that avoids miniaturization of the cell fragments. It allows the release of high number of soluble molecules and energy saving. Moreover, this strategy can avoid the high degree of comminution, which often causes problems in the following fractionation of the microalgal components (Safi et al., 2017; Montalescot PhD thesis).

Other works already analysed the product release during the bead milling. Postma et al., (2015) proposed a first order kinetic for describing the proteins and the pigments release similarly to the disruption kinetic. They found higher kinetic constant for protein release than for cell disruption and pigments release. In a successive work (Postma et al., 2017), they proposed the use of small beads, associated to low specific energy consumption, for increasing the kinetic of disruption and protein release. The present study proposes a strategy for optimization of the bead milling condition for the recovery of the product of interest by using low energy centrifuge parameters. Moreover, the results highlight that modulated energetic input produces the best results in terms of product repartition, recovery and selectivity. Low energy input is associated to lower beads diameters and higher level of comminution contrasting with an effective separation of the resulting products.

The understanding of the different repartition of the product in function of the energy requirement for the disruption is a crucial point for the design of downstream process in function of the target product and the refinery application. It opens the way to a customization of the disruption parameters in function of the value and the fragility of the target product. Moreover, it gives information about the composition of the recovered fraction and the by-products. Another perspective could regard the selection of bead milling parameters for the disruption of a selected cell size classes for the recovery of specific products known to be accumulated in bigger and older cells (e.g. carotenoids), and recirculate the little cells in the culture system (upon cells debris removal). For these applications, additional studies are required (Zinkone et al. to be submitted).

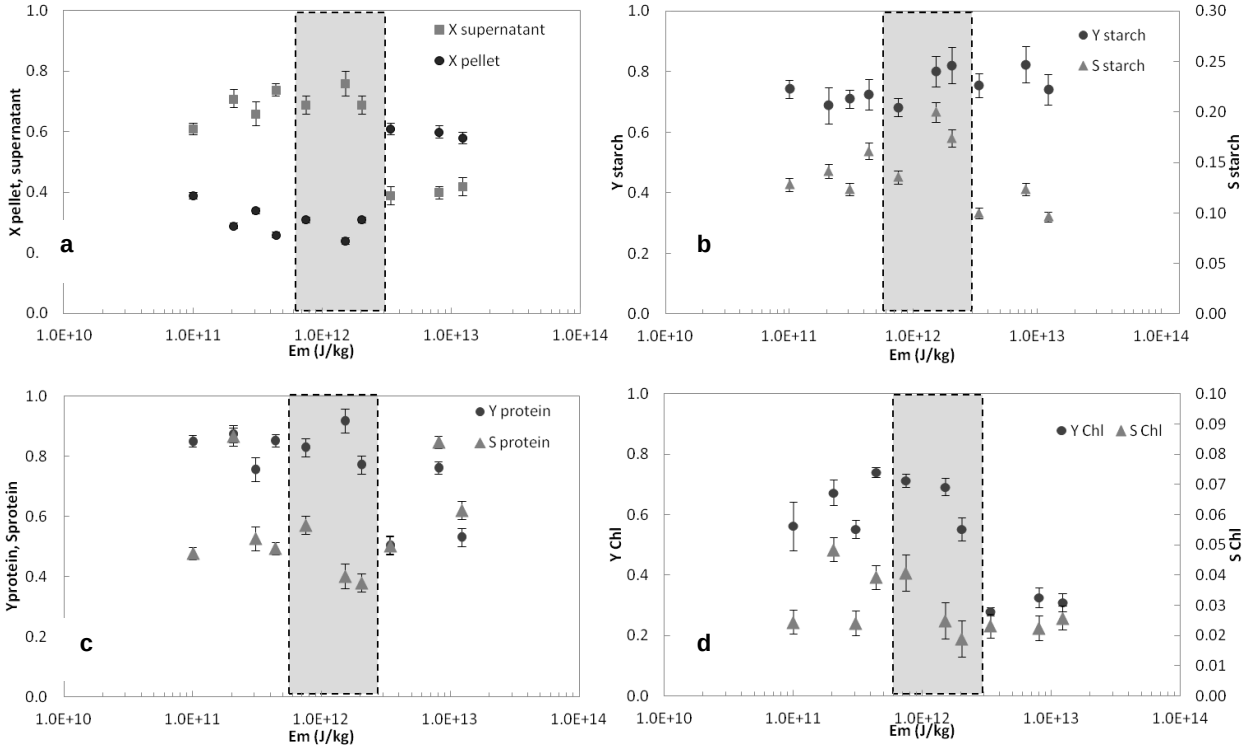

Figure 6.2.3: At different specific energy for 90% of disruption (E_m) is plotted: a) the distribution of the dry weight in pellet and supernatant; b) starch yield and selectivity of its recovery in the pellet; c) protein yield and selectivity and d) chlorophyll yield and selectivity in the supernatant fraction; after bead milling disruption and mild centrifugation.

Conclusion

The recovery of starch, proteins and chlorophyll after bead milling disruption and mild centrifugation was studied as function of the bead milling parameters. Stress model was applied and the specific energy of bead milling step was related to the yield and selectivity of the products recovery. A clear behaviour was identified, suggesting the possibility of customizing the fractionation and the selectivity of the product recovery on the basis of the disruption conditions. Lower energy consumption in the bead milling was found to be not related to mild disintegration and comminution, but it results in higher miniaturisation of the cell debris and lower selectivity for proteins recovery. The critical energy range identified by the stress model, ensure the best compromise for starch yield and selectivity in the pellet, high protein yield in the supernatant and lowest selectivity for chlorophyll in the supernatant.

6.3 Purification of microalgal protein fraction by three-steps membrane filtration: advancements and feasibility

I. Gifuni[a], L. Lavenant[c], J. Pruvost[b], L. Marchal[b], A. Masse[b]*

[a] Dipartimento di Ingegneria Chimica, dei Materiali e della Produzione Industriale, Università degli Studi di Napoli "Federico II", Piazzale Tecchio, 80, Naples, Italy.
[b] GEPEA, UMR CNRS 6144, University of Nantes, 37 bd de l'Université 44602 Saint Nazaire Cedex, France
[c] UR1268 Unite´ de Recherches Biopolyme`res Interactions Assemblages, INRA, F–44300 Nantes, France

Abstract

Microalgae proteins are recognized as source of proteins for nutraceuticals, food additives and animal feed production. The exploitation of protein fraction can be easily integrated in the biorefinery of microalgae biomass. Membrane filtration is one of the most sustainable and cost-effective technique for the proteins purification in the biorefienry, but the procedure need to be improved. This study proposes a three-step filtration for the recovery, the purification and the concentration of proteins extracted from microalgae biomass. The three-step filtration was performed on the supernatant obtained from a mechanic cell disruption and mild centrifugation of a culture of *Chlorella sorokiniana*. It was designed as: 1) PREFILTATION (0.22 µm – ceramic membrane) for removing impurities; 2) DIAFILTRATION (0.22 µm – ceramic membrane) for recovering the proteins retained in the first step; 3) CONCENTRATION (3 kDa – ceramic membrane) for concentrating the protein in the retentate. The overall yield of the filtration process was not satisfying, 12% of the initial proteins were recovered in the retentate of the concentration step and the purity was low as well (18%). The inadequate result was identified in several bottlenecks of the procedures and different solutions have been proposed.

Introduction

Microalgae are widely studied as sources of renewable feedstock for food and energy production (Vanthoor-Koopmans et al. 2013; Wijffels and Barbosa 2010). The biorefinery of the microalgal biomass, for the valorisation of several components, was already proposed in order to have a cost-effective refinery as well as biomass cultivation. Before any economic evaluation, the feasibility to refine the biomass has to be proved from a technical point of view. As already seen, the biorefinery should allow the recovery of most of the microalgal components without causing harm to the other fraction (Chew et al. 2017). Mild and low-cost techniques are advisable. Membrane filtration is one of the techniques widely applied in several industrial fields, from the desalinization and purification of the water to the recovery of high value and sensitive compounds (Massé et al., 2013; Castro-Munoz et al., 2017). No chemical addition is needed and the operating conditions (temperature, shear stress, pressure) are relatively soft. The membrane filtration is already used at large scale and constitutes a mature technology. Membrane filtration was proposed for example, for TAG separation (Giorno et al., 2013; Lorente et al., 2016); phycoerythrin pre-purification (Denis et al., 2009), polysaccharides purification and for proteins recovery (Ba et al., 2016; Safi et al., 2017). In particular, the recovery of proteins fractions by membrane filtration can be considered as one of the best techniques preserving the functional and nutritional properties of the proteins (Ursu et al., 2014), removing or reducing the strong chlorophyll colour and taste (Schwenzfeier et al., 2011). The membrane filtration, for proteins recovery, is generally subsequent to the microalgal cells disruption. It was

already proved that the best compromise between the quantity of proteins released and the quality of the proteins is ensured by mechanical disruption method, such as bead milling (Safi *et al.* 2015). The separation of the microalgal components from the whole bead milling lysate was tested by Safi *et al.* (2014). They proposed a strategy of two-step membrane filtration for the separation of microalgal components. In particular, they used 100 kDa and 10 kDa polyethersulfone membranes for the separation of a model suspension reproducing cells lysate of *T. suecica*. The approach seemed interesting, but not conclusive for the fractionation of the molecule classes. Some proteins are lost in the retentate of the first filtration step and the retentate of the second filtration do not separate the proteins chlorophyll. Moreover, fouling seemed to be important for all the pressure tested (0.69-2.07 bar). Other authors worked on proteins separation from microalgal lysate after centrifugation focusing also on the characterization of the recovered proteins (Schwenzfeier et al., 2014; Ursu et al., 2014). These studies demonstrated that the separation process and their operating conditions not only influence the yield of the protein recovery, but also the protein quality (especially emulsifying activity). In particular, the emulsifying activity can be attributed to soluble fraction of the microalgal protein.

Safi et al. (2017) proposed a new strategy composed of disruption, centrifugation step, membrane filtration and diafliltration for the recovery of soluble proteins. Three different membrane cut off 300, 500 and 1000 kDa were tested to identify the optimal cut off for recovering proteins in the permeate. The best performances for proteins recovery and fouling mitigation were observed for 300 kDa membrane. Concerning the fractionation of microalgal extracts by membrane filtration, the fouling of the membrane is often a key issue to be resolved in view of a large-scale production. The fouling can act on the production flow rates as well as the selectivity/retention of the process and it is largely influenced by the disruption parameters. Thus, the current challenge is the integration of membrane technology into the biorefinery chain for the fractionation of microalga components (Gerardo et al., 2014).

Our previous work optimized the bead milling disruption for the recovery of dense and unsoluble particles (i.e. starch) in the pellet after a mild centrifugation (2500g for 5 min). This study starts from the already optimized protocol of disruption and centrifugation and deals with the membrane separation of proteins from the supernatant obtained. The membrane filtration process was designed with three steps: prefiltration, diafiltration, concentration in order to retain the impurities, increase the transmission of proteins through the membrane, and concentrate the proteins, respectively. The repartition of sugars and chlorophyll during the filtration stages was followed and the properties the obtained protein enriched fraction was characterised in terms of purity. It is worth noting that this part of the thesis consists in a study of the feasibility to partially purify the proteins and concentrate them. No optimization was carried out.

Materials and Methods

Microalgal culture and proteins extraction

The green microalga *Chlorella sorokiniana* was cultivated in continuous mode in a 5 L flat panel PBR using modified BBM medium (Van Vooren et al., 2012). About 2 L of biomass, with a concentration of 1 g L^{-1} were harvested every 24 hours and directly processed in bead milling, without previous concentration. The bead milling operated in a single step continuous mode as described by Montalescot *et al.* (2015). The bead milling conditions have been selected in the previous study (Gifuni *et al. section 6.1*) and they consist in the use of 0.6 mm glass beads, velocity of 14 m s^{-1} and flow rate of

200 mL min^{-1}. The disrupted biomass suspension was centrifuged for 5 min at 2500 g in order to recover most of the starch and insoluble particles in the pellet. The supernatant was collected for several days before to reach enough volume to perform filtration experiment (7 L). In order to preserve the proteins during the storage, the supernatant was heated at 60°C for 1 min for protease inactivation, then 0.02% m/v of sodium azide was added for inhibition of bacterial growth.

Preliminary analysis: DLS and SDS-PAGE

The supernatant produced by disruption and centrifugation was analysed for particles and protein size to define rationally the choice of the membrane cut off. The dynamic light scattering (DLS) was used to measure the size distribution of the particles suspended in the supernatant. The supernatant sample was measured without treatment and after filtration with 0.8, 0.45 and 0.22 µm cellulose filter. The preliminary filtration, with cellulose filter, allow to reduce the interferences and to have a clearer signal by the instrument. The proteins present in the supernatant were analysed by SDS-PAGE in order to determine the molecular mass of the soluble proteins under denaturing conditions. The SDS_PAGE protocol followed Laemmli (1970). 20 µL of protein solution were loaded on 10% SDS gel. Protein standard (26614 *Thermo Scientific*) was used as marker of molecular weight. The gel were stained overnight using Comassi Brilliant blue R250. The destaining was carried out with distilled water. DLS and SDS-PAGE were also performed on the final products of the filtration: permeate and retentate of the three steps.

Membrane filtration process

The membrane process for the proteins isolation was composed of three steps showed in the Figure 6.3.1. 1) Prefiltration, with a 0.22 µm membrane, for removing the big particles and retain them in the retentate while the proteins passed through the membrane. The final volume reduction factor was equal to about 10 (initial volume 7 L) 2) Diafiltration of the final retenate of the previous step, with 0.22 µm membrane, for recovering the proteins that are still in the retentate. Six diavolumes of demineralized water has been added during this step. 3) Concentration of the protein rich permeates produced in the step 2 and 3, with a 3 kDa membrane. The permeates of the previous two steps were mixed and concentrated 10 folds (initial volume of 8 L). The filtration process was conducted with a pilot plant operating with a feed volume ranges from 5-10 L. All membranes used (0.22 µm and 3 kDa) were made of ceramic to minimize interactions between the compounds and the membrane as previously seen from previous GEPEA experiments. The filtration area of the 7 channels tubular membrane was 0.032 m^2. The transmembrane pressure (TMP) was arbitrary fixed at 2 bar for 0.22 µm membrane and 5 bar for 3 kDa which corresponds to classical transmembrane pressures for such operation. The recirculation flow rate was fixed at 250 L h^{-1}, that means a cross-flow velocity inside the channel lumen equal to 2.5 m s^{-1}. The temperature was maintained between 22 and 25°C. The permeate flux was monitored every 20 min. After each trial, the membranes were washed with 5 L of demineralized water at room temperature, 2 L of water at 50°C and 2 L of NaOH (15 g L^{-1}, pH=12) at 3 and 6 bar for 0.22 µm and 3 kDa respectively. Finally, the membrane was flushed with demineralized water at 20°C until the pH of the permeate was equal to the demineralized water pH. Then the water permeability of the membrane was measured. The washing protocol was repeated if the membrane did not recover at least the 80% of the initial permeability (before filtration experiment).

Proteins quantification

Protein concentration was quantified using BCA kit assay by *Thermo Scientific*. The quantification of the proteins was performed on the sample before the filtration, for the

samples collected during the filtrations and in the final permeate and retentate recovered for the three filtration steps. The sensitivity of the method allows detecting proteins from 0.05 to 1 g L^{-1}. Samples that were more concentrated were opportunely diluted.

Additional biochemical analysis

Sugars and chlorophyll were assayed in the initial supernatant and in the final permeate and retentate of each filtration step to have an indication of the repartition of these molecules during the filtration. Sugars were quantified by Dubois's method (DuBois *et al.*, 1956). Pigments were assayed according to the protocol reported by Safi *et al.* (2017). Chlorophyll and carotenoids concentration were determined using the equations proposed by Ritchie *et al.* (2006).

Calculations

Permeate flux (J) during the filtration was calculated according to the following equation:

$$J = \frac{V_{permeate}}{\Delta t \times A_{filtration}} \quad (6.3.1)$$

The volume of permeate ($V_{permeate}$) was reported in L; Δt is the time necessary to collect the permeate volume (h); $A_{filtration}$ is the filtration area (m^2).

The permeate flux will be reported as function of the volume reduction factor (VRF) in the section 3. VRF is defined as:

$$VRF = \frac{V_0}{V_{retentate}} \quad (6.3.2)$$

Where V_0 is the initial volume of the supernatant to be treated (L) and $V_{retentate}$ is the volume of the retentate in the feed tank at the instant of the sampling.

The mean retention factor (TR) of the proteins was calculated by the following equation:

$$C_r = C_0 \cdot VRF^{TR} \quad (6.3.3)$$

Here, C_r is the protein concentration in the retentate (g L^{-1}), C_0 is the protein concentration in the initial feed solution (g L^{-1}), and VRF was already defined before. It is worth noting that TR can change during the filtration. We reported the TR corresponding to the mean retention rate in the course of operation.

For the diafiltration step, the relative flux and the diavolume are considered. The relative flux is defined as the ratio between permeate flux of the diafiltration and the permeate flux at the end of the beginning of the diafiltration step (J/J_0).

The diavolume (DV) is the relative volume of demineralized water added (V_{added}) during the process with respect to the initial volume in the feed tank (V_0):

$$DV = \frac{V_{added}}{V_0} \quad (6.3.4)$$

The protein yield or protein recovery rate (Y) was calculated independently for the three filtration steps and for the entire filtration process:

$$Y_{prefiltration} = \frac{C_p^1 \cdot V_p^1}{C_0 \cdot V_0} \qquad Y_{concentration} = \frac{C_r^3 \cdot V_r^3}{C^{1+2} \cdot V^{1+2}}$$

$$Y_{diafiltration} = \frac{C_p^2 \cdot V_p^2}{C_r^1 \cdot V_r^1} \qquad Y_{tot} = \frac{C_r^3 \cdot V_r^3}{C_0 \cdot V_0} \quad (6.3.5)$$

Here, C and V represent the protein concentration and the volume respectively (g L^{-1}; L). The subscript $i; f; p; r$ refers to the initial and final solution, the permeate and the retentate. The superscript $1; 2; 3$ refers respectively to the prefiltration, diafiltration and concentration steps; 1+2 for the solution resulting from the mixing of the permeates from the prefiltration and diafiltration steps. The protein yield of the full process is reported as Y_{tot}.

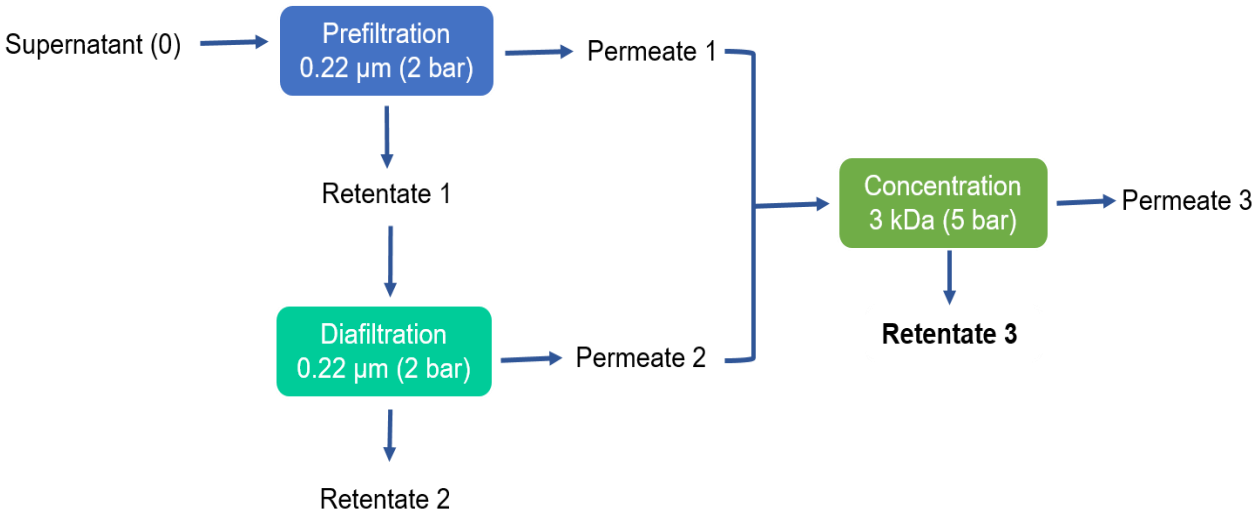

Figure 6.3.1: Schematic representation of the three-step filtration process.

Results and Discussion

This study has the aim to concentrate and pre-purify the soluble components of the supernatant produced after a mild and industrially feasible centrifugation (2500 g). In the previous work we found that, for a known energy input provided to the bead milling (critical value), after the mild centrifugation, most of the particles are dispersed in the supernatant. In particular, more than 80% of the initial proteins are in the supernatant with 75% of the initial pigments. In the pellet, it is possible to recover 80% of the initial starch with high purity. The choice of the membrane cut off for prefiltration and concentration step (Figure 6.3.1) has been made on the basis of a preliminary DLS and SDS analysis of the particles and proteins contained into the supernatant. The mean particle diameters resulted about 0.6 µm, while the smallest proteins detected by the SDS-PAGE presented a mean size of 20 kDa. The filtration of the supernatant has been carried out in triplicates and the result of each filtration step is reported in the section hereinafter.

Prefiltration

In the Figure 6.3.2, the results of the prefiltration step are reported. In particular, the figure 2.A shows the permeate flux as function of the VRF. The data of the test 3 are not presented, because of the low stability of the permeate flux. The permeate flux decreases slowly with the VRF. The permeate flux seems to became almost constant to 70 $L.m^{-1}.h^{-1}$ from the VRF of 6. Thus, no severe fouling seems to take place during the prefiltration. The values of the permeate fluxes are generally considered in the order of magnitude of an aconomically feasible microfiltration process. In the figure 2.B the concentration of protein in the retentate is reported. The relationship between protein concentration and the VRF follows a power law, reported in the equation 3. The

exponent represents the mean retention rate of the proteins (TR). It was estimated to be equal to 0.78. The concentration of the proteins recovered in the permeate slightly increase during the prefiltration step, since the retention rate remain almost constant from the beginning to the end of the filtration (0.71 to 0.88 respectively) (Figure 2.C). The final recovery yield of this step was 23 ± 5 %. It is known that the bigger protein-chlorophyll complex is in the order of 670 kDa (Ursu et al., 2014) that normally allows a transmission through the membrane of 0.22 µm. The retention of a part of proteins could find explanation in different hypothesis. I) A fouling (cake, adsorption, pore blocking), formed by the components of the supernatant, is established and it limits the transmission of proteins through the membrane. II) The proteins released in the supernatant after the disruption are still linked to little cell debris that cannot pass through the membrane. III) The protocol for the storage (heating at 60°C for 1 min) or the storage itself (10 days at 4°C) causes aggregations protein-protein or protein-debris and the final size of the aggregate cannot pass through the 0.22 µm membrane. IV) proteins can be adsorbed on the membrane material.

Diafiltration

The figure 6.3.3 shows the permeate flux during the dialfiltration step. Six diavolumes (DV) were added. The goal of the diafiltration is to continue the transmission of proteins through the 0.22 µm membrane. Indeed, it seems not acceptable to lose too much protein during the concentration and purification chain. The permeate flux was almost constant during the diaflilfiltration, while the protein concentration within the permeate decrease from 0.05 g L^{-1} at the beginning of the test, to 0.01 g L^{-1} after 5 DV (results not shown). The proteins recovery rate of the diafiltration was equal to 14 ± 3 %. These results are comparable with that obtained by Safi *et al.* (2017) using high-pressure disrupter (16, 10, 4 % with 300. 500 and 100 kDa membrane).

Concentration

The figure 6.3.4 reports the results of the concentration step with 3 kDa ceramic membrane. The figure 4.A shows the trend of the permeate flux (J) along the VRF. The flux decreases of about 15% at the VRF of 2, then it remains constant until the end of the process. Low deviation is noted among the three different tests performed. The fouling seems to be low. The figure 4.B shows the increase of the protein concentration in the retentate (C_r) as the VRF increases. The mean retention factor (TR) is 0.91 and then most of the proteins are retained. Anyway, The yield of protein recovery in the concentration step was 54 ±3 %, while 31% of the proteins are recovered in the permeate. Ursu *et al.* (2014) recovered 87% of the proteins in the retentate with 300 kDa membrane. Then, the use of 3 kDa membrane should have ensured the retention of all the proteins recovered in the first two steps. Probably, the proteins that pass through the membrane of this step, are already degraded and characterized by a reduced size.

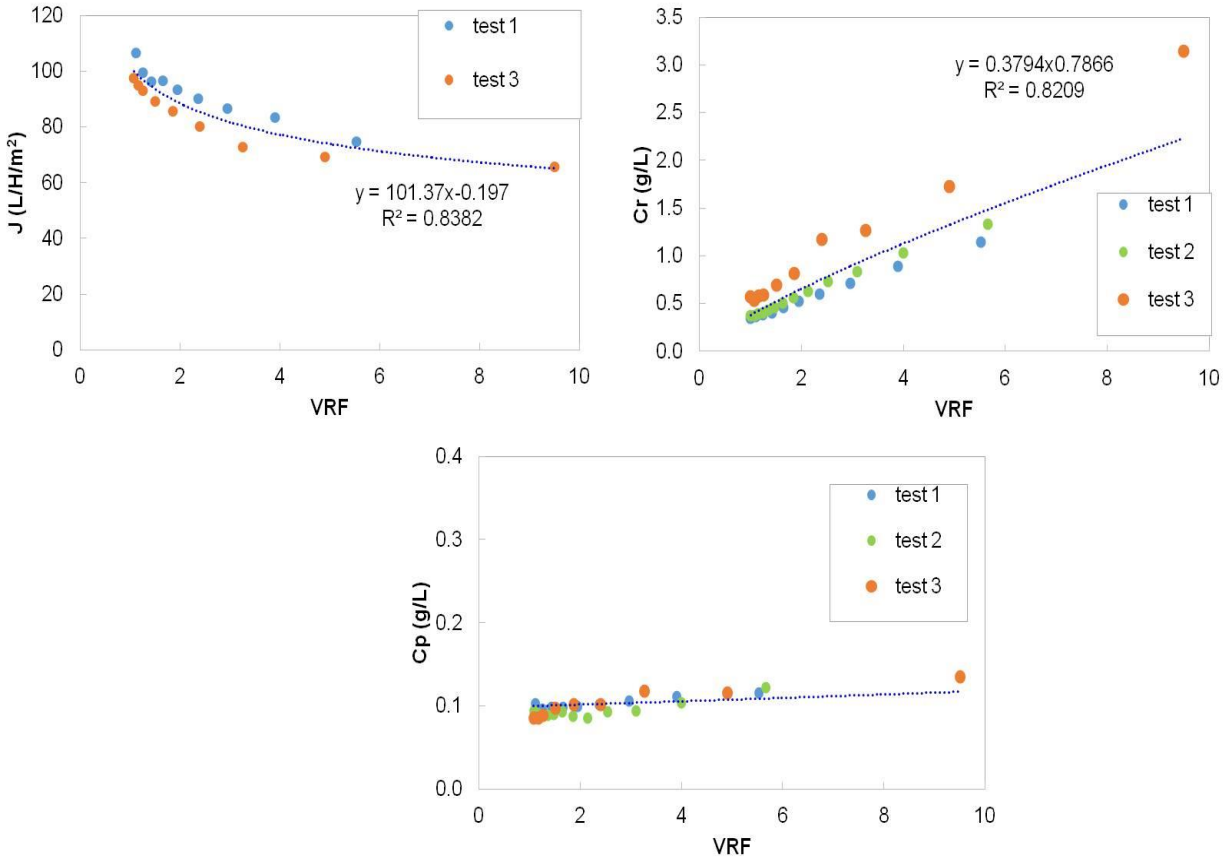

Figure 6.3.2.: Prefiltration results about A) permeate flux (J, L $h^{-1}m^{-2}$); B) protein concentration in the retentate (C_r, g L^{-1}); C) protein concentration in the permeate (C_r, g L^{-1}) as function of the volume reduction factor (VRF).

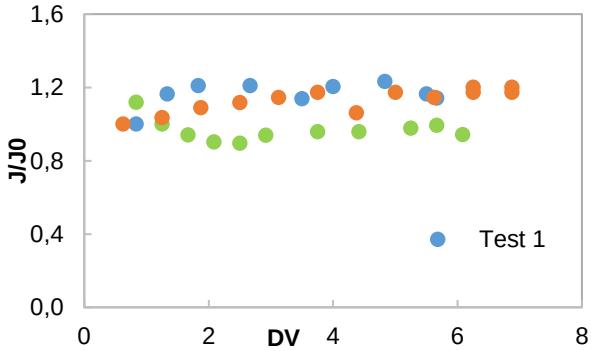

Figure 6.3.3: The ratio between permeate flux of the diafiltration and the permeate flux at the end of the prefiltration (J/J_0), is reported as function of the diavolumes added (DV).

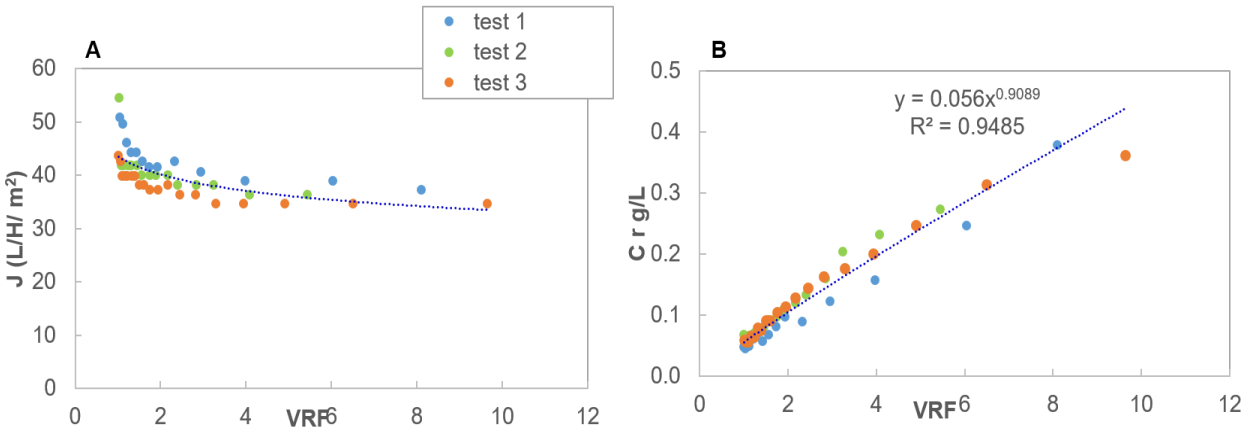

Figure 6.3.4: A) The permeate flux (J) and B) the protein concentration in the retentate (C_r) along the volume reduction factor (VRF) for the concentration step (3 kDa membrane).

Process performance

The characterization of the permeate and retentate of each filtration step has been carried out in order to assess the process efficiency. In the figure 6.2.5, the draft of the overall process is shown and the composition of permeate and retentate of each step is reported in terms of proteins, chlorophyll and total sugars. The proposed application for the proteins isolate was food additives with emulsifying properties. Thus, the amount of sugars that could not be separated from the proteins is an important information, as well as the content of chlorophyll that give to the protein isolate a green colour. We can notice that the chlorophyll is removed with the prefiltration and the diafiltration and uncoloured permeate solution is obtained after the first two steps. This is a good result, since the green colour is not desirable for all the food-applications. The retention of the chlorophyll could be due to the storage protocol. In fact, the heating could cause aggregation of the chlorophyll complex to other molecules and their retention by the membrane. Otherwise, the complex chlorophyll-proteins can be absorbed by the membrane. However, not only the pigments are retained but also most of the proteins. The sugars retained by the 0.22 µm membrane are probably represented by polysaccharides: little starch granules that are not able to precipitate in the previous centrifugation, damaged starch granules that lose their granular structure during the disruption step, other polysaccharides produced by the algae or simple sugars (mono-, di- saccharides) by adsorption. The sugars that are recovered in the retentate of the concentration step (on 3kDa) are probably part of glycoproteins, while the sugars of permeate are mainly simple sugars. The final yield of protein recovery after the entire filtration process is just 12 ± 3%. Even if the low yield seems to be strongly influenced by the storage protocol, these results are preliminary and fundamental for the effective integration of the membrane filtration in the microalgal biorefinery. It gives many starting points for further tests and the introduction of a storage protocol is not really far from the reality. Indeed, many times the microalgal production platform is not localized near the processing platform. Then logistic problem forces the use of a storage strategy. The results of this study suggest that many factors should be taken into account when delicate molecules, such as proteins, want to be recovered. Furthermore, in deep analysis of molecules size, molecules-molecules interaction and target molecules activity during the biomass processing should be performed for the achievement of the biorefinery concept.

Additional studies are required for the optimisation of the membrane material, molecular weight cut off and operating condition of the filtration plant (pressure, velocity) to reach a feasible process. Nevertheless, based on the permeate flux values

in the course of each steps, the fouling if the membrane seems to not be too much important and the use of membrane remains relevant.

Conclusions

A membrane filtration chain was suggested for the recovery and the preliminary concentration of the soluble microalgal proteins. The integration of the filtration strategy with the optimized disruption step and mild centrifugation, really contribute to the fulfilment of the microalgal biorefinery. The hydraulic performances of the membrane filtration chain are promising; the fouling seems not so high. The final recovery yield is not attractive (just 12% of the initial proteins are recovered) and new strategies should to be studied to reduce the loss of proteins during the process. New strategies could be investigated for the integration of membrane filtration in the microalgal biorefinery. This field is still in its infancy, but it has great potential. The selection of the appropriate membrane material and operating conditions, give an efficient alternative to the centrifugation (used after the disruption step for the separation of dense and insoluble particles) and to the solvent extraction for the recovering of the lipid fraction. Granular filtration also offers an alternative to the centrifugation and the prefiltration steps for removing the cellular debris. However, reasonable process design could be obtained with an in deep characterization of the structure, the size, and the interaction of the different molecules in the suspension obtained after the disruption.

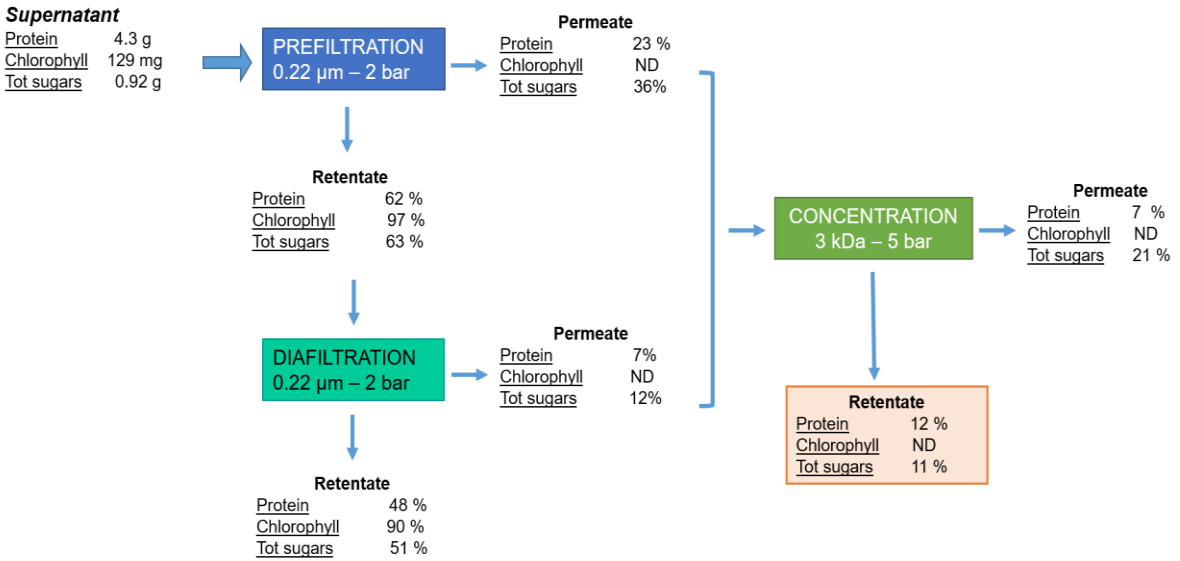

Figure 6.25: Process diagram and recovery of proteins, chlorophyll and sugars in the three-step filtration. All the percentages are referred to the initial amount in the supernatant. The values are the results of an average of three different experiments; the standard deviation is not reported in the diagram. The standard deviation was always ≤ 5%.

ND: not detected

7. DISCUSSION

The environmental problems of our era have let to increase efforts in new and sustainable feedstock for food and energy. Fuel-dedicated cultures divide scientific and popular opinion between the safeguard of the biodiversity and the human nutrition, and the necessity of “green” fuel. Microalgae are an alternative and sustainable source of feedstock (Williams, 2014). In particular, microalgae are considered as sunlight-driven cell factories able to convert CO_2 in biofuels, food, feed and high-value compounds (Chisti, 2006). The species used for commercial applications are: *Spirulina*, *Chlorella*, *Dunaliella*, *Haematococcus*, *Botrycoccus*, *Phaeodactilum* and *Porphyridium*. However, many other species have been isolated and probably thay are composed of new substances characterized by unknown functionalities. The exploitable microalgal products are mainly triglycerides for biodiesel production, poly-unsaturated fatty acid, antioxidants, proteins and pigments (Moreno-garcia, 2017). The microalgal cultures are generally carried out in open ponds and photobioreactors: they differ for investment and operating cost and also for performances and productivity (Wang et al., 2014). The microalgae can grow under autotrophic, heterotrophic, and mixotrophic conditions: the sustainable production of consumer goods mainly consider the autotrophic growth. The nutrients of autotriphic growth are the waste products of human activity such as nitrogen and phosphorus compounds, metals, and carbon dioxide. The photosynthesis is able to convert inorganic substrates into organic components by the support of solar energy. The microalgal biomass components are potential feedstock for the industrial production of chemicals, energy and commodities (Figure 7.1). It is unanimously accepted by the scientific community that the exploitation of a single microalgal product is not cost-effective and it generates unsuitable waste. The biorefinery approach is now applied to the microalgal production. The biorefinery allows the exploitation of all the microalgal potential through the recovery and the separation of biomass components.

Several companies and start-ups have been founded with the aim of gaining profit from the microalgal cultures (***Algal Scientific***, ***Cellana***, ***Fermentalg***, ***Microphyt***, ***KeyNatura***, ***SpirAlps***). Hawever, many challenges still limit the fulfilment of the microalgae potential and they will be analysed in the following sections.

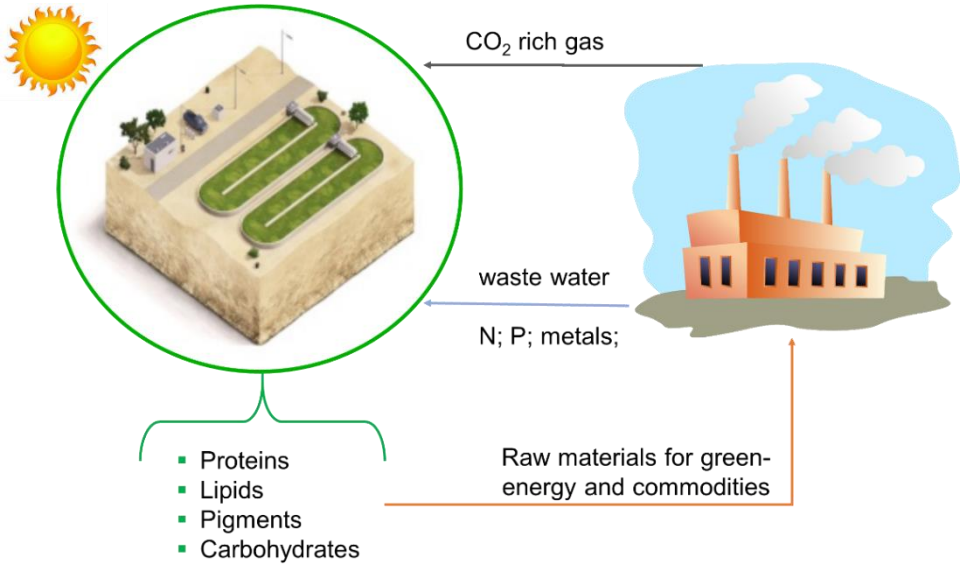

Figure 7.1: Microalgae as feedstock for energy and commodities.

7.1 Economic bottlenecks of the microalgal production

Microalgae boast a large spectrum of products and multiple applications and their productivity largely exceed the crops cultures (Thomassen et al., 2017). However, high production costs inhibit the large-scale industrial success of algae. The main bottlenecks are:

- Limited or expensive nutrients;
- Low biomass conversion efficiency;
- High harvesting costs;
- Not assessed strategy for biomass fractionation.

The nutrients used for autotrophic microalgal growth are generally no expensive (inorganic salts, CO_2 and light). However, some inorganic nutrients - such as nitrogen and phosphorus are also used as fertilizer for crops culture (Coons et al., 2014) and their use for intensive production of microalgae for industrial application may interfere with the fertilizier supply. A solution may be the use of wastewater that typically contain high concentration of nitrogen and phosphorus (Chen et al., 2017). Other strategies involve the nutrient limitation for increasing the accumulation of the product of interests (lipids, carotenoids). CO_2 is also an inexpensive nutrient produced by the anthropic activity and the CO_2 sequestration is a benefit for the microalgal culture for reducing the “green-house” effect. However, 80-90% of the CO_2 supplied to the culture escape to the air due to the low gas-liquid exchanhge efficiency. Often the microalgal culture are not located close to the industrial plant producing the exhausted gas emissions and an additional cost should be included for the CO_2 deliver to the microalgal culture system (Moreno-garcia et al., 2017).

The efficiency of the light-to-biomass conversion is influenced by the photosynthetic efficiency of the microalgal strain and by the PBR configuration. As the biomass concentration increases in the PBR, a dark fraction is established due to the shadowing effect of the algae. Then, the light availability is reduced and not all the light provided to the culture is converted into biomass (Janssen, 2016). Many studies are now focused on the reduction of the optical path of the culture system to increase the biomass concentration and productivity (Qiang and Richmond, 1996; Doucha and Livànski, 2006; Pruvost et al., 2017). Moreover, the outdoor conditions with light-dark cycle also reduce the productivity and the variable climatic conditions make difficult to have a constant microalgal and product productivity.

Harvesting costs are due to the dilute nature of autotrophic culture: the dewatering must precede the fractionation and the recovery of the products. The dewatering is the major factor preventing the scalability of microalgal production and it is about the 40% of the operating costs (Davis et al., 2016). New flocculation strategies and filtration processes have been proposed and the strategies are dependent on the properties of microalgal specie used (Gerardo et al., 2014). Decreasing the processing volume (increase of the microalagal concentration) is a crucial point for the feasibility of the extraction and fractionation strategies.

The fractionation of the different microalgal components requires mild and eco-friendly processes to preserve the integrity and the quality of the products. Generally, sequential extraction has been proposed (Gilbert-lòpez et al., 2017; Ansari et al., 2017). However, Lorente et al. (2016), pointed out that a few studies have been published on the fractionation step.

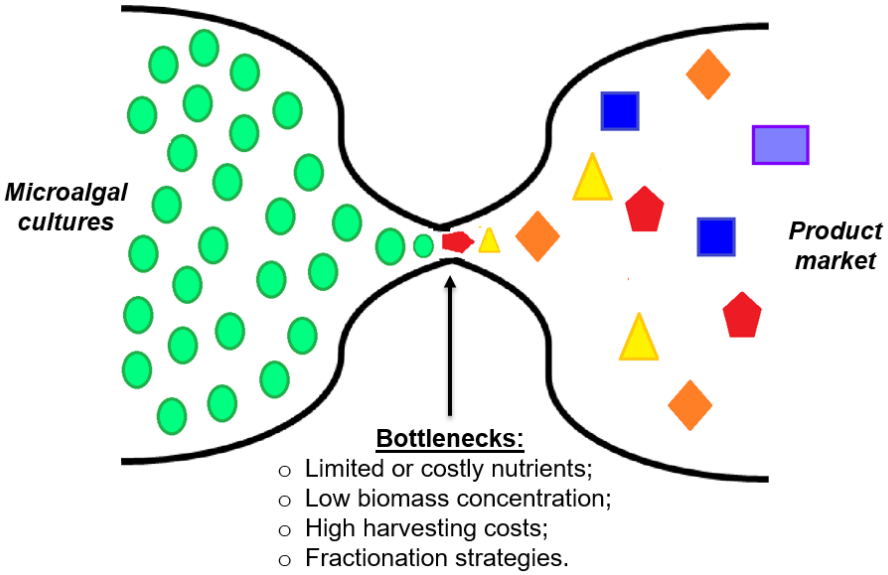

Figure 7.2: Bottleneck of mmicroalgal production

7.2 Culture strategy: co-exploitable products

The nutrient requirement is generally specie-specific for microalgae. The main constituent of microalagal biomass are: C, H, O, N, P. During autotrophic growth CO_2 is supplied as carbon source, hydrogen and oxygen are produced from the water, nitrogen, phosphorus, sulphur and other microelements are supplied as salts. The energy for the synthesis of organic constituents is captured as electron from the light by the photosystem. The electrons received are distributed in the synthesis of lipids (TAGs), starch, proteins (functional biomass) and part of them are used in catabolic reaction or dissipated (Figure 7.3).

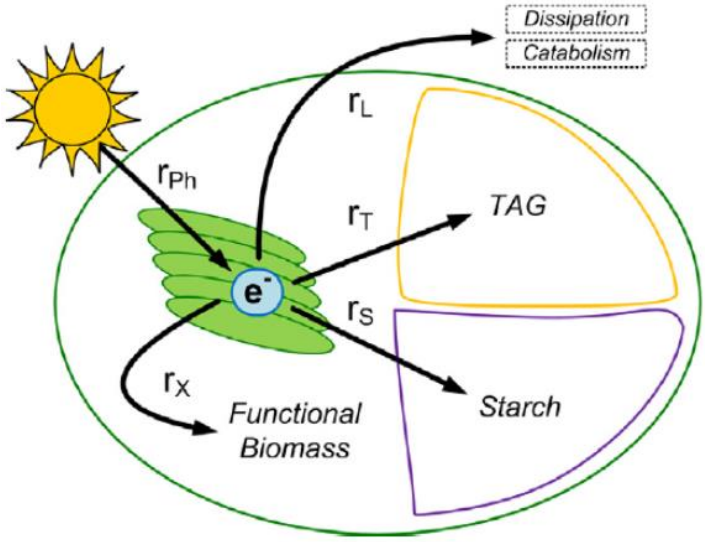

Figure 7.3: Schematic representation of the electron allocation in microalgal constituents and dissipation/catabolism (Klok et al., 2013).

Several studies report the change in biochemical composition of the microalgae and nutrient regime were designed to induce specific metabolic pathway overproducing target metabolites. For example, nutrient depletion has been adopted for carotenoid accumulation in *Dunaliella salina* (Lamers et al., 2012) and it has been proposed for lipids accumulation in *Scenedesmus obliquus* (Breuer et al., 2013) for

biodiesel production propose. Moreover, nutrient depletion is also effective to enhance starch accumulation in *Chlorella* and *Chlamydomonas* species (Mizuno et al., 2013; Msanne et al., 2012). The maximization is generally focused on a single component.

Lipids accumulations strategies are focused on the increase of CO_2 concentration but limiting the nitrogen and/or phosphorus concentration (Lari et al., 2016; Breuer et al., 2014; Klok et al., 2013). The nutrient limitation also induces a decrease in biomass and then lipids productivity. To overcome this problem, different culture strategies have been proposed for optimizing the lipid production: fed-batch followed by semi-continuous mode in N-depletion, repeated batch (Olivieri et al., 2011; Benvenuti et al., 2016).

Carbohydrates (starch and polysaccharides) are generally accumulated during the early nitrogen depletion and during the light period (Fernandes et al., 2013; Klok et al., 2013). Nitrogen and phosphorus limitation (Dragone et al, 2011; Yao et al., 2013) and increase of CO_2 and light intensity (Brànikovà et al., 2010; Tanadul et al., 2014) are the strategies used to enhance carbohydrates accumulation. Anyway, the right metabolic balance should be respected because no starch accumulation occurs when light is not available, even though nitrogen depletion is applied (Gifuni et al., 2017). Moreover, the cell composition is the result of a synergic combination of chemical and physical factors activating specific metabolic response in the different microalgal species (Richmond, 2013). For example, no nutrient limitation coupled with physical stress (such as high light irradiance or high metal concentration) could increase the production of antioxidant pigments avoiding the arrest of the cell growth.

Some strategies are used both for carbohydrates and lipids accumulation, but the time scale of the maximum accumulation of each component is sometimes sequential and the preference on lipids or carbohydrates is strain dependent (Msanne et al., 2012). On one hand, the nutrient limitation strategy (especially N-limitation) is based on the reduction of the protein synthesis and prolonged depletion can cause the reduction in chlorophyll content. On the other hand, the concentration of antioxidant pigments, such as astaxantin (Rosenberg et al., 2008), increases and, when the depletion is coupled with high light irradiance, some strains are able to accumulate carotenoids (Lamers et al., 2012). Therefore, the maximization of a single component is based on a metabolic imbalance, which divert the electron energy towards the selected target to the detriment of the other components.

The biorefinery challenge is in the maximization of the microalgal potential as a prtofolio of products and not as a single product producer, then strategies considering the co-exploitation of different microalgal components are preferred. The co-exploitation is the only sustainable solution for the production of mass-market products, which really play a part in the environmental pollution. Stress conditions for microalgal cultures (nutrient depletion, high light irradiance, high metal concentration) typically promote the accumulation of several interesting compounds (carotenoids, starch, lipids) but they are unfavourable for growth and accumulation of other exploitable components (proteins). Therefore, a compromise should be established. To this aim, Gifuni et al. (chapter 3) proposed the nitrogen depletion onset as optimal condition for the simultaneous exploitation of starch, proteins and lipids. Moreover, ethanol extract of microalgae harvested in this phase pointed out the presence of pigments and lipids with significant antioxidant activity (Petruk et al., appendix).

7.3 Intensive culture systems

Microalgal culture productivity largely exceed crops culture (Vaz et al., 2016), but the costs associated to the culture and the processing are still important. The key

issue for reducing the culture and the harvesting costs is the increase in the biomass concentration. The low mass concentration of microalgae currently produced is due to the low light penetration in the culture system then, a remarkable increase of the biomass concentration can be reached reducing the optical path of the culture (Richmond and Hu, 2013). Many research groups payed attention to the light supply and thin culture systems were developed. Generally, culture characterized by an optical path in the order of 1 cm are considered thin culture and they can reach biomass concentration of 10 g L^{-1} (Figure 7.4). Some innovative examples of thin reactors are reported hereinafter.

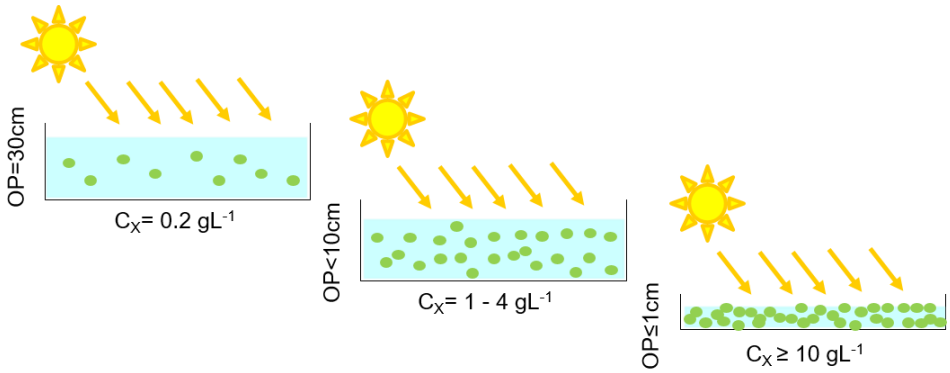

Figure7.4: Reduction of the optical path (OP; cm) is associated to the increase of the biomass concentration (C_X; gL^{-1}).

Flat plate PBRs reported by Qiang and Richmond (1996) were made of glass. They had a thickness of 26 mm and consisted of three tanks. Each tank had a volume of 2.4 L and 0.1 m^2 of illuminated area. The tanks were equipped with a perforated tube that extended along the entire lower part of them and provided the flow of compressed air for mixing. Recirculating cool water, in the back chambers of the reactor, acted as temperature controller. Cuaresma et al. (2011) proposed a new and thin version of the flat plate characterized by a thickness of 14 mm. The length of the reactor was 60 cm, the width was 24.9 cm and the volume 1.7 L with an illuminated surface of 0.019 m^2. This reactor was able to reach a microalgal concentration of 6 g L^{-1} (*C. sorokiniana*). An ultra-thick model of flat panel -UFP- has been proposed in this thesis (Gifuni et al., chapter 5). This thin panel is characterized by a thickness of 3 mm and can reach 24 g L^{-1} of biomass (*C. sorokiniana*). The advantages of this system are in the easy scale-up and operation and the possibility to modulate the light intensity by orienting them in different angles. The problem associated to the scale-up are the power costs necessary to ensure the efficient mixing with the bubbling (Tredici et al., 2010). The integration of vertical flat panel PBR into building facade offers opportunities for an efficient integration. For example, microalgae can fix the CO_2 contained in the flue gas emitted from the building or reduce the energy consumption for the thermal regulation of the building and the PBR (Pruvost et al., 2016).

Cascade systems were firstly proposed by Doucha and Lìvansky (2006). They consisted in two inclined cultivation lanes made of 2 x 1 m glass sheets 1.7% inclination): the upper lane and the lower lane with two different circulation directions. Below the lower lane, a retention tank received the culture. In the retention tank, CO_2 was supplemented to maintain the dissolved concentration at 0.15%v/v and the culture was pumped in the upper edge of the culture system. The mean velocity of the suspension flowing down the inclined area was 0.6 m s^{-1}, the thickness of the culture was 6 mm. Two lanes had a culture area of 224 m^2 and a circulating volume of 2000

L. Microalgal concentration in this system ranged between 40 and 50 g L^{-1} (*Chlorella sp.*). This system, as open ponds, had low cost for the installation and operations but contaminations, temperature and CO_2 escape to the air were not controllable.

AlgoFilm© was patented by Pruvost et al. (2017). It is an upgrade of the falling film principle as the cascade system, but was completely closed and controlled. The AlgoFilm was composed by a titled surface; the culture was injected at the top of the surface, fall down and collected in a tank, then pumped again to the top. A glass plate closes the titled surface but it was not in contact with the cultures, a gas phase flows in the headspace between culture and glass. The gas stream was composed by air and CO_2 was supplemented to control the pH. The gas flow did not recirculate the system (as in airlift), but it avoids the oxygen accumulation. The volume of culture was 0.18 L, the illuminated area 0.3 m^2. The AlgoFilm provided high specific illuminated area, typical of thin-culture system, and fully controlled conditions. The culture thickness ranged between 1.3 and 2.2 mm. The highest biomass concentration achieved was 17 and 30 g L^{-1}, in semi-continuous and batch mode respectively.

Thin culture systems improve the light utilization. The reduced thickness increases the light availability in the culture. It results in the increase of biomass concentration and productivity. In particular, the biomass concentration increases 10 times the concentration of open ponds of traditional PBR, resulting in a proportional decrease of the downstream costs (Souliés et al., 2016).

Figure 7.5: Example of thin-culture system: flat panel of different scale and thickness, cascade open and closed.

7.4 Downstream for the recovery of multiple products

The process framework of a single product production from microalgae consists in: culture, harvest, disruption (extraction), recovery (purification), as reported in the figure 7.6.

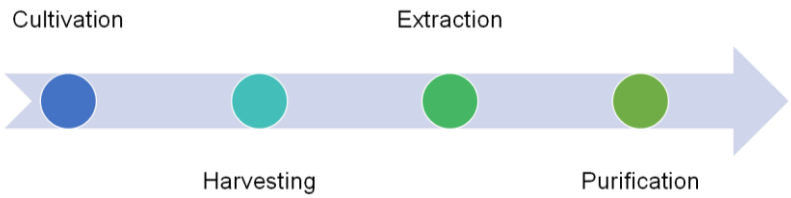

Figure 7.6: Process framework for microalgal products.

The downstream operations start with the harvesting step. The harvesting is required to reduce the processing volume and it is associated to high energy input because of the small size of the cells (4-15 μm), their negative charge, low concentration and density close to that of the water (Packer, 2009). Several technologies have been proposed for the microalgae harvesting: mechanical, electrical, biological and chemical methods. However, recent developments sustain the use of more eco-friendly technologies such as bioflocculation and microfiltration (Ummalyma et al., 2017; Gerardo et al., 2015).

The extraction step is associated with the celluar disruption and the release of the intracellular molecules. The disruption techniques can be divided in: physics (pulsed electric field, microwave, ultrasonication); mechanicals (bead milling, high pressure homogenisation); chemicals; and enzymatic. The selection of the appropriate disruption method is dependent on the cell wall characteristics of the microalgal species and it is drived by the effect of the method on bioproduct quality and recovery (Günerken et al., 2015). Mild disruption conditions are generally required for the extraction of functional products such as proteins.

Purification concerns the separation of the target molecules from the mixture produced during the disruption. Although the solution (aqueous or of the extracting solvent) containing the product extracted is successfully separated from the other cells fractions, the achievement of a satisfactory purity is not an easy task. Indeed, the soluble fraction is a mixture of proteins, sugars and sometimes chlorophyll related to soluble proteins. The hydrophobic fraction contains different lipids classes with different application fields, which need to be separated (carotenoids, TAG, PUFAs, sterols). The separation of molecules belonging to the same fraction needs sophisticated techniques such as chromatography (Manirafasha et al., 2016).

Extraction and purification steps have been widely studied for lipids, phycobiliproteins, carotenoids, astaxantin. However, they were always focused on the maximization of the single product yield. For example, hydrophobic lipids and pigments are extracted by organic solvents, ionic liquids, supercritical CO_2 (Rezaie et al., 2015; Kim et al., 2015; Mubarak et al., 2015). The exploitation of the microalgal potential by sequential extractions of different components, proposed by Zhu and Hiltunen (2016), also consider the maximization of a product class recovery and then consider the valorisation of the residues. This kind of sequential extraction considers the extraction priority in function of the component value. Then, pigments, antioxidant, nutraceuticals are firstly recovered. On the residue, the lipid extraction is applied for biodiesel production. The remaining biomass (containing carbohydrates and proteins) is used as substrate for anaerobic fermentation for biomass production (Figure 7.7).

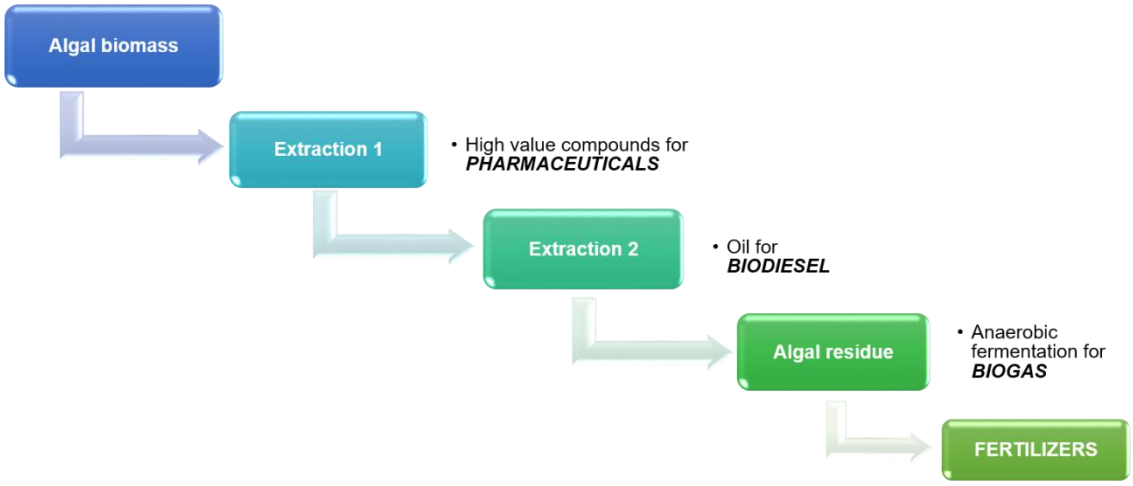

Figure 7.7: Sequential extraction proposed by Zhu and Hiltunen (2016).

The scheme proposed by Zhu and Hiltunen (2016) does not valorise the proteins and the carbohydrates, they are damaged by the extraction of high value compounds and biodiesel. Anyway, it can be a strategy to adopt when specific microalgal cultures are finalized to the accumulation and the recovery of high values (carotenoids, astaxantin, phycobiliproteins, recombinant proteins, active compounds for human disease).

The same strategy does not create profit when large market products are considered (biofuel from oil, food additives from proteins, bioplastics from polysaccharides). Some high value compounds are present in the microalgal biomass whatever the strain or the culture conditions selected (pigments, PUFAs or antioxidant molecules). Their exploitation cannot be excluded, but innovative solution should consider a sequential extraction based on both product value and sensitivity. For example, if high value compounds (such as antioxidants or pigments) are not damaged by aqueous proteins extraction, the latter can precede the high value compounds recovery. Moreover, the lipids extraction should consider non-invasive and sustainable techniques in order to recover the polysaccharides (starch) from the residue fraction. A new ideal skeme is proposed in the figure 7.8, based on the results of the present thesis (Chapter 4 and 6) and appendix article (Petruk et al., Appendix). This scheme considers the application of cell disruption for component release of water soluble components and the recovery of two fraction after a mild centrifugation: pellet and supernatant. In this case, most of the soluble proteins and simple sugars will be recovered in the supernatant, together with other impurities. Then, membrane filtration or two-phase extraction can aid the proteins purification and concentration with consequent application as food additives. The pellet is supposed to contain lipids, pigments, polysaccharides (starch) probably included in cell debries. Based on the respective content of the different unsoluble molecules, two different extraction can be selected: the saponification and recovery of oil ester for biodiesel purpose and the recovery of high values antioxidants (used for pharmaceuticals application). An optimistic scenario can consider a lipids extraction and the separation of the different lipid classes by chromatography for the simultaneous production of biodiesel and antioxidants. The exhausted pellet, resulted from lipids/antioxidants extraction, will be enriched of unsoluble polysaccharides, debries and residual proteins. This fraction can be valorised, upon physic and chemical characterization, by extrusion and bioplastic production or as food additives (flour or emulsifying agent containing no fats).

However, the subject of the sequential extraction of the different microalgal products is still in its infancy, and further studies are required to reach an optimized strategy. Different strategies should be designed on the basis of the microalgal strain selected and its main product.

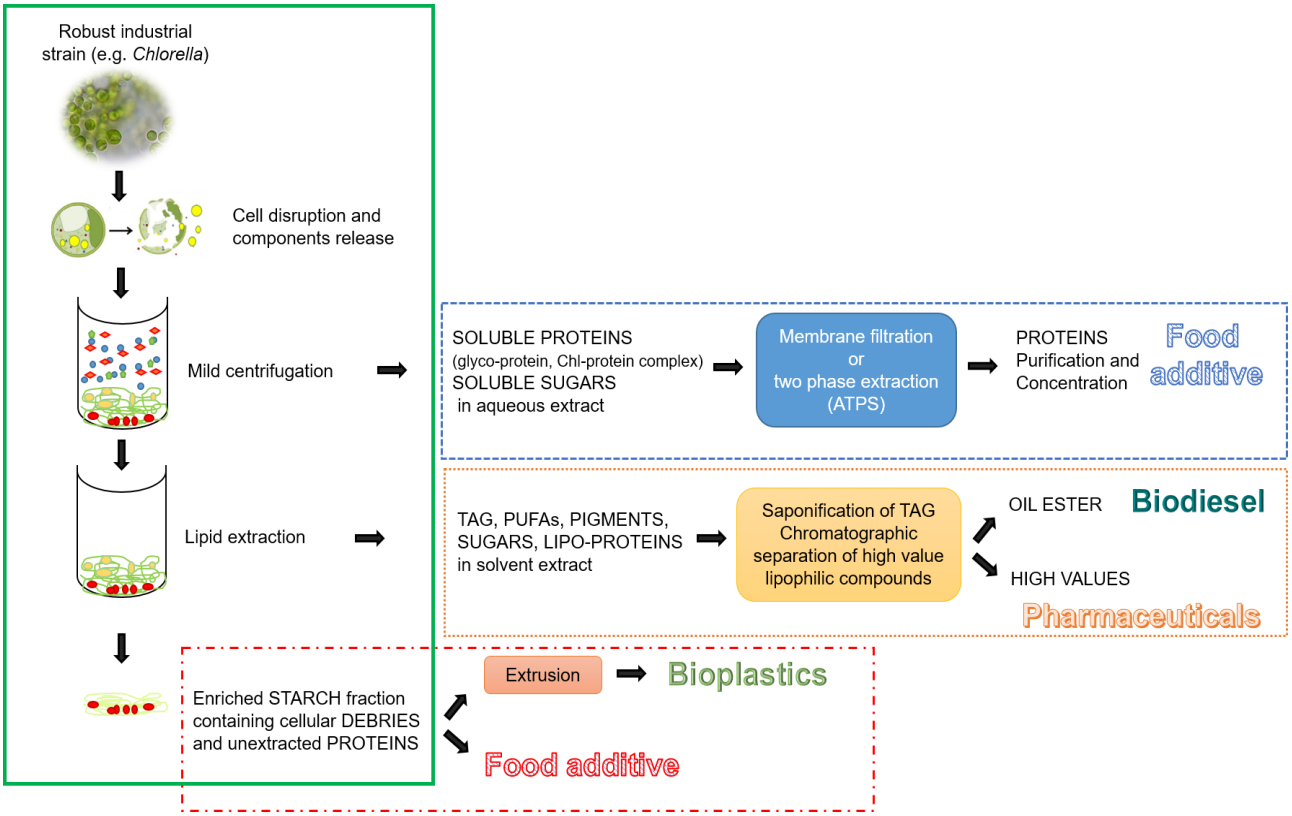

Figure 7.8: Innovative and sustainable biorefinery scheme.

7.5 Future prospective

The results of the present PhD study valorize the potential and the innovation of a biorefinery scheme focused on the exploitation of multiple microalgal components representing not-only-fuel products. Since the goal was to maximize the income from the selling of the product portfolio from the microalgae, the culture was not focused on the maximization of a single product, but on the selection of the nutrient supply and culture conditions able to provide high productivity of multiple components (Chapter 3). The valorization of the starch fraction of the microalgae was supported by a preliminary characterization of the physic-chemical properties and identification of the application opportunities (Chapter 4). Innovative thin culture system was proposed for the intensification of the microalgal biomass production with the aim of reducting the processing costs and increasing the light/biomass conversion (Chapter 5). Relation between energy input of mechanical cell disruption (bead milling) and product recovery selectivity was established (Chapter 6.1). The integration of mechanical cell disruption, mild centrifugation and three-step membrane filtration was studied for the simultaneous recovery of starch and proteins (Chapter 6.2). Starch purification was coupled with not-invasive solvent extraction of the pigments, and the value of the solvent extract as antioxidant mix was demonstrated in vitro and in vivo on eukaryotic cells (Appendix). Finally, the innovative biorefinery scheme was drawn (Figure 7.8).

Further investigation is required for the fulfillment of the multiple product biorefinery scheme. The issues to be investigated can be divided in three groups listed hereinafter.

New properties of microalgal biomass and residual fraction

Many microalgal products are still not explored. The present study was focused on the valorization of the starch fraction, but depending on the separation techniques selected, high value products are mixed with the target component in the extract or they are wasted in the residual fraction (protein, pigments or antioxidands). For example, the extraction/purification of starch requires the pigments removal (Derlue et al., 1992). Solvent-assisted extraction transfer most of the lipids, carotenoids, chlorophyll and astaxantin in the extract. The obtained extract is a mix of powerful antioxidant molecules (Petruk et al., appendix) which can be used in cosmetics and pharmaceutics or they can be furtherly separated in several fractions with application in different industrial fields. Fractions characterized by higher antioxidant activity can be sold as pharmaceuticals, while the remaining fractions should be characterized to establish the potential applications (biodiesel, colorants, edible oil). The costs of fractionation step of the initial extract should be validated by the market opportunity of the obtained fractions, by techno-economic analysis. The same argumentation can be done for the soluble proteins recovery. Aqueous proteins extraction and further purification by membrane filtration or precipitation (Ursu et al., 2014; Safi et al., 2017) produce a mix of proteins with promising applications as food additives (Schwenzfeier et al., 2011). A further separation by chromatography could reveal new antioxidant functions or techno-functional proteins for food preservation or proteins enrichment in long-life products.

Optimization and scale-up of thin-culture system

Thin-culture system is not applied in large-scale microalgal cultures. The high cost for the plant installation and operation and the high surface required are the main limitation. The building-integrating solution proposed by (Pruvost et al., 2016) offers an interesting solution, which could be applied also to the ultra-thin flat panel proposed in this work (Chapter 5). Further investigation is required to establish the maximum microalgal concentration achievable in this culture system and which is the effect of the day/night cycle on the maximum concentration and productivity. An interesting idea could be the evaluation of a “single day culture-harvesting strategy”. Since the growth rate in the ultra-thin PBR can reach high values and the night period reduce the accumulation of interesting compounds (starch, lipids, pigments), the approach could imagine a semi-continuous mode with the harvesting of high concentrated culture in the end of the day, before the night period. The remaining cells will divide in the night and restart the growth again in the morning to reach high concentration in the end of the day and for the new harvesting. In this way, the culture can continue in parallel with the processing but ensuring high concentration. The “single day culture-harvesting strategy” needs many tests for understanding the feasibility and many factors should be taken into account for the real application (effect of the season, light/dark cycle, nutrients supply strategy, techno-economic feasibility).

Integration and co-optimization of upstream and downstream processes

Currently, the optimization studies mainly regard one or two steps of the microalgae production process (Figure 7.6). Integration studies should be carried out to optimize the single process step as a function of the overall process. For example, optimization of biomass concentration and productivity of the culture system should consider the optimum concentration for the downstream processes. This evaluation should not consider only the consecutive step (cell disruption) but the complete

processing line (separations, two or three steps extraction, purifications). Normally, the disruption procedure can work at biomass concentration of 100 g L^{-1} (Postma et al., 2016) with high energy saving. This condition can cause difficulties in the following separations, indeed the precipitation of unsoluble particles and the recovery of the soluble one in the supernatant, require high-speed centrifugations, which absorb important amount of energy. Moreover, mild and sustainable purification strategies, such as filtration, chromatography exhibit better performance with not extremely concentrated solutions (see fouling effect or obstruction of the separation column). The optimization of the single step parameters has to be studied in the integrated system to ensure the technical and the economic feasibility of the process.

It worth to consider that the present study has also other interesting research material to be developed. For example, the further valorization and increase of starch productivity and quality. Indeed, there has been in the last decades a growing interest in modification of starch granules to generate new properties for applications in the fields of renewable polymers and food additives (Slattery et al., 2000; Hoover et al., 2010). Physic and chemical modifications of the purified starch granules is the current methodology adopted. Less pollutant strategies consider the engineering of the starch during its synthesis inside the plant by modifying the DNA and by adding enzymes able to introduce the desired customization. With this strategy, the amylose/amylopectine content can also be customized on the basis of the industrial necessity. In this context, the use of microalgae as starch producers can improve the efficiency of starch customization. In fact, it is reported that microalgae engineering is more feasible than plant's (Yoo et al., 2015; Wilkie et al., 2015). Then, the engineering of microalgae for generating novel starches can be considered an interesting subject of study.

REFERENCES

Acién, F.G., Fernàndez, J.M., Magàn, J.J., Molina, E., 2012. Production cost of a real microalgae production plant and strategies to reduce it. Biotechnol. Adv. 30, 1344–1353. doi:10.1016/j.biotechadv.2012.02.005

Adesanya, V.O., Davey, M.P., Scott, S.A., Smith, A.G., 2014. Kinetic modelling of growth and storage molecule production in microalgae under mixotrophic and autotrophic conditions. Bioresour. Technol. 157, 293–304. doi:10.1016/j.biortech.2014.01.032

Ansari, F.A., Shriwastav, A., Gupta, S.K., Rawat, I., Bux, F., 2017. Exploration of Microalgae Biorefinery by Optimizing Sequential Extraction of Major Metabolites from Scenedesmus obliquus. Ind. Eng. Chem. Res. 56, 3407–3412. doi:10.1021/acs.iecr.6b04814

Ariede, M.B., Candido, T.M., Jacome, A.L.M., Velasco, M.V.R., de Carvalho, J.C.M., Baby, A.R., 2017. Cosmetic attributes of algae - A review. Algal Res. 25, 483–487. doi:10.1016/j.algal.2017.05.019

Arora, N., Patel, A., Pruthi, P.A., Pruthi, V., 2015. Synergistic dynamics of nitrogen and phosphorous influences lipid productivity in Chlorella minutissima for biodiesel production. Bioresour. Technol. 213, 79–87. doi:10.1016/j.biortech.2016.02.112

Ba, F., Violeta, A., Laroche, C., Djelveh, G., 2016. Bioresource Technology Haematococcus pluvialis soluble proteins : Extraction , characterization , concentration / fractionation and emulsifying properties. Bioresour. Technol. 200, 147–152. doi:10.1016/j.biortech.2015.10.012

Balasundaram, B., Skill, S.C., Llewellyn, C.A., 2012. A low energy process for the recovery of bioproducts from cyanobacteria using a ball mill. Biochem. Eng. J. 69, 48–56.

Becker, E.W., 2007. Microalgae as a source of proteins. Biotechnol. Advanc. 25,.207-210.

Belotti, G., Bravi, M., Caprariis, B., De Filippis, P., De Scarsella, M., 2013. Effect of Nitrogen and Phosphorus Starvations on Chlorella vulgaris Lipids Productivity and Quality under Different Trophic Regimens for Biodiesel Production. Am J Plant Sci. 4, 44–51. doi:10.4236/ajps.2013.412A2006.

Benvenuti, G., Lamers, P.P., Breuer, G., Bosma, R., Cerar, A., Wijffels, R.H., Barbosa, M.J., 2016. Microalgal TAG production strategies: why batch beats repeated-batch. Biotechnol. Biofuels 9, 64. doi:10.1186/s13068-016-0475-4

Bikker, P., van Krimpen, M.M., van Wikselaar, P., Houweling-Tan, B., Scaccia, N., van Hal, J.W., Huijgen, W.J.J., Cone, J.W., López-Contreras, A.M., 2016. Biorefinery of the green seaweed Ulva lactuca to produce animal feed, chemicals and biofuels. J. Appl. Phycol. 28, 3511–3525. doi:10.1007/s10811-016-0842-3

Bilger, W., Schreiber, U., Bock, M., 1995. Determination of the quantum efficiency of photosystem II and of non-photochemical quenching of chlorophyll fluorescence in the field. Oecologia 102, 425–432. doi:10.1007/BF00341354

Biliaderis, C.G., Juliano, O.B., 1993. Thermal and mechanical properties of concentrated rice starch gels of varying composition. Food Chemistry. 48, 243-250.

Bold, H.C., Wynne, M.J., 1978. Introduction to the Algae. Structure and Reproduction. Englewood Cliffs. New Jersey, Prentice-Hall.

Brányiková, I., Maršálková, B., Doucha, J., Brányik, T., Bišová, K., Zachleder, V., Vítová, M., 2011. Microalgae-novel highly efficient starch producers. Biotechnol. Bioeng. 108, 766–776. doi:10.1002/bit.23016

Breuer, G., de Jaeger, L., Artus, V.P.G., Martens, D.E., Springer, J., Draaisma, R.B., Eggink, G., Wijffels, R.H., Lamers, P.P., 2014. Superior triacylglycerol (TAG) accumulation in starchless mutants of Scenedesmus obliquus: (II) evaluation of TAG yield and productivity in controlled photobioreactors. Biotechnol. Biofuels 7, 70. doi:10.1186/1754-6834-7-70

Breuer, G., Evers, W.A.C., de Vree, J.H., Kleinegris, D.M.M., Martens, D.E., Wijffels, R.H., 2013. Analysis of Fatty Acid Content and Composition in Microalgae. J Vis Exp. 5, 1–9. doi:10.3791/50628.

Breuer, G., Lamers, P.P., Martens, D.E., Draaisma, R.B., Wijffels, R.H., 2012. The impact of nitrogen starvation on the dynamics of triacylglycerol accumulation in nine microalgae strains. Bioresour. Technol. 124, 217–226. doi:10.1016/j.biortech.2012.08.003

Breuer, G., Lamers, P.P., Martens, D.E., Draaisma, R.B., Wijffels, R.H., 2013. Effect of light intensity, pH, and temperature on triacylglycerol (TAG) accumulation induced by nitrogen starvation in Scenedesmus obliquus. Bioresour. Technol. 143, 1–9. doi:10.1016/j.biortech.2013.05.105

Buleòn, A., 1998. Starch granules : structure and biosynthesis. Int. J. Biol. Macromol. 23, 85–112.

Carvalho, A.P., Silva, S.O., Baptista, J.M., 2011. Light requirements in microalgal photobioreactors : An overview of biophotonic aspects Light requirements in microalgal photobioreactors : an overview of biophotonic aspects. doi:10.1007/s00253-010-3047-8

Castro-Munoz, R., Barragàn-Huerta, B.E., Fìla, V., Denis, P.C., Ruby-Figueroa, R., 2017. Current role of membrane technology: from the treatment of agro-industrial by-products up to the valorization of valuable compounds. Waste Biom. Valor. DOI 10.1007/s12649-017-0003-1.

Chauhan, K., Kaur, J., Singh, P., Sharma, P., Sharma, P., Chauhan, G.S., 2015. An Efficient and Regenerable Quaternary Starch for Removal of Nitrate from Aqueous Solutions. Industrial and Ing Chem Res. 55 (9), 2507–2519.

Cheali, P., Loureiro, da Costa Lira Gargalo, C., Gernaey, K., Sin, G., 2015. A Framework for Sustainable Design of Algal Biorefineries: Economic Aspects and Life Cycle Analysis. Prokop A, Bajpai RK, Zappi ME (edn) Springer, 511-535.

Chen, C.Y., Zhao, X.Q., Yen, H.W., Ho, S.H., Cheng, C.L., Lee, D.J., 2013. Microalgae-based carbohydrates for biofuel production. Biochem Eng J. 78, 1–10. doi:10.1016/j.bej.2013.03.006.

Chen, Y., Vaidyanathan, S., 2013. Simultaneous assay of pigments, carbohydrates, proteins and lipids in microalgae. Anal Chim Acta. 776, 31–40. doi:10.1016/j.aca.2013.03.005.

Chen, Y., Xu, C., Vaidyanathan, S., 2017. Critical Reviews in Biotechnology Microalgae : a robust " green bio-bridge " between energy and environment. Crit. Rev. Biotechnol. 0, 1–18. doi:10.1080/07388551.2017.1355774

Chew, W., K., Ying, J., Loke, P., Hui, N., Ching, J., Chuan, T., Lee, D., Chang, J., 2017. Bioresource Technology Microalgae biorefinery : High value products perspectives. Bioresour. Technol. 229, 53–62. doi:10.1016/j.biortech.2017.01.006

Chisti, Y., 2006. Environmental Pollution and Monitoring MICROALGAE AS SUSTAINABLE CELL FACTORIES 5, 261–274.

Christaki, E., Florou-Paneri, P., Bonos, E., 2011. Microalgae: a novel ingredient in nutrition. Int J Food Sci Nutr. 62, 794–799.

Collos, Y., Mornet, F., Sciandra, A., Waser, N., Larson, A., Harrison, P.J., 1999. An optical method for the rapid measurement of micromolar concentrations of nitrate in marine phytoplankton cultures. J Appl Phycol. 11, 179–184.

Coons, J.E., Kalb, D.M., Dale, T., Marrone, B.L., 2014. Getting to low-cost algal biofuels : A monograph on conventional and cutting-edge harvesting and extraction technologies. ALGAL 6, 250–270. doi:10.1016/j.algal.2014.08.005

Copeland, L., Blazek, J., Salman, H., Tang, M.C., 2009. Form and functionality of starch. Food Hydrocoll. 23, 1527–1534. doi:10.1016/j.foodhyd.2008.09.016

Crawshaw, R., 2004. Co-product feeds: animal feeds from the food and drinks industries. Nothingham University Press

Cuaresma, M., Janssen, M., van den End, E.J., Vílchez, C., Wijffels, R.H., 2011. Luminostat operation: A tool to maximize microalgae photosynthetic efficiency in photobioreactors during the daily light cycle? Bioresour. Technol. doi:10.1016/j.biortech.2011.05.076

Cuaresma, M., Janssen, M., Vìlchez, C., Wijffels, R.H., 2009. Productivity of Chlorella sorokiniana in a short light-path (SLP) panel photobioreactor under high irradiance. Biotechnol. Bioeng. 104, 352–359. doi:10.1002/bit.22394

Cuellar-Bermudez, S.P., Aguilar-Hernandez, I., Cardenas-Chavez, D.L., Ornelas-Soto, N., Romero-Ogawa, M.A., Parra-Saldivar, R., 2015. Extraction and purification of high-value metabolites from microalgae: Essential lipids, astaxanthin and phycobiliproteins. Microb. Biotechnol. 8:190–209. doi: 10.1111/1751-7915.12167.

Davis, R., Markham, J., Kinchin, C., Grundl, N., Tan, E.C.D., Humbird, D., Davis, R., Markham, J., Kinchin, C., Grundl, N., Tan, E.C.D., Humbird, D., 2016. Process Design and Economics for the Production of Algal Biomass.

De Farias Silva, C.E., Sforza, E., 2016. Carbohydrate productivity in continuous reactor under nitrogen limitation: Effect of light and residence time on nutrient uptake in Chlorella vulgaris. Process Biochem. 51, 2112–8. doi:10.1016/j.procbio.2016.09.015.

De Farias Silva, C.E., Sforza, E., Bertucco, A., 2017. Effects of pH and Carbon Source on Synechococcus PCC 7002 Cultivation: Biomass and Carbohydrate Production with Different Strategies for pH Control. Appl Biochem Biotechnol. 181, 682–98. doi:10.1007/s12010-016-2241-2.

Denis, C., Massé, A., Fleurence, J., Jaouen, P., 2009. Concentration and pre-purification with ultrafiltration of a R-phycoerythrin solution extracted from macro-algae Grateloupia turuturu : Process definition and up-scaling 69, 37–42. doi:10.1016/j.seppur.2009.06.017

Derlue, B., Fontaine, T., Routier, F., Decq, A., Ball, S., 1992. Waxy Chlamydomonas reinhardtii : Monocellular Algal Mutants Defective in Amylose Biosynthesis and Granule-Bound Starch Synthase Activity Accumulate a Structurally Modified Amylopectin. Starch J. 174, 3612–3620.

Doucha, J., Lívanský, K., 2006. Productivity, CO2/O2 exchange and hydraulics in outdoor open high density microalgal (Chlorella sp.) photobioreactors operated in a Middle and Southern European climate. J. Appl. Phycol. 18, 811–826. doi:10.1007/s10811-006-9100-4

Doucha, J., Lívanský, K., 2009. Outdoor open thin-layer microalgal photobioreactor: Potential productivity. J. Appl. Phycol. 21, 111–117. doi:10.1007/s10811-008-9336-2

Doucha, J., Lívanskyˊ, K., 2008. Influence of processing parameters on disintegration of Chlorella cells in various types of homogenizers. Appl. Microbiol. Biotechnol. 81, 431–440.

Draaisma, R.B., Wijffels, R.H., Slegers, P.M., Brentner, L.B., Roy, A., Barbosa, M.J., 2013. Food commodities from microalgae. Curr. Opin. Biotechnol. 24, 169–177. doi:10.1016/j.copbio.2012.09.012

Dragone, G., Fernandes, B.D., Abreu, A.P., Vicente, A.A., Teixeira, J.A., 2011. Nutrient limitation as a strategy for increasing starch accumulation in microalgae. Appl. Energy 88, 3331–3335. doi:10.1016/j.apenergy.2011.03.012

Elmi Sharlina, M.S., Yaacob, W.A., Lazim, A.M:, Fazry, S., Lim, S.J., Abdullah, S., Noordin, A., Kumaran, M., 2017. Physicochemical Properties of Starch from Dioscorea pyrifolia tubers. Food Chem. 220, 225-232.

FAO: Food and Agriculture Organization of the United Nations. Rome, 2002. The state of food and agriculture.

Fernandes, B., Teixeira, J., Dragone, G., Vicente, A.A., Kawano, S., Bišová, K., Přibyl, P., Zachleder, V., Vítová, M., 2013. Relationship between starch and lipid accumulation induced by nutrient depletion and replenishment in the microalga Parachlorella kessleri. Bioresour. Technol. 144, 268–274. doi:10.1016/j.biortech.2013.06.096

Ferreira, S., Sant'Anna, C., 2017. Impact of culture conditions on the chlorophyll content of microalgae for biotechnological applications. World J. Microbiol. Biotechnol. 33, 1–8. doi:10.1007/s11274-016-2181-6

Filippov, S.K., Sergeeva, O.Y., Vlasov, P.S., Zavyalova, M.S., Belostotskaya, G.B., Garamus, V.M., Khrustaleva, R.S., Stepanek, P., Domnina, N.S., 2015. Modified hydroxyethyl starch protects cells from oxidative damage. Carbohydr. Polym. 134, 314–323. doi:10.1016/j.carbpol.2015.07.062

Fuller, M. F., 2004. The encyclopedia of farm animal nutrition. CABI Publishing Series, 606 pp

Garay, L.A., Boundy-Mills, K.L., German, J.B., 2014. Accumulation of high-value lipids in single-cell microorganisms: A mechanistic approach and future perspectives. J. Agric. Food Chem. 62, 2709–2727. doi:10.1021/jf4042134

Gardner, R.D., Lohman, E., Gerlach, R., Cooksey, K.E., Peyton, B.M., 2013. Comparison of CO2 and bicarbonate as inorganic carbon sources for triacylglycerol and starch accumulation in Chlamydomonas reinhardtii. Biotechnol Bioeng. 110, 87–96. doi:10.1002/bit.24592.

Gargano, I., Olivieri, G., Spasiano, D., Andreozzi, R., Pollio, A., Marotta, R., D'Ambrosio, N., Marzocchella, 2015. A. Kinetic characterization of the photosynthetic reaction centres in microalgae by means of fluorescence methodology. J. Biotechnol. 212: 1-10.

Garrido, F., Banerjee, U.C., Chisti, Y., Moo-Young, M., 1994. Disruption of a recombinant yeast for the release of B-galactosidase. Bioseparation 4, 319–328.

Gerardo, M.L., Hende, V. Den, Vervaeren, H., Coward, T., Skill, S.C., 2015. Harvesting of microalgae within a biore fi nery approach : A review of the developments and case studies from pilot-plants 11, 248–262. doi:10.1016/j.algal.2015.06.019

Gerardo, M.L., Oatley-Radcliffe, D.L., Lovitt, R.W., 2014. Integration of membrane technology in microalgae biorefineries. J. Memb. Sci. 464, 86–99. doi:10.1016/j.memsci.2014.04.010

Ghisellini, P., Cialani, C., Ulgiati, S., 2016. A review on circular economy: The expected transition to a balanced interplay of environmental and economic systems. J. Clean. Prod. 114, 11–32. doi:10.1016/j.jclepro.2015.09.007

Gifuni, I., Olivieri, G., Pollio, A., Franco, T.T., Marzocchella, A., 2017. Autotrophyc starch production by *Chlamydomonas* species. J Appl Phycol, 28:1-10.

Gifuni, I., Olivieri, G., Russo, I., Errico, G.D., Pollio, A., Marzocchella, A., 2017. Microalgae as New Sources of Starch : Isolation and Characterization of Microalgal Starch Granules. 57, 1423–8. doi:10.3303/CET1757238.

Gilbert-lópez, B., Mendiola, J.A., Broek, L.A.M. Van Den, Houweling-tan, B., Sijtsma, L., Cifuentes, A., Herrero, M., Ibáñez, E., 2017. Green compressed fl uid technologies for downstream processing of Scenedesmus obliquus in a biore fi nery approach 24, 111–121. doi:10.1016/j.algal.2017.03.011

Giorno, F., Mazzei, R., Giorno, L., 2013. Purification of triacylglycerols for biodiesel production from Nannochloropsis microalgae by membrane technology. Bioresour. Technol. 140, 172–178. doi:10.1016/j.biortech.2013.04.073

Global Industry Analysts, Inc, 2014. Online Learning Industry Poised for $107 Billion. McCue, T.J. Distance Education Report 2015, 18:8.

Goiris, K., Van Colen, W., Wilches, I., León-Tamariz, F., De Cooman, L., Muylaert, K., 2015. Impact of nutrient stress on antioxidant production in three species of microalgae. Algal Res 7: 51–57

Gouveia, A.P. Batista, A. Miranda, J. Empis, A. Raymundo, L., 2007. Chlorella vulgaris biomass used as colouring source in traditional butter cookies, Innov. Food Sci. Emerg. Technol. 8, 433–436. doi:10.1016/j.ifset.2007.03.026

Guihé, F., Stengel, D.B., 2013. Carbon Availability in the Marine Haptophyte Pavlova lutheri 4246–4266. doi:10.3390/md11114246

Guiry, M.D., 2012. How many species of algae are there? J. Phycol. 48, 1057–1063. doi:10.1111/j.1529-8817.2012.01222.x

Günerken, E., D'Hondt, E., Eppink, M.H.M., Garcia-Gonzalez, L., Elst, K., Wijffels, R.H., 2015. Cell disruption for microalgae biorefineries. Biotechnol. Adv. 33, 243–260. doi:10.1016/j.biotechadv.2015.01.008

Heim, A., Kamionowska, U., Solecki, M., 2007. The effect of microorganism concentration on yeast cell disruption in a bead mill. J. Food Eng. 83, 121–128. doi:10.1016/j.jfoodeng.2007.02.047

Ho, S.H., Huang, S.W., Chen, C.Y., Hasunuma, T., Kondo, A., Chang, J.S., 2013. Bioethanol production using carbohydrate-rich microalgae biomass as feedstock. Bioresour Technol. 135, 191–8. doi:10.1016/j.biortech.2012.10.015.

Hoover, R., Hughes, T., Chung, H.J., Liu, Q., 2010. Composition, molecular structure, properties, and modification of pulse starches: A review. Food Research International. 43 (2), 399-413. doi.org/10.1016/j.foodres.2009.09.001.

Hussain, F., Shah, S.Z., Zhou, W., Iqbal, M., 2017. Microalgae screening under CO2 stress: Growth and micro-nutrients removal efficiency. J. Photochem. Photobiol. B Biol. 170, 91–98. doi:10.1016/j.jphotobiol.2017.03.021

Janssen, M., 2016. Microalgal Photosynthesis and Growth in Mass Culture, 1st ed, Photobioreaction Engineering. Elsevier Inc. doi:10.1016/bs.ache.2015.11.001

Jerez, C.G., Malapascua, J. R., Sergejevová, M., Figueroa, F.L., Masojídek, J., 2016. Effect of Nutrient Starvation under High Irradiance on Lipid and Starch Accumulation in Chlorella fusca (Chlorophyta). Mar Biotechnol. 18, 24-36

Jong, E. De, Jungmeier, G., 2015. Biorefinery Concepts in Comparison to Petrochemical Refineries, Industrial Biorefineries and White Biotechnology. doi:10.1016/B978-0-444-63453-5.00001-X

Kandilian, R., Pruvost, J., Legrand, J., Pilon, L., 2014. Influence of light absorption rate by Nannochloropsis oculata on triglyceride production during nitrogen starvation. Bioresour. Technol. 163, 308–319. doi:10.1016/j.biortech.2014.04.045

Kim, S.S., Ly, H.V., Kim, J., Lee, E.Y., Woo, H.C., 2015. Pyrolysis of microalgae residual biomass derived from Dunaliella tertiolecta after lipid extraction and carbohydrate saccharification. Chem. Eng. J. 263, 194–199. doi:10.1016/j.cej.2014.11.045

Klok, A.J., Lamers, P.P., Martens, D.E., Draaisma, R.B., Wijffels, R.H., 2014. Edible oils from microalgae: Insights in TAG accumulation. Trends Biotechnol. 32, 521–8. doi:10.1016/j.tibtech.2014.07.004.

Klok, A.J., Verbaanderd, J.A., Lamers, P.P., Martens, D.E., Rinzema, A., Wijffels, R.H., 2013. A model for customising biomass composition in continuous microalgae production. Bioresour. Technol. 146, 89–100. doi:10.1016/j.biortech.2013.07.039

Kwade, A., Schwedes, J., 2002. Breaking characteristics of different materials and their effect on stress intensity and stress number in stirred media mills. Powder Technol. 122, 109–121. doi:10.1016/S0032-5910(01)00406-5

Kwade, A., Schwedes, J., 2007. Chapter 6 wet grinding in stirred media mills. In: Agba, M.G., Salman, D., Michael, J.H. (Eds.), Handbook of Powder Technology, vol. 12. Elsevier Science B.V., pp. 251–382.

Lamers, P.P., Janssen, M., De Vos, R.C.H., Bino, R.J., Wijffels, R.H., 2012. Carotenoid and fatty acid metabolism in nitrogen-starved Dunaliella salina, a unicellular green microalga. J. Biotechnol. 162, 21–27. doi:10.1016/j.jbiotec.2012.04.018

Lari, Z., Moradi-kheibari, N., Ahmadzadeh, H., 2016. Bioprocess engineering of microalgae to optimize lipid production through nutrient management. J. Appl. Phycol. 3235–3250. doi:10.1007/s10811-016-0884-6

Lavín, P.L., Lourenço, S.O., 2005. An evaluation of the accumulation of intracellular inorganic nitrogen pools by marine microalgae in batch cultures. Brazilian J Oceanogr. 53, 55–67. doi:10.1590/S1679-87592005000100006.

Li, T., Gargouri, M., Feng, J., Park, J.J., Gao, D., Miao, C., 2015. Regulation of starch and lipid accumulation in a microalga *Chlorella sorokiniana*. Bioresour Technol. 180, 250–7. doi:10.1016/j.biortech.2015.01.005.

Lindeboom, N., Chang, P.R., Tyle,r R.T., 2004. Analytical, biochemical and physicochemical aspects of starch granule size, with emphasis on small granule starches. A review. Starch J. 56, (3-4), 89-99.

Lopes, T., Gouveia, L., Reis, A., 2014. Integrated microbial processes for biofuels and high value-added products : the way to improve the cost effectiveness of biofuel production 1043–1053. doi:10.1007/s00253-013-5389-5

Lorente, E., Haponska, M., Clavero, E., Torras, C., Salvad??, J., 2016. Microalgae fractionation using steam explosion, dynamic and tangential cross-flow membrane filtration. Bioresour. Technol. 237, 3–10. doi:10.1016/j.biortech.2017.03.129

Lupatini, A.L., de Oliveira Bispo, L., Colla, L.M., Costa, J.A.V., Canan, C., Colla, E., 2016. Protein and carbohydrate extraction from S. platensis biomass by ultrasound and mechanical agitation. Food Res. Int. 99, 1028–1035. doi:10.1016/j.foodres.2016.11.036

Manirafasha, E., Ndikubwimana, T., Zeng, X., Lu, Y., Jing, K., 2016. Phycobiliprotein : Potential microalgae derived pharmaceutical and biological reagent. Biochem. Eng. J. 109, 282–296. doi:10.1016/j.bej.2016.01.025

Marzocchella, A., Andreozzi, R., Bartalini, G., Filippone, E., Olivieri, G., Pinto, G., Salatino, P., 2010. A techno-economic assessment of biofuels production by microalgae. Chem. Eng. Trans. doi:10.3303/CET1020029

Masojídek, J., Torzillo, G., 2014. Mass Cultivation of Freshwater Microalgae☆. Ref. Modul. Earth Syst. Environ. Sci. 2226–2235. doi:10.1016/B978-0-12-409548-9.09373-8

Massé, A., Thi, H.N., Roelens, G., Legentilhomme, P., Jaouen, P., 2013. Seawater ultrafiltration: Role of particles on organic rejections and permeate fluxes. Environ. Technol. (United Kingdom) 34, 2553–2561. doi:10.1080/09593330.2013.777127

Mata, T.M., Mendes, A.M., Caetano, N.S., Martins, A.A., 2014. Sustainability and economic evaluation of microalgae grown in brewery wastewater. Bioresour. Technol. 168, 151–158. doi:10.1016/j.biortech.2014.04.091

Mizuno, Y., Sato, A., Watanabe, K., Hirata, A., Takeshita, T., Ota, S., Sato, N., Zachleder, V., Tsuzuki, M., Kawano, S., 2013. Sequential accumulation of starch and lipid induced by sulfur deficiency in Chlorella and Parachlorella species. Bioresour. Technol. 129, 150–155. doi:10.1016/j.biortech.2012.11.030

Mohan, S.V., Nikhil, G.N., Chiranjeevi, P., Reddy, C.N., Rohit, M. V, Kumar, A.N., 2016. Bioresource Technology Waste biorefinery models towards sustainable circular bioeconomy : Critical review and future perspectives. Bioresour. Technol. 215, 2–12. doi:10.1016/j.biortech.2016.03.130

MojioviĆ, L.M., Pejin, D., Ć, O.G., Rakin, M., Ć, M.V., Ć, S.N., Ć, D.S., 2009. PROGRESS IN THE PRODUCTION OF BIOETHANOL ON STARCH-BASED FEEDSTOCKS * 15, 211–226. doi:10.2298/CICEQ0904211M

Monari, C., Righi, S., Olsen, S.I., 2016. Greenhouse gas emissions and energy balance of biodiesel production from microalgae cultivated in photobioreactors in Denmark: A life-cycle modeling. J. Clean. Prod. doi:10.1016/j.jclepro.2015.08.112

Montalescot, V., Rinaldi, T., Touchard, R., Jubeau, S., Frappart, M., Jaouen, P., Bourseau, P., Marchal, L., 2015. Optimization of bead milling parameters for the cell disruption of microalgae: Process modeling and application to Porphyridium cruentum and Nannochloropsis oculata. Bioresour. Technol. 196, 339–346. doi:10.1016/j.biortech.2015.07.075

Moraes, B.S., Junqueira, T.L., Pavanello, L.G., Cavalett, O., Mantelatto, P.E., Bonomi, A., Zaiat, M., 2014. Anaerobic digestion of vinasse from sugarcane biorefineries in Brazil from energy, environmental, and economic perspectives: Profit or expense. Appl. Energy 113, 825–835. doi:10.1016/j.apenergy.2013.07.018

Moreno-garcia, L., Adjallé, K., Barnabé, S., Raghavan, G.S. V, 2017. Microalgae biomass production for a biore fi nery system : Recent advances and the way towards sustainability 76, 493–506. doi:10.1016/j.rser.2017.03.024

Morton Satin, 2012, Functional properties of starches, FAO publication report.

Msanne, J., Xu, D., Konda, A.R., Casas-Mollano, J.A., Awada, T., Cahoon, E.B., Cerutti, H., 2012. Metabolic and gene expression changes triggered by nitrogen deprivation in the photoautotrophically grown microalgae Chlamydomonas reinhardtii and Coccomyxa sp. C-169. Phytochemistry 75, 50–59. doi:10.1016/j.phytochem.2011.12.007

Mubarak, M., Shaija, A., Suchithra, T. V., 2015. A review on the extraction of lipid from microalgae for biodiesel production. Algal Res. 7, 117–123. doi:10.1016/j.algal.2014.10.008

Mulders, K.J.M., Janssen, J.H., Martens, D.E., Wijffels, R.H., Lamers, P.P., 2014. Effect of biomass concentration on secondary carotenoids and triacylglycerol (TAG) accumulation in nitrogen-depleted Chlorella zo fi ngiensis. ALGAL 6, 8–16. doi:10.1016/j.algal.2014.08.006

Olivieri, G., Gargano, I., Andreozzi, R., Marotta, R., Marzocchella, A., Pinto, G., Pollio, A., 2013. Effects of photobioreactors design and operating conditions on *Stichococcus bacillaris* biomass and biodiesel production. Biochem Eng J. 70, 8-1424

Olivieri, G., Guida, T., Salatino, P., Marzocchella, A., 2013. A techno-economic analysis of biodiesel production from microalgae. Environ Eng Manag J;12:1563-1573.

Olivieri, G., Marzocchella, A., Andreozzi, R., Pinto, G., Pollio, A., 2011. Biodiesel production from Stichococcus strains at laboratory scale. J. Chem. Technol. Biotechnol. 86, 776–783.

Packer, M., 2009. Algal capture of carbon dioxide; biomass generation as a tool for greenhouse gas mitigation with reference to New Zealand energy strategy and policy. Energy Policy 37, 3428–3437. doi:10.1016/j.enpol.2008.12.025

Penloglou, G., Chatzidoukas, C., Kiparissides, C., 2016. A Microalgae-based biorefinery plant for the production of valuable biochemicals: design and economics. Computer Aided Chem Eng. 38:1731-1736.

Pérez, S., Bertoft, E., 2010. The molecular structures of starch components and their contribution to the architecture of starch granules: A comprehensive review. Starch/Staerke 62, 389–420. doi:10.1002/star.201000013

Pérez-Pacheco, E., Moo-Huchin, V.M., Estrada-León, R.J., Ortiz-Fernández, A., May-Hernández, L.H., Ríos-Soberanis, C.R., Betancur-Ancona, D., 2014. Isolation and characterization of starch obtained from *Brosimumalicastrum* Swarts Seeds. Carbohyd Polym.101:920-927.

Perin, G., Segalla, A., Basso, S., Simionato, D., Meneghesso, A., Sforza, E., Bertucco, A., Morosinotto, T., 2014. Biotechnological optimization of light use efficiency in nannochloropsis cultures for biodiesel production. Chem Eng Trans. 37, 763-768.

Phong, W.N., Le, C.F., Show, P.L., Chang, J-S, Ling, T.C., 2017. Extractive disruption process integration using ultrasonication and an aqueous two-phase system for proteins recovery from Chlorella sorokiniana. Eng. Life Sci. 17, 357-369.

Pireto, C.V.G, Ramos, F.D., Estrada, V., Villar, M.A., 2017.Optimization of an integrated algae-based biorefinery for the production of biodiesel, astaxanthin and PHB. Energy. 139, 1159-1172.

Postma, P.R., Miron, T.L., Olivieri, G., Barbosa, M.J., Wijffels, R.H., Eppink, M.H.M., 2014. Mild disintegration of the green microalgae Chlorella vulgaris using bead milling. Bioresour. Technol. 184, 297–304.

Postma, P.R., Miron, T.L., Olivieri, G., Barbosa, M.J., Wijffels, R.H., Eppink, M.H.M., 2015. Mild disintegration of the green microalgae Chlorella vulgaris using bead milling. Bioresour. Technol. 184, 297–304. doi:10.1016/j.biortech.2014.09.033

Postma, P.R., Pataro, G., Capitoli, M., Barbosa, M.J., Wijffels, R.H., Eppink, M.H.M., Olivieri, G., Ferrari, G., 2016. Selective extraction of intracellular components from the microalga Chlorella vulgaris by combined pulsed electric field-temperature treatment. Bioresour. Technol. 203, 80–88. doi:10.1016/j.biortech.2015.12.012

Postma, P.R., Suarez-Garcia, E., Safi, C., Olivieri, G., Olivieri, G., Wijffels, R.H., Wijffels, R.H., 2017. Energy efficient bead milling of microalgae: Effect of bead size on disintegration and release of proteins and carbohydrates. Bioresour. Technol. 224, 670–679. doi:10.1016/j.biortech.2016.11.071

Procházková, G., Brányiková, I., 2014. Effect of nutrient supply status on biomass composition of eukaryotic green microalgae 1359–1377. doi:10.1007/s10811-013-0154-9

Pruvost, J., Cornet, J.F., Goetz, V., Legrand, J., 2012. Theoretical investigation of biomass productivities achievable in solar rectangular photobioreactors for the cyanobacterium Arthrospira platensis. Biotechnol Prog. 28, 699–714.

Pruvost, J., Le Borgne, F., Artu, A., Legrand, J., 2017. Development of a thin-film solar photobioreactor with high biomass volumetric productivity (AlgoFilm??) based on process intensification principles. Algal Res. 21, 120–137. doi:10.1016/j.algal.2016.10.012

Pruvost, J., Le Gouic, B., Lepine, O., Legrand, J., Le Borgne, F., 2016. Microalgae culture in building-integrated photobioreactors: Biomass production modelling and energetic analysis. Chem. Eng. J. 284, 850–861. doi:10.1016/j.cej.2015.08.118

Pruvost, J., Van Vooren, G., Le Gouic, B., Couzinet-Mossion, A., Legrand, J., 2011. Systematic investigation of biomass and lipid productivity by microalgae in photobioreactors for biodiesel application. Bioresour. Technol. 102, 150–158. doi:10.1016/j.biortech.2010.06.153

Qiang, H., Richmond, A., 1996. Productivity and photosynthetic efficiency of Spirulina platensis as affected by light intensity, algal density and rate of mixing in a flat plate photobioreactor. J. Appl. Phycol. 8, 139–145. doi:10.1007/BF02186317

Reddy, C.K., Vidya, P.V., Vijina, K., Haripriya, S., 2015. Modification of poovan banana (Musa AAB) starch by c-irradiation: effect on in vitro digestibility, molecular structure and physico-chemical properties 1778–1784. doi:10.1111/ijfs.12846

Rezaie, M., Farhoosh, R., Iranshahi, M., Sharif, A., Golmohamadzadeh, S., 2015. Ultrasonic-assisted extraction of antioxidative compounds from Bene (Pistacia atlantica subsp . mutica) hull using various solvents of different physicochemical properties. FOOD Chem. 173, 577–583. doi:10.1016/j.foodchem.2014.10.081

Richmond, A., Hu, Q., 2013. Phycology, A., n.d. Handbook of Microalgal Culture.

Rosenberg, J.N., Oyler, G.A., Wilkinson, L., Betenbaugh, M.J., 2008. A green light for engineered algae: redirecting metabolism to fuel a biotechnology revolution. Curr. Opin. Biotechnol. 19, 430–436. doi:10.1016/j.copbio.2008.07.008

Rossi, F., Olguìn, E.J., Diels, L., De Philippis, R., 2015. Microbial fixation of CO2 in water bodies and in drylands to combat climate change, soil loss and desertification. N. Biotechnol. 32, 109–120. doi:10.1016/j.nbt.2013.12.002

Ruiz, J., Olivieri, G., de Vree, J., Bosma, R., Willems, P., Reith, J.H., Eppink, M.H.M., Kleinegris, D.M.M., Wijffels, R.H., Barbosa, M.J., 2016. Towards industrial products from microalgae. Energy Environ Sci 9: 3036–3043.

Safi, C., Cabas Rodriguez, L., Mulder, W.J., Engelen-Smit, N., Spekking, W., van den Broek, L.A.M., Olivieri, G., Sijtsma, L., 2017. Energy consumption and water-soluble protein release by cell wall disruption of Nannochloropsis gaditana. Bioresour. Technol. 239, 204–210. doi:10.1016/j.biortech.2017.05.012

Safi, C., Frances, C., Ursu, A.V., Laroche, C., Pouzet, C., Vaca-Garcia, C., Pontalier, PY., 2015. Understanding the effect of cell disruption methods on the diffusions of Chlorella vulgaris proteins and pigments in acquous phase. Algal Res. 8, 61-68.

Safi, C., Ursu, A.V., Laroche, C., Zebib, B., Merah, O., Pontalier, P.Y., Vaca-Garcia, C., 2014. Aqueous extraction of proteins from microalgae: Effect of different cell disruption methods. Algal Res. 3, 61–65. doi:10.1016/j.algal.2013.12.004

Schwartz, D.; Whistler, R. L., 2009. History and future of starch. In: BeMiller, J. N.; Whistler, R. L. (Eds). Starch: Chemistry and Technology. 3rd edition. Academic Press. Elsevier

Schwenzfeier, A., Wierenga, P.A., Eppink, M.H.M., Gruppen, H., 2014. Effect of charged polysaccharides on the techno-functional properties of fractions obtained from algae soluble protein isolate. Food Hydrocoll. doi:10.1016/j.foodhyd.2013.07.019

Schwenzfeier, A., Wierenga, P.A., Gruppen, A., 2012. Isolation and characterization of soluble protein from the green microalgae *Tetraselmis* sp. Bioresour Technol. 102, 9121-9127.

Schwenzfeier, A., Wierenga, P.A., Gruppen, H., 2011. Isolation and characterization of soluble protein from the green microalgae Tetraselmis sp. Bioresour. Technol. 102, 9121–9127. doi:10.1016/j.biortech.2011.07.046

Sforza, E., Enzo, M., Bertucco, A., 2014. Design of microalgal biomass production in a continuous photobioreactor: An integrated experimental and modeling approach. Chem. Eng. Res. Des. doi:10.1016/j.cherd.2013.08.017

Shiratake, T., Sato, A., Minoda, A., Tsuzuki, M., Sato, N., 2013. Air-Drying of Cells , the Novel Conditions for Stimulated Synthesis of Triacylglycerol in a Green Alga , Chlorella kessleri 8. doi:10.1371/journal.pone.0079630

Skrede, A., Mydland, L.T., Ahlstrøm, Ø., Reitan, K.I., 2011. Evaluation of microalgae as sources of digestible nutrients for monogastric animals * 131–142.

Slattery, C.J., Kavakli, I.H., Okita, T.W., 2000. Engineering starch for increased quantity and quality. Trends in Plant Science. 5 (7), 291-298. doi.org/10.1016/S1360-1385(00)01657-5.

Soh, L., Montazeri, M., Haznedaroglu, B.Z., Kelly, C., Peccia, J., Eckelman, M.J., 2014. Evaluating microalgal integrated biorefinery schemes: Empirical controlled growth studies and life cycle assessment. Bioresour Technol. 151:19–27. doi:10.1016/j.biortech.2013.10.012.

Souliés, A., Legrand, J., Marec, H., Pruvost, J., Castelain, C., Burghelea, T., Cornet, J.F., 2016. Investigation and modeling of the effects of light spectrum and incident angle on the growth of Chlorella vulgaris in photobioreactors. Biotechnol. Prog. 32, 247–261. doi:10.1002/btpr.2244

Souliès, A., Pruvost, J., Legrand, J., Castelain, C., Burghelea, T.I., 2013. Rheological properties of suspensions of the green microalga Chlorella vulgaris at various volume fractions. Rheol. Acta 52, 589–605. doi:10.1007/s00397-013-0700-z

Stengel, D.B., Walker, J.M., 2015. Natural Products From Marine Algae, Natural Products From Marine Algae. doi:10.1007/978-1-4939-2684-8

Suzuki, E., Suzuki, R., 2013. Variation of Storage Polysaccharides in phototrophic microorganisms. Journal of Applied Glycoscience, 60, p. 21-27

Takeshita, T., Ota, S., Yamazaki, T., Hirata, A., Zachleder, V., Kawano, S., 2014. Starch and lipid accumulation in eight strains of six Chlorella species under comparatively high light intensity and aeration culture conditions. Bioresour Technol. 158, 127–34. doi:10.1016/j.biortech.2014.01.135.

Tanadul, O. u ma, Vandergheynst, J.S., Beckles, D.M., Powell, A.L.T., Labavitch, J.M., 2014. The impact of elevated CO2 concentration on the quality of algal starch as a potential biofuel feedstock. Biotechnol. Bioeng. 111, 1323–1331. doi:10.1002/bit.25203

Thomassen, G., Dael, M. Van, Lemmens, B., Passel, S. Van, 2017. A review of the sustainability of algal-based biore fi neries : Towards an integrated assessment framework. Renew. Sustain. Energy Rev. 68, 876–887. doi:10.1016/j.rser.2016.02.015

Tibbetts, S.M., Yasumaru, F., Lemos, D., 2017. In vitro prediction of digestible protein content of marine microalgae (Nannochloropsis granulata) meals for Paci fi c white shrimp (Litopenaeus vannamei) and rainbow trout (Oncorhynchus mykiss). ALGAL 21, 76–80. doi:10.1016/j.algal.2016.11.010

Tilman, D., Clark, M., 2014. Global diets link environmental sustainability and human health. Nature 515, 518–522. doi:10.1038/nature13959

Tredici, M.R., 2010. Photobiology of microalgae mass cultures: understanding the tools for the next green revolution. Biofuels 1, 143–162. doi:10.4155/bfs.09.10

Tredici, M.R., Rodolfi, L., Biondi, N., Bassi, N., Sampietro, G., 2016. Techno-economic analysis of microalgal biomass production in a 1-ha Green Wall Panel (GWPII) plant. Algal Res. 19, 253–263. doi:10.1016/j.algal.2016.09.005

Ummalyma Beevi, S., Gnansounou, E., Sukumaran, R.K., Sindhu, R., Pandey, A., Sahoo, D., 2017. Bioresource Technology Bioflocculation : An alternative strategy for harvesting of microalgae – An overview. Bioresour. Technol. 242, 227–235. doi:10.1016/j.biortech.2017.02.097

Ursu, A.V., Marcati, A., Sayd, T., Sante-Lhoutellier, V., Djelveh, G., Michaud, P., 2014. Extraction, fractionation and functional properties of proteins from the microalgae Chlorella vulgaris. Bioresour. Technol. 157, 134–139. doi:10.1016/j.biortech.2014.01.071

Van Vooren, G., Le Grand, F., Legrand, J., Cuiné, S., Peltier, G., Pruvost, J., 2012. Investigation of fatty acids accumulation in Nannochloropsis oculata for biodiesel application. Bioresour. Technol. 124, 421–432.

Vanthoor-Koopmans, M., Wijffels, R.H., Barbosa, M.J., Eppink, M.H.M., 2013. Biorefinery of microalgae for food and fuel. Bioresour. Technol. 135, 142–149. doi:10.1016/j.biortech.2012.10.135

Vaz, S., Moreira, J.B., Morais, M.G. De, Alberto, J., Costa, V., 2016. ScienceDirect Microalgae as a new source of bioactive compounds in food supplements. Curr. Opin. Food Sci. 7, 73–77. doi:10.1016/j.cofs.2015.12.006

Vigani, M., Parisi, C., Rodríguez-Cerezo, E., Barbosa, M.J., Sijtsma, L., Ploeg, M., Enzing, C., 2015. Food and feed products from micro-algae: Market opportunities and challenges for the EU. Trends Food Sci. Technol. 42, 81–92. doi:10.1016/j.tifs.2014.12.004

Wang, L., Li, Y., Sommerfeld, M., Hu, Q., 2013. A flexible culture process for production of the green microalga Scenedesmus dimorphus rich in protein, carbohydrate or lipid. Bioresour Technol. 129, 289–95. doi**:**10.1016/j.biortech.2012.10.062

Wang, S., Stiles, A.R., Guo, C., Liu, C., 2014. Microalgae cultivation in photobioreactors : An overview of light characteristics 550–559. doi:10.1002/elsc.201300170

Wase, N., Black, P.N., Stanley, B.A., Dirusso, C.C., 2014. Integrated quantitative analysis of nitrogen stress response in Chlamydomonas reinhardtii using metabolite and protein profiling. J Proteome Res. 13,1373–96. doi:10.1021/pr400952z.

Welkie DG, Lee BH, Sherman LA (2015) Altering the Structure of Carbohydrate Storage Granules in the Cyanobacterium Synechocystis PCC 6803 through Branching-Enzyme Truncations. J Bacteriol. 198(4):701-10.

Wijffels, R.H., Barbosa, M.J., 2010. An outlook on microalgal biofuels. Science 329 (5993), 796–799.

Wilhelm, E.P., Mullen, R.E., Keeling, P.L., Singletary, G.W., 1999. Heat Stress during Grain Filling in Maize: Effects on Kernel Growth and Metabolism. American Society of Agronomy. 39 (6), 1733-1741

Williams, Peter J. le B., Brook, B.W., 2014. Kyoto : doing our best is no longer enough Biofuel : microalgae cut the Kyoto : doing our best is. doi:10.1038/450478d

Winck, F.V., Orlando, D., Melo, P., Fernando, A., Barrios, G., 2013. Carbon acquisition and accumulation in microalgae Chlamydomonas : Insights from " omics " approaches ScienceDirect

Carbon acquisition and accumulation in microalgae Chlamydomonas : Insights from " omics " approaches. doi:10.1016/j.jprot.2013.09.016

www.acuf.net

www.ellenmacarthurfoundation.org

www.newfoodmagazine.com/innova-market-insights

www.foodnavigator.com/Market-Trends/Changing-diets-Plant-protein-sustainability-crucial-for-food-security

www.viaspace.com

Yao, C.H., Ai, J.N., Cao, X.P., Xue, S., 2013. Characterization of cell growth and starch production in the marine green microalga Tetraselmis subcordiformis under extracellular phosphorus-deprived and sequentially phosphorus-replete conditions. Appl Microbiol Biotechnol. 97, 6099–110. doi:10.1007/s00253-013-4983-x.

Yoo SH, Lee BH, Li L, Perris SD, Spalding MH, Han SY, Jane JL (2015)Biocatalyticrole of potato starch synthase III for α-glucan biosynthesis in Synechocystis sp.PCC6803 mutants. Int J BiolMacromol. 81:710-7.

Zhang, W., Zhang, Z., Yan, S., 2015. Effects of various amino acids as organic nitrogen sources on the growth and biochemical composition of *Chlorella pyrenoidosa*. Bioresour Technol. 197, 458–464.

Zhu, L., 2015. Biorefinery as a promising approach to promote microalgae industry : An innovative framework. Renew. Sustain. Energy Rev. 41, 1376–1384. doi:10.1016/j.rser.2014.09.040

Zhu, L.D., Hiltunen, E., 2016. Application of livestock waste compost to cultivate microalgae for bioproducts production: A feasible framework. Renew. Sustain. Energy Rev. 54, 1285–1290. doi:10.1016/j.rser.2015.10.093

ARTICLES

1. I. Gifuni, G. Olivieri, A. Pollio, T. T. Franco, A. Marzocchella. “Autotrophic starch production by five Chlamydomonas species” Journal of Applied Phycology 2016, 1-10.
2. I. Gifuni, G. Olivieri, A. Pollio, A. Marzocchella. “Identification of an industrial microalgal strain for starch production in biorefinery context: the effect of nitrogen and carbon concentration on starch accumulation”. Accepted to New Biotechnology Journal.
3. I. Gifuni, G. Olivieri, I. Russo Krauss, G. D’ Errico, A. Pollio, A. Marzocchella. “Microalgae as new sources of starch: characterization of microalgal starch granules” Chemical Engineering Transactions 2017, 1423-1428.
4. I. Gifuni, A. Marzocchella, A. Pollio, G. Olivieri. “New designed ultra-flat photobioreactor for intensive microalgal production: the effect of light irradiance”. Submitted to Algal Research.
5. G. Petruk, I. Gifuni, A. Illiano, M. Roxo, G. Pinto, A. Amoresano, A. Marzocchella, R. Piccoli, M. Wink, G. Olivieri, D. M. Monti. “Simultaneous production of antioxidant and renewable molecules from microalga *Chlorella sorokiniana*”. Submitted to Algal Research.
6. I. Gifuni, T. R. Zinkone, J. Pruvost, L. Marchal. “Effect of bead milling parameters on the products recovery in microalgal biorefinery”. To be submitted to Bioresource Technology.

CONFERENCES

- Petruk G., Gifuni I., Roxo M., Olivieri G., Marzocchella A., Piccoli R., Wink M., Monti D. Microalgae in circular economy: from waste to high-value products. 19th International Conference on Oxidative Stress Reduction, Redox Homeostasis and Antioxidants. June 26-27, 2017, Paris (FR).
- Gifuni I., Olivieri G., Pollio A. and Marzocchella A. “Effects of light irradiance on growth and biochemical composition of *Chlorella sorokiniana* cultures in new designed ultra-flat photobioreactors”. 6th Congress of the international society for applied phycology. June 18-23, 2017, Nantes (FR).
- Olivieri G., Gifuni I., Pollio A., Pinto G., Marzocchella A. “Biorefinery of microalgae and cyanobacteria for fuel, food and chemicals” Italian Forum on Industrial Biotechnology and Bioeconomy.September 24-25, 2015, Rome (IT).
- Gifuni I., G. Olivieri, A. Pollio, A. Marzocchella. “Factors influencing starch accumulation in microalga *Chlorella sorokiniana*” European Congress of Biotechnology. July 2-7, 2016, Crakow (PL).
- Carpine R., Ferone M., Gifuni I., Marzocchella A., S. Niglio, Olivieri G., Peirce S., Procentese A., Raganati F., Russo M.E., Salatino P., Salemme L. Intensification systems in bioconversion processes. Convegno GRICU 2016 “Gli orizzonti 2020 dell’Ingegneria Chimica”., September 12 – 14, 2016, Anacapri (NA).
- Gifuni I., Olivieri G., D’Errico G., Pollio A. and Marzocchella A. “Starch production by autotrohicmicroalgal cultures for bioplastic applications”. 8th European Symposium on Biopolymers. September 15-17, 2015, Rome (IT).

COLLABORATIONS WITH FOREIGN RESEARCH INSTITUTION

06.01.2017 – 06.07.2017: Research activity at Laboratoire GEPEA- Genie des Procédés Environnement-Agroalimentaire, University of Nantes (FRANCE).

Topic: **Downstream processes of *Chlorella sorokiniana* for the recovery of starch and proteins.**

COURSES AND SEMINARIES

• “Structuring and Writing Manuscripts for Publication in Scholarly Journals: Adding Value to the Scientific Literature”–Prof. Barnett Parker, 15-17/06/2015
• “Impianti dell’industria di processo” parte del corso – Prof. Antonio Marzocchella- November-December 2014

1. Carlos Regalando “Edible films and coatings to increase shelf life of fresh foods”, 09/07/2015
2. Blanca Garcia “Microbial study of Listeria monocytogenes biofilms”, 09/07/2015
3. Rafaele Porta “Le transglutaminasi: dalle poliammine alle bioplastiche”, 30/06/2015
4. Peter Gotz “Microbial production of polysaccharides as feed additives”, 14/04/2015
5. Alfredo Ronca “Bioactive composite scaffolds for bone regeneration: from the process to the biological validation”, 25/03/2015
6. Piero Salatino “Fluidizzazione di solidi granulari e mobilità di flussi piroclastici densi”, 29/01/2015
7. Angelo Fierro “Il Grafalloon del bioetanolo di seconda generazione: il caso studio per la regione Campania”, 11/02/2015
8. Roberto Lauri “Aspetti di sicurezza relativi a processi industriali finalizzati alla produzione di biocombustibili e bioplastiche”, 28/012015
9. Biotecnologie per lo sviluppo sostenibile: applicazioni e sicurezza” - Prof. Biancamaria Pietrangeli, 28/01/2015
10. Franco Terlizzese “La strategia italiana per l’utilizzo delle materie prime e il loro impatto ambientale: idrocarburi e geotermia”, 17/11/2015
11. Thierry Tron “Functionalized and artificial enzymes: new bio-derived catalysts , 14/01/2016
12. Angharad Gatehouse “Biopesticides which target voltage-gated ion channels: efficacy and biosafety ,14/01/2016
13. Barbara Sherwood Lollar “New development in isotopic investigation of source and fateoh halogenated hydrocarbon compounds, 17/05/2016
14. Lars Rehmann “Fermentative butanol production form unconventional resource,14/06/2016
15. Angelo Fontana “Research and exploitation of marine genetic resources: from ecophysiology to biotechnology, 13/07/2016
16. Bogdan Bjola, Michele Maremonti “La protezione brevettuale: opportunità, procedure, casi di studio, 30/09/2016
17. Edgardo Filippone: “Dalle piante alle microalghe, il mondo biotech si tinge di verde”, 26/10/2016
18. Dionysio Dionysiou: “Treatment of cyanotoxins and contaminants of emerging concern in water using advanced oxidation processes”, 27/10/2016
19. Tomaso Zambelli: “FluidFM for single cell manipulation”, 18/10/2016
20. Tomaso Zambelli: “Development of FluidFM and its application for 2D patterning as well as 3D microprinting”, 18/10/2016
21. Tomas Morosinotto: “Algae: metabolic engineering for the sustainable production of bio-commodities”, 06/12/16
22. Raffaele Scoccianti: “Effective comunication in industry (and tips for building a strong CV)”, 23/11/2016

APPENDIX

The last aim of the present PhD, regarding the recovery of microalgae starch in the biorefinery context, has been improved by a fertile collaboration with another PhD student in Biotechnology (XXX°cicle), Ganna Petruk. The collaboration rose from shared interests in the recovery of natural and renewable products of commercial interest, in particular starch (present thesis) and antioxidants (colleague's thesis). The collaboration was focused on: i) the estimation of the antioxidant activity of ethanol extract of the microalga *Chlorella sorokiniana* and ii) the estimation of the starch recovery in the extracted pellet. The results were promising and resulted in a submitted article reported hereinafter.

Simultaneous production of antioxidants and renewable molecules from microalga Chlorella sorokiniana

Ganna Petruk[a], Imma Gifuni[b], Anna Illiano[a], Mariana Roxo[c], Gabriella Pinto[a], Angela Amoresano[a], Antonio Marzocchella[b], Renata Piccoli[a,d], Michael Wink[c], Giuseppe Olivieri[b*], Daria Maria Montia,[d*]

[a]Department of Chemical Sciences, University of Naples Federico II, Complesso Universitario Monte Sant'Angelo, via Cinthia 4, 80126, Naples, Italy
[b]Department of Chemical Engineering, of Materials and Industrial Production, University of Napoli "Federico II", Napoli, Italy;
[c]Institute of Pharmacy and Molecular Biotechnology, University of Heidelberg, Heidelberg, Germany;
[d]Istituto Nazionale di Biostrutture e Biosistemi (INBB), Rome, Italy

Abstract

In recent years, microalgae have gained considerable importance as potential source of biofuels and bioplastics. However, these markets are still developing, as the high cost of cultivation ask for exploiting microalgae into new areas and with a biorefinery approach towards a multicomponent cascade extraction process. To exploit microalgae as a multicomponent source, starch was extracted with high yield from *Chlorella sorokiniana* in biocompatible conditions. Then, to minimize waste production, the extract residue was tested as a potential source of antioxidants. We found that it was able to elicit a strong protective activity towards oxidative stress either *in vitro* on human colon cancer cells and in *vivo on C. elegans* worms, by inhibiting ROS production and activating DAF-16/FOXO transcription factor pathway. We observed that a pool of molecules from three different classes (fatty acids, photosynthetic pigments and carotenoids) were synergistically responsible for this activity. To our knowledge, this is the first report on the obtainment, from a "waste" fraction, of a high value product endowed with antioxidant activity tested in a cell-based model and *in vivo*.

Keywords
Antioxidants; *Chlorella sorokiniana*; eukaryotic cells; microalgae; *C. elegans*

Abbreviations: **DCF**, 2',7'-dichlorofluorescein; **DTNB**, 5,5′-dithiobis-2-nitrobenzoic acid; **EDTA**, ethylene diamine tetra acetic acid; **EE**, ethanol extract; **H_2-DCFDA**, 2',7'-dichlorodihydrofluorescein diacetate; **P-p38**, phosphorylated p38 MAP kinase; **P-MAPKAPK-2**, phosphorylated MAP kinase-activated protein kinase; **ROS**, reactive oxygen species; **r.t.**, room temperature; **TFA**, trifluoroacetic acid; **TNB**, 5-thio-2-nitrobenzoic acid.

1. Introduction

The circular bioeconomy, based on the biorefinery approach, seems to be a good and long-term solution to harmonise the use of natural resources with the sustainability of the economic growth, ensure human wellness, reduce the increase of CO_2 concentration in the air and reduce waste production. Microalgae have been often indicated as a potential candidate for biorefinery as they are an incredible reservoir of compounds endowed with biological activities that could be used in different fields [1]. Microalgal biomass is renewable, as the industrial byproduct CO_2 and the sun light energy, are both required for their growth. As no competition exists with food culture on the use of arable land, many recent studies have been focused on the exploitation of various microalgal component in order to obtain the maximum economic benefit, as the conversion of biomass into different products produces minimal waste to the environment. Currently, the research is mainly focused on the use of microalgae as sources of lipids for biodiesel production [2], carbohydrates for methane production via anaerobic fermentation [3], proteins for animal nutrition [4] and food additives. On one hand, several process alternatives to exploit microalgal components in a multi-product biorefinery have been proposed in literature [5], but most of them have been tested as raw fractions, not characterized in their single components to validate them as potential products in the market. As an example, it is frequently claimed that the pigment fraction can turn positive the economic balance of the whole process (cultivation plus biorefinery), by assuming that all the pigments can potentially be sold at an antioxidant-like price. But if this is the case, or if only a small fraction of the extracted pigments can have these properties, is far to be verified.

We recently reported the use of *Chlorella sorokiniana* to extract starch carbohydrates for bioplastics production [6]. However, from the economic point of view, the exploitation of other components apart from starch is mandatory to render the process more attractive. In particular, *C. sorokiniana*, during nitrogen depletion conditions (required for starch accumulation) increases the production of pigments endowed with antioxidant activity [7]. Indeed, microalgae are normally exposed to high oxygen and radical stress in their natural environment, thus they have developed several efficient protective systems against reactive oxygen species (ROS) and free radicals [8]. For this reason, pigments from microalgae, such as chlorophylls carotenoids, xanthophylls and phycobiliproteins, could be used in food, cosmetic, nutraceutical and pharmaceutical industries [7]. In particular, astaxanthin, β-carotene, zeaxanthin and lutein are endowed with antioxidant activity higher than α-tocopherol [9]. However, to date, the main bottleneck of microalgal exploitation as a multicomponent source is to separate the raw extract in different fractions preserving the activity of their components.

Here, taking advantage of the extraction technique we recently reported to obtain starch from *C. sorokiniana* [6], we used the waste material as a starting point for antioxidant production. We found that this material was rich in molecules endowed with antioxidant activity which were validated as potential products by testing their properties in a real applicative environment, i.e. either on a cell-based model and *in vivo* on a *C. elegans* model.

2. Results and discussion

Recently, a laboratory scale protocol for starch purification by Gifuni et al. [6] highlighted the need of removing pigments form the microalgal biomass before recovering starch. To this end, taking into account that in a biorefinery perspective each component of the microalgal biomass should be valorized, the extraction of pigments from the microalgal biomass was performed not to obtain the highest amount of pigments, but with the aim of extracting interesting antioxidant molecules without damaging, or drastically reducing, the starch recovery yield. For the same reason, ethanol, already proved not to damage starch, was used. Moreover, ethanol belongs to the permitted solvents exploitable for the extraction of compounds used in food industries (law 2009/32/CE), thus suggesting the possibility to use the extracted antioxidants, or the molecules recovered from the pellet, also as food additives. Finally, this solvent has a low evaporation temperature (78 °C), so it can be easily recovered by evaporation and with low energetic investment.

2.1 Pigments extraction

The microalgal biomass was harvested and dried at the early stage of nitrogen depletion. Pigments extraction was performed by using ethanol on dried biomass, as reported in Materials and Methods section. The composition in starch, simple sugars, proteins and lipids was analysed on the initial biomass and on the extracted biomass pellet (herein denoted as EP), and is reported in Table I. The microalgal biomass was found to be composed by starch (39.2 ± 1.0%), proteins (29.1 ± 1.1%), lipids (19.8 ± 0.4%) and simple sugars (10.0 ± 0.3%). After pigments extraction, the weight loss of the EP was about 35%, with respect to the initial biomass. In particular, the EP composition with respect to the initial biomass dry weight (Table I) showed that starch content was 26.4 ± 0.6%, proteins were 18.5 ± 0.1%, simple sugars were 13.7 ± 0.4%. Lipid content was 4.1 ± 0.1%, thus indicating that lipids were almost completely extracted by the solvent. With the extraction protocol proposed, it was possible to recover 82.9% of the initial starch, and a significant amount of proteins (78.3%). Only 17.0% of the initial lipid content remained in the pellet after the extraction. Therefore, starch recovery was considered satisfying. Simple sugars seem to increase in the pellet with respect to the untreated biomass, probably because part of the initial starch is reduced in simple sugars during the treatment. The composition in proteins and lipids of EP suggests applications as feedstock for bioplastics or as feed or food complements without further treatments. By introducing further separation steps, all the components of the pellet could be separated and exploited as biochemicals in different industrial fields with higher profit. For example, proteins could be used for animal feed [10], starch as bulk chemicals in food or pharmaceutical industries [6] and lipids as food emulsifier or for biofuel production.

When the ethanol extracted fraction (herein denoted as EE) was analyzed, besides the presence of lipids (29.5 ± 3.6 mg), proteins (12.5 ± 1.3 mg) and sugars (4.9 ± 0.8 mg), carotenoids, chlorophyll *a* and *b* were detected (0.17 ± 0.23 mg, 0.79 ± 0.11 mg and 0.66 ± 0.09 mg, respectively). Thus, the EE was chosen to test the protective antioxidant activity on human cells against oxidative stress injury.

Table I. Total composition of biomass, of the extracted biomass pellet (EP) and of ethanol extracted fraction (EE).

	Biomass composition (%DW)	EP composition (%DW)	EE composition (mg)
Simple sugars	10.0 ± 0.3	13.7 ± 0.4	4.9 ± 0.8
Starch	39.2 ± 1.0	26.4 ± 0.6	-
Proteins	29.1 ± 1.1	18.5 ± 0.1	50.2 ± 1.3
Lipids	18.8 ± 0.4	4.1 ± 0.1	65.8 ± 3.6
Weight loss	0	35	-
Chl a	-	0	0.79 ± 0.23
Chl b	-	0	0.66 ± 0.11
Carotenoids	-	0	0.17 ± 0.09

2.2 *In vitro* biocompatibility and antioxidant activity of microalgae extract

Human cancer colon cells (LoVo) were chosen as a proof of concept to study the protective effects of EE. For this reason, we first evaluated the biocompatibility of EE by treating cells for 24 and 48 h with increasing amounts (from 20 µg mL^{-1} to 2 mg mL^{-1}) of the extract. At the end of incubation, cell viability was assessed by the 3-(4,5-dimethylthiazol-2-yl)-2,5-diphenyl tetrazolium bromide (MTT) reduction assay, used as an indicator of metabolically active cells, as only alive cells are able to convert MTT to formazan salts. The results of dose-response experiments are reported in Figure 1A. In particular, no toxicity was observed up to 200 µg mL^{1} of microalgae extract at any time analysed, whereas, at higher concentrations (1 and 2 mg mL^{-1}), cell viability was found to be significantly lower in a dose- and time- dependent manner.

Based on these results, we selected 200 µg mL^{-1} microalgae extract as the optimal concentration to analyse the ability of the extract to protect cells from oxidative stress induced by sodium arsenite (SA). Cells were pre-treated with 200 µg mL^{-1} EE for 24 h (B, grey bars) or 48 h (C, grey bars) in the presence or absence of 300 µM SA and then cell viability was measured. As shown in Figure 1, cells incubated in the presence of SA, showed a low survival rate (67 and 61% after 24 and 48h, respectively) when compared to untreated cells (Figure 1B and C, black bars). Interestingly, the treatment of cells with EE before inducing oxidative stress was able to keep unaltered cell viability, which was found to be comparable to that of untreated cells (Figure 1B and C, grey bars).

As it is well documented that SA induces high ROS production and consequently GSH oxidation in eukaryotic cells [11,12], we analysed EE ability to maintain unaltered intracellular ROS and GSH levels. As shown in Figure 1D, the pre-treatment of LoVo cells with the extract reduced ROS levels of about 3.5 times with respect to cells exposed to SA. Similarly, total intracellular GSH levels were significantly higher (about 40%) in cells pre-treated with microalgae extract and then exposed to the stress, compared to cells exposed to SA (Figure 1E).

Finally, we analyzed the phosphorylation levels of p38 and its direct target MAPKAPK-2 (Figures 1F-G). These proteins belong to the family of mitogen-activated protein kinases (MAPK) and are directly involved in oxidative signaling stress pathways. Consistently with the results reported above, we observed a significant increase in the phosphorylation level of both proteins after oxidative stress injury (Figure 1F, third lane). On the other hand, the pre-treatment of cells with the microalgae extract prior to SA resulted in the inhibition of the phosphorylation of the above mentioned markers (Figure 1F, fourth lanes). It is worth to notice that, in all the experiments described, no

induction of oxidative stress was observed when cells were incubated with the microalgae extract.

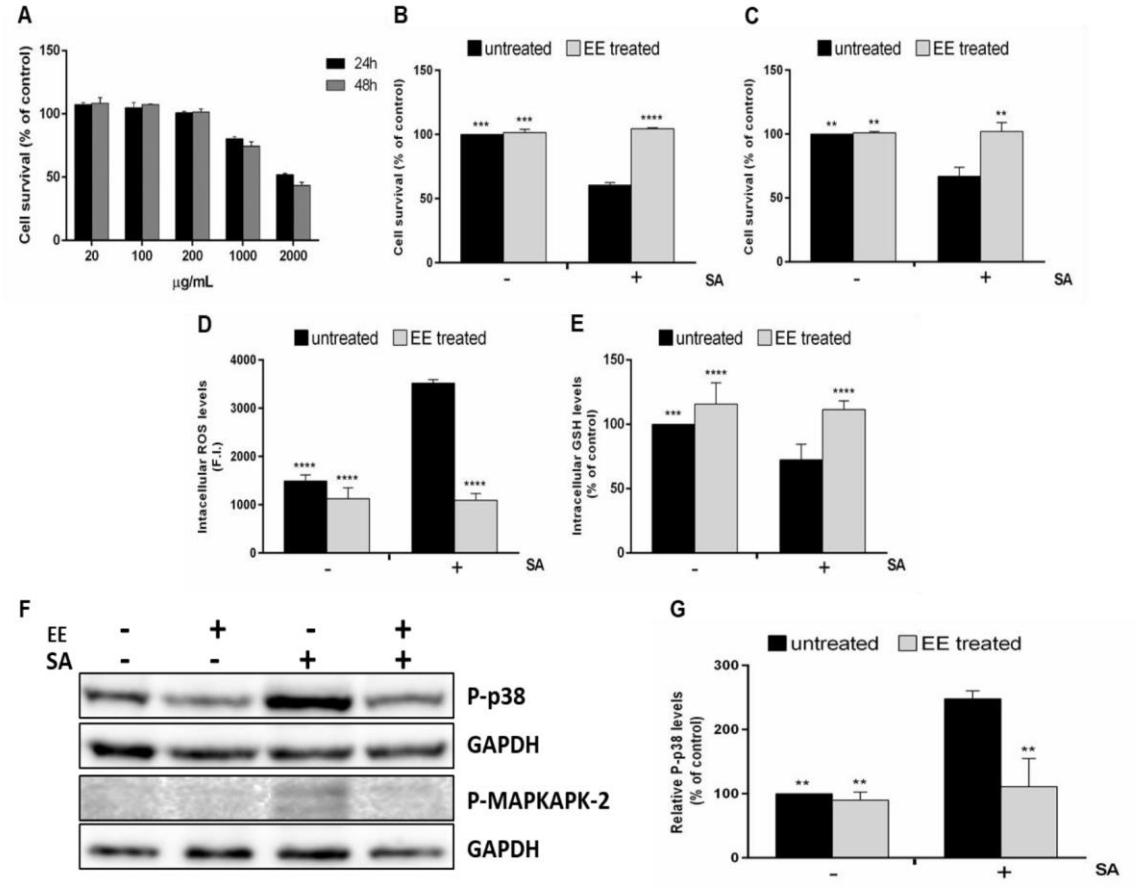

Figure 1: *In vitro* antioxidant activity of microalgae extract. A, LoVo cells were treated with increasing concentrations of EE (from 20 to 2000 µg mL^{-1}) for 24 (black bars) and 48 h (grey bars). Cell viability was assessed by the MTT assay. B, C, LoVo cells were pre-incubated with 200 µg mL^{-1} EE (grey bars) for 24 (B) and 48 h (C) and then treated with 300 µM SA for 45 min. Cell viability was assessed by the MTT assay. D, E, LoVo cells were incubated with of 200 µg mL^{-1} EE prior to be stressed by 300 µM sodium arsenite (SA) for 45 min at 37 °C. D, Intracellular ROS levels were determined by DCFDA assay. Values are expressed as fold increase with respect to control (i.e. untreated) cells. E, intracellular GSH levels determined by DTNB assay. F, Representative images of Western blots of cells incubated with EE. Cells were treated as described above and, after SA-treatment, incubated for 90 min at 37 °C. In Western blots the phosphorylation level of P-p38 and P-MAPKAPK-2 is reported. GAPDH was used as internal standard. In B, C, D, E, G histograms, black bars refer to control cells, grey bars refer to cells pre-treated with EE, untreated (−) or treated with SA (+).
Values are expressed as fold increase with respect to control (i.e. untreated) cells. Data shown are the means ± S.D. of three independent experiments. ** indicates $p<0.005$; *** indicates $p<0.001$; **** indicates $p<0.0001$

2.3 *In vivo* biocompatibility and antioxidant activity of microalgae extract

The protective activity of EE against oxidative stress was then evaluated on an *in vivo* system, i.e. *Caenorhabditis elegans*. We first analyzed the variation of brood size, widely accepted as a toxicity marker [49], after treatment with the microalgae extract, and we did not find any significant difference with respect to untreated worms (169 ± 7 vs 177 ± 6, respectively). Then, the antioxidant activity was evaluated by treating N2 wild-type worms, in L1 larval stage, with EE (200 µg mL^{-1}), for 48 h at 20 °C. Epigallocatechin-3-gallate (EGCG) 100 µg mL^{-1} was used as a positive control, whereas DMSO was used to verify that buffer was not responsible for side effects. In

the adult stage, worms were transferred to fresh media and grouped in populations of approximately 80 individuals and treated with lethal dose of 80 µM 5-hydroxy-1,4-naphthalenedione (juglone) [48]. After 24 h, dead and live worms were counted. The worms were considered dead when they did not respond to a gentle touch stimulus.
As showed in Figure 2A, worms pre-treated with EE showed a significantly higher survival rate (46 ± 7 worms, light grey bar) with respect to worms treated with juglone (23 ± 4 worms, black bar) or juglone and DMSO (25 ± 4 worms, dark grey bar). Afterwards, the ability of EE in counteracting ROS production was evaluated. As reported in the histograms of Figure 2B, a significant lower fluorescence intensity was observed in nematodes N2 treated with EE (about 50%, light grey bar) with respect to the untreated control group (black and darker grey bars). Subsequently, the expression of heat shock protein *hsp-16.2* was evaluated. The family of HSPs proteins is found in almost all living organisms and its expression is mainly induced by heat shock or oxidative stress (REF). Thus, the mutant strain TJ375, which has a *hsp-16.2* promoter fused with a GFP reporter was incubated with EE (72 h) in the presence of 20 µM juglone (24 h). Worms pre-treated with the extract showed extremely low expression of *hsp-16.2* (about 60%, Figure 3C, light grey bar) when compared to stressed worms (Figure 2C, black and dark grey bars). As SOD is believed to act as the first line of defense in the disposal of ROS, the effect of EE (72 h) on *sod-3* expression was analyzed by using the mutant strain CF1553, which has a *sod-3* promoter fused to a GFP reporter. A significant higher expression of *sod-3*::GFP was detected in worms treated with EE (about 42% increase, Figure 2D, light grey bar) in comparison with control worms (Figure 2D, black and dark grey bars). Therefore, these results indicate that EE extract exerts its antioxidant activity not only by scavenging ROS production, but also by modulating the expression of stress response genes, such as sod-3 and hsp-16.2 and.

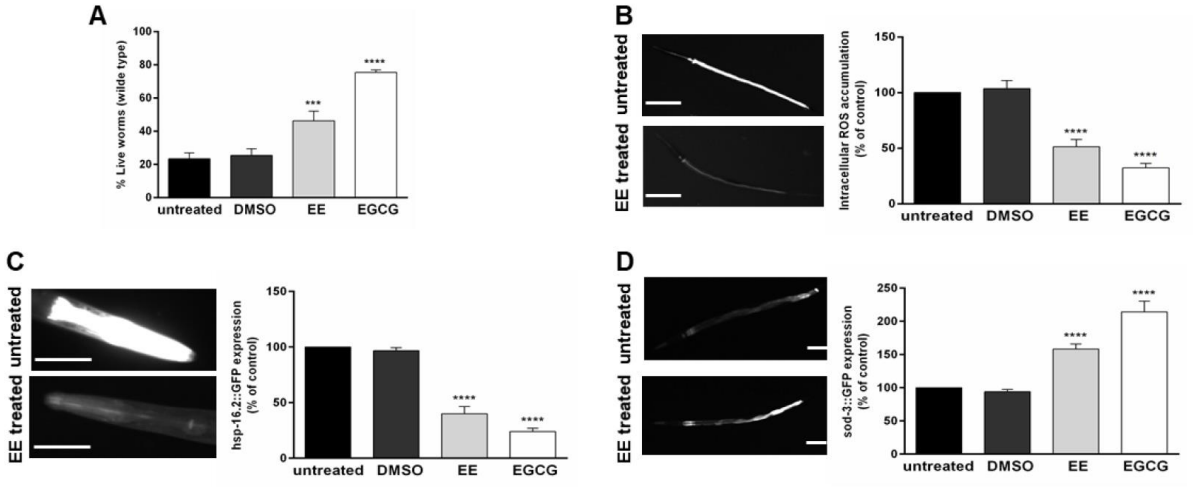

Figure 2: *In vivo* antioxidant activity of microalgae extract. A, wild type N2 worms were treated with 200 µg mL^{-1} EE extract for 48 h and then exposed to lethal dose of juglone (80 µM). After 24 h, alive and dead worms were counted and survival rate were reported in histograms. B, wild type N2 worms were treated with 200 µg mL^{-1} EE extract for 48 h and then incubated with DCF fluorescent probe. After 1 h incubation, accumulation of intracellular ROS levels was evaluated. On the left, representative images of DCF fluorescence in untreated worms (up) and in worms treated with EE (below); On the right, quantification of the fluorescence intensity of the whole body determined densitometrically by using ImageJ software. C, transgenic TJ375 worms were treated with 200 µg mL^{-1} EE extract for 72 h and then exposed to juglone (20 µM). After 24 h, the expression of GFP::*hsp-16.2* was evaluated. On the

left, representative images of GFP fluorescence in untreated worms (up) and in worms treated with extract (below); On the right, the relative fluorescence of the heads determined densitometrically by using ImageJ software. D, transgenic CF1553 worms were treated with 200 µg mL^{-1} EE extract for 72 h and then the expression of GFP::*sod-3* was evaluated. On the left, representative images of GFP fluorescence in untreated worms (up) and in worms treated with extract (below); On the right, the relative fluorescence of the tails determined densitometrically by using ImageJ software. In the Figure, black bars refer to control worms, light grey bars refer to worms treated with EE, white bars refer to worms treated with EGCG (used as positive control), whereas dark grey bars refer to worms treated with buffer (DMSO). In B, C and D histograms data are presented as percentage of the mean pixel intensity of each treatment, with respect to control worms (mean ± SD, n=40, replicated at least 3 times). Images were taken with BZ9000 from Keyence, scale bar = 100 µm. *** indicates p< 0.001, **** indicates p< 0.0001, compared to the untreated worms by one-way ANOVA followed by Bonferroni (post-hoc).

Finally, we analyzed the subcellular localization of DAF-16/FOXO, which is the main transcription factor involved in the regulation of stress response genes. Under physiological conditions, DAF-16/FOXO remains inactive in the cytosol, whereas, some environmental or stress conditions can stimulate its translocation to the nucleus, where it induces the expression of different genes involved in stress response, metabolism and longevity.
The mutant strain TJ356 has a *daf-16* fused to a GFP reporter and was used to detect *daf-16*::GFP localization. As shown in Figure 3A, worms pretreated in the presence of EE (24 h) showed a higher percentage of *daf-16*::GFP nuclear localization (about 70%), with respect to untreated worms (12%). This pathway was further confirmed by performing survival assays with a *daf-16* loss-of-function mutant (CF1038) and a *daf-16* null mutant (GR1307) grown in the presence of EE (48 h). In both cases, the extract had no effect on the survival rate of the worms (Figure 3B and C, light grey bars), in contrast to the results obtained with N2 worms (Figure 2A).

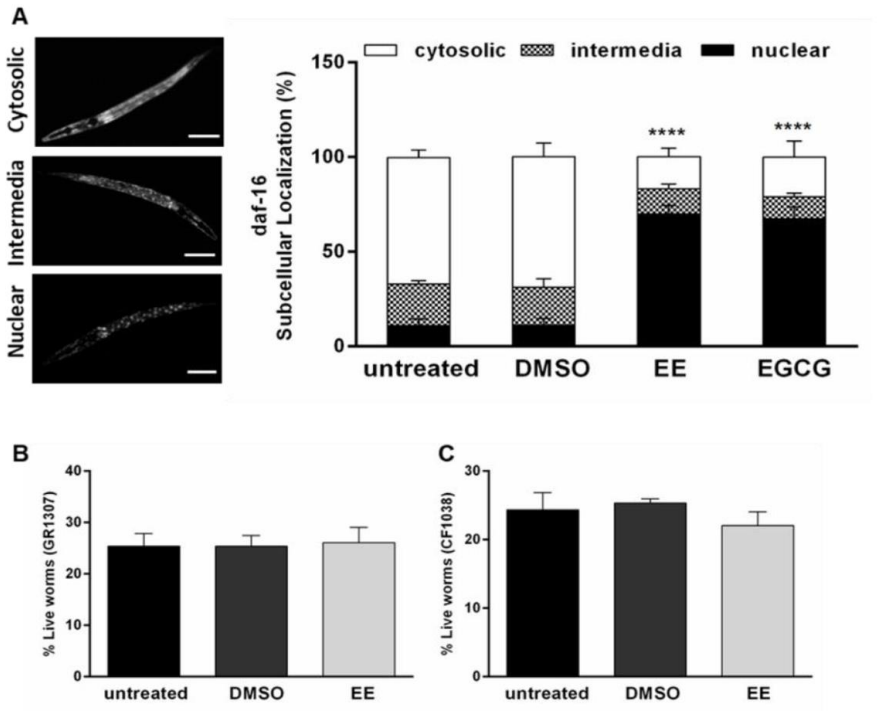

Figure 3: Pathway activated by EE in *C. elegans*. A, transgenic TJ356 worms were treated with 200 µg mL^{-1} EE extract for 24 h and then GFP::*daf-16* localization was evaluated. On the top, representative images of different GFP localization. Below, histograms reporting the percentage of worms exhibiting a DAF-16 sub-cellular localization pattern, namely cytosolic (white bars), intermediate (checked bars) and

nuclear (black bars). Data are presented as mean ± SD (n=40, replicated at least 3 times). Images were taken with BZ9000 from Keyence, scale bar = 100 µm. **** indicates p< 0.0001, compared to the untreated worms by one-way ANOVA followed by Bonferroni (post-hoc). B-C, a *daf-16* null mutant (GR1307) and *daf-16* loss-of-function mutant (CF1038) worms were treated with 200 µg mL^{-1} EE extract (light grey bars) for 48 h and then exposed to lethal dose of juglone (80 µM). After 24 h, alive and dead worms were counted and the survival rate was reported. Data are presented as mean ± SD (n=40, replicated 3 times).

2.4 Identification of active compounds

EE was then fractionated by HPLC and the elution profile is shown in Figure 4A. Thirteen fractions were manually collected and tested for antioxidant activity on LoVo cells by measuring intracellular GSH in the presence or absence of oxidative stress (300 µM SA). As shown in Figure 4B, fractions 8, 9, 11 and 12 had no effect on GSH levels when tested alone, but showed a high protective effect against oxidative stress. To verify the occurrence of additive effects, the active fractions were combined and tested on LoVo cells, in the presence or absence of SA damage, and the results, shown in Figure 4B, suggested the presence of additive effects.

The active fractions were further analyzed by LC-MS and MALDI-TOF/TOF for the identification of the main agents responsible for their bioactivity. The LC-MS TIC chromatogram of each fraction is reported in Figure 4C-F. A similar profile for the four fractions was observed, although relevant differences in their relative abundance were recorded. The base peak chromatogram of an ethanol extract with the identification of the most abundant peaks is reported in the Supporting information (Figure S1) while mass spectral identification of each peak is reported in Table II. The assignment of species to each mass peak is based on the interpretation of MALDI-TOF/TOF spectra and on the comparison with literature data [13–16]. By LC-TOF analysis, we found several saturated and polyunsaturated chain fatty acids, consisting of their radical species, dimeric forms and sodium adducts (Table II), as shown as an example in Figure S2. This finding is not surprising, as Bergé et colleagues [17] reported the analysis of fatty acids (FAs) from different microalgae strains. Although a variable content of proteins and lipids depending on the specific algal strain and growth conditions was detected in microalgae [18], they show a high amount of lipids [19]. In this context, Richards et al. demonstrated that long chain polyunsaturated fatty acids (LC-PUFAs) of the omega-3 series act as indirect antioxidants *in vitro* [20].
Besides FAs, different antioxidant molecules, well documented in the literature, were identified by LC-TOF analysis and confirmed by tandem MS. In particular, carotenoids, such as astaxanthin and its sodiated form (596.4 Da,), and porphyrins, as chlorophyll c2 (609.3 Da), pheophorbide a (593.3 Da) and thioether porphyrin (611.4 Da) were found to be present [21,22]. A MALDI-TOF/TOF spectrum is reported for chlorophyll C2, with the structures drawn for the most intense fragments (Figure S3). Interestingly, the chlorophylls esterified with unsaturated long chain fatty acid, e.g. Pheophytin a' (871.2 Da, Figure S4) and hydroxylated chlorophyll a (908.9 Da, Figure S5), were detected only by MALDI.
The other fragmentation spectra were collected in Supporting information (Figures S6-9). Finally, a derivate quercetin and some triacylglycerols were found exclusively in fractions 8 and 9, respectively.

Table II. Identification of each peak of TIC chromatogram with relative retention time and relative abundance

Species	Measured m/z	Detected Ion	MALDI-TOF/TOF Fragments	Rt (min)	Relative abundance (%)			
					8	9	11	12
Fatty acid C18:3	278.2	$M^{\bullet+}$		15.4	1.5	3.1	2.4	2.5
Dimeric form of C18:3	555.5	$[M+H]^+$						
Fatty acid C19:2	294.2	$M^{\bullet+}$		16.2/16.7	3.1	3.7	3.6	2.8
Dimeric form of Fatty acid C19:2	587.4 609.3	$[M+H]^+$, $[M+Na]^+$						
Dimeric form of C19:0	595.5 617.5	MH^+ $[M+Na]^+$		17.1	1.9	1.7	0.7	1.8
Fatty acid C19:1	296.2	$M^{\bullet+}$		18.6	0.8	2.4	1.4	0.3
Dimeric form of Fatty acid C19:1	591.5	$[M+H]^+$, $[M+Na]^+$						
Fatty acid C18:3	279.3	$[M+H]^+$		18.9	0.4	n.d.	n.d.	n.d.
S Porphyrin (SEt)	611.3	$[M+H]^+$	567.4 Da, 547.3 Da, 537.3 Da, 493.3 da, 465.3 Da	19.4	1.7	n.d.	1.4	n.d.
Luteolin dihexoside	611.4	$[M+H]^+$	579.4 Da, 565.4 Da					
Delphinidine 3-O p-coumaroyl-monoglucoside	611.4	$[M+H]^+$	519.3 da, 465.31, 493.3 (malvidine 3-0 monoglucoside)					
Fatty acid C18:4	277.2	$[M+H]^+$		19.9	0.4	n.d.	1.4	n.d.
Fatty acid C19:2	295.2	$[M+H]^+$						
Fatty acid C22:5	330.2	$M^{\bullet+}$						
S-Porphyrin (SEt)	611.4	$[M+H]^+$	567.4 Da, 547.3 Da, 537.3 Da, 493.3 da, 465.3 Da					
Luteolin dihexoside	611.4	$[M+H]^+$	579.4 Da, 565.4 Da					
Delphinidine 3-O p-coumaroyl-monoglucoside	611.4	$[M+H]^+$	519.3 da, 465.31, 493.3 (malvidine 3-0 monoglucoside)					
Fatty acid C19:0	298.2	$M^{\bullet+}$		20.3	0.5	1.9	1.1	1.3
Dimeric form of Fatty acid C19:0	595.5 617.5	$[M+H]^+$ $[M+Na]^+$						
Fatty acid C14:0	228.2	$M^{\bullet+}$		21.9	0.3	0.3	0.3	2.3
Dimeric form of C14:0	455.4	$[M+H]^+$						
Fatty acid C16:1	254.2 $M^{\bullet+}$	$M^{\bullet+}$		23.4	0.3	0.4	0.6	1.9
Fatty acid C22:4	332.2	$M^{\bullet+}$						
Dimeric form of C16:1	507.5	$[M+H]^+$						
Fatty acid C18:2	280.2	$M^{\bullet+}$		24.8 25.4 26.2	2.3 5.2 2.4	4.8 8.6 3.7	4.3 8.7 4.0	5.2 9.6 5.2
Dimeric form of C18:2	559.5	$[M+H]^+$ $[M+Na]^+$						
Fatty acid C16:0	256.3	$M^{\bullet+}$		27.5	7.7	7.3	8.5	9.7
Dimeric form of C16:0	511.5 533.5	$[M+H]^+$ $[M+Na]^+$						
Fatty acid C18:1	282.3	$M^{\bullet+}$		28.3 29.0	32.0 20.3	27.6 16.6	28.5 20.9	23.2 18.6
Dimeric form of C18:1	563.5 585.5	$[M+H]^+$ $[M+Na]^+$						
Fatty acid C17:0	270.3	$M^{\bullet+}$		32.6	n.d.	n.d.	n.d.	0.7
Dimeric form of C17:0	539.5 561.5	$[M+H]^+$ $[M+Na]^+$						
Quercetin 3-(2"-p-hydroxybenzoyl-4"-p-coumarylrhamnoside)	715.3	$[M+H]^+$	699.1 Da, 669.1 Da, 561.1 Da, 311.4 Da, 283.4 Da	30.9	0.4	n.d.	n.d.	n.d.
Chlorophyll c2	609.3	$[M+H]^+$	579.4 Da, 549.4 Da, 455.3 Da, 429.05 Da	31.1	5.7	0.5	n.d.	1.3
Pheophorbide a	593.3	$[M+H]^+$	533.3 Da, 459.3 Da	32.8 33.8	n.d.	n.d.	n.d.	0.7 0.3
Fatty acid C18:0	284.4	$M^{\bullet+}$		32.7	6.4	5.8	4.8	3.2
Dimeric form of C18:0	567.6 589.5	$[M+H]^+$ $[M+Na]^+$						
Fatty acid C20:1	310.3	$M^{\bullet+}$		33.2	3.7	4.2	n.d.	2.8
Pheophorbide a	593.3	$[M+H]^+$	533.3 Da, 459.3 Da					
Dimeric form of C20:1	619.6 641.6	$[M+H]^+$ $[M+Na]^+$						
Pheophytin a'	871.2	$[M+H]^+$	593.2 Da, 714.9 Da					
Hydroxylated Chlorophyll a	908.9	$[M+H]^+$	752.9 Da ,311.3 Da ,283.2 Da					
Fatty acid C20:1	310.3	$M^{\bullet+}$		34.0	0.4	0.6	0.4	0.9
Astaxanthin	596.4	$[M+H]^+$						
Dimeric form of C20:1	619.6 641.6	$[M+H]^+$ $[M+Na]^+$						
TG(16:0/18:1(9Z)/18:2	874.7	$[M+NH_4]^+$		35.5	n.d.	1.9	n.d.	n.d.
TG(18:1(9Z)/18:1(9Z)/18:1(9Z)	902.7	$[M+NH_4]^+$						
Fatty acid C22:1	338.3	$M^{\bullet+}$		38.0	0.8	1.9	1.6	1.8
Dimeric form of C22:1	675.7 697.5	$[M+H]^+$ $[M+Na]^+$						

A

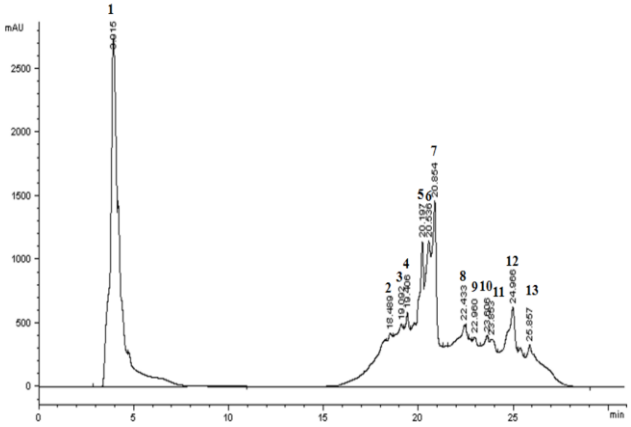

B

Cells incubated with:	% of intracellular GSH levels (with respect to untreated cells)	
	Unstressed cells	**SA-stressed cells**
untreated	100	69 ± 2
EE	100 ± 10	113 ± 9
#1	75 ± 9	62 ± 1
#2	71 ± 6	60 ± 8
#3	63 ± 4	76 ± 5
#4	59 ± 5	67 ± 5
#5	74 ± 2	82 ± 3
#6	66 ± 6	94 ± 3
#7	75 ± 3	74 ± 2
#8	92 ± 5	91 ± 8
#9	82 ± 8	99 ± 3
#10	82 ± 8	82 ± 13
#11	95 ± 2	95 ± 3
#12	80 ± 1	105 ± 4
#13	85 ± 2	58 ± 1
mix #7,8,11 and 12	113 ± 10	115 ± 11

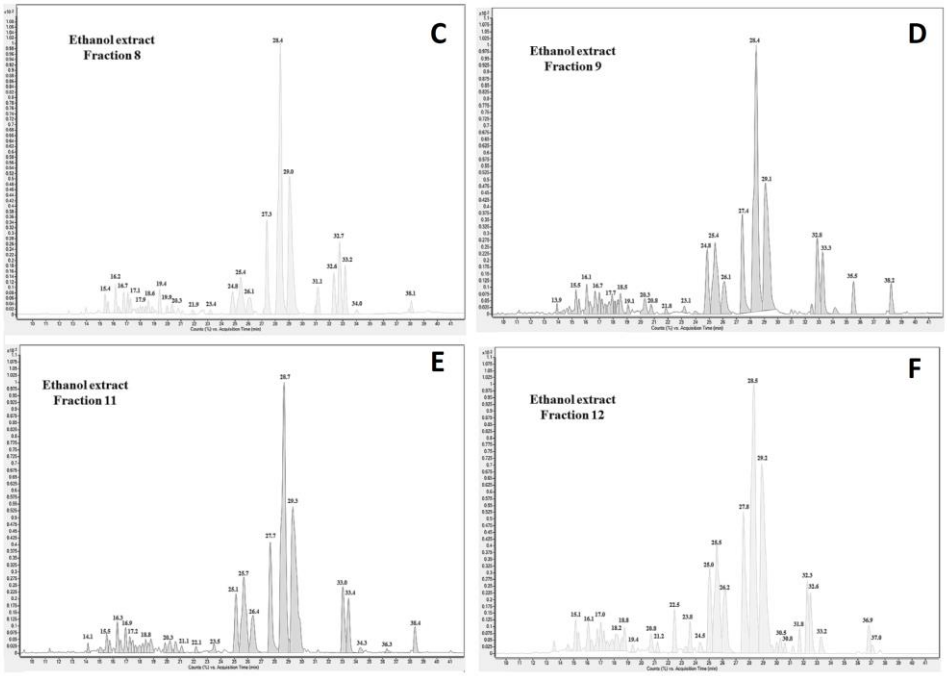

Figure 4: Characterization of EE. A, HPLC chromatogram of EE, in which eluted fractions are marked in the profile. B, Analysis of the antioxidant activity of microalgae fractions by DTNB assay. LoVo cells were pre-incubated in the presence of 200 µg mL^{-1} EE or equivalent amount of each fraction after HPLC for 120 min and then cells were stressed by SA treatment (300 µM) for 45 min and intracellular GSH levels determined, as described in Materials and Methods section. Values are reported as % of untreated cells. C-F, TIC chromatogram of the fractions with the highest biological activity.

3. Conclusions

In this study, a new strategy for a sequential recovery of starch and antioxidants was proposed and validated. We found that, after starch extraction from *C. sorokiniana*, the waste product was able to counteract oxidative stress, both in a cell-based model and *in vivo*, as many carotenoids, chlorophylls and FAs are present. While the antioxidant activity of the first two class of molecules identified is well documented, the literature is still quiescent on the FAs antioxidant activity. However, some studies are reported on the impact of polyunsaturated fatty acids (PUFAs) intake on oxidative stress, as omega-3 PUFAs have been shown to reduce lipoperoxidation levels, advance

glycation end products, increase SOD/CAT enzymatic ratio in the livers of diabetic rats fed with a high fat thermolyzed diet (rich in advanced glycation end-products) [20,23]. These properties, together with the reported inhibition of hepatic lipogenesis afforded by EPA and DHA [24], suggest a multifaceted healthful activity of omega-3 fatty acids supplementation in liver disorders. We still do not know to which class of molecules the antioxidant activity is due, or if there is a synergistic effect among them, and further analysis will be performed to shed light on this issue. It has to be taken into account, however, that, to date, papers claim the multiproduct biorefinery of algae, but no cascade or validation of the obtained products are reported [5,25,26]. The physic-chemical characterization of the starch granules, extracted with the method here reported, was already carried out [6] and its properties suggest interesting industrial application: emulsifier for food and pharmaceuticals, bioplastics, textiles and paper preservation. The novelty of the present work is in the proved feasibility of the cascade approach to isolate two different high value products, starch and antioxidants in developing markets.

4. Materials and Methods

4.1 Microalgal strain and culture conditions

Chlorella sorokiniana Shihiraet Krauss strain ACUF 318 (http://www.acuf.net) is a fresh water terrestrial alga. The culture medium used was Bold's Basal Medium (BBM) containing $NaNO_3$ as nitrogen source at concentration of 0.25 g L^{-1}. The growth was carried out in inclined square bubble column photobioreactors, as reported by Olivieri et al. [27]. The culture was continuously irradiated with white fluorescent lamps on the front side of the reactors with a light intensity of 300 µmol m^{-2} s^{-1}. Aeration and mixing was provided by feeding air supplemented with 2% of CO_2. Gas flow rate was set at 0.2 vvm. The temperature was maintained at 25 °C by air-conditioning system. Nitrogen depletion was reached after the regular uptake of $NaNO_3$ for biomass growth and the biomass was harvested in the second day of nitrogen depletion, optimal condition for starch accumulation and productivity (Gifuni et al. under review).

4.2 Pigments extraction

A conventional solvent extraction method was performed in order to determine the antioxidant activity of *C. sorokiniana* extract. Pure ethanol (99.8%, Sigma-Aldrich) was used as solvent. The extraction protocol follows that reported by Aremu et al. [28] with some modifications. Briefly, the microalgal biomass was dried and ground to 0.150 mm powder. 200 mg of microalgal powder were suspended in 2 mL of ethanol and disrupted by bead beater (2000 g for 3 cycles of 1 min space out with 2 min breaks in ice) equipped by 0.5 mm glass beads. The disrupted biomass was moved to dark flaks and the beads were washed twice with ethanol and the final volume was led to 20 mL. The mixture was shaken for 24 h at 250 rpm in the dark on a magnetic stirrer. Then the mixture was centrifuged at 12000 g for 10 min. The supernatant, dried using N_2 stream, represents the ethanol extract (EE). Then, the extract was solubilized in 1 mL of DMSO for further analysis on ca cell-based model and *in vivo*. The remaining pellet (EEP) was also collected and dried to assay the recovered starch.

4.3 Biochemical composition

Initial microalgal biomass and the pellet after extraction were characterized in terms of lipids, proteins, total sugars, starch and proteins. The extracts were assayed for pigments, proteins and total sugars concentration, lipids were calculated as difference between the biomass content and the pellet content using mass balance.

Lipids were extracted according to the protocol by Breuer et al. [29] followed by gravimetric quantification of the chloroform extract, previously dried at 100°C for 1 h.

Proteins were assayed by BCA Protein Assay Kit (Thermo Scientific). 10 mg of sample (biomass and dried pellet) was dissolved in 1 mL of lysis buffer (60 mM Tris, 2% SDS) and disrupted by bead beater (700 g for 3 cycles of 4 min space out with 1 min breaks in ice) equipped by 0.5 mm glass beads. The samples were incubated at 100 °C for 30 min for the extraction of membrane proteins and then centrifuged at 2500 g for 10 min. Supernatants were analyzed by BCA Kit.
Total sugars concentration was measured by spectrophotometric method of Anthrone modified with respect to that described by Chen and Vaidyanathan [30]. In particular, the disruption of the biomass and of the pellet was carried out according to the procedure described for proteins.
Starch was measured using Total Starch kit by Megazyme (Wicklow, Ireland) and according the manufacture's protocol with some modifications. The amount of sample was set at 10 mg the microalgal samples and the cells disruption was carried out by the bead beater, as previously reported [31].
Pigments were directly measured by spectrophotometric measurements at 663, 646 and 470 nm. chlorophyll a, b and carotenoids concentration were calculated according to Wellburn [32].
The composition assays were performed in triplicates.
Simple sugars are calculated as difference between total sugars concentration and starch concentration.
The recovery yields of the biomolecules were calculated through mass balances. The recovery yield ($Y, \%$) is defined as reported in the following formula:

$$Y = \frac{m_{x\ EP}}{m_{x\ initial}} \cdot 100\%$$

Where $m_{x\ EP}$ is the amount (mg) of the compound x (proteins, lipids, total sugars, starch) in EP and $m_{x\ initial}$ is the amount (mg) of the compound x in the initial biomass.

4.4 Cell culture and cell survival assay

Human epithelial colorectal adenocarcinoma cells (LoVo) were obtained from ATCC and cultured in Dulbecco's Modified Eagle's Medium (Sigma-Aldrich), supplemented with 10% foetal bovine serum (HyClone), 2 mM L-glutamine and antibiotics, all from Sigma-Aldrich, in a 5% CO_2 humidified atmosphere at 37 ºC. Every 3-4 days the culture medium was removed and cells were rinsed with PBS, detached with trypsin-EDTA and diluted in fresh complete growth medium for sub-culturing.
For dose-dependent survival assays cells were seeded in 96-well plates (100 µL/well) at a density of 4 x 10^4 cells/cm^2. 24 h after seeding, increasing amount of microalgae extract (from 20 µg mL^{-1} to 2 mg mL^{-1}) were added to the cells for 24-48 h. At the end of treatment, cells were incubated with 3-(4,5-dimethylthiazol-2-yl)-2,5-diphenyl tetrazolium bromide (MTT) reagent and the cells were incubated for 4 h at 37 °C in a humidified 5% CO_2 incubator. At the end of the incubation, medium was removed and the converted dye was solubilized with isopropanol containing 0.01 mol L^{-1} HCl (100 µL per well). Absorbance was measured at a wavelength of 570 nm using an automatic plate reader (Microbeta Wallac 1420, PerkinElmer, Waltham, MA, USA). Cell survival was expressed as percentage of viable cells in the presence of the microalgae extract under test compared with control cells grown in the absence of the extract. The assay was carried out in triplicates for at least 3 times. Control experiments were performed either by growing cells in the absence of the extract or by adding to the cell cultures identical volumes of DMSO. The method used avoids any possibility of a DMSO effect on the final results.

4.5 Oxidative stress

To analyze if EE was able to protect cells from oxidative stress, LoVo cells were plated at a density of 4 x 10^4 cells/cm^2. 24 h after seeding, cells were incubated for different length of time (24 or 48 h) in the presence or absence of EE (200 µg mL^{-1}), and then incubated in the presence of 300 µM SA for 45 min at 37 °C. At the end of treatment, cell viability was assessed by the MTT assay as reported above.

To detect the minimal pre-treatment time, cells were plated as reported above and then incubated for different length of time (5-120 min) with EE (200 µg mL^{-1}). Then, cells were exposed to oxidative stress as reported above and a DTNB assay was performed (described more in detail in paragraph 4.6). The result of the experiment is reported in Figure S10.

Once defined the minimum pre-treatment, in all further experiments cells were pre-treated with EE for 30 min and then exposed to SA for 45 min. After incubation, different assays were performed, as reported below.

4.6 Measurement of intracellular total GSH levels

Total reduced glutathione levels were estimated by using the procedure previously described [33]. Briefly, at the end of incubation, cells were detached by trypsin, lysed and protein concentration was determined by the Bradford assay. Then, 50 µg of proteins were incubated with 3 mM EDTA, 144 µM 5,5′-dithiobis-2-nitrobenzoic acid (DTNB) in 30 mM TrisHCl pH 8.2, centrifuged at 14,000 *g* for 5 min at 4 °C and the absorbance of the supernatant was measured at 412 nm by using a multiplate reader (Biorad). GSH levels were expressed as the percentage of TNB absorbance in the sample under test with respect to the untreated sample. Values are the mean of three independent experiments, each with triplicate determinations.

4.7 Measurement of intracellular ROS levels on cells

ROS intracellular levels were evaluated by using a cells permeable probe, 2',7'-dichlorodihydrofluorescein diacetate (H_2-DCFDA, Sigma-Aldrich). In particular the protocol described in [34] was followed. Briefly, at the end of incubation cells were incubated with the nonfluorescent H_2DCFDA becomes fluorescent product, 2',7'-dichlorofluorescein (DCF), in the presence of different species of ROS. Fluorescence intensity was measured by a Perkin-Elmer LS50 spectrofluorimeter (525 nm emission wavelength, 488 nm excitation wavelength, 300 nm/min scanning speed, 5 slit width for both excitation and emission). ROS production was expressed as percentage of DCF fluorescence intensity of the sample under test, with respect to the untreated sample. Each value was assessed by three independent experiments, each with three determinations.

4.8 Western blot analyses

LoVo cells were plated at a density of 4 x 10^4 cells/cm^2 in complete medium for 24 h and then treated as described above (paragraph 4.5). After treatment time, cells were detached and lysed in 100 mM Tris-HCl, 300 mM sucrose with addiction of inhibitors of proteases and phosphatases. These lysates were analyzed by Western blotting as reported by Del Giudice et al [35]. Phosphorylation levels of p38 and MAPKAPK-2 were detected by using specific antibodies purchased from Cell Signal Technology (Danvers, MA, USA). To normalize protein intensity levels, a specific antibody against anti-GAPDH (ThermoFisher, Rockford, IL, USA) was used. The chemiluminescence detection system (SuperSignal® West Pico) was from Thermo Fisher.

4.9 *Caenorhabditis elegans* strains and culture conditions

Nematode strains were obtained from the Caenorhabditis Genetic Center (CGC). All *C. elegans* strains were cultured on solid nematode growth media (NGM) plates fed with living *Escherichia coli* OP50 and maintained at 20 °C in a temperature-controlled

incubator. Prior to each assay eggs were isolated to obtain age synchronized cultures and kept in M9 buffer (3 g KH_2PO_4, 6 g Na_2HPO_4, 5 g NaCl, 1 mL 1 M $MgSO_4$, H_2O to 1 L) for hatching, as described by Stiernagle [36].

4.10 Brood size

Synchronized N2 worms at L4 stage were sorted and placed one by one on individual NGM agar plates. In the treatment group, the bacterial lawn was supplemented with microalgae extract (200 µg mL^{-1}). 100 µg/mL of epigallocatechin gallate (EGCG, Sigma-Aldrich GmbH, Steinheim, Germany) was used as positive control, whereas DMSO was used to verify that buffer was not responsible for side effects. Adult worms were transferred daily to fresh medium to separate them from their progeny. Eggs were counted every day for 5 days using a dissecting microscope. The results are presented as mean brood size.

4.11 *Caenorhabditis elegans* survival assay under oxidative stress

24 h after bleaching, N2 wild-type worms and transgenic worms (CF1038, GR1307), in L1 larval stage, were pre-treated with 200 µg mL^{-1} EE and maintained 48 h at 20 ºC. EGCG and DMSO were used as indicated above. In the adult stage, worms were transferred to fresh media and grouped in populations of approximately 80 individuals and treated with 80 µM juglone (5-hydroxy-1,4-naphthalenedione) [37]. After 24 h, dead and live worms were counted. The worms were scored dead when they did not respond to a gentle touch stimulus. The results are expressed as percentage of living worms.

4.12 Intracellular ROS accumulation in *Caenorhabditis elegans*

Synchronized N2 worms at L1 larval stage were pre-treated with 200 µg mL^{-1} EE and maintained 48 h at 20 ºC. EGCG and DMSO were used as indicated above. At the end of the treatment, worms were washed with M9 buffer and then incubated with 50 µM H_2DCFDA solution for 1 h at 20 °C. Worms were then mounted on a glass slide with a drop of 10 mM sodium azide (used to paralyze them) and photographed by the BIOREVO BZ-9000 fluorescent microscope (Keyence Deutschland 200 GmbH, Neu-Isenburg, Germany) equipped with a mercury lamp. Images were taken for at least 30 worms at constant exposure time (λ Ex 480/20 nm; λ Em 510/38 nm) using a 10 X objective lens. The relative fluorescence of the whole body was determined densitometrically by using ImageJ software 6.01. The results are expressed as percentage of fluorescence intensity of the worms under test compared to untreated worms.

4.13 Quantification of hsp-16.2::GFP expression

The expression of hsp-16.2p::GFP construct was quantified in the strain TJ375. Worms at larval stage L1 were pre-treated with 200 µg mL^{-1} EE and maintained 72 h at 20 °C. EGCG (50 µg/mL) and DMSO were used as indicated above. Then, worms were exposed to 20 µM juglone for 24 h and analyzed as described above

4.14 Quantification of sod-3::GFP expression

The worms of transgenic strain CF1553 at larval stage L1 were pre-treated with 200 µg mL^{-1} EE and maintained 72 h at 20 ºC. EGCG (100 µg/mL) was used as positive control, whereas DMSO was used as negative control. After treatment, the worms were analyzed as described above.

4.15 Quantification of DAF-16::GFP localization

The nematode worms of transgenic strain TJ356 at larval stage L1 were pre-treated with EE (200 µg mL^{-1}) and maintained 24 h at 20 ºC and analyzed as described above. EGCG and DMSO were used as indicated above.

4.16 Reverse-phase HPLC Analyses

Metabolites from ethanol extracts were separated by reverse-phase HPLC on a Phenomenex Jupiter C18 column (250 × 2.00 mm 5 µm, 300 Å pore size) (Phenomenex, Torrance, California, USA) at a flow rate of 200 µL/min. A linear gradient from 5% to 95% acetonitrile in 0.1% formic acid (Sigma Aldrich, Milan, Italy) was used over a time of 40 min and a wavelength of 278 nm was used for monitoring the elution. The eluate was collected in thirteen fractions to be directly analyzed by MALDI-TOF and LC-MS.

4.17 Mass Spectrometry Analyses

Matrix-assisted laser desorption/ionization (MALDI) mass spectrometry (MS) experiments were performed on a 5800 MALDI-TOF-TOF ABSciex equipped with a nitrogen laser (337 nm) (AB SCIEX, Milan, Italy). Aliquots of HPLC fractions (0.5 µL) were mixed (1:1, v/v) with a solution of 2.5 dihydroxybenzoic acid (DHB, Sigma Aldrich, Milan, Italy) at a concentration of 10 mg/mL in acetonitrile:water (90:10) solution. Standards Kit for Calibration of AB SCIEX MALDI-TOF was from AB SCIEX calibration mixture. For metabolite identification, MS and tandem mass (MSMS) spectra were acquired in reflector positive mode, by using a mass (m/z) range of 100–4000 Da. Laser power was set to 3500 V for MS spectra acquisition. Each spectrum represents the sum of 3000 laser pulses from randomly chosen spots per sample position. For CID experiments, ambient air was used as collision gas with medium pressure of 10^{-6} Torr. The data were reported as monoisotopic masses. LCMS analyses were performed by LC-MS equipped by an Agilent HPLC system (1260 Series) on a reverse-phase C18 column (Agilent Life Sciences Extend-C18, 2.1x50mm,1.8um) coupled to an Agilent 6230 TOF mass spectrometer. The HPLC separation was carried out by using water and acetonitrile as mobile phases A and B, respectively, both acidified with 0.1% formic acid. A linear gradient was employed over 40 min (0–2 min: 2% B, 2–8 min: 2-40% B, 8–20 min: 40%-60% B, 20-30 min: 60-80%, 30-40 min, 80-95) at a flow rate of 0.3 mL min^{-1}. The injection volume was 20 µL and The MS source was an electrospray ionization (ESI) interface in the positive ion mode with capillary voltage of 3000 V, gas temperature at 325 °C, dry gas (N_2) flow at 5 l min^{-1} and the nebulizer at 35 psi. The MS spectra were acquired in a mass range of 150-1000 m/z with a rate of 1 spectrum/s, time of 1000 ms/spectrum and transient/spectrum of 9961.

4.18 Statistical Analyses

In all the experiments samples were analyzed in triplicate. The results are presented as mean of results obtained after three independent experiments (mean ± SD) and compared by one-way ANOVA following Bonferroni's method (posthoc) using Graphpad Prism for windows, Version 6.01.

5. References

1. Chew KW, Yap JY, Show PL, Suan NH, Juan JC, Ling TC, Lee D-J, Chang J-S (2017) Microalgae biorefinery: High value products perspectives. *Bioresour Technol* **229**: 53–62.
2. Chiara Monari Serena Righi Stig Irving Olsen (2016) Greenhouse gas emissions and energy balance of biodiesel production from microalgae cultivated in photobioreactors in Denmark: a life-cycle modeling. *J Clean Prod* **112**: 4084–4092.
3. Santos-Ballardo DU, Rossi S, Reyes-Moreno C, Valdez-Ortiz A (2016) Microalgae potential as a biogas source: current status, restraints and future trends. *Rev Environ Sci Bio/Technology* **15**: 243–264.
4. Carboni S, Clegg SH, Hughes AD (2016) The use of biorefinery by-products and

natural detritus as feed sources for oysters (Crassostrea gigas) juveniles. *Aquaculture* **464**: 392–398.
5. Ruiz J, Olivieri G, de Vree J, Bosma R, Willems P, Reith JH, Eppink MHM, Kleinegris DMM, Wijffels RH, Barbosa MJ (2016) Towards industrial products from microalgae. *Energy Environ Sci* **9**: 3036–3043.
6. Gifuni I, Olivieri G, Krauss IR, D'Errico G, Pollio A, Marzocchella A (2017) Microalgae as new sources of starch: Isolation and characterization of microalgal starch granules. *Chem Eng Trans* **57**: 1423–1428.
7. Goiris K, Van Colen W, Wilches I, León-Tamariz F, De Cooman L, Muylaert K (2015) Impact of nutrient stress on antioxidant production in three species of microalgae. *Algal Res* **7**: 51–57.
8. Pulz O, Gross W (2004) Valuable Product from Biotechnology of Microalgae. *Appl Microbiol Biotechnol* **65**: 635–648.
9. Shimidzu N, Goto M, Miki W (1996) Carotenoids as Singlet Oxygen Quenchers in Marine Organisms. *Fish Sci* **62**: 134–137.
10. Zhu L (2015) Biorefinery as a promising approach to promote microalgae industry: An innovative framework. *Renew Sustain Energy Rev* **41**: 1376–1384.
11. Akanda M, Tae H, Kim I, Ahn D, Tian W (2017) Hepatoprotective Role of Hydrangea macrophylla against Sodium Arsenite-Induced Mitochondrial-Dependent Oxidative Stress via the Inhibition of MAPK/. *Int J Mol Sci* **18**: 1–15.
12. Maheshwari N, Khan F, Mahmood R (2017) Sodium meta-arsenite induced reactive oxygen species in human red blood cells: impaired antioxidant and membrane redox systems, haemoglobin oxidation, and morphological changes. *Free Radic Res* **51**: 1–49.
13. Juin C, Bonnet A, Nicolau E, Bérard J, Devillers R (2015) UPLC-MSE Profiling of Phytoplankton Metabolites: Application to the Identification of Pigments and Structural Analysis of Metabolites in Porphyridium. *Mar Drugs* **13**: 2541–2558.
14. Gilbert-López B, Mendiola J, Fontecha J (2015) Downstream processing of Isochrysis galbana: a step towards microalgal biorefinery. *Green Chem* **17**: 4599–4609.
15. Lang I, Hodac L, Friedl T (2011) Fatty acid profiles and their distribution patterns in microalgae: a comprehensive analysis of more than 2000 strains from the SAG culture collection. *BMC Plant Biol* **11**: 124.
16. Flamini R, Traldi P (2010) *Mass Spectrometry in grape and wine analysis*.
17. Bergé JP, Barnathan G (2005) Fatty acids from lipids of marine organisms: Molecular biodiversity, roles as biomarkers, biologically active compounds, and economical aspects. *Adv Biochem Eng Biotechnol* **96**: 49–125.
18. Duong VT, Ahmed F, Thomas-Hall SR, Quigley S, Nowak E, Schenk PM (2015) High protein- and high lipid-producing microalgae from northern australia as potential feedstock for animal feed and biodiesel. *Front Bioeng Biotechnol* **3**: 53.
19. Sharma K, Li Y, Schenk P (2014) UV-C-mediated lipid induction and settling, a step change towards economical microalgal biodiesel production. *Green Chem* **16**: 3539–3548.
20. Richard D, Kefi K, Barbe U, Bausero P, Visioli F (2008) Polyunsaturated fatty acids as antioxidants. *Pharmacol Res* **57**: 451–455.
21. Serrano, Gustavo A. MN (2014) Natural astaxanthin, antioxidant protection power for healthy eyes. *Agro FOOD Ind Hi Tech* **25**:.
22. Wang E, Wink M (2016) Chlorophyll enhances oxidative stress tolerance in Caenorhabditis elegans and extends its lifespan. *PeerJ* **4**: e1879.
23. de Assis AM, Rech A, Longoni A, Rotta LN, Denardin CC, Pasquali MA, Souza

DO, Perry MLS, Moreira JC (2011) Ω3-Polyunsaturated fatty acids prevent lipoperoxidation, modulate antioxidant enzymes, and reduce lipid content but do not alter glycogen metabolism in the livers of diabetic rats fed on a high fat thermolyzed diet. *Mol Cell Biochem* 1–10.

24. Lamaziere A, Wolf C, Barbe U, Bausero P, Visioli F (2013) Lipidomics of hepatic lipogenesis inhibition by omega 3 fatty acids. *Prostaglandins Leukot Essent Fat Acids* **88**: 149–154.
25. Laurens LML, Markham J, Templeton DW, Christensen ED, Van Wychen S, Vadelius EW, Chen-Glasser M, Dong T, Davis R, Pienkos PT (2017) Development of algae biorefinery concepts for biofuels and bioproducts; a perspective on process-compatible products and their impact on cost-reduction. *Energy Environ Sci* **10**: 1716–1738.
26. Safi C, Liu DZ, Yap BHJ, Martin GJO, Vaca-Garcia C, Pontalier P-Y (2014) A two-stage ultrafiltration process for separating multiple components of Tetraselmis suecica after cell disruption. *J Appl Phycol* **26**: 2379–2387.
27. Olivieri G, Gargano I, Andreozzi R, Marotta R, Marzocchella A, Pinto G, Pollio A (2013) Effects of photobioreactors design and operating conditions on Stichococcus bacillaris biomass and biodiesel production. *Biochem Eng J* **74**: 8–14.
28. Aremu AO, Masondo NA, Molnár Z, Stirk WA, Ördög V, Van Staden J (2016) Changes in phytochemical content and pharmacological activities of three Chlorella strains grown in different nitrogen conditions. *J Appl Phycol* **28**: 149–159.
29. Breuer G, Evers WAC, de Vree JH, Kleinegris DMM, Martens DE, Wijffels RH, Lamers PP (2013) Analysis of fatty acid content and composition in microalgae. *J Vis Exp*.
30. Chen Y, Vaidyanathan S (2013) Simultaneous assay of pigments, carbohydrates, proteins and lipids in microalgae. *Anal Chim Acta* **776**: 31–40.
31. Gifuni I, Olivieri G, Pollio A, Franco TT, Marzocchella A (2017) Autotrophic starch production by Chlamydomonas species. *J Appl Phycol* **29**: 105–114.
32. Wellburn AR (1994) The Spectral Determination of Chlorophylls a and b, as well as Total Carotenoids, Using Various Solvents with Spectrophotometers of Different Resolution. *J Plant Physiol* **144**: 307–313.
33. Petruk G, Raiola A, Del Giudice R, Barone A, Frusciante L, Rigano MM, Monti DM (2016) An ascorbic acid-enriched tomato genotype to fight UVA-induced oxidative stress in normal human keratinocytes. *J Photochem Photobiol B Biol* **163**: 284–289.
34. Del Giudice R, Petruk G, Raiola A, Barone A, Monti DM, Rigano MM (2017) Carotenoids in fresh and processed tomato (Solanum lycopersicum) fruits protect cells from oxidative stress injury. *J Sci Food Agric* **97**: 1616–1623.
35. Del Giudice R, Raiola A, Tenore GC, Frusciante L, Barone A, Monti DM, Rigano MM (2015) Antioxidant bioactive compounds in tomato fruits at different ripening stages and their effects on normal and cancer cells. *J Funct Foods* **18**: 83–94.
36. Stiernagle T (2006) *Maintenance of C. elegans*.
37. Abbas S, Wink M (2014) Green Tea Extract Induces the Resistance of Caenorhabditis elegans against Oxidative Stress. *Antioxidants* **3**: 129–143.

Supplemental materials

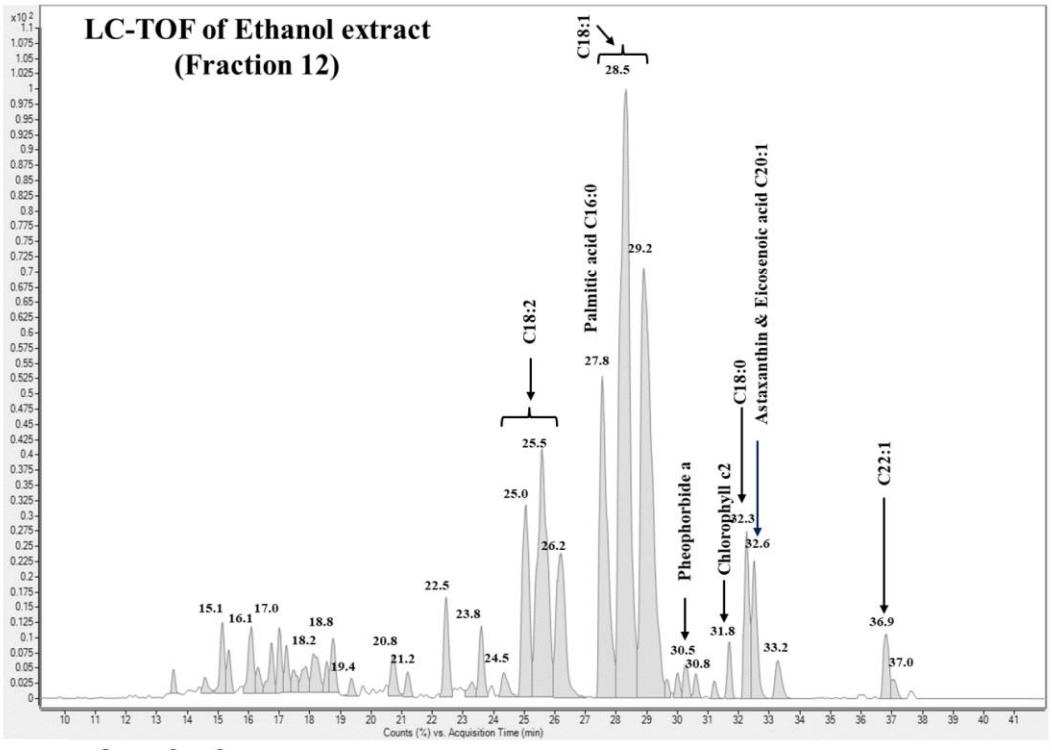

Figure S1: LC-TOF of EE (Fraction 12)

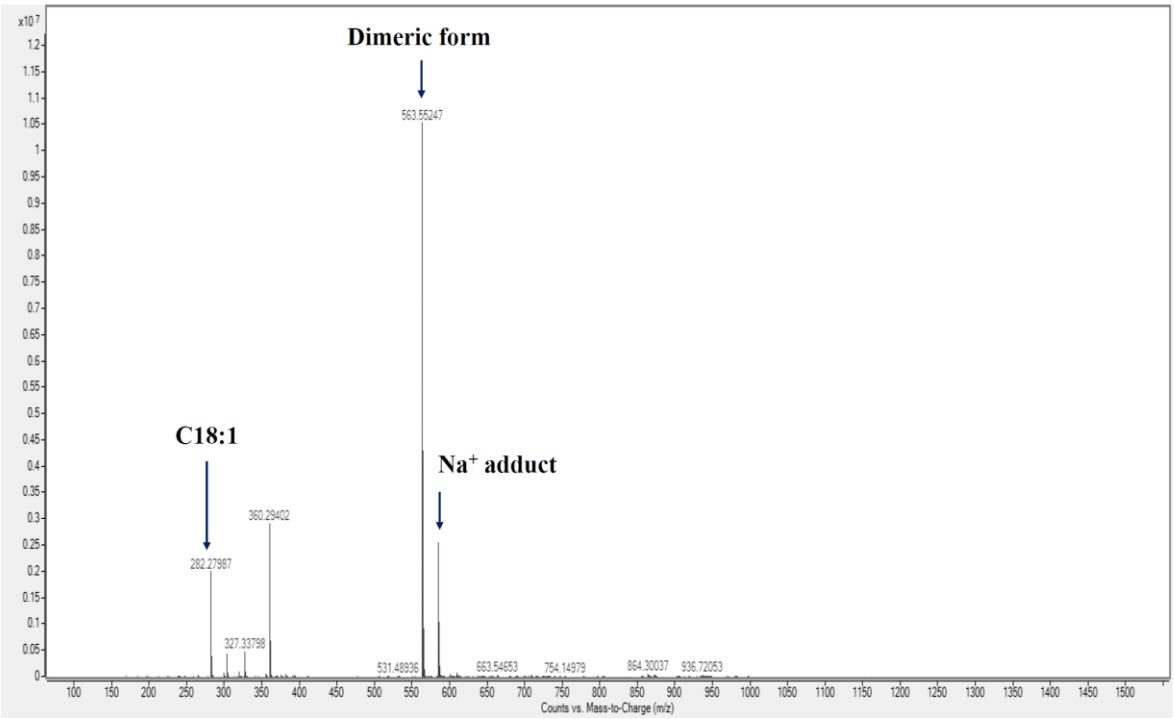

Figure S2: LC-TOF spectrum of ethanol extract (Fraction 12) at 28.5 min

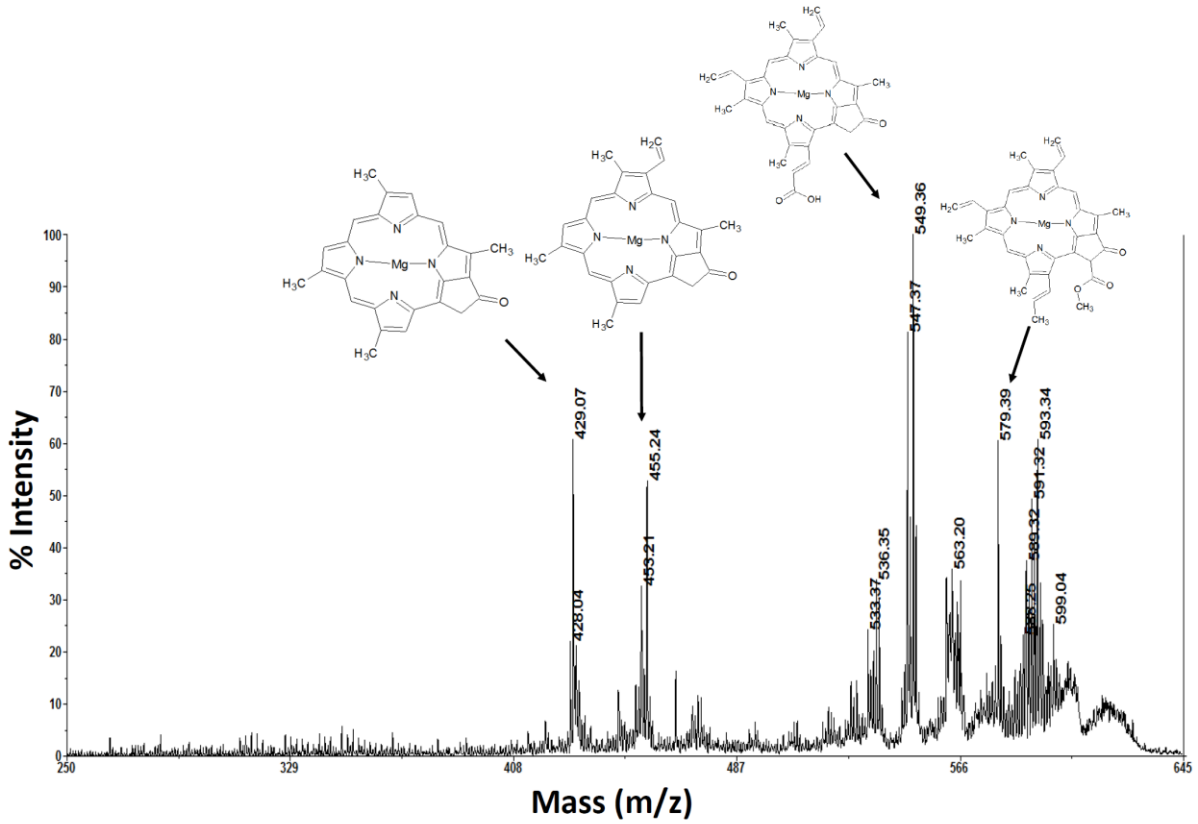

Figure S3: MALDI-TOF/TOF spectrum of Chlorophyll C2 (609.3 Da)

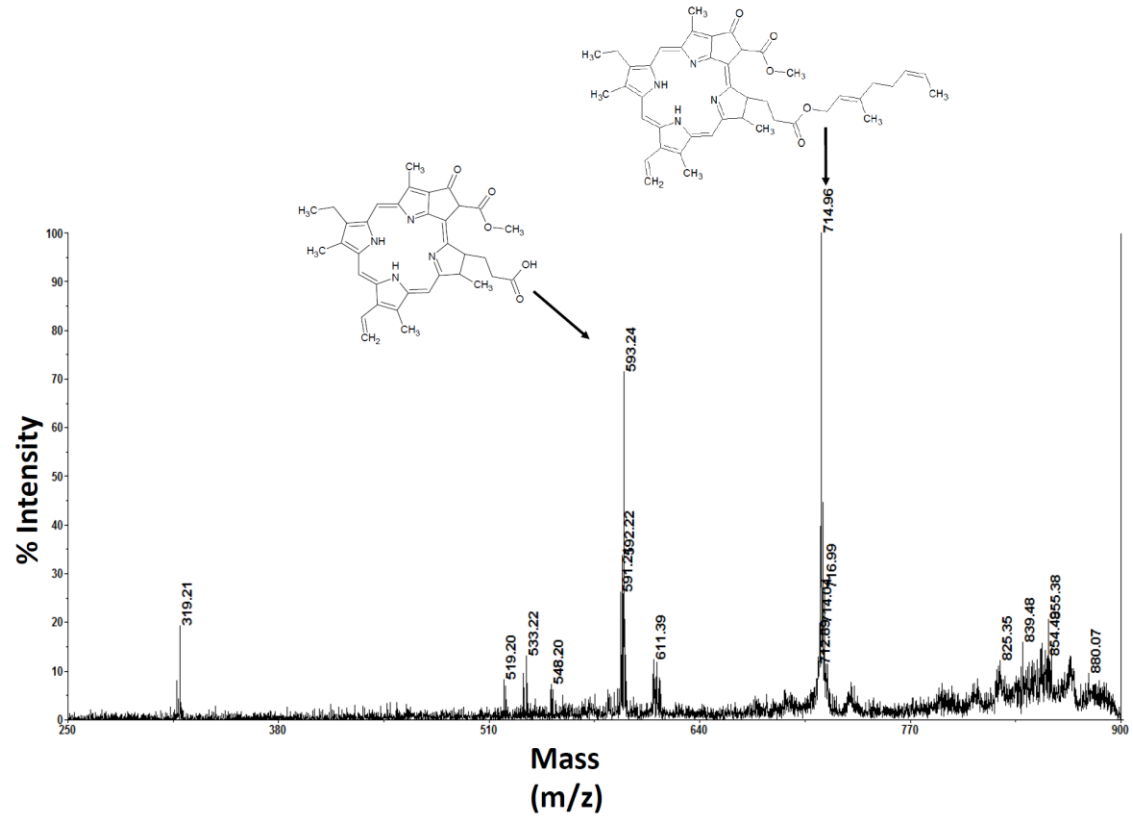

Figure S4: MALDI-TOF/TOF spectrum of Pheophytin a' (871.2 Da)

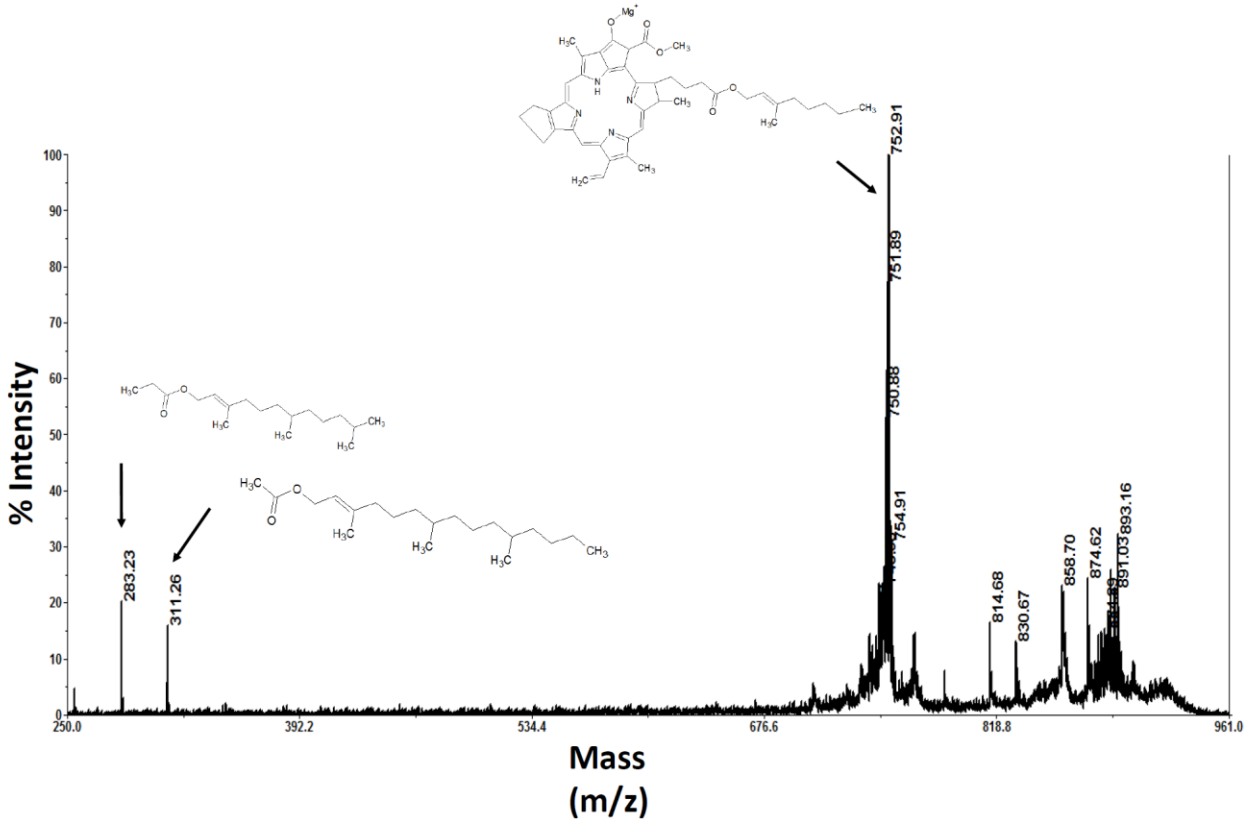

Figure S5: MALDI-TOF/TOF spectrum of hydroxylated chlorophyll a (908.9 Da)

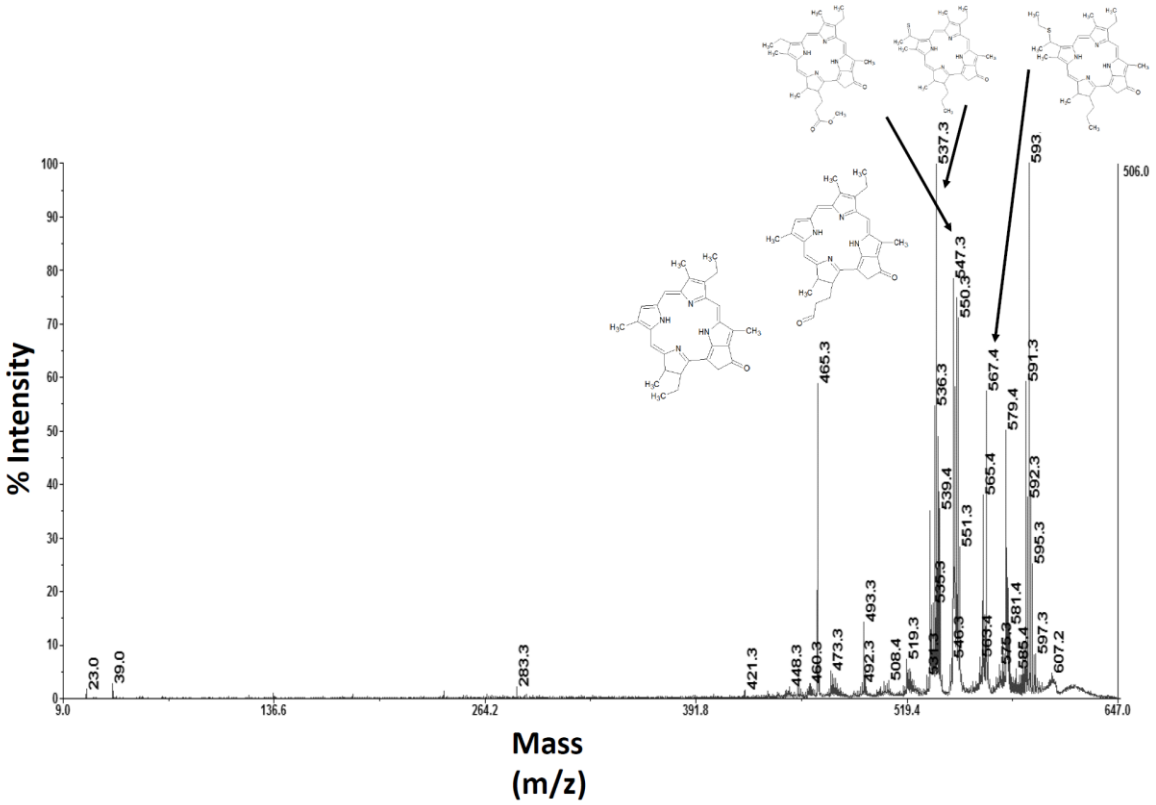

Figure S6: MALDI-TOF/TOF spectrum of S-Et Porphyrin at 611.3 Da

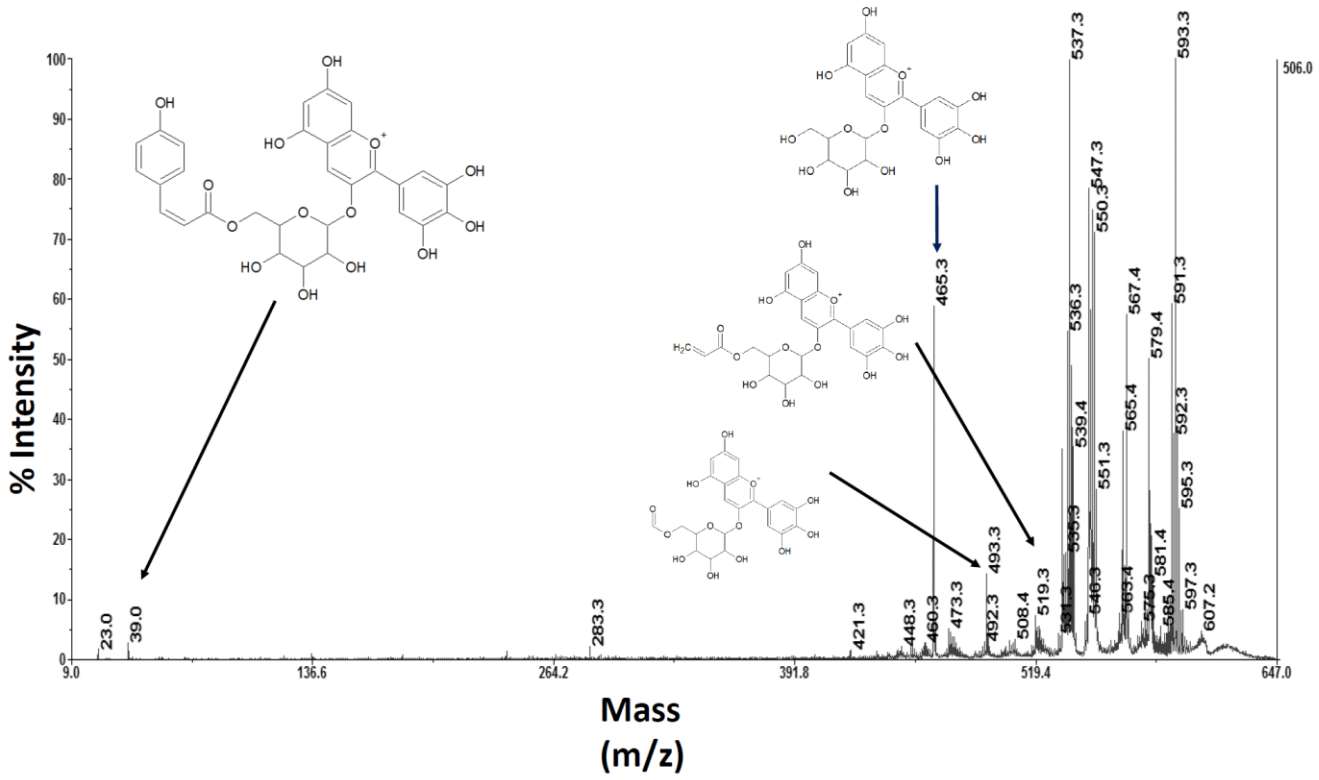

Figure S7: MALDI-TOF/TOF spectrum of Delfinidin – p-coumaroyl glucoside at 611.3 Da

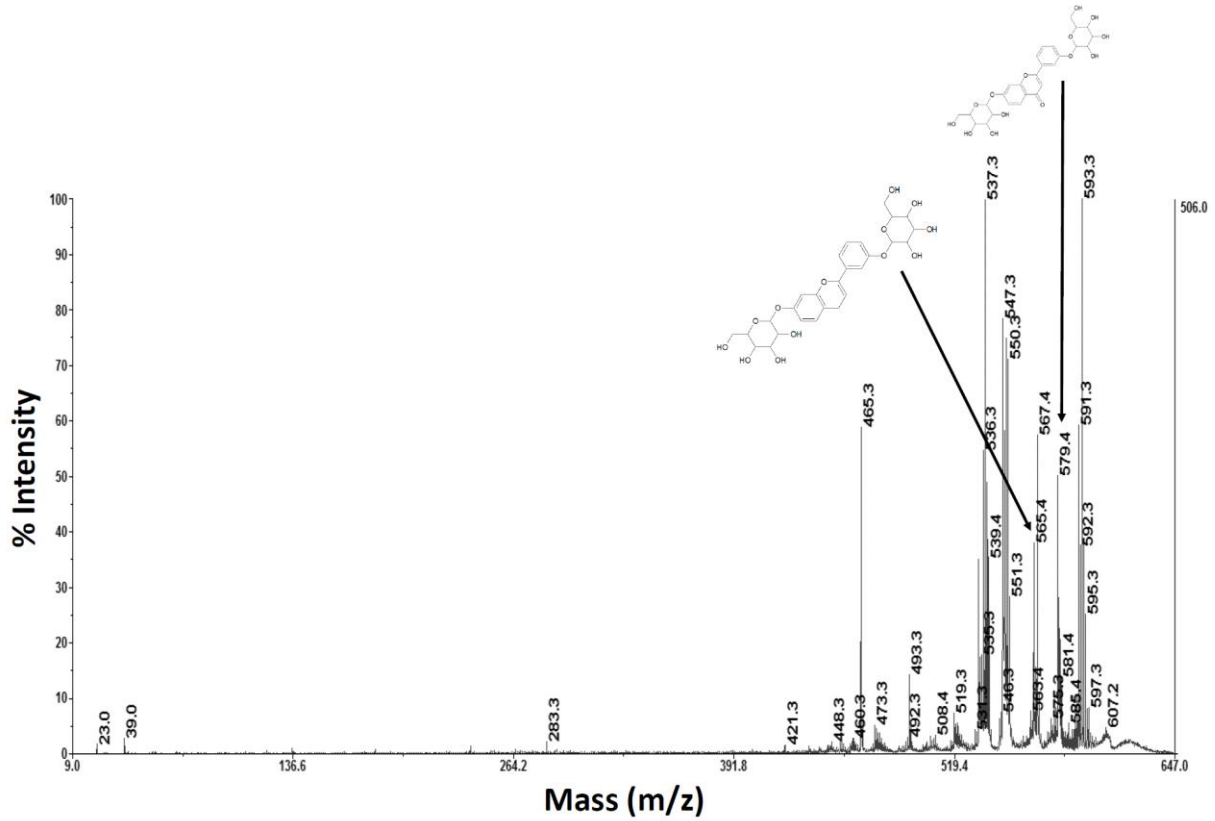

Figure S8: MALDI-TOF/TOF spectrum of Luteolin dihexoside at 611.3 Da

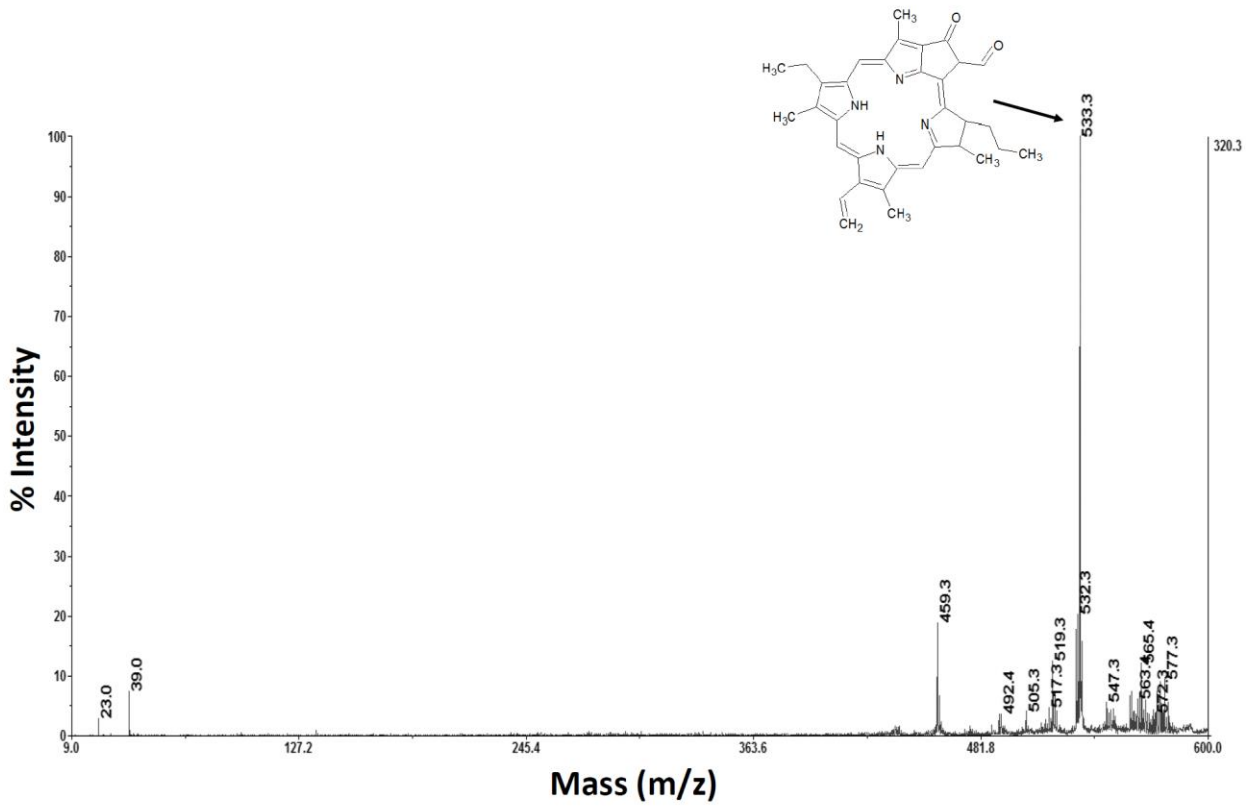

Figure S9: MALDI-TOF/TOF spectrum of pheophorbide at 593.3 Da

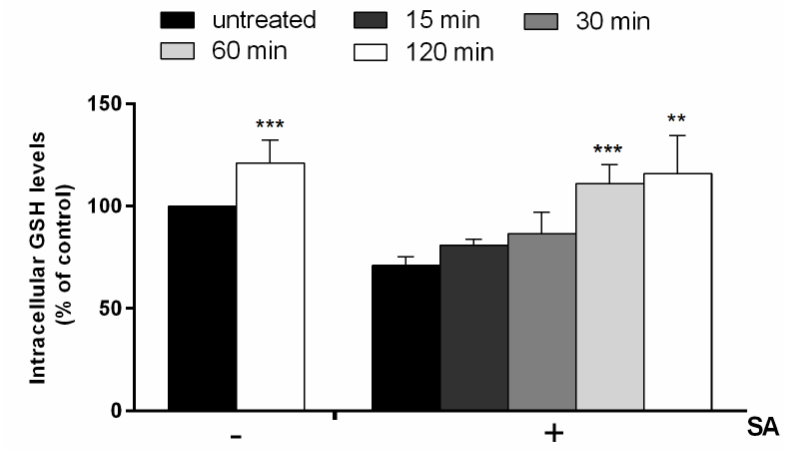

Figure S10: GSH levels in LoVo cells stressed by SA in the presence of EE. Cells were pre-incubated in the presence of 200 µg mL^{-1} EE for different lengths of time prior to be stressed by 300 µM SA for 45 min. Intracellular GSH levels determined by DTNB assay. Control cells, black bars; cells pre-treated with EE are indicated by: dark grey bars (15 min of pre-incubation), grey bars (30 min of pre-incubation), light grey bars (60 min of pre-incubation) and white bars (120 min of pre-incubation). Values are expressed as fold increase with respect to control (i.e. untreated) cells. Data shown are the means ± S.D. of three independent experiments. ** indicates $p<0.005$, *** indicates $p<0.001$.

Conflict of interest

The authors declare no competing financial interest.

The research activity carried out during my master thesis, produced many interesting results which were analyzed and elaborated during the PhD and resulted in a scientific publication here reported.

J Appl Phycol (2017) 29:105–114
DOI 10.1007/s10811-016-0932-2

Autotrophic starch production by *Chlamydomonas* species

Imma Gifuni[1] · Giuseppe Olivieri[1] · Antonino Pollio[2] · Telma Teixeira Franco[3] · Antonio Marzocchella[1]

Received: 19 May 2016 / Revised and accepted: 9 August 2016 / Published online: 4 September 2016

Abstract Microalgal autotrophic cultures may be used as starch feedstocks for a wide spectrum of food and non-food applications, starch-based plastics production included. *Chlamydomonas* is known to accumulate carbohydrates, but only *Chlamydomonas reinhardtii* is widely studied. This is the first paper that analyzes the starch content and production rate of four non-conventional *Chlamydomonas* species and compares their performances to the benchmark *C. reinhardtii*. Two culture systems—shaken flasks and inclined bubble column (IBC) photobioreactors—and nitrogen depletion conditions were characterized. The irradiance was set at 95 μmol photons m^{-2} s^{-1} for flask system and at 220 μmol photons m^{-2} s^{-1} for photobioreactors. CO_2 and light depletion in shaken flasks strongly affected growth rate and starch production. Under these limiting condition, *Chlamydomonas applanata* had the best starch productivity of 1.2 mg L^{-1} day^{-1}. In IBC photobioreactors, the microalgal growth rate and starch production improved with respect to the flask system and nitrogen depletion promoted starch accumulation. The best results of starch productivity and maximum starch fraction were 53 mg L^{-1} day^{-1} and 45%$_{DW}$ for *Chlamydomonas oblonga* and *Chlamydomonas moewusii*, respectively. This was 49 % more than the studied benchmark. A fast and simple method for starch localization in the microalgal cells was also proposed. The starch granules surrounded the pyrenoid under the growth phase, while they fill the whole cell under nutrient depletion.

Keywords Bioplastics · *Chlamydomonas* · Culture systems · Microalgae · Starch

Electronic supplementary material The online version of this article (doi:10.1007/s10811-016-0932-2) contains supplementary material, which is available to authorized users.

✉ Giuseppe Olivieri
giolivie@unina.it

[1] Dipartimento di Ingegneria Chimica, dei Materiali e della Produzione Industriale, Università degli Studi di Napoli Federico II, Piazzale Tecchio 80, 80125 Naples, Italy

[2] Dipartimento di Biologia, Università degli Studi di Napoli Federico II, Via Foria 223, 80139 Naples, Italy

[3] Faculdade de Engenharia Química–University of Campinas, Av. Albert Einstein, 500, Campinas, SP CEP 13083-852, Brazil

Introduction

The increasing demand of starch, as feedstock for many food and non-food products, has been reported by Srinivas (2007) and by LM International (2002). One of the consolidated starch industrial applications is starch plastic (e.g., thermoplastic starch, TPS) production, which is now the most widespread biobased plastic. Starch-plastic producers (e.g., Novamont) exploit starch accumulated by plants as carbon/energy source (Busi et al. 2014). Plant starch is made up of two polymers of D-glucose: amylose (unbranched) and amylopectin (highly branched). Amylopectin chains may form helical structures that may crystallize promoting the formation of the granule structure (Buléon et al. 1998).

The current main sources of starch are potato, maize, wheat, and sorghum. However, social, environmental, and commercial issues ask for alternative sources characterized by constant supply rate, selected quality, low cost and environmental impact, and production systems that do not compete for arable land.

The interest in microalgae as potential source for starch is related to their fast growth rate—compared with terrestrial

plants—and their wide range of industrial applications including food, biofuels, drugs, cosmetics, and bioremediation. Moreover, microalgal cultures do not compete for arable land, and in autotrophic cultures, they combine the biomass production with CO_2 capture. Regarding microalgae as bioplastic feedstock, the attention of researchers has been mainly focused on the characterization of processing both the whole microalgal biomass and the microalgal proteins for bioplastic production. At Algix, researchers have investigated the capacity of microalgal proteins to form polymers and an algae-to-plastic facility for algae powder extrusion with resin and additives has been built in Missisipi, USA (www.algix.com). However, there is industrial interest concerning also the use of the microalgal starch fraction in bioplastic production as well as in food industries. The process breakthrough is the selection of the optimal culture conditions (i.e., culture strategy and culture systems) to maximize starch accumulation in microalgae.

Ho et al. (2012) reported that it is possible to enhance starch production in microalgae by tuning the microalgal culture conditions such as irradiance, nutrient depletion, temperature variation, pH shift, and CO_2 supply (Brown et al. 1997; Renaud et al. 2002; Khalil et al. 2010; Chen et al. 2013). However, the most common strategy to enhance the accumulation of carbon-rich molecules in microalgae is nitrogen depletion (Dragone et al. 2011; Breuer et al. 2012; Fernandes et al. 2013; Kamalanathan et al. 2016). Under nitrogen depletion, starch is accumulated in the early starvation phase, whereas in late starvation phase, lipid accumulation is promoted. *Chlamydomonas* is known to accumulate a large amount of sugars as starch (Chen et al. 2013), but the most studied species is still *Chlamydomonas reinhardtii* because it is widely characterized from the metabolic and genetic point of view. More than 400 *Chlamydomonas* species have been recognized, and molecular analyses showed that the genus *Chlamydomonas* is polyphyletic and should be divided into eight independent lineages (Demchenko et al. 2012). No information is available about carbohydrates and starch content of other *Chlamydomonas* species. We have investigated four interesting species, in addition to *C. reinhardtii* (used as benchmark):

- *Chlamydomonas pitschmannii*, coming from thermoacidic environment, studied for lipid production and resistance to the presence of metals in the medium (Abou-Shanab et al. 2011; Pollio et al. 2005)
- *Chlamydomonas oblonga* for which only phylogenetic, taxonomic, and structural analyses are reported in literature
- *Chlamydomonas applanata* characterized by a high range of pH tolerance
- *Chlamydomonas moewusii* widely studied for hydrogen production in the last decades (Meuser et al. 2009)

No information is available in the literature about the carbohydrate and starch content of these four species.

The aim of this work was to investigate starch production by the mentioned non-conventional *Chlamydomonas* species and to select the best starch producer. Moreover, to the authors' knowledge, there is no systematic analysis of culture conditions and culture systems on microalgal starch accumulation. For this reason, the effect of two culture systems has been investigated: shaking flasks and prismatic photobioreactors.

A cytological study about the localization of starch in the cells was also carried out by means of a staining assay coupled with optical microscope observation, in order to localize the amount and the distribution of the granules in the different *Chlamydomonas* species.

Materials and methods

Microorganisms and medium

Chlamydomonas species were from the ACUF collection of the Department of Biology at the Università degli Studi di Napoli "Federico II" (www.acuf.net). Five *Chlamydomonas* species were investigated: *Chlamydomonas reinhardtii* Dangeard (strain number (s.n.) 027); *Chlamydomonas pitschmannii* Ettl (s.n.118); *Chlamydomonas oblonga* Pringsheim (s.n.157); *Chlamydomonas applanata* Pringsheim (s.n.159); and *Chlamydomonas moewusii* Gerloff (s.n.163). The strains were grown in Bold Basal Medium (BBM) as described by Olivieri et al. (2013). The BBM pH was about 6.8.

Analytical methods

Culture samples were collected and characterized in terms of microalgae and medium composition. The samples were centrifuged at 5000×*g* for 20 min (Eppendorf-5804R) to harvest cells from the liquid phase.

Microalgal analysis

The microalgal concentration was measured as optical density at wavelength of 750 and 600 nm (OD_{750} and OD_{600}). The OD values were converted to biomass concentration via appropriate calibration between OD and dry cell weight. The dry cell weight was determined by filtering 50-mL aliquots of culture through a Whatman filter. The filter was dried at 60 °C until constant weight and weighed. This procedure was repeated for several biomass concentrations. The biomass concentration estimated according the conversion factor assessed by processing OD_{750} and OD_{600} did not change within the experimental error.

Total carbohydrates were assayed according to phenol-sulfuric acid method (Miller 2010). The microalgal pellet was dispersed in distilled water to prepare a suspension at 1 g_{DM} L^{-1} cell concentration. One milliliter of the suspension was mixed with 1 mL of phenol (5 %) and 5 mL of sulfuric acid (96 %). The mixture was cooled at 25 °C. The absorbance of the solution was measured at 488 nm. The concentration of carbohydrates was calculated using a calibration curve based on glucose.

Ten milligram of dry microalgae was used to measure the microalgal starch content. Microalgae were suspended in a buffer solution (pH = 7) and processed in a French press for mechanical rupture. The microalgal lysate was centrifuged, re-suspended in an aqueous solution of ethanol (80 %), and incubated at 80–85 °C for 5 min to extract the pigments. Starch content was assayed by an enzymatic kit (Megazyme, Ireland) containing amylase, amyloglucosidase, and oxidase-peroxidase enzymes and adopting the protocol provided by the manufacturers.

The starch granules in microalgal cells were stained with Lugol dye and observed in a microscope (Nikon eclipse E800, bright field). Lugol's dye is a solution of elemental iodine and potassium iodide in water. The solution was mixed with culture samples at a volumetric ratio of 1:3 (Muller et al. 1998). Elemental iodine solutions stain just starches because iodine interacts with the coil structure of the polysaccharide and provides dark-blue/black starch colorization after 10 min of mixing. Simple sugars—such as glucose and fructose—do not interact with Lugol dye. Microscope pictures were analyzed by ImageJ (open sources image processing software by National Institutes of Health, USA) as reported by Schulze et al. (2011), in order to measure the cell area and the cell area filled by starch.

Medium analysis

Liquid phase was characterized in term of pH, nitrate, and total sugar concentration. The pH was measured by a pH meter (InLab Routine series probe, 0–14 pH | FE20 – FiveEasy meter, Mettler Toledo).

Nitrate concentration was determined spectrophotometrically according to Collos et al. (1999). Twenty microliter of 1 M HCl was added to 1 mL of liquid sample to remove carbonate interferences and nitrate content was measured as optical density at 220 nm (OD_{220}) using a UV/VIS spectrophotometer (Varian Cary50). A calibration curve was made vs. $NaNO_3$ to assess the conversion factor between OD_{220} and concentration of NO_3^- ions.

The sugar concentration was assayed using the Phenol-Sulfuric Acid method previously described (see section "Microalgal analysis").

Apparatus, operating conditions, and procedures

Two culture systems were used for *Chlamydomonas* growth: Erlenmeyer flasks and inclined bubble column photobioreactors. All experiments were carried out in triplicates and the standard deviation was calculated on the basis of these tests.

Erlenmeyer flasks of 2 L were set on a Plexiglass shaking plate housed in a thermosted room at ~25 °C. The flasks were lighted from the bottom by fluorescent lamps (Philips, TLD 30W/55) at an irradiance of 95 μmol photons m^{-2} s^{-1}. The irradiance was measured with a LI-COR LI-190 quantum sensor.

The head of the flask was closed by means of a gauze filter to prevent contamination and to allow free gas exchange between the flask and the atmosphere. CO_2 and O_2 exchange between the culture and the gas present in the flask was provided by continuous shaking of the cultures. Flasks with 500 mL medium were autoclaved for 20 min at 121 °C. pH was not controlled during the cultivation. Fifty milliliter of concentrated medium was added each week to the culture to restore the initial volume and nutrient concentration and to prevent nutrient depletion. Sterilized distilled water was supplemented to the flasks for counterbalance the effect of evaporation.

The inclined square bubble column photobioreactors had a volume of 2 L, thickness of 8 cm, and the longitudinal axis was inclined of 30° with respect to the horizontal (Gargano et al. 2013). The working volume was 1.5 L. The photobioreactors were housed in a climate chamber (HeraeusVötsch GmbH; type: HPS 500) at 25 ± 1 °C. Fluorescence lamps (M2M engineering) fixed at the ceiling of the climate chamber continuously illuminated photobioreactors at an irradiance of 220 μmol photons m^{-2} s^{-1}. The volumetric flow rate of the gas stream fed at each photobioreactor was controlled by means of needle valves and was set at 0.22 vvm. The CO_2 concentration in the gas stream was set at 2 %. The photobioreactors with the medium were autoclaved for 20 min at 121 °C. Batch cultures were carried out in these photobioreactors; the pH was maintained at 7 by continuous addition of CO_2 to offset the increase in pH during microalgal growth (Moheimani and Borowitzka 2006). Culture was sampled daily and no medium was added to culture to allow nitrogen depletion.

The biomass-light yield $Y_{X/E}$ was calculated as ratio of the biomass produced and the light energy irradiated over the cultivation time. The produced biomass was assessed as the product of the culture volume, V (L) and the difference of the biomass concentration measured at the culture end, X (g L^{-1}) and the inoculation time X_0 (g L^{-1}). The irradiated energy was assessed as the product of the irradiated surface A (m^2), the irradiance E) (μmol photons m^{-2} s^{-1}) and the culture time t (s). The $Y_{X/E}$ (g_X $mol_{photons}^{-1}$) was:

$$Y_{X/E} = \frac{(X - X_0)V}{AEt} \quad (1)$$

The ratio φ between the area occupied by the starch in a cell and the area of the cell was assessed by processing cell digital images with ImageJ program. Under a set of operating conditions, φ was calculated as the average of the ratio, assessed for N observation, with N larger than 100:

$$\varphi = \frac{1}{N}\sum_{N}\frac{(\text{starch area})}{(\text{cell area})} \quad (2)$$

The standard deviation of ratio was also assessed.

Biomass productivity, r_X (g L^{-1} day^{-1}) was assessed as the ratio between biomass concentration and culture time according to the relationship:

$$r_{X(t)} = \frac{X(t) - X_0}{t - t_0} \quad (3)$$

where $X(t)$ is the biomass concentration (g L^{-1}) at a specific time of the culture, t (d), while t_0 (d) is the beginning of the culture time.

Starch productivity, r_S (g L^{-1} day^{-1}) was assessed as the ratio between starch concentration (g_{starch} L^{-1}) and culture time, $t - t_0$ (d):

$$r_{S(t)} = \frac{\omega_{starch}(t) \cdot X(t)}{t - t_0} \quad (4)$$

where $\omega_{starch}(t)$ is the starch fraction of the dry microalgal dry mass measured at the instant t and t_0 is the inoculation time. The starch mass in the inoculum was not included in Eq. (4) because it was negligible.

Starch and sugar content of microalgae were calculated as the ratio between the starch and the sugar concentration and the dry mass of microalgae analyzed.

Results

Flask culture system

The cultures in flasks were carried out for about 1 month. The culture volume was kept constant during the test and nutrient concentration was never limiting because nutrients were periodically added. The supply of CO_2 to the culture was for dispersion of the CO_2 of the air across the free suspension surface. Culture irradiance was set at 95 μmol photons m^{-2} s^{-1}.

Figure 1 shows the growth curve in the flask system of the five investigated species. The cell concentration (X) increased linearly with time for all species, although there are noticeable differences in growth performances. *Chlamydomonas applanata* and *C. reinhardtii* growth rates are almost comparable, as well as *C. oblonga* and *C. pitschmannii*, while *C. moewusii* is characterized by the slowest growth rate. The

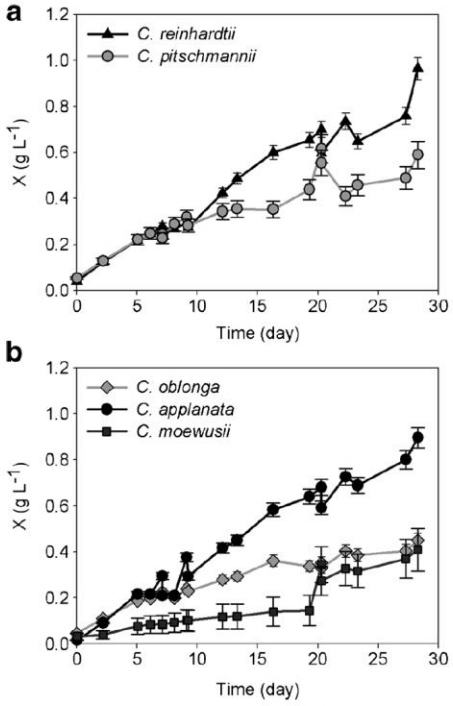

Fig. 1 *Chlamydomonas* species growth in flasks: **a** *C. reinhardtii, C. pitschmannii*; **b** *C. oblonga*, *C. applanata*, *C. moewusii*. Operating conditions: volume 500 mL; temperature 25 °C; pH 6.7; irradiance 95 μmol photons m^{-2} s^{-1}. All points represent the average ± s.d. of three independent experimental replicates

biomass-light yield ($Y_{X/E}$) ratio for the investigated cultures (see Fig. S1, supplemental material) according to Eq. (1) decreased with the time and after about 2 weeks they approached a constant value characteristic of each strain. Table 1 reports the $Y_{X/E}$ for the *Chlamydomonas* strains at the end of the culture time (4 weeks). *Chlamydomonas reinhardtii* and *C. applanata* were characterized by the best yields: 0.183 and 0.172 g_x mol^{-1} photons, respectively. Lower values were observed for the others strains.

Table 1 also reports the starch fraction of *Chlamydomonas* species and the starch productivity for the flask system. *Chlamydomonas applanata* and *C. reinhardtii* were characterized by the best biomass and starch productivity: 0.034, 0.032 g L^{-1} day^{-1} and 1.1, 1.2 x 10^{-3} g starch L^{-1} day^{-1}. Although the starch contents were not the highest among the five strains, these strains were characterized by the highest growth rate and biomass productivity under the operating conditions tested. The highest starch content (5 %) for cultures in the flask system was measured for *C. oblonga*.

The concentration of sugar secreted in the medium is also reported in Table 1. Secreted sugar concentration increased with the time for all species and was as high as 0.2 g L^{-1}.

Table 1 Main data assessed for the cultures of the investigated *Chlamydomonas* species

Chlamydomonas species	$Y_{X/E}$ (g_x $mol_{photons}^{-1}$)	Biomass productivity (g L^{-1} day^{-1})	Starch productivity (g L^{-1} day^{-1})	Total sugar concentration in biomass ($\%_W$)	Starch concentration in biomass ($\%_{DW}$)	Secreted sugar (g L^{-1})
C. reinhardtii	0.183 ± 0.009	0.034 ± 0.004	1.1 ± 0.1 x 10^{-3}	27.21 ± 0.72	3.1 ± 0.28	0.108 ± 0.002
C. pitschmannii	0.119 ± 0.006	0.021 ± 0.002	0.5 ± 0.1 x 10^{-3}	22.18 ± 0.08	4.6 ± 0.56	0.198 ± 0.007
C. oblonga	0.104 ± 0.005	0.019 ± 0.005	0.8 ± 0.2 x 10^{-3}	27.85 ± 0.09	5.2 ± 1.15	0.157 ± 0.008
C. applanata	0.172 ± 0.009	0.032 ± 0.002	1.2 ± 0.3 x 10^{-3}	19.91 ± 0.23	3.7 ± 1.03	0.190 ± 0.009
C. moewusii	0.086 ± 0.003	0.015 ± 0.007	0.6 ± 0.2 x 10^{-3}	14.84 ± 0.68	4.04 ± 0.97	0.083 ± 0.008

Cultivation system: flasks. CO_2 feeding: diffusion of air at the culture surface. Irradiance 95 μmol photons m^{-2} s^{-1}. All points represent the average ± s.d. of three independent experimental replicates

Cell growth and starch production rate in photobioreactors

Figure 2 reports the concentration of microalgal cells vs. time for cultures in inclined square bubble column photobioreactors (IBCPs) irradiated with cold white fluorescent lamps at 220 μmol photons m^{-2} s^{-1}. The photobioreactors were fed with 2 % CO_2 air streams. A two-phase pattern of the microalgal cell growth was recognized: a 5–6 day growth phase followed by a stationary phase. The lag phase was almost absent because of the high inoculum size.

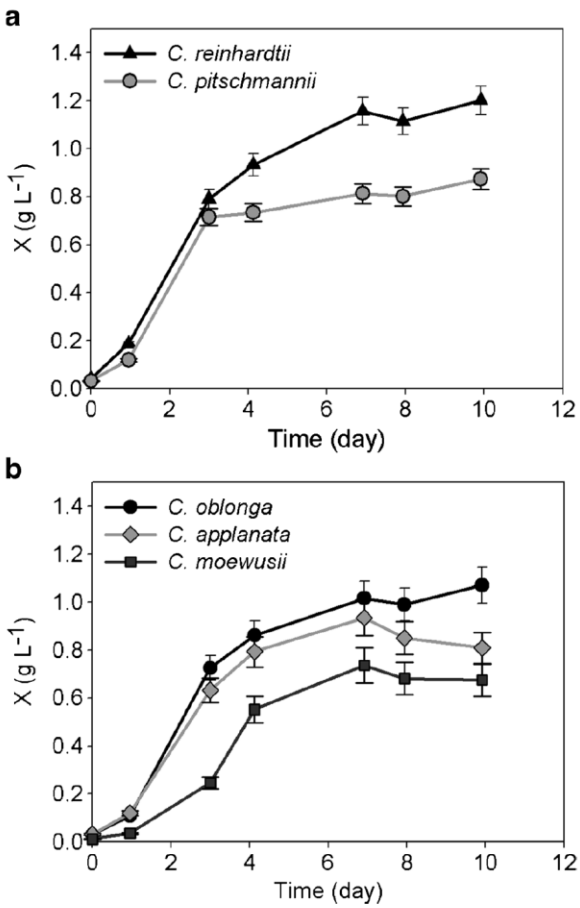

Fig. 2 Growth of the *Chlamydomonas* species in photobioreactors. **a** *C. reinhardtii*, *C. pitschmannii*; **b** *C. oblonga*, *C. applanata*, *C. moewusii*. Operating conditions: inoculum size 0.1 g L^{-1}; BBM; volume: 1.6 L; temperature 25 °C; pH 6.7; air flow 0.22 vvm; CO_2 concentration 2 %; irradiance 220 μmol photons m^{-2} s^{-1}. All points represent the average ± s.d. of three experimental replicates

Figure 3 reports the biomass productivity—assessed according to Eq. 3—as a function of culture time. The maximum productivity was measured at about day 3 after the inoculation and the value depended on the species. The total carbohydrate fraction, the starch fraction of the biomass and the starch productivity—assessed according to Eq. 4—are reported in Table 2 and Fig. 4, respectively. Both total carbohydrate and starch fractions of the biomass increased from early growth phase (day 1 in Fig. 2) to early N-starvation phase (day 7 in Fig. 2). As N-starvation was extended (day 10 in Fig. 2), the total carbohydrate fraction decreased mainly as a consequence of the reduction of the non-starch components. The highest biomass productivity was reached by *C. reinhardtii*, but the non-conventional strains showed the highest starch content and starch productivity. In particular, *C. moewusii* sugar content reached 73 % of microalgal DW and the starch fraction was 45 % of DW, while the highest starch productivity was measured for *C. oblonga* and was 0.53 g L^{-1} day^{-1}.

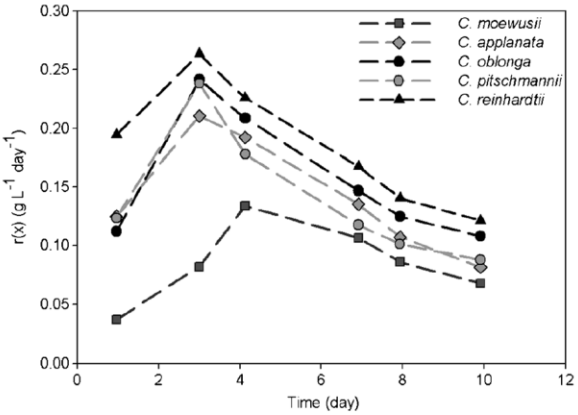

Fig. 3 Biomass productivity of the *Chlamydomonas* species during cultivation time in photobioreactors

Table 2 Carbohydrate content and starch content of the biomass and secreted sugars measured during the cultures of the investigated *Chlamydomonas* species

	Total carbohydrates in biomass (% of $_{DW}$)	Starch in biomass (% of $_{DW}$)	Secreted sugar (g L^{-1})
Early growth phase (day 1 in Fig. 2)			
C. reinhardtii	10.01 ± 0	4.83 ± 0.32	34.45 ± 5.24 x 10^{-3}
C. pitschmannii	17.93 ± 0.69	7.09 ± 0.16	41.90 ± 1.51 x 10^{-3}
C. oblonga	28.4 ± 3.61	12.07 ± 0.62	31.77 ± 1.16 x 10^{-3}
C. applanata	33.64 ± 5.81	22.58 ± 0.19	25.37 ± 0.81 x 10^{-3}
C. moewusii	47.84 ± 0.98	6.46 ± 0.85	21.07 ± 2.44 x 10^{-3}
First day under N-depletion (day 7 in Fig. 2)			
C. reinhardtii	48.31 ± 1.98	22.14 ± 0.49	54.59 ± 5.90 x 10^{-3}
C. pitschmannii	50.34 ± 2.51	29.58 ± 0.68	70.25 ± 4.62 x 10^{-3}
C. oblonga	72.58 ± 1.46	37.73 ± 1.12	57.21 ± 5.62 x 10^{-3}
C. applanata	50.34 ± 1.34	31.76 ± 2.24	51.62 ± 5.47 x 10^{-3}
C. moewusii	72.76 ± 5.72	44.65 ± 3.33	48.65 ± 7.72 x 10^{-3}
Third day under N-depletion (day 10 in Fig. 2)			
C. reinhardtii	43.83 ± 2.5	26.36 ± 0.44	126.77 ± 2.23 x 10^{-3}
C. pitschmannii	48.78 ± 3.61	30.38 ± 0.13	83.69 ± 5.59 x 10^{-3}
C. oblonga	74.56 ± 4.95	43.89 ± 0.57	71.76 ± 3.87 x 10^{-3}
C. applanata	55.47 ± 5.41	29.94 ± 1.82	59.19 ± 2.04 x 10^{-3}
C. moewusii	79.04 ± 1.01	36.04 ± 1.01	88.00 ± 5.70 x 10^{-3}

See caption of Fig. 2 for operating conditions and culture system. All points represent the average ± s.d. of three independent experimental replicates

The secreted sugar concentration in the medium increased with the time for all the investigated species.

Starch distribution in microalgal cells grown in photobioreactors

Figure 5 shows microscope pictures of *C. oblonga* cells stained with Lugol dye. The cells were harvested in the growth phase (Fig. 5a) and in the N-starvation phase (Fig. 5Bb). The dark regions represent the pyrenoids surrounded by starch granules. The microscope observation of the cell highlighted that the pyrenoid was in the central-basal position for *C. reinhardtii* and *C. moewusii*, in a sub-apical position against the cell wall in *C. pitschmannii* and *C. applanata* (see Fig. S2, supplemental material), and in the central position in *C. oblonga* (Fig. 5a). Under nitrogen starvation conditions, the starch filled the cell in all the strains (Fig. 5Bb).

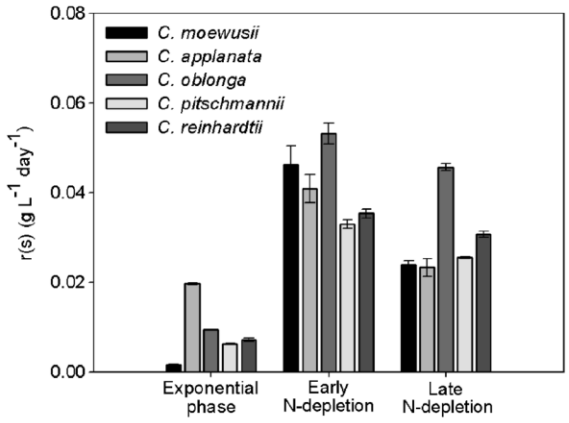

Fig. 4 Starch productivity of the *Chlamydomonas* species investigated (see Fig. 2 for operating conditions). Data refer to the three phases of growth: phase, early N-depletion, after 3 days in N-starvation. All *bars* represent the average ± s.d. of three experimental replicates

Table 3 reports the ratio φ between the area occupied by the starch in a cell and the area of the cell, assessed according to Eq. 2 in the growth phase and the N-starvation phase. It can be seen that during N-starvation, the area of the cells and the fraction of cell area occupied by starch increase with respect to the exponential phase. Cell fattening was observed for all the investigated *Chlamydomonas* species under N-depletion conditions.

Discussion

Flask system vs. IBC for starch production studies The linear growth observed for the test carried out in flask system (Fig. 1) may be due to some nutrient limitations that prevented exponential growth. The biomass productivity reported in Table 1 was constant for each species throughout the culture time because the biomass concentration increased linearly with the time. The growth-limiting factors did not include N- and P-sources because they were periodically

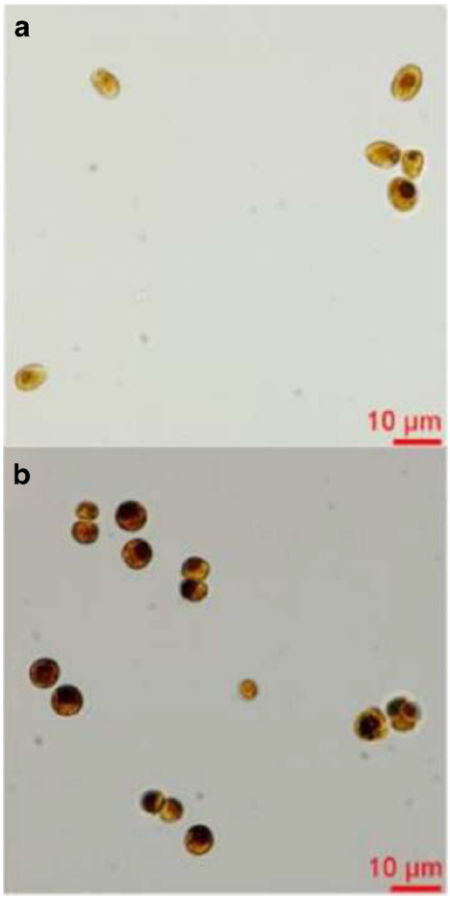

Fig. 5 Light micrographs of *C. oblonga* cells stained with Lugol dye to highlight the starch granules (*dark region*). Cell harvested under **a** growth phase and **b** N-starvation phase

supplemented at sufficient mass rate to avoid N- and P-depletion. The two factors that could have limited the cell growth are CO_2 and light. The flask irradiation was definitively low and this kind of culture system did not allow efficient conversion of the light provided into biomass as shown by the $Y_{X/E}$ values. Kliphuis et al. (2012) reported $Y_{X/E}$ for *C. reinhardtii CC1690* in steady-state cultures irradiated at constant irradiance for 24/24 h. The irradiance was changed between 80 and 1000 (μmol photons m^{-2} s^{-1}). They found that the $Y_{X/E}$ decreased from 1.25 to 0.51 g_x mol^{-1} photons when the irradiance increased between 80 and 1000 μmol photons m^{-2} s^{-1}. The yield assessed in the present study was about one order of magnitude less than that observed by Kliphuis et al. (2012) at approximately equal irradiance. It may be inferred that some factors limited the light conversion into biomass. Indeed, Kliphuis et al. (2012) sparged the cultures with air at 5 % of CO_2, while the CO_2 concentration in the present tests was about 0.035 %. Nascimento et al. (2013) reported a biomass productivity of 0.24 g L^{-1} day^{-1} when *Chlamydomonas* species were grown in shaken flasks, at 80 μmol photons m^{-2} s^{-1} with air supplied at 2 % CO_2, much higher than those obtained in our experiment (Table 1). Analysis of the data in Table 1 and those reported by Kliphuis et al. (2012) and Nascimento et al. (2013) suggests that CO_2 diffusion from air to liquid promoted by flask shaking was not adequate for supplying the cultures.

The presence of limiting factors also affects starch accumulation and productivity in flasks system. Indeed, the obtained results of 5 % of starch on DW and $1.1x10^{-3}$ g L^{-1} day^{-1} are definitely not attractive for a mass production.

The biomass and starch productivities measured in the IBC photobioreactors were higher than those measured in the flasks (Table 2). The high performance in the IBCs with respect to the performance in the flasks is probably due to the improved supply of CO_2 and to the light availability. Indeed, the mixing induced by the bubble flow promoted cell movement between the dark and the light zones (Olivieri et al. 2013). Moreover, as reported by Yao et al. (2012), for the microalga *Tetraselmis subcordiformis*, the increase in light energy causes a superior starch accumulation, as well as increased biomass productivity. According to Johnson and Alric (2013) and Chen et al. (2013), appropriate irradiance offers energy that may be stored as carbohydrates. Indeed, *C. reinhardtii* can accumulate carbohydrates up to 60 % of dry biomass, and about 55 % of these carbohydrates is starch. Fernandes et al. (2013) reported that the starch content in *Chlorella vulgaris* increased from 8.5 % (dry weight basis) to 40 % when the light intensity was increased from 215 to

Table 3 Microalgal cell area and fraction of area occupied by starch (φ)

	Growth phase		N-starvation phase	
	Cell area (μm²)	φ	Cell area (μm²)	φ
C. reinhardtii	23.4 ± 8.1	25.0 ± 11.8	44.8 ± 8.4	40.1 ± 18.6
C. pitschmannii	32.3 ± 8.1	22.8 ± 15.5	47.5 ± 22.5	47.0 ± 22.5
C. oblonga	29.1 ± 7.9	33.3 ± 11.9	35.8 ± 10.2	47.4 ± 21.4
C. applanata	23.6 ± 9.1	31.4 ± 10.6	35.8 ± 6.1	43.5 ± 22.2
C. moewusii	43.5 ± 16.5	27.6 ± 16.1	26.5 ± 7.6	46.4 ± 16.3

All points represent the average ± s.d. of 100 independent analytical replicates

330 μmol photons m^{-2} s^{-1}. Therefore, the optimization of the operating conditions—e.g., light irradiance and CO_2 availability—may remarkably improve starch content and production. The analysis of the results of the present tests proves that a simple growth system as that used in the present investigation (shaking flasks) is not well designed for the study of microalgal starch production, because CO_2 supply is limited to the diffusion of the fraction present in the air and there is a limitation in light availability.

Regarding the secreted sugars, their concentration in the medium for cultures carried out in the IBC photobioreactors (Table 2) is lower than that measured in cultures carried out in flasks for most of the strains (Table 1). The high concentration of secreted sugars measured in the flasks could be due to cell lysis and/or due to the stress conditions (CO_2-depletion): microalgae secrete sugars to make a protective habitat. However, secreted sugar concentrations of 0.05–0.1 g L^{-1} were reached in the PBR system. Bafana (2013) pointed out that *Chlamydomonas*-secreted sugars are EPS (exopolysaccharides) and that these sugars are characterized by significant antioxidant activity typically utilized in food, cosmetics, and pharmaceuticals. These sugars can be considered as byproducts of starch production, and their utilization may improve the economics of the starch production process.

Starch accumulation in non-conventional *Chlamydomonas* species In the flask system, where limiting factors occur, *C. reinhardtii* and *C. applanata* showed the best growth and the highest starch productivity of about 0.001 g L^{-1} day^{-1}. Therefore, these two species can be considered the strains characterized by the highest robustness and ability to convert light into biomass (Table 1).

In the IBC, photobioreactors characterized by substantial improvement of light and CO_2, *C. reinhardtii* still had the best growth, but similar growth was recorded by *C. oblonga* which had the highest starch productivity of 0.053 g L^{-1} day^{-1}. The highest starch content of 45 % of DW was reached by *C. moewusii* in this culture system.

The comparison of the maximum biomass productivity (Fig. 3) and the maximum starch productivity (Fig. 4) for a given species deserves some comments. The expected starch productivity at the instance of the maximum biomass productivity—assuming the starch fraction is constant under exponential growth phase—was typically less than half the maximum starch productivity assessed during early N-depletion. This result is in agreement with the conclusion of Yao et al. (2012) about starch accumulation in *T. subcordiformis*: starch accumulation is uncoupled with growth and the reduction of nitrogen sources concentration causes an increase in starch content and productivity at the expense of biomass productivity.

In particular, the analysis of Fig. 3 points out that the prolonged nitrogen starvation was associated to a reduction in starch productivity for all species. Moreover, data in Table 2 confirm that the decrease of starch productivity is species dependent and it is remarkable mainly for *C. moewusii*. Msanne et al. (2012) proposed that the reduction of starch content during prolonged N-starvation is the result of a microalgal metabolism shift to TAG synthesis. Results reported by Siaut et al. (2011) for *C. reinhardtii* cultures support the hypothesis that starch is converted to reserve lipids. On one hand, the production rates of TAG and carbohydrates are affected by the competition for common precursors: intermediates of the central carbon metabolism, e.g., glyceraldehyde-3 phosphate or acetyl coenzyme A (Breuer et al. 2014). On the other hand, the metabolism responsible for cellular growth and maintenance uses starch as energy and carbon sources under nutrient depletion. The result of both phenomena is starch content reduction during N-starvation.

The present investigation confirms the effectiveness of the nitrogen starvation to drive the carbohydrate increase, and the differences among species in the amount of carbohydrate accumulated during N-starvation prove that the accumulation process is species dependent.

Although the model species *C. reinhardtii* exhibited the best growth performances and biomass productivity in both culture systems, a significant improvement of 49 % in starch productivity was obtained by the lesser known species, *C. oblonga*. A real advantage could come from the use of unconventional species for starch production.

Advantages of a simple localization method of starch inside the cells Typically, the pyrenoid is located in the centre of the chloroplast and as starch concentration increases a variable number of starch granules wraps the pyrenoid (Barsanti et al. 2013; Gorelova et al. 2015). This study highlights that there are small differences in starch localization in *Chlamydomonas* species and that nitrogen concentration influences the area occupied by the starch granules inside the chloroplast.

It is known that, as the starch is synthesized, it forms a sheath around the pyrenoid, a subcellular microcompartment where RuBisCO (ribulose-1,5-bisphosphate carboxylase/oxygenase) enzymes and CCM (CO_2-concentrated mechanisms) enzymes act. The observations of the starch-cell system, reported in the literature, make use of advanced diagnostics (e.g., scanning electron microscope, transmission electron microscope, fluorescent microscopy) (Brányiková et al. 2011; Tanadul et al. 2014). The comparison between our observation and those reported in the literature (Muller et al. 1998) proves that the diagnostic tool adopted—staining with Lugol dye coupled with optical microscope observation and image analysis—is a simple, fast, and cheap method to highlight the starch distribution in microalgal cells.

The picture analysis by ImageJ program does not provide quantitative data because the standard deviation of the measured data was not negligible (10–20 %),

notwithstanding the quite high number of cells observed under each operating condition. The high value of the standard deviation is a figure of the wide variability in the cell populations. However, this analysis provides information about the physiological condition of growing and starved cells. The increase of cell area, simultaneously with the increase of the area occupied by starch, is in agreement with the well-known observation that microalgae do not duplicate under nutrient depletion conditions, but accumulate high-energy compounds and increase their average size (Dragone et al. 2011; Fernandes et al. 2013; Johnson and Alric 2013; Gorelova et al. 2015). The observed phenomenon was particularly obvious for *C. applanata* and *C. oblonga* (see Table 2).

Concluding remarks Batch cultures of *Chlamydomonas* species in flasks proved that simple culture systems that do not provide adequate light and CO_2 supply to the cultures (i.e., open pounds) are not suitable for starch production investigation.

The tests of *Chlamydomonas* species in inclined bubble column photobioreactors identified two non-conventional *Chlamydomonas* species characterized by promising starch productivity. *Chlamydomonas oblonga* and *C. moewusii* showed the highest starch productivity with respect to the investigated species (0.053 and 0.046 g L^{-1} day^{-1}, respectively) during early nitrogen depletion. Moreover, a significant increase of 49 % in starch productivity can result from the use of *C. oblonga* instead of the known benchmark *C. reinhardtii*. Interesting results are also related to *C. moewusii*, characterized by high carbohydrate (73%$_{DW}$) and starch content (45 % $_{DW}$), features that facilitate product recovery and reduce downstream process costs.

A method based on Lugol dye starch staining coupled with optical microscope observation and image analysis provided a simple, fast, and cheap method to highlight the presence of starch in microalgal cells and its distribution during different growth phases.

Further studies about the physical and chemical characterization of starch (e.g., amylose and amylopectin content) are needed to verify the real industrial application of microalgal starch.

Acknowledgments The authors thank the Regione Campania (Italy) for the financial support to the project P.O.R. FESR 2007/2013 BioIndustrial Processes—BIP (CUPB25C13000290007).

References

Abou-Shanab RAI, Matter IA, Kim SN, Oh YK, Choi J, Jeon BH (2011) Characterization and identification of lipid-producing microalgae species isolated from a freshwater lake. Biomass Bioenergy 35: 3079–3085

Bafana A (2013) Characterization and optimization of production of exopolysaccharide from *Chlamydomonas reinhardtii*. Carbohyd Polym 20:746–752

Barsanti L, Frassanito AM, Passarelli V, Evangelista V (2013) *Tetraflagellochloris mauritanica* gen. et sp. nov. (Chlorophycae), a new flagellated alga from the Mauritanian Desert: morphology, ultrastructure, and phylogenetic framing. J Phycol 49:178–193

Brányiková I, Maršálková B, Doucha J, Brányik T, Bisová K, Zachleder V, Vitová M (2011) Microalgae-novel highly efficient starch producers. Biotechnol Bioeng 108:766–776

Breuer G, Lamers PP, Martens DE, Draaisma RB, Wijffells RH (2012) The impact of nitrogen starvation on the dynamics of triacylglycerol accumulation in nine microalgae strains. Bioresour Technol 124: 217–226

Breuer G, De Jaeger L, Artus VPG, Martens DE, Draaisma RB, Wijffells RH (2014) Superior triacylglycerol (TAG) accumulation in starchless mutants of *Scenedesmus obliquus*: evaluation of TAG yield and productivity in controlled photobioreactors. Biotechnol Biofuels 7:70–82

Brown MR, Jeffrey SW, Volkman JK, Dunstan GA (1997) Nutritional properties of microalgae for mariculture. Aquaculture 151:315–331

Buléon A, Colonna P, Planchot V, Ball S (1998) Starch granules: structure and biosynthesis. Int J Biol Macromol 23:85–112

Busi MV, Barchiesi J, Martin M, Gomez-Casati DF (2014) Starch metabolism in green algae. Starch 66:28–40

Chen CY, Zhao XQ, Yen HW, Ho SH, Cheng C-L, Lee DJ, Bai F-W, Chang JS (2013) Microalgae-based carbohydrates for biofuel production. Biochem Eng J 78:1–10

Collos Y, Mornet F, Sciandra A, Waser N, Larson A, Harrison PJ (1999) An optical method for the rapid measurement of micromolar concentrations of nitrate in marine phytoplankton cultures. JAppl Phycol 11:179–184

Demchenko E, Mikhailyuk T, Coleman AW, Pröschold T (2012) Generic and species concepts in *Microglena* (previously the *Chlamydomonas monadina* group) revised using an integrative approach. Eur J Phycol 47:264–290

Dragone G, Fernandes BD, Abreu AP, Vicente AA, Teixeira JA (2011) Nutrient limitation as a strategy for increasing starch accumulation in microalgae. Appl Ener 88:3331–3335

Fernandes B, Teixeira J, Dragone G, Vicente AA, Kawano S, Bisová K, Pribyl P, Zachleder V, Vitová M (2013) Relationship between starch and lipid accumulation induced by nutrient depletion and replenishment in the microalga *Parachlorella kessleri*. Bioresour Technol 144:268–274

Gargano I, Olivieri G, Andreozzi R, Marotta R, Marzocchella A, Pinto G, Pollio A (2013) Effects of photobioreactor depth on *Stichococcus* cultures aimed at biodiesel production. Chem Eng Trans 32:1117–1122

Gorelova O, Baulina O, Solovchenko A, Selyakh I, Chiukunova O, Semenova L, Scherbakov P, Burakova O, Lobakova E (2015) Coordinated rearrangements of assimilatory and storage cell compartments in a nitrogen-starving symbiotic chlorophyte cultivated under high light. Arch Microbiol 197:181–195

Ho SH, Chen CY, Chang JS (2012) Effect of light intensity and nitrogen starvationon CO_2 fixation and lipid/carbohydrate production of an indigenous microalga *Scenedesmus obliquus* CNW-N. Bioresour Technol 113:244–252

Johnson X, Alric J (2013) Central carbon metabolism and electron transport in *Chlamydomonas reinhardtii*: metabolic constraints for carbon partitioning between oil and starch. Eukaryotic Cell 12:776–793

Kamalanathan M, Pierangelini M, Shearman LA, Gleadow R, Beardall J (2016) Impacts of nitrogen and phosphorus starvation on the

physiology of *Chlamydomonas reinhardtii*. J Appl Phycol 28:1509–1520

Khalil ZI, Asker MS, El-Sayed S, Kobbia IA (2010) Effect of pH on growth and biochemical responses of *Dunaliella bardawil* and *Chlorella ellipsoidea*. World J Microbiol Biotechnol 26:1225–1231

Kliphuis AMJ, Klok AJ, Martens DE, Lamers PP, Janssen M, Wijffles RH (2012) Metabolic modeling of *Chlamydomonas reinhardtii*: energy requirements for photoautotrophic growth and maintenance. J Appl Phycol 24:253–266

LMC International Ldt (2002) Evaluation of the community policy for starch and starch products. Prepared for: European Commission – DG Agriculture Rue de la Loi 200/Wetstraat 200 B-1049 Bruxelles/Brussel

Meuser JE, Ananyev G, Wittiga LE, Kosourovc S, Ghirardi ML, Seibert M, Dismukes GC, Posewitz MC (2009) Phenotypic diversity of hydrogen production in chlorophycean algae reflects distinct anaerobic metabolisms. J Biotechnol 142:21–30

Miller BJN (2010) Food analysis. Nielsen SS, 4th edn. Springer, New York

Moheimani NR, Borowitzka MA (2006) The long-term culture of the coccolithophore *Pleurochrysis carterae* (Haptophyta) in outdoor raceway ponds. J Appl Phycol 18:703–712

Msanne J, Xu D, Konda AR, Casas-Mollano JA, Awada T, Cahoon EB, Cerrutti H (2012) Metabolic and gene expression changes triggered by nitrogen deprivation in the photoautotrophically grown microalgae *Chlamydomonas reinhardtii* and *Coccomyxa* sp. C-169. Phytochemistry 75:50–59

Muller T, Bleiss W, Martin C-D, Rogaschewski S, Fuhr G (1998) Snow algae from northwest Svalbard: their identification, distribution, pigment and nutrient content. Polar Biol 20:14–32

Nascimento IA, Marques SSI, Cabanelas ITD, Pereira SA, Druzian JI, de Suoza CO, Vich DV, de Carvalho GC, Nascimento MA (2013) Screening microalgae strain for biodiesel production: lipid productivity and estimation of fuel quality based on fatty acids profiles as selective criteria. Bioenergy Res 6:1–13

Olivieri G, Gargano I, Andreozzi R, Marotta R, Marzocchella A, Pinto G, Pollio A (2013) Effects of photobioreactors design and operating conditions on *Stichococcus bacillaris* biomass and biodiesel production. Biochem Eng J 74:8–14

Pollio A, Cennamo P, Ciniglia C, De Stefano M, Pinto G, Huss VA (2005) *Chlamydomonas pitschmannii* Ettl, a little known species from thermoacidic environments. Protist 156:287–302.

Renaud SM, Thinh LV, Lambrinidis G, Parry DL (2002) Effect of temperature on growth, chemical composition and fatty acid composition of tropical Australian microalgae grown in batch culture. Acquaculture 211:195–214

Schulze K, Lòpez DA, Tillich UM, Frohme M (2011) A simple viability analysis for unicellular cyanobacteria using a new autofluorescence assay, automated microscopy, and Image J. BMC Biotechnol 11:118–126

Siaut M, Cuiné S, Cagnon C, Fessler B, Nguyen M, Carrier P, Beyly A, Beisson F (2011) Oil accumulation in the model green alga *Chlamydomonas reinhardtii*: characterization, variability between common laboratory strains and relationship with starch reserves. BMC Biotechnol 11:7–22

Srinivas T (2007) Industrial demand for cassava starch in India. Starch 59:477–481

Tanadul O, Vandergheynst JS, Beckles DM, Powell ALT, Labavitch JM (2014) The impact of elevated CO_2 concentration on the quality of algal starch as a potential biofuel feedstock. Biotechnol Bioeng 111:1323–1331

Yao C, Ai J, Cao X, Xue S, Zhang W (2012) Enhancing starch production of marine green microalga *Tetraselmis subcordiformis* through nutrient limitation. Bioresour Technol 118:438–444

Mosaic of micloalgae colours

Rea Giulia